INSTITUTE OF GEOPHYSICS
POLISH ACADEMY OF SCIENCES

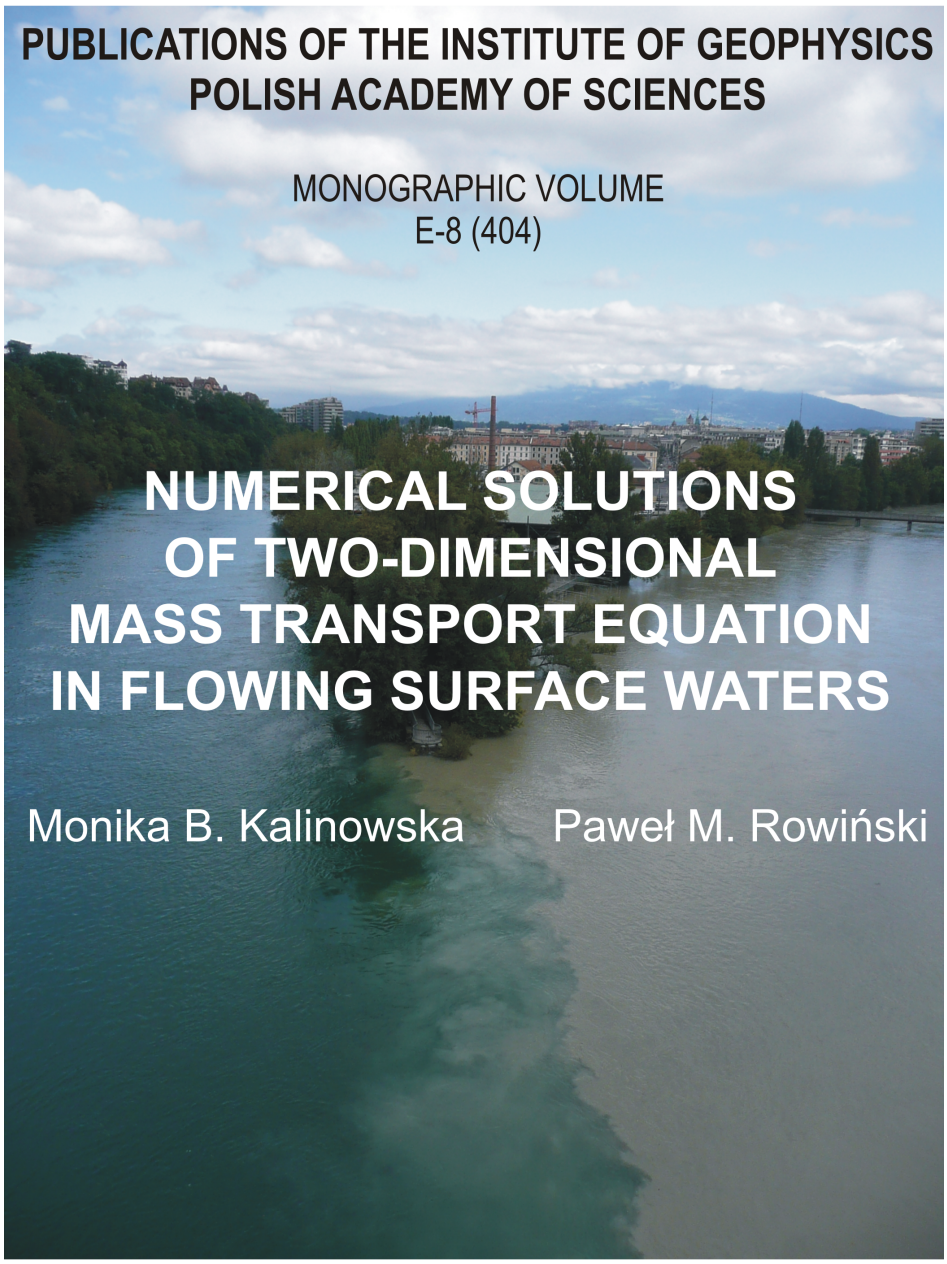

PUBLICATIONS OF THE INSTITUTE OF GEOPHYSICS
POLISH ACADEMY OF SCIENCES

MONOGRAPHIC VOLUME
E-8 (404)

NUMERICAL SOLUTIONS OF TWO-DIMENSIONAL MASS TRANSPORT EQUATION IN FLOWING SURFACE WATERS

Monika B. Kalinowska Paweł M. Rowiński

Warsaw 2008

„All models are wrong but some models are useful”
George Box

Acknowledgements

This work was supported by grant 2 P04D 026 29 from the Ministry of Education and Science, Poland. The authors would like to express gratitude to Professor Ian Guymer from the School of Engineering at the University of Warwick who has kindly provided the unique data, very helpful in verification of the model. Ian Guymer was also a host of the first author devoting his time and sharing his knowledge on the processes of spread of pollutants in open channels. The authors had also the privilege to discuss various aspects of the research presented in the book with Dr. Steve Wallis from Hariot-Watt University in Edinburgh, UK.

Contents

1 Introduction **1**

2 Mass Transport in Open Channels **7**
2.1 Introduction 7
2.2 Physical bases for modeling mass transport in open channels . . 8
2.3 Two-dimensional equation of mass transport 16
2.4 Dispersion coefficients 18
2.5 Solving 2D transport equation 20

3 Simplifications of 2D Mass Transport Equation **23**
3.1 Introduction 23
3.2 Determination of the dispersion tensor coefficients 24
3.2.1 Rotation 25
3.2.2 Quasi rotation 27
3.2.3 Vector-like rotation 27
3.2.4 Identity transformation 29
3.3 Computational tests 29
3.3.1 Instantaneous release of solute 32
3.3.2 Continuous inflow of solute 39

4 Numerical Methods for 2D Transport Equation **45**
4.1 Introduction 45
4.2 Finite Difference Method 46
4.3 Discretization of 2D transport equation 49
4.3.1 Upwind explicit, forward/backward space scheme 52

4.3.2 Crank-Nicolson scheme with central finite difference spatial approximation . . . 54
4.3.3 Alternating Direction Implicit method with central finite difference spatial approximation . . . 58
4.4 Initial and boundary conditions . . . 65

5 Properties of Considered Numerical Schemes 67
5.1 Introduction . . . 67
5.2 Accuracy – truncation error . . . 68
5.2.1 Modified Equation Approach . . . 69
5.2.2 Truncation error for Alternating Direction Implicit method 84
5.3 Computation speed and stability . . . 89

6 Description of RivMix Model 97
6.1 Introduction . . . 97
6.2 Simulation parameters . . . 97
6.3 Algorithm . . . 99

7 Model Verification 105
7.1 Introduction . . . 105
7.2 Wide rectangular channel . . . 105
7.2.1 Instantaneous discharge of pollutants . . . 106
7.2.2 Continuous inflow of pollutants . . . 113
7.3 Laboratory compound channel . . . 117

8 Concluding remarks 129

A 2D Transport Equation 133

B Difference Operators Used in the Book 135

C Dispersion Tensor Simplifications 137
C.1 Instantaneous release of solute . . . 137
C.2 Continuous inflow of solute . . . 148

D Boundary Conditions 159

E Modified Equation 171

List of symbols 175

List of acronyms 179

List of figures 181

List of tables 186

References 189

Index 198

Chapter 1

Introduction

The problem of water quality receives an increasing attention of the public, politicians, decision makers nowadays. People have to answer how to achieve any given level and pattern of water quality in particular watercourses and also how to mitigate the catastrophes that are inseparable elements of civilization. The EU water framework directive, which came into force at the end of 2000 (Directive, 2000), changes the way of monitoring, assessing and managing water in European countries. Three groups of quality elements (biological, hydromorphological and physico-chemical) have been identified in the water framework directive as necessary to classify the ecological status of a particular water body. One should also mention about other EU directives, like the dangerous substances directive, drinking water directive, IPCC directive which in general should lead towards reduction and elimination of pollution by hazardous substances, phasing out emissions, losses and discharges of them. In general, achievement of levels protecting human health and aquatic ecosystems is expected. There are however many significant shortfalls and gaps not only in the countries information but also at the basic understanding of the physical processes occurring in various water bodies and consequently on the modeling of pollution transport.

Water quality predictions in rivers require development of a model that is able to capture the basic physical features of the process and depends only on the variables that are available in case under consideration. A very crucial and often made assumption is the limitation to the neutrally buoyant substances. The analysis of such micropollutants like heavy metals (e.g. mercury, cadmium, lead) would go along different line. The reason is that these substances may be present in three states in the system considered: in dissolved form as well as in

solid phase mostly present in the suspended solids and in the sediment below. In case when these pollutants are in the solid form, the relevant description of their transport should appeal to the dynamics of two-phase flows.

We will further assume that the considered mixture is passive that is one, in which the fluid-particle interaction does not affect the dynamics of the flow. Otherwise, one would have to include momentum considerations in order to properly represent certain two-phase flows. Further limitation is the consideration of the fate of solutes only, i.e. the substances that are dissolved in the water. Throughout this volume, we use the macroscopic treatment, i.e. the theory of continuum. Because of practical importance, we do not care about the motion of individual particles of the matter and are interested only in the resultant effects due to the motion of a large number of particles. It is possible because in practical problems the smallest length scales of interest are much larger than the distance between molecules.

In principle, the physical processes during the transport of any constituent are three dimensional and should be described by three dimensional (3D) advection-diffusion equation together with the description of 3D velocity field. Advection-diffusion equation (ADE) already imposes the so-called one-way coupling, i.e. the particles dispersed in a carrier flow have negligible effect on turbulence. It means that particle spread in this regime depends on the state of turbulence but due to the negligible concentration of the particles, the momentum transfer from the particles to the turbulence has an insignificant effect on the flow (Elgobashi, 1994). In most cases, it is an acceptable assumption. Three dimensional ADE is, however, still too demanding in respect to data, and the data for such models are mainly available for academic purposes. Therefore, further simplifications are usually sought in practice.

In the general three-dimensional case, construction of the mass transport equation for a dissolved quantity requires the application of the Reynolds hypothesis allowing for the decomposition of the velocities and concentrations into mean and fluctuating values, and further additional information about the turbulent mass flux, based for example on a linear relationship between the turbulent flux and the gradient of the mean concentration. The main obstacles to progress in that approach are the lack of reliable theory which relates the spatial variation of turbulent diffusion coefficients to flow and boundary conditions, mathematical difficulties in solving the transport equation for variable diffusion coefficients and realistic spatial domains. Another important problem is the lack of knowledge of the realistic detailed 3D velocity field. Three dimensional approach is probably suitable in the vicinity of the injection point in the river when one is interested in studying the heterogeneity in vertical and lateral

directions. Such strong heterogeneity may occur due to the variability of river geometry like meanders, or the ones caused by fairways and weirs.

Various simplifications of the model are necessary to tackle real life problems. One option is to eliminate one or two dimensions in cases where such operation is justified by the conditions in the considered river reach. This elimination may be realized by relevant averaging of the governing equations (both hydrodynamics and mass transfer equation at the same time). It is usually the case that in the mid-field region the governing equations may be averaged over the depth giving two-dimensional (2D) models. In the far field, in case when the river geometry allows, one is mostly interested in the cross-sectionally averaged concentrations. The governing equations may be then averaged over the cross-section, which results in a one-dimensional (1D) model of the spread of the constituent under consideration. Two-dimensional case will be considered in more detail in the next section. Let us therefore briefly discuss the problem of 1D modeling. A long tradition in the application of the longitudinal dispersion model exists. Such a model is very useful for designing outfalls or water intakes and first of all for evaluating risks from, for example, accidental releases of hazardous contaminants. 1D models are the easiest in application and not such detailed knowledge about the hydraulic characteristics of the considered reach is required as in case of 2D and 3D approaches.One has to be aware, however, of the restrictions that 1D models are burdened (Jirka & Weitbrecht, 2005; Rutherford, 1994; Sukhodolov *et al.*, 1998). 1D model in the traditional Fickian form applies only in relatively simple river reaches (in terms of the geometry) and only after some initial mixing period (the solute concentration should be well distributed over the channel width). The advection-dispersion equation has been successfully applied for many real cases; nevertheless, very often the questions about its applicability arise. The tail of a solute tracer pulse is often more pronounced than can be accounted for by the traditional advection-dispersion model. A common method for simulating these long tails has been to allow for storage zones along the stream channel (Czernuszenko *et al.*, 1998; Rowiński & Piotrowski, 2008; Van Mazijk & Veling, 2005). These storage zones are assumed to be stagnant relative to the longitudinal flow of the stream and to obey a first-order mass transfer type of exchange relationship. Very often a quicker decrease of the concentration maximum following from the Fickian equation is observed. Also a nonlinear growth of the concentration distribution variance and dependence of the dispersion coefficient on time has been often manifested in experimental studies.

As mentioned before, in situations where the concentration is rather uniform along each individual vertical line, the depth averaging of every quantity

is made to reduce the dimensionality of the problem. As a result, the depth-averaged, two-dimensional advection-diffusion transport equation is readily obtained. Discussion of efficient methods of the solutions of thus obtained model will constitute the main aim of this volume. In this study the full version of the transport equation has been considered. Special attention has been paid to the often-encountered practice of neglecting the mixed derivatives in the transport equations independently of the complexity of the domain of computations. The credible investigation of mixing processes in open-channels has stimulated the development of various numerical solvers for advection-diffusion equations. However, the requirements regarding the accuracy and efficiency for these methods are constantly becoming stricter and therefore there is still a need to find better numerical schemes (Grima & Newman, 2004; Juntunen & Tsiboukis, 2000; MacKenzie & Roberts, 2003, e.g.,). Understanding of the theoretical truncation error is therefore a must when concrete numerical schemes are applied. Such an error is in fact the difference between the actual solution and the approximate solution due solely to the numerical scheme. We do realize that the root of finite-difference schemes is a Taylor expansion. Since it is impossible to compute all the terms in an infinite series, a numerical scheme necessarily uses a truncated series. Most of the studies aimed at the evaluation of numerical errors associated with the finite-difference solutions of relevant equations were either devoted to one-dimensional cases (Ataie-Ashtiani *et al.*, 1996, 1999; Dehghan, 2004; Fletcher, 1991; Karahan, 2006) or in case of two-dimensional transport processes – they were usually restricted to the simple case in which mixed derivatives were avoided (Ataie-Ashtiani & Hosseini, 2005a,b; Noye & Tan, 1989; Noye, 1984; Peyret & Taylor, 1986). Such an approach is very common in hydraulic research, and taking into account complex natural geometries that we deal with in natural channels is not well justified (Rowiński & Kalinowska, 2006). One should note a recent study of Ataie-Ashtiani & Hosseini (2005a) in which full 2D advection-dispersion equation with a reaction term has been analysed but the authors restricted their considerations to just numerical diffusion error. Numerical dispersion, another source of truncation error, is an undesired nonphysical effect inherently present in the finite-difference schemes commonly used in environmental hydraulics. It will be studied in this book as well. Some of alike literature studies were devoted to the pure advection equation – see e.g. (Fletcher, 1991; Grandjouan, 1990; Odman, 1997; Thomas, 1995; Zoppou & Roberts, 1993) in one-dimensional case, or (Bielecka-Kieloch, 1998; Szymkiewicz, 2006) in two-dimensional case. The method of the present study pertains to the so-called Modified Equation approach proposed by Warming & Hyett (1974). Recently Szymkiewicz (2006) has provided a detailed review of

this method. The modified equation is derived by first expanding each term of the applied difference scheme in a Taylor series and then eliminating time derivatives higher than the first-order by specially designed mathematical manipulations.

On top of analyzing the numerical schemes, this work aims to provide a comprehensive model and the description of the computer program **RivMix** (River Mixing Model) together with its application to a few case studies. The computer program was created in C++ computing language and compiled under Linux Red Hat operating system. Visualization of results was done with use of an Object Oriented Data Analysis Framework ROOT – the program created in CERN – European Organization for Nuclear Research (Brun & Rademakers, 1997). The **RivMix** model has been verified and tested using the comparison with analytical solution for a simple case, when such solution could be obtained. Data from the experiment performed at Sheffield Hallam University and provided by Ian Guymer has been used for validation of the model.

The presented model with its numerical implementations holds great promise for future applications to real cases studies. This model still lacks verification for a wide range of prototype situations. This circumstance is due in part to the complexity of performing two dimensional experiments and a giant step forward toward further development of the method requires high quality laboratory and field data.

We hope that the results of the study presented in this book will be helpful for researchers and students dealing with numerical modeling of mass transport in open channels. The numerical aspects may also be treated more universally and definitely may be used by a broader audience, namely by everybody working on solving the advection-diffusion equation in natural flows but also in industrial applications.

Chapter 2

Mass Transport in Open Channels

2.1 Introduction

Monitoring the quality of waters and control of pollutants released into them, as well as development of ways of acting in case of possible contamination make us create models describing processes of water flow and the transport of substances dissolved in it. This volume considers processes of transport and mixing of substances dissolved in surface flowing waters, e.g. rivers and open channels. The transport of passive and conservative substances which dissolve in water after a short time is taken into account. In the natural environment, the significant number of admixtures is of passive nature (Szymkiewicz, 2000). Such substances do not have any influence upon the water velocity field, which allows to limit the consideration to single phase flows. Conservative substances are substances whose total mass does not change in time. Therefore, the generation and disappearance of solute are not taken into consideration. Otherwise, the mass transport equation described further in the volume would have to include terms representing equations of chemical, physical or biological reactions or transformations describing the process of generation or dissolution of the source factor. Those terms obviously depend on the kind of the process and the dissolved substance under consideration. The ways of their parameterisation may be found in literature (e.g. Rowiński & Kwiatkowski, 2008; Sawicki, 2003).

The description of the basic transport processes and the ways of modeling them mathematically are broadly discussed in the literature on the subject. The review of the basic theories relating to open channels is presented, among others, by: Czernuszenko (1990, 2000a,b); Czernuszenko & Rowiński (1994); Fischer

et al. (1979); Holley & Jirka (1986); Rutherford (1994); Szymkiewicz (2000). A comprehensive work describing mass and energy transport is "Migration of Pollutants" (Sawicki, 2003), and the monograph "Water Quality Hazards and Dispersion of Pollutants" (Czernuszenko & Rowiński, 2005), including a collection of works by leading experts dealing with various aspects of modeling of spreading of pollutants in rivers.

The equations describing the transport of dissolved substances result from one of the basic laws of physics, which is the mass conservation law (derivation can be found in, e.g.: Czernuszenko, 1990; Sawicki, 2003; Szymkiewicz, 2000). In the most general case this will be a three-dimensional advection-diffusion equation, but in practice its averaged versions are usually applied, leading to two-dimensional or one-dimensional equations.

2.2 Physical bases for modeling mass transport in open channels

The basic measure of the amount of a substance dissolved in water is ***concentration*** defined by the proportion of the mass of the solute to the volume of water in which it is dissolved:

$$c = \frac{M}{V} \left[\frac{\mathrm{kg}}{\mathrm{m}^3} \right], \tag{2.1}$$

where:

c – concentration,
M – mass of the solute,
V – volume of the liquid.

One may find other definitions in literature, but relation (2.1) will be consequently used in this book.

The process of transport of any solute in water is the result of operation of two basic mechanisms: ***advection***, which is the mechanism connected with the movement of water, and ***diffusion***, which is an intrinsive mechanisms of transporting the substance in the direction of decreasing concentration. Diffusion, unlike advection, is an irreversible process. To describe the advection process, one needs to solve the complicated equation of motion, while the diffusion process is usually described by well-known diffusion coefficients.

The equation which allows to determine the concentration field in the most general three-dimensional case results from mass conservation law and can be

written as follows (Czernuszenko, 2000b):

$$\frac{\partial c(\mathbf{x},t)}{\partial t} + \operatorname{div}\Big[\underbrace{\mathbf{v}(\mathbf{x})c(\mathbf{x},t)}_{\text{advection term}} - \underbrace{\mathbf{D_M}\operatorname{grad} c(\mathbf{x},t)}_{\text{diffusion term}}\Big] = 0; \tag{2.2}$$

where:

t – time,
$\mathbf{x} = (x, y, z)$ – position vector,
$c(\mathbf{x}, t)$ – concentration,
$\mathbf{v}(\mathbf{x})$ – velocity vector,
$\mathbf{D_M}$ – molecular diffusion tensor.

The exact determination of the value of concentration at a given point in space in a given time instant is not possible, therefore, in practice, we look for concentration values which are averaged over time. The most general three-dimensional case of the equation for transport of the solute requires the application of Reynolds' hypothesis, allowing for decomposition of the concentration and velocity values into their average values and fluctuating (turbulent) values:

$$\mathbf{v} = \bar{\mathbf{v}} + \mathbf{v}';$$
$$c = \bar{c} + c';$$

where:

$\bar{\mathbf{v}}$ – mean velocity vector,
$\mathbf{v}'$ – turbulent velocity vector,
$\bar{c}$ – mean point concentration,
c' – concentration fluctuation.

This procedure described in detail e.g. in (Czernuszenko, 2000b; Czernuszenko & Rowiński, 2005; Rowiński, 2002; Sawicki, 2003; Szymkiewicz, 2000) introduces an additional mechanism of turbulent mass transport called ***turbulent diffusion***. The solution of the equation requires the acceptance of a hypothesis that makes the turbulent mass stream dependent on the average concentration gradient (Czernuszenko, 2000b):

$$\overline{\mathbf{v}'c'} = -\mathbf{D_T}\operatorname{grad}\bar{c}; \tag{2.3}$$

where:

$\mathbf{D_T}$ – turbulent diffusion tensor.

Table 2.1: Orders of magnitude of various mixing coefficients in rivers (Smith, 1992)

Coefficient	Order of Magnitude in $\frac{m^2}{s}$
molecular diffusion	from 10^{-10} to 10^{-9}
turbulent diffusion	from 10^{-3} to 10^{-1}
dispersion	from 1 to 10^3

Turbulent diffusion tensor appears in the transport equation, which has nine components in the general case. The equation can be written as follows:

$$\frac{\partial \bar{c}(\mathbf{x},t)}{\partial t} + \operatorname{div}\Big[\bar{\mathbf{v}}(\mathbf{x})\bar{c}(\mathbf{x},t) - (\mathbf{D_M} + \mathbf{D_T}(\mathbf{x}))\operatorname{grad}\bar{c}(\mathbf{x},t)\Big] = 0. \tag{2.4}$$

The values of the molecular diffusion coefficients are usually much smaller than those of the turbulent diffusion coefficients (see table 2.1), and therefore they are often omitted. Hence, the three-dimensional transport equation can be written in the form:

$$\frac{\partial c(\mathbf{x},t)}{\partial t} + \nabla\Big[\mathbf{v}(\mathbf{x}) \cdot c(\mathbf{x},t)\Big] - \nabla\Big[\mathbf{D_T}(\mathbf{x}) \cdot \nabla c(\mathbf{x},t)\Big] = 0; \tag{2.5}$$

where, for simplicity the mean velocity ($\bar{\mathbf{v}}$) and concentration ($\bar{c}$) values are written without the overhead dash.

With appropriately selected system of coordinates, the turbulent diffusion tensor is diagonal and has only three non-zero components (Czernuszenko, 2000b; Sawicki, 2003). Although any solution of a full three-dimensional equation requires information not only on turbulent diffusion coefficients which are difficult to establish, but also on exact measurements of the velocities and depth, which are seldom available in reality. At the same time the computational costs of the solution of a three-dimensional task are very high.

In practice, the information on the three-dimensional concentration field is usually not necessary. Apart from that, the majority of natural rivers and channels is shallow as compared to their width, and therefore the mixing process along the depth runs relatively fast, both in case of large and small rivers (see table 2.2). We may assume that the complete vertical mixing takes place at the distance equal to a few dozens of depths at most (Jirka & Weitbrecht, 2005).

Table 2.2: Examples for the complete mixing of a passive point source located at water surface and at bank of a river (Jirka & Weitbrecht, 2005)

River	Distance to complete mixing	
	vertical (along the depth)	horizontal (along the width)
Large river B = 250 m, H = 3 m	150 m	160 000 m
Small river B = 5 m, H = 0.5 m	25 m	400 m

B – river width
H – average depth

Treating the process of spreading of pollutants (except for the short initial distance) as two-dimensional seems natural. The equation describing it (presented further on in the volume – see equation (2.6)) is obtained by the averaging of the three dimensional equation along the depth. The averaging process (analogous to time averaging) introduces the additional transport mechanism called ***dispersion***, which will be described in detail further in the book. The mathematical description of the averaging process can be found in many works (e.g.: Czernuszenko, 1990, 2000b; Fischer *et al.*, 1979; Rowiński, 2002; Rutherford, 1994). In practice, it is mainly attempted to describe the process of spreading of pollutants with the application of a one-dimensional advection-diffusion equation obtained by the averaging of the three dimensional equation in the given cross-section of the channel. Such an approach can be very useful; however, it is often insufficient. Although the complete vertical mixing takes place relatively fast, the mixing along the width can take a very long time (see table 2.2). In large rivers, in an extreme case, these may be distances of hundreds of kilometers. Figures 2.1, 2.2 and 2.3 illustrate the process very well. The one-dimensional approach can, therefore, be effectively applied only starting from the moment when complete mixing of the substance along the cross-section of the channel took place. For a typical river (B/H = 10 to 100) this will be a section of the length equal 100 to 1000 times the width of the river (Endrizzi *et al.*, 2002; Jirka & Weitbrecht, 2005).

Figure 2.1: Aerial photograph (ca. 1960) of an industrial discharge located near the middle of the regulated River Rhine upstream of Lake Constance (Bodensee); photograph courtesy of D. Vischer, Zurich; source: (Jirka & Weitbrecht, 2005)

Therefore, we can distinguish three characteristic zones conditioning the dimension of the problem:

- **NEAR FIELD ZONE** – the shortest one – starting at the discharge point (figs. 2.4 and 2.5) and continuing to the point of complete vertical mixing. Its length depends mainly on the depth and the way of discharging of the pollutants. Vertical mixing prevails in this zone.
- **MID FIELD ZONE** – may continue for a very long distance (figs. 2.1, 2.2 and 2.3) – it stretches down the river until the point where a complete mixing in the cross-section of the channel takes place. Horizontal mixing prevails in this zone.

Figure 2.2: Tracer study of horizontal mixing in Missouri river in USA (river width: from $B = 150\,\mathrm{m}$ to $B = 240\,\mathrm{m}$, maximum depth: $H = 7.5\,\mathrm{m}$); source: (Holley, 2001)

Figure 2.3: Rhodamine dye study of hydrology of stream-lake interactions (Spring Creek lake); source: http://www.aslo.org/, author: Prof. Wayne Wurtsbaugh

Figure 2.4: Tracer test performed in a natural Narew river in the North-East of Poland in June 2005; dye release

Figure 2.5: Tracer test performed in a small river (river width: $B = 5\,\mathrm{m}$, height: $H = 1\,\mathrm{m}$); dye release; source: (Holley, 2001)

- **FAR FIELD ZONE** – starting after the complete mixing along the depth and width of the channel (fig. 2.6) – where the transport of the solute takes place only downstream. Longitudinal mixing prevails here.

Mixing in each zone should be modeled, respectively, with the application of three-, two- or one-dimensional equations. In the literature, generally the attempts to model the process with application of the one-dimensional diffusion-advection equation, or its various modifications, may by found (for example see: Beer & Young, 1983; Cheong & Seo, 2003; Czernuszenko *et al.*, 1998; Karahan, 2006; Tsai *et al.*, 2001). Although the modeling of the near field, in which the three-dimensional approach has to be applied (sample works: Chau & Jiang, 2002; Czernuszenko & Rylov, 2005), due to a short distance along which it takes place, has small practical applicability, in the analysis of phenomena related to the discharge of pollutants, the mid field is very often significant, where the full spreading of the pollutant across the channel has not yet taken place. In such situations, the one-dimensional approach is, as mentioned earlier, insufficient. The subject of this study is often disregarded, yet significant, transition zone,

Figure 2.6: Tracer test performed in a natural Narew river in the North-East of Poland in June 2005 (Rowiński *et al.*, 2007, 2008); after complete mixing along the river width

the modeling of which requires solving an averaged two-dimensional transport equation. The two-dimensional approach is necessary also in the situation of mixing of rivers (joining of two or more rivers, tributaries), and allows to take into consideration a complicated geometry (e.g., bends) which is present in case of natural channels. Note that all the presented equations must be supplemented by proper initial and boundary conditions.

2.3 Two-dimensional equation of mass transport

The majority of rivers are shallow in relation to their length and width, which, as mentioned earlier, guarantees relatively fast vertical mixing of the admixture. In this case, the transport of passive substances dissolved in water may be represented by a depth-averaged, two-dimensional advection-diffusion differential equation (Czernuszenko, 1990):

$$h(\mathbf{x})\frac{\partial c(\mathbf{x},t)}{\partial t} + \underbrace{h(\mathbf{x})\Big[\mathbf{v}(\mathbf{x})\cdot\nabla c(\mathbf{x},t)\Big]}_{\text{advection term}} - \underbrace{\nabla\Big[h(\mathbf{x})\mathbf{D}(\mathbf{x})\cdot\nabla c(\mathbf{x},t)\Big]}_{\text{diffusion term}} = 0; \tag{2.6}$$

where:

$\mathbf{x} = (x, y)$ – position vector,
$c(\mathbf{x}, t)$ – depth-averaged concentration,
$h(\mathbf{x})$ – local depth,
$\mathbf{v}(\mathbf{x})$ – depth-averaged velocity vector,
$\mathbf{D}(\mathbf{x})$ – dispersion tensor.

The result of the depth-averaging of the equation (or cross-section averaging) is the occurrence of additional coefficients in the transport equation, resulting from the non-uniformity of concentrations and velocities along the depth of the flow. Those coefficients represent an additional, significant transport mechanism called dispersion or shear dispersion. Dispersion is not a physical process but only a consequence of the averaging of the equation. Like in the case of turbulent diffusion, it is assumed that dispersion flow is proportional to the average concentration gradient (Czernuszenko, 2000b; Rowiński, 2002; Rutherford, 1994). This proportionality is determined by the so-called ***dispersion coefficients*** ($D_{xx}, D_{xy}, D_{yx}, D_{yy}$), which, in the general case in the Cartesian coordinate system, create the non-diagonal tensor:

$$\mathbf{D} = \begin{bmatrix} D_{xx} & D_{xy} \\ D_{yx} & D_{yy} \end{bmatrix}. \tag{2.7}$$

Note that usually the turbulent diffusion coefficients are included in the dispersion coefficients. For a properly selected coordinate system, when the direction of flow is parallel to the x- or y-axis, off-diagonal elements of the tensor equal zero. In such a situation, instead of the full equation:

$$h\left(\frac{\partial c}{\partial t}+v_x\frac{\partial c}{\partial x}+v_y\frac{\partial c}{\partial y}\right) - \frac{\partial}{\partial x}\left(hD_{xx}\frac{\partial c}{\partial x}+hD_{xy}\frac{\partial c}{\partial y}\right)-\frac{\partial}{\partial y}\left(hD_{yy}\frac{\partial c}{\partial y}+hD_{yx}\frac{\partial c}{\partial x}\right)=0, \quad (2.8)$$

a simplified differential equation (2.9) can be solved, where the mixed derivatives are not present:

$$h\left(\frac{\partial c}{\partial t}+v_x\frac{\partial c}{\partial x}+v_y\frac{\partial c}{\partial y}\right)-\frac{\partial}{\partial x}\left(hD_{xx}\frac{\partial c}{\partial x}\right)-\frac{\partial}{\partial y}\left(hD_{yy}\frac{\partial c}{\partial y}\right)=0; \quad (2.9)$$

where:

v_x, v_y – depth-averaged components of the velocity vector in x and y direction respectively.

In practice, we seldom find a channel for which the flow direction is parallel to the x- or y-axis in all points of flow, and therefore the full equation (2.8) should be applied, including mixed derivatives. Nevertheless, in the literature, even for complex geometries, the simplified versions (2.9) of the equation are applied without a proper justification (Rowiński & Kalinowska, 2006). This problem is discussed in detail in Chapter 3.

If at a given point the axes of the coordinate system are directed along the main directions of flow, then the dispersion coefficient D_{xx} is called the ***longitudinal dispersion coefficient*** denoted by D_L, and the D_{yy} is the ***transverse dispersion coefficient*** denoted by D_T. Then the dispersion tensor has the following form:

$$\mathbf{D}=\begin{bmatrix} D_{xx} & 0 \\ 0 & D_{yy}\end{bmatrix}=\begin{bmatrix} D_L & 0 \\ 0 & D_T\end{bmatrix}. \quad (2.10)$$

The knowledge of the dispersion coefficients is, beside the information regarding the velocity field, necessary for the solution of two- or one-dimensional transport equations.

2.4 Dispersion coefficients

The dispersion coefficients influencing the velocity of spreading of pollutants in the channel are in fact the most important and the most difficult to determine factors characterizing the mixing processes (Czernuszenko, 1990, 2000b). These coefficients depend on many factors relating to the geometry of the channel and the dynamics and turbulence of the flow. In practice, they are determined by means of tracer experiments carried out in the considered channel, or on the basis of available empirical relationships, determined earlier.

The longitudinal and transverse dispersion coefficients, due to their significance and the difficulties connected with their determination, are the subject of many considerations in the literature. The majority of research relates to the attempts to determine "universal" empirical formulae determining the values of the coefficients on the basis of known parameters characteristic for a river or a channel of the given type. The selection of the proper formula, in the discussed case, is not a simple matter. Relations true for one river are not always such for another; straight channels must be treated differently from meandering ones (Deng *et al.*, 2002; Guymer, 1998). According to Czernuszenko (1990), laboratory measurements, in case of spreading of pollutants in a rectangular channel, lead to a general relation:

$$D = aHu_* \,; \tag{2.11}$$

where:

D – longitudinal or transverse dispersion coefficient,
H – average depth,
u_* – friction (shear) velocity,
a – dimensionless coefficient.

The bulk friction velocity is most often calculated from the formula:

$$u_* = \sqrt{gRS_0} \,; \tag{2.12}$$

where:

R – hydraulic radius,
S_0 – slope of the channel,
g – gravitation.

In literature, however, more complex formulae for determination of the friction velocity are known (see e.g. Rowiński *et al.* (2005a)). In some cases, the relations determining the D_L factor use the average flow velocity (U) instead of

Table 2.3: Parameter a values for transverse dispersion coefficient (Rutherford, 1994)

Type of channel	Range of the values of parameter a
straight channels	from 0.15 to 0.3
meandering channels	from 0.3 to 1.0
strongly curved channels	from 1.0 to 3.0

friction velocity, and the width of the channel (B) instead of the average depth, or a combination of all these parameters. The coefficient a is different for longitudinal dispersion and transverse dispersion, and it also depends on the type of the river in question, its sinuosity, etc. In case of longitudinal dispersion, the value $a = 5.93$, is very often seen, determined with the assumption of logarithmic distribution of velocity (Elder, 1959). For transverse dispersion, Rutherford (1994) suggests using the values presented in table 2.3 depending on the curvature of the channel. Czernuszenko (1990) gives example ranges for coefficient a: for transverse dispersion in a rectangular channel – from 0.1 to 0.25 and for longitudinal dispersion in a trapezoidal channel – from 150 to 400. In the same work, we can also find a description of how to determine dispersion coefficients on the basis of tracer measurements. The presented methods were applied to determine the longitudinal and transverse dispersion coefficients for the Vistula river within the area of Warsaw. The average values of those coefficients are, respectively, $D_L = 2.77\,\frac{\mathrm{m}^2}{\mathrm{s}}$, $D_T = 0.24\,\frac{\mathrm{m}^2}{\mathrm{s}}$, for the average depth of the river being $H = 1.42\,\mathrm{m}$ and the average flow velocity $U = 0.67\,\frac{\mathrm{m}}{\mathrm{s}}$. It is worth noticing that in this case the value of the longitudinal dispersion coefficient is about 12 times greater than the value of the transverse dispersion coefficient.

In majority of cases, there are separate works devoted to the processes of longitudinal and transverse mixing. The dispersion coefficients are usually determined in the situation of actual discharge of pollutants at the stage when the full mixing along the width of the channel has already taken place. The description of methods of determining and comparing, and the discussion of various empirical relations enabling to determine the D_L factor can be found, among others, in the following works: (Guymer *et al.*, 1999; Rieckermann *et al.*, 2005; Sukhodolov *et al.*, 1998; Wallis *et al.*, 2007; Wallis & Manson, 2004). The research concerning transverse mixing usually concerns situations of continuous discharge of pollutants (Boxall *et al.*, 2003; Holley & Abraham, 1973a,b; Rutherford *et al.*, 1992; Seo *et al.*, 2006), when we can assume that $\frac{\partial c}{\partial t} = 0$. The review of empirical formulae used to determine the value of the transverse dis-

persion coefficient D_T, may be found in the article of Jeon *et al.* (2007). The D_T coefficient is in some cases called the transverse mixing coefficient. On the basis of tracer experiments, databases of dispersion coefficients for individual rivers are created, together with the description of their basic parameters (e.g.: Deng *et al.*, 2002; Kashefipour *et al.*, 2002; Lau & Krishnappan, 1981; Rutherford, 1994; Sukhodolov *et al.*, 1998), which can in turn be useful for similar rivers. Also artificial intelligence models for the estimation of dispersion coefficients on the basis of such data as the depth, width and curvature of the riverbed are created using such data (e.g.: Kashefipour *et al.*, 2002; Piotrowski, 2005; Piotrowski *et al.*, 2006; Rowiński *et al.*, 2005b; Tayfur & Singh, 2005).

However, the best source of information on the dispersion coefficients of the given river is still a tracer test. If there is no possibility to carry out the experiment, then using both the available data and empirical relations or models provided to determine the coefficients, we must always take into account both the conditions and the rivers for which they were created.

2.5 Solving 2D transport equation

The advection-diffusion transport equation (2.8) may be also presented, without loosing its general character, as:

$$\frac{\partial c}{\partial t} + v'_x \frac{\partial c}{\partial x} + v'_y \frac{\partial c}{\partial y} - D_{xx} \frac{\partial^2 c}{\partial x^2} - 2D_{xy} \frac{\partial^2 c}{\partial x \partial y} - D_{yy} \frac{\partial^2 c}{\partial y^2} = 0; \tag{2.13}$$

where in most cases one can assume: $v'_x = v_x, \quad v'_y = v_y$.

The equation can be effectively applied in the situation of constant depth of the channel and constant dispersion coefficients, or when the changes in depth and coefficients are insignificant. In case of significant variability in the x or y directions, the averaged components of the velocity in equation (2.13) should be replaced with the previously determined values (see Appendix A):

$$v'_x = v_x - \frac{1}{h} \frac{\partial (hD_{xx})}{\partial x} - \frac{1}{h} \frac{\partial (hD_{xy})}{\partial y},$$

and

$$v'_y = v_y - \frac{1}{h} \frac{\partial (hD_{yy})}{\partial y} - \frac{1}{h} \frac{\partial (hD_{xy})}{\partial x}. \tag{2.14}$$

The information concerning the dispersion coefficients, two-dimensional velocity field, the depth of the channel and the boundary and initial conditions is necessary to solve the two-dimensional transport equation. Unfortunately, in

natural flow conditions, the advection-diffusion equation (2.13) with real boundary and initial conditions does not have an analytical solution, and therefore, in practice, it has to be solved numerically. Such a problem appears for many issues in fluid mechanics. There are, of course, analytical solutions for individual flow conditions and boundary conditions as well as for specific geometries, but they have little application in practice. Suggestions for various analytical solutions for specific cases are presented, e.g. by Boczar (1980, 1991), Rutherford (1994) and Socolofsky & Jirka (2005).

In case of instantaneous release of pollutants (as the initial condition) and constant dispersion coefficients and constant velocity field in a rectangular channel of constant depth, the solution of the two-dimensional transport equation in situation where the axes of the coordinate system are parallel to the main flow directions can be written in the form of bivariate Gaussian distribution (Rutherford, 1994):

$$c(x,y,t) = M \frac{\exp\left[-\frac{(x-\mu_x)^2}{4\pi D_{xx} t}\right]}{\sqrt{4\pi D_{xx} t}} \frac{\exp\left[-\frac{(y-\mu_y)^2}{4\pi D_{yy} t}\right]}{\sqrt{4\pi D_{yy} t}}; \tag{2.15}$$

where:

(x_0, y_0) – release point;
$\mu_x = x_0 + v_x t$, $\mu_y = y_0 + v_y t$;
M – mass injected at point (x_0, y_0) and time $t = 0$.

The solution is true for an infinite domain (as the boundary conditions), far away from the banks, i.e. when the pollutant has not reached the walls of the channel.

For the equation with the off-diagonal dispersion tensor, with the same assumptions, we can analogically write:

$$c(x,y,t) = \frac{M}{4\pi t\sqrt{D}} \exp\left[-\frac{(x-\mu_x)^2}{4tD/D_{yy}} - \frac{(y-\mu_y)^2}{4tD/D_{xx}} + \frac{(x-\mu_x)(y-\mu_y)}{2tD/D_{xy}}\right]; \tag{2.16}$$

where:

$D = D_{xx}D_{yy} - D_{xy}^2$.

To write down the above analytical solution, a solution presented in the work of Smith (1992) was used. It was checked that the suggested solution meets the advection-diffusion equation given in the form (2.13). Example analytic

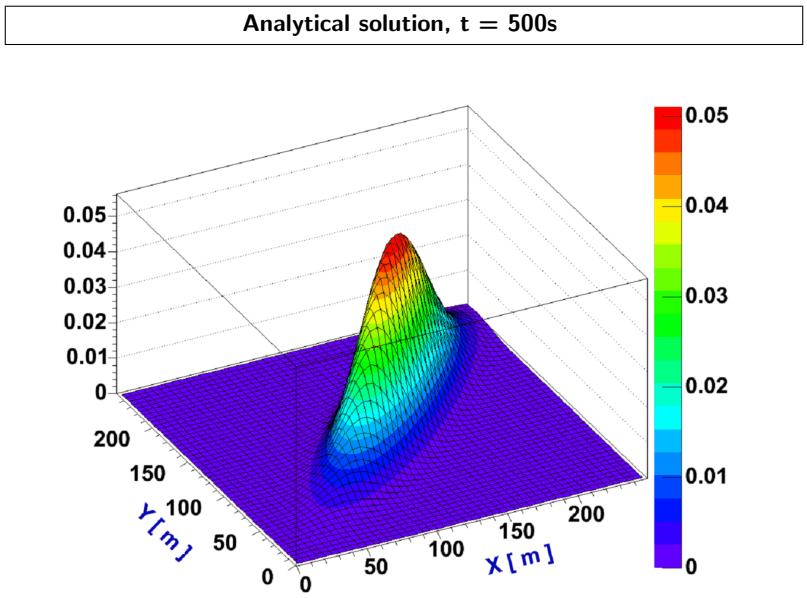

Figure 2.7: An example of an analytical solution (eq. 2.16) after time $t = 500\,\mathrm{s}$, for $v_x = v_y = 0.28\,\frac{\mathrm{m}}{\mathrm{s}}$, $D_{xx} = D_{yy} = 1.6\,\frac{\mathrm{m}^2}{\mathrm{s}}$, $D_{xy} = 1.4\,\frac{\mathrm{m}^2}{\mathrm{s}}$ and $M = 10\,\mathrm{a.u.}$ released at point $(x_0, y_0) = (0, 0)$ and time $t = 0\,\mathrm{s}$

solutions for selected values of velocity and the dispersion coefficients, in case of instantaneous discharge of mass equivalent to 10 arbitrary units, is presented in figure 2.7.

The analytical solutions presented above will be used further on in the book for verification of the numerical model, tests of numerical schemes, and also in analyses concerning the simplification of the off-diagonal dispersion tensor.

Chapter 3

Simplifications of Two-Dimensional Mass Transport Equation

3.1 Introduction

Transport of a substance dissolved in water is described, in general case, by a three-dimensional advection-diffusion equation. Solving such an equation, as mentioned in the previous chapter, requires a large amount of data which are difficult to obtain in the majority of real-life cases. Moreover, the calculation costs of a numerical solution for such an equation would be also large. Therefore, in practice, various kinds of simplifications are used, resulting in one- or two-dimensional equations by averaging the three-dimensional equation and/or omitting elements which seem to be small in comparison with others. In Chapter 2 it was demonstrated that in case of rivers and open channels whose depth is small in comparison with their length and width, the two-dimensional approach can be effectively applied to describe the transport of solute. The two-dimensional transport equation was written in its full form (2.8) and the simplified form (2.9). The simplified version can be applied if the main flow directions follow the axes of the coordinate system. Unfortunately, a very common practice is to use the easier to solve version (2.9) of the equation without the mixed derivatives, even if a complex geometry of a channel is under consideration. The approach accounting only for the diagonal components of the dispersion tensor, as pointed out by Sawicki (2003) for an analogical problem in case of turbulent diffusion tensor, may lead to results too far away from reality.

The resultant error is influenced by the geometry of the channel and the way in which the off-diagonal components of dispersion tensor were omitted. The tests presented in this chapter allow for comparison of errors and indicate when the individual simplifications can be applied. The analyses were carried out for two basic situations encountered in real-life conditions: instantaneous release (e.g. catastrophic release) or continuous inflow of pollutants (e.g. constant inflow of warm or hot water from cooling processes into reservoirs).

In case of the two-dimensional transport equation, the applied practice is to solve the equation in a curvelinear coordinate system, sometimes called the natural coordinate system (e.g.: Czernuszenko, 1987, 1990; Guan & Zhang, 2005; Holley & Jirka, 1986; Lau & Krishnappan, 1981; Manson *et al.*, 2002), where the dispersion tensor is always diagonal. The idea of the natural coordinate system is that the longitudinal coordinate axis approximately follows the meandering longitudinal direction of channel flow. Yet such an approach brings about problems of another kind, connected with the determination of coefficients describing the geometry of the channel, especially if we deal with a complex geometry. Those coefficients are the so-called metric coefficients introduced to correct for differences between distances along curved coordinate surfaces and those measured along the respective axes. Very often those coefficients are taken to be equal to unity which is far from being true, particularly in sharp bends or in wide meandering rivers. To avoid those problems, the traditional Cartesian coordinate system has been adopted in this study.

3.2 Determination of the dispersion tensor coefficients

From the data and empirical formulae available in the literature, or on the basis of experimental data, we obtain information on the longitudinal D_L and transverse D_T dispersion coefficient for a given river or channel. If it is impossible to direct the axes of the coordinate system along the main flow directions (see fig. 3.1) then, based on them, all the elements of the dispersion tensor have to be determined for each flow point (D_{xx}, D_{xy}, D_{yx}, D_{yy}), transforming the diagonal tensor $\mathbf{D_D}$ into the non-diagonal tensor $\mathbf{D}$:

$$\mathbf{D_D} = \begin{bmatrix} D_L & 0 \\ 0 & D_T \end{bmatrix} \longrightarrow \mathbf{D} = \begin{bmatrix} D_{xx} & D_{xy} \\ D_{yx} & D_{yy} \end{bmatrix}. \tag{3.1}$$

The correct way of determining those coefficients, which is the rotation of the tensor – ***Rotation*** for short, and the simplified methods of determining

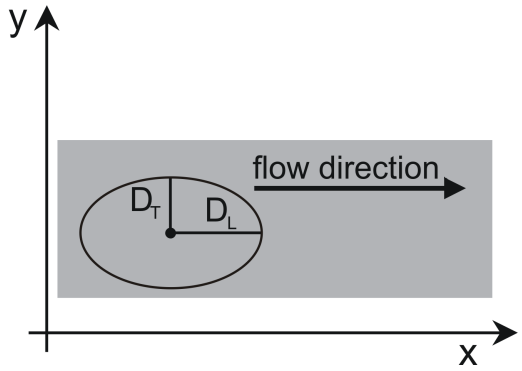

(a) x-axis of the coordinate system directed along the flow direction

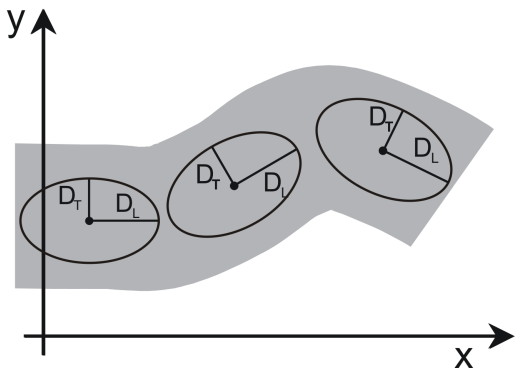

(b) x-axis of the coordinate system directed off the flow direction

Figure 3.1: Schematic representation of the dispersion tensor in the Cartesian coordinate system

elements D_{xx} and D_{yy} (without off-diagonal elements) conventionally called: ***Quasi rotation***, ***Identity transformation*** and ***Vector-like rotation*** are described below.

3.2.1 Rotation

$$\mathbf{D_D} = \begin{bmatrix} D_L & 0 \\ 0 & D_T \end{bmatrix} \xrightarrow{\text{TENSOR ROTATION}} \mathbf{D} = \begin{bmatrix} D_{xx} & D_{xy} \\ D_{yx} & D_{yy} \end{bmatrix} \tag{3.2}$$

The correct approach allowing for obtaining the full dispersion tensor $\mathbf{D}$ is the rotation of the diagonal tensor, $\mathbf{D_D}$ (fig. 3.2) by the angle created at a given point by the velocity (flow direction) vector with the x-axis of the coordinate system:

$$\mathbf{D} = \mathbf{R}(\alpha) \cdot \mathbf{D_D} \cdot \mathbf{R}^{-1}(\alpha)\,; \tag{3.3}$$

where:

$$\mathbf{R}(\alpha) = \begin{bmatrix} \cos\alpha & -\sin\alpha \\ \sin\alpha & \cos\alpha \end{bmatrix} \text{ – rotation matrix,}$$

α – the angle between the flow direction (velocity vector) and the x-axis in a given point.

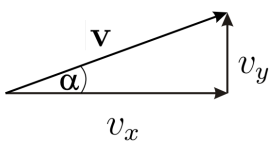

$$\sin\alpha = \frac{v_y}{|\mathbf{v}|} \qquad \cos\alpha = \frac{v_x}{|\mathbf{v}|}$$

The rotation of the tensor leads to the following relationships:

$$D_{xx} = D_T + D\frac{v_x^2}{v^2}\,, \qquad D_{xy} = D_{yx} = D\frac{|v_x v_y|}{v^2}\,, \qquad D_{yy} = D_T + D\frac{v_y^2}{v^2}\,; \tag{3.4}$$

where:

$$D = D_L - D_T\,, \quad v = \sqrt{v_x^2 + v_y^2}\,.$$

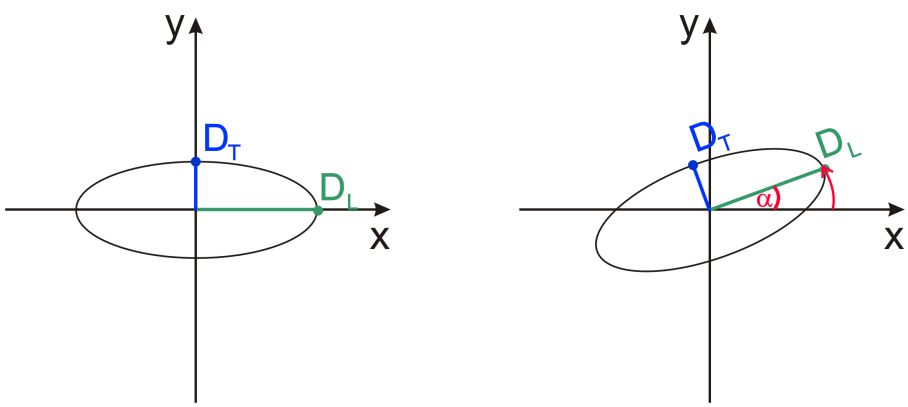

Figure 3.2: $\mathbf{D_D}$ tensor rotation by angle α

3.2.2 Quasi rotation

$$\mathbf{D_D} = \begin{bmatrix} D_L & 0 \\ 0 & D_T \end{bmatrix} \xrightarrow{\text{TENSOR ROTATION}} \mathbf{D} = \begin{bmatrix} D_{xx} & \cancel{D_{xy}} \\ \cancel{D_{yx}} & D_{yy} \end{bmatrix} \tag{3.5}$$

In this approach, the correct way of determining the components of the tensor is applied as defined by (3.3). In order for the resultant tensor to be diagonal, the off-diagonal elements are disregarded (it is arbitrarily assumed that they equal 0). Therefore, the tensor components are, respectively:

$$D_{xx} = D_T + D\frac{v_x^2}{v^2}\,, \qquad D_{xy} = D_{yx} = 0\,, \qquad D_{yy} = D_T + D\frac{v_y^2}{v^2}\,. \tag{3.6}$$

This simplification is met in situations when unwanted equation terms with mixed derivatives are disregarded – with the assumption that the off-diagonal elements of the dispersion tensor are very small. However, complex geometry of a channel often makes such an assumption impossible.

3.2.3 Vector-like rotation

$$\mathbf{D_V} = \begin{bmatrix} D_L \\ D_T \end{bmatrix} \xrightarrow{\text{VECTOR-LIKE ROTATION}} \mathbf{D} = \begin{bmatrix} D_{xx} \\ D_{yy} \end{bmatrix} \tag{3.7}$$

It is assumed that elements D_L and D_T create vector $\mathbf{D_V}$ (fig. 3.3). Coefficients D_{xx} and D_{yy} are obtained by rotating $\mathbf{D_V}$ according to the vector rotation rule (fig. 3.4) by the angle it creates at a given point by the velocity (flow direction) vector with the x-axis of the coordinate system:

$$\mathbf{D} = \mathbf{R}(\alpha) \cdot \mathbf{D_V}\,. \tag{3.8}$$

If, after rotation, the value of any component of the vector is negative, then its absolute value is to be taken into consideration. The values of the determined coefficients will be:

$$D_{xx} = \left| D_L\frac{v_x}{v} - D_T\frac{v_y}{v} \right|\,, \quad D_{xy} = D_{yx} = 0\,, \quad D_{yy} = \left| D_L\frac{v_y}{v} + D_T\frac{v_x}{v} \right|\,. \tag{3.9}$$

Such an approach is incorrect, because the matrix of dispersion coefficients makes a second-order tensor. This simplification is usually used unintentionally.

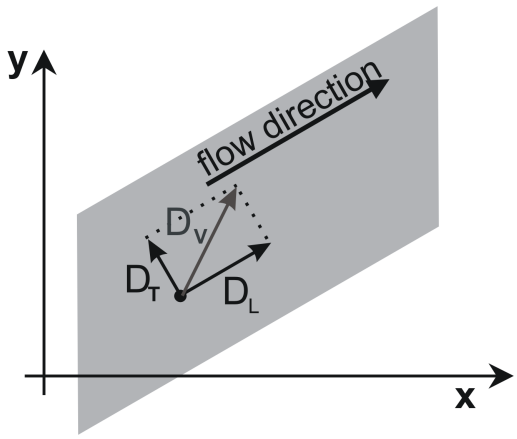

Figure 3.3: Diagram representation of $\mathbf{D_V} = [D_L, D_T]$ for a rectangular channel whose main axis is not parallel to the x-axis

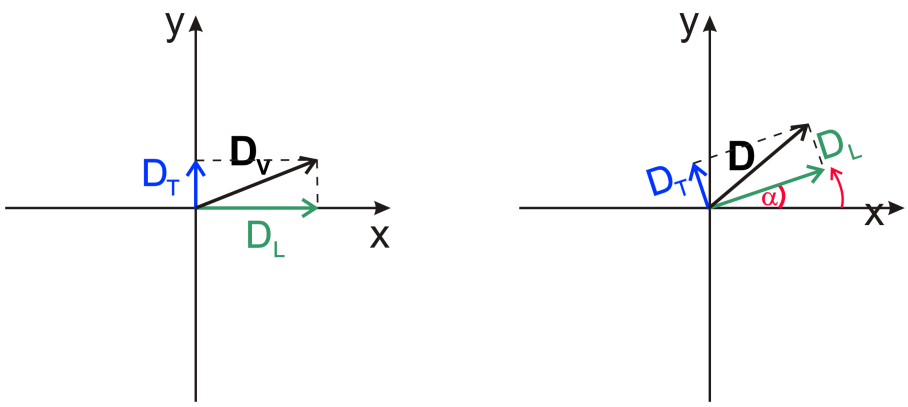

Figure 3.4: Vector $\mathbf{D_V}$ rotation by angle α

3.2.4 Identity transformation

$$\mathbf{D} = \begin{bmatrix} D_{xx} & D_{xy} \\ D_{yx} & D_{yy} \end{bmatrix} \quad \overset{\text{IDENTITY TRANSFORMATION}}{\equiv} \quad \mathbf{D_D} = \begin{bmatrix} D_L & 0 \\ 0 & D_T \end{bmatrix} \tag{3.10}$$

In this approach, we simply assume that the elements D_{xx} and D_{yy} are equal to longitudinal and transverse dispersion coefficients, respectively, without taking into consideration coefficients D_{xy} and D_{yx}:

$$D_{xx} = D_L\,, \qquad D_{xy} = D_{yx} = 0\,, \qquad D_{yy} = D_T\,. \tag{3.11}$$

It is the practice often applied in the literature on the subject, in many cases without the awareness of the consequences and the influence upon the obtained results.

Each of the simplifications described above introduces some error. Further considerations allow to determine and compare the values of the introduced error in situations equivalent to instantaneous and continuous release of solute.

In order to simplify the notation, the following symbols have been adopted for the charts presented in the further part of this book:

- *Rotation* – **R**,
- *Quasi rotation* – **Q**,
- *Identity transformation* – **T**,
- *Vector-like rotation* – **V**.

3.3 Computational tests

The tests for the methods described above were carried out for a broad rectangular channel whose axis formed various angles with the coordinate system. An area situated far away from the banks was taken into consideration for which analytical solution of the problem (eq. 2.16) is known. Figure 3.5 presents schematically the geometry in question. The analyses were carried out for a number of values of angle α within the range between 0 and 90 degrees. The calculations were performed with the use of the implemented **RivMix** computer program described in detail in Chapter 6. The Alternating Direction Implicit method (see Section 4.3.3), was used, which, as demonstrated in Chapter 5, was proven

to be an exact, stable and relatively fast method. All methods of determination of the dispersion tensor for various angles α, described in Section 3.2, were compared. In order to simplify the interpretation of the results, a uniform distribution of velocity of $|\mathbf{v}| = 0.15\,\frac{\mathrm{m}}{\mathrm{s}}$, was assumed, directed parallel to the axis of the channel. The depth of the channel was assumed constant. The parameters of simulation are presented in table 3.1.

Table 3.2 contains the values of dispersion coefficients D_{xx}, D_{xy} and D_{yy} obtained with the methods described above for the given $D_L = 0.75\,\frac{m^2}{s}$ and $D_T = 0.1\,\frac{m^2}{s}$. It can be observed that the differences between the coefficients are the smallest for angles close to 0 and 90 degrees. The exception is the *identity transformation*, for which the difference for the angle of 90 degrees is the biggest. The significant values of the off-diagonal dispersion coefficients for angles α close to 45 degrees in case of correct determination of the off-diagonal tensor coefficient (*rotation*) are also worth stressing. The dependency of the D_{xy} coefficient on the angle α was shown in figure 3.6. Particularly for the values of α close to 45°, D_{xy} is of the order of magnitude of D_L.

It also does matter whether the case in question relates to instantaneous

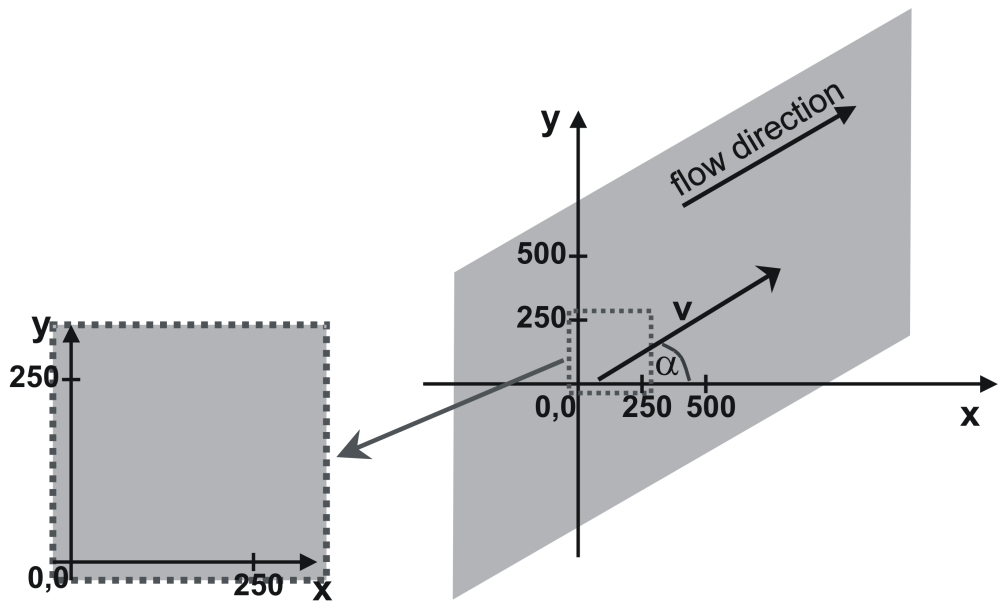

Figure 3.5: Scheme of straight, rectangular channel, used for computations

Table 3.1: Simulation parameters used in the numerical tests

Velocity components		Dispersion coefficient		Spatial steps		Time Steps
$v_x \left[\frac{\mathrm{m}}{\mathrm{s}}\right]$	$v_y \left[\frac{\mathrm{m}}{\mathrm{s}}\right]$	$D_L \left[\frac{\mathrm{m}^2}{\mathrm{s}}\right]$	$D_T \left[\frac{\mathrm{m}^2}{\mathrm{s}}\right]$	$\Delta x[\mathrm{m}]$	$\Delta y[\mathrm{m}]$	$\Delta t[\mathrm{s}]$
$0.15\cos\alpha$	$0.15\sin\alpha$	0.75	0.1	1	1	1

Table 3.2: Dispersion coefficients (in $\frac{\mathrm{m}^2}{\mathrm{s}}$) calculated for various α on the basis of the considered methods

	Method of determination of the dispersion tensor											
	Rotation			Quasi rotation			Vector-like rotation			Identity transformation		
α	D_{xx}	D_{xy}	D_{yy}	D_{xx}	D_{xy}	D_{yy}	D_{xx}	D_{xy}	D_{yy}	D_{xx}	D_{xy}	D_{yy}
0°	0.75	0	0.1	0.75	0	0.1	0.75	0	0.1	0.75	0	0.1
5°	0.745	0.056	0.105	0.745	0	0.105	0.738	0	0.165	0.75	0	0.1
10°	0.730	0.111	0.119	0.730	0	0.119	0.721	0	0.229	0.75	0	0.1
15°	0.706	0.162	0.143	0.706	0	0.143	0.698	0	0.290	0.75	0	0.1
30°	0.587	0.281	0.262	0.587	0	0.262	0.599	0	0.461	0.75	0	0.1
45°	0.425	0.325	0.425	0.425	0	0.425	0.460	0	0.601	0.75	0	0.1
60°	0.262	0.281	0.587	0.262	0	0.587	0.288	0	0.699	0.75	0	0.1
90°	0.1	0	0.75	0.1	0	0.75	0.1	0	0.75	0.75	0	0.1

– calculations were made for $D_L = 0.75\,\frac{\mathrm{m}^2}{\mathrm{s}}$ and $D_T = 0.1\,\frac{\mathrm{m}^2}{\mathrm{s}}$
– values were rounded off to the nearest thousandth

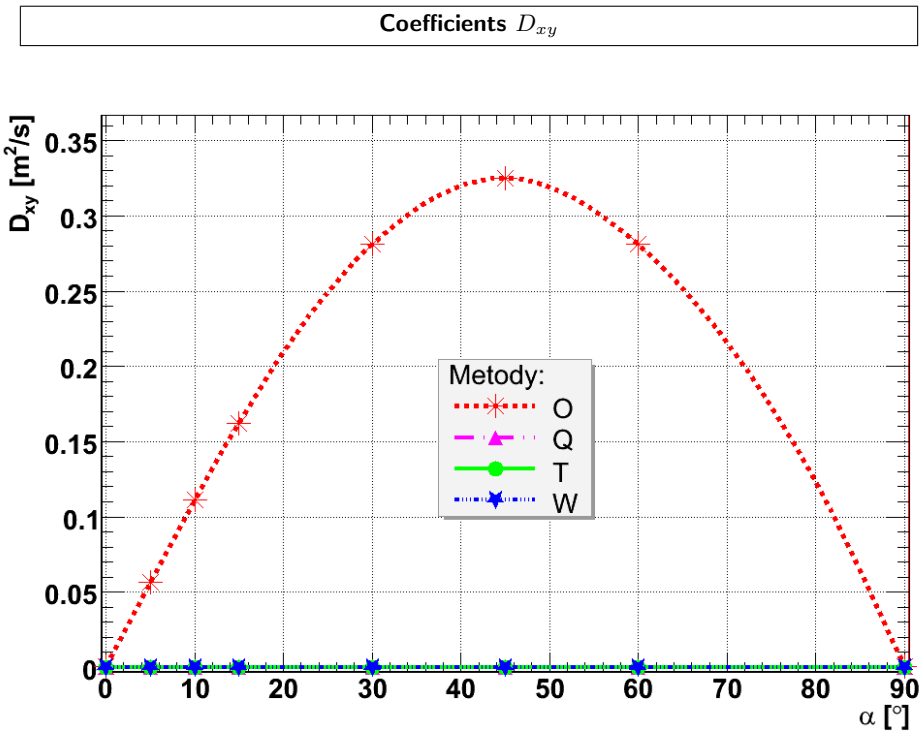

Figure 3.6: Dependence of the D_{xy} coefficient on the angle α for the considered methods; $D_L = 0.75\,\frac{\mathrm{m}^2}{\mathrm{s}}$ and $D_T = 0.1\,\frac{\mathrm{m}^2}{\mathrm{s}}$

or continuous discharge of solute. Therefore, the two cases were analysed separately below.

3.3.1 Instantaneous release of solute

The two-dimensional mass transport equation (2.13) with the initial conditions set by the Dirac delta describes a situation equivalent to instantaneous release of solute. By the moment of reaching the banks of the channel by the substance, the distribution of concentration at time t after the discharge can be determined using the analytical solution given by equation (2.16). In the considered situation the discharge of mass $M = 10$ a.u. took place at point $x_0 = 50\,\mathrm{m}$, $y_0 = 50\,\mathrm{m}$. To avoid the errors resulting from a large gradient of concentration on the computational grid, the analytical solution after 200 seconds was used as the initial condition in the tests ($t_0 = 200$ s). Unwanted oscillations appear in the numerical solution if the initial concentration distribution (at the time

$t_0 = 0$ s) was given by Dirac delta. Below the numerical solutions with the application of each discussed method of determination of the dispersion tensor are discussed.

The solutions for angle $\alpha = 45°$ after 400 steps of simulation are presented in figures 3.8, 3.10, 3.12 and 3.14. The obtained results can be compared with the exact analytical solution (fig. 3.7) equivalent to them. The errors (differences between the numerical and analytical solutions) for each of the considered methods are presented in figures 3.9, 3.11, 3.13 and 3.15.

It is difficult to notice a difference between the distributions of concentrations presenting the analytical solution (fig. 3.7) and the numerical solution by means of *rotation* method (fig. 3.8). The maximum difference is of order of 10^{-6} (see fig. 3.9). In case of other methods the difference is conspicuous both in the shape of distribution of concentrations and in the obtained values. Figures 3.8 – 3.15 illustrate the most extreme situation for angle $\alpha = 45°$, when the divergences between the methods in question are the most visible. The values "*Mean x*" and "*Mean y*" marked in the charts denote the location of maximum concentration in the given area (its value is represented by the "*Max*" variable). The value "*Integral*" represents the total mass present in the area shown in the chart. In case of *vector-like rotation* and *identity transformation* it is smaller than the initial 10 arbitrary units. It means that a part

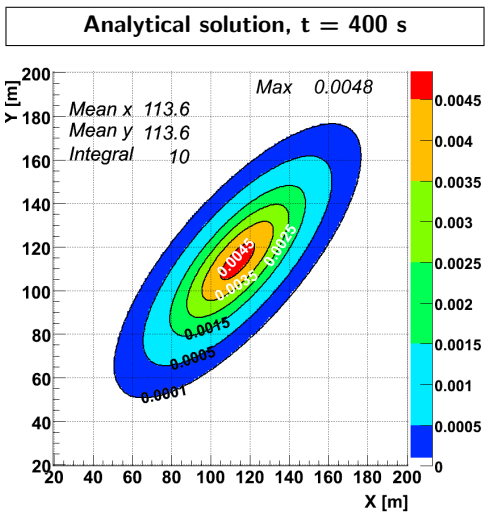

Figure 3.7: Analytical solution for the pulse release of the substance after 400 seconds from t_0

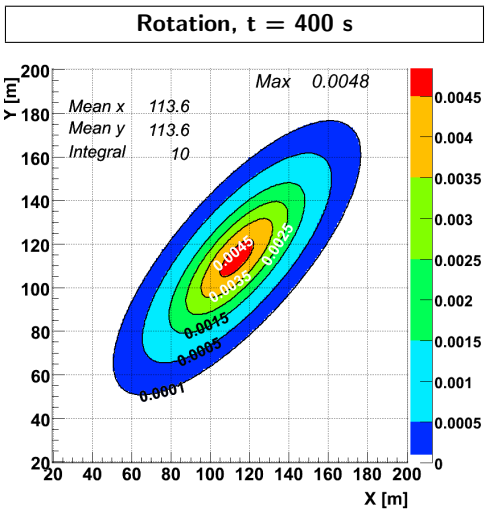

Figure 3.8: Numerical solution by means of full tensor *rotation* method for the pulse release after 400 time steps, $\alpha = 45°$

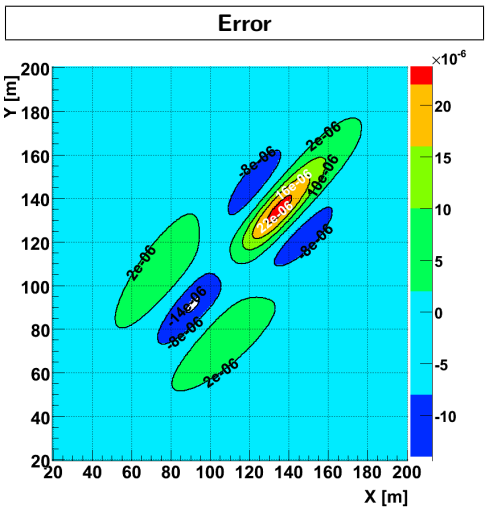

Figure 3.9: Difference between the analytical and numerical (*rotation*) solutions, for the pulse release after 400 time steps, $\alpha = 45°$

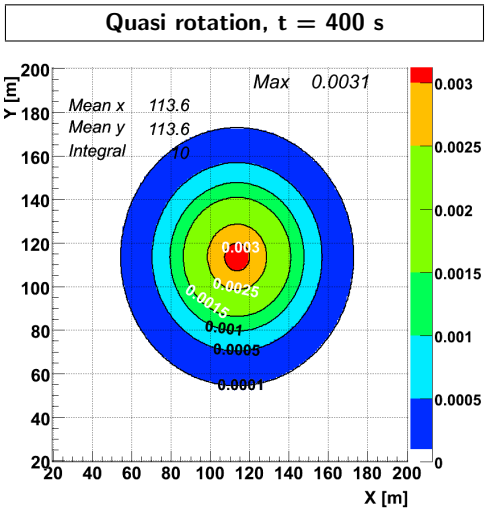

Figure 3.10: Numerical solution by means of *quasi rotation* method for the pulse release after 400 time steps, $\alpha = 45°$

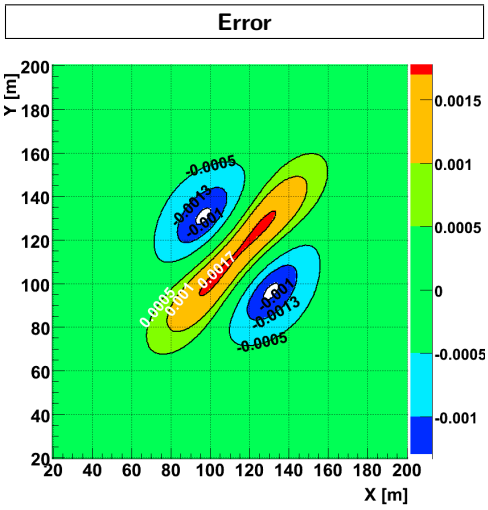

Figure 3.11: Difference between the analytical and numerical (*quasi rotation*) solutions, for the pulse release after 400 time steps, $\alpha = 45°$

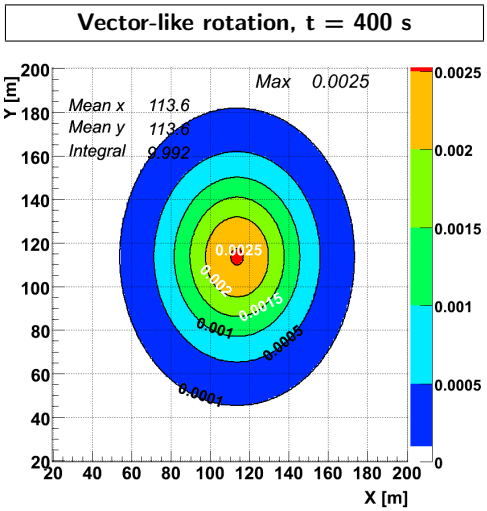

Figure 3.12: Numerical solution by means of *vector-like rotation* method for the pulse release after 400 time steps, $\alpha = 45°$

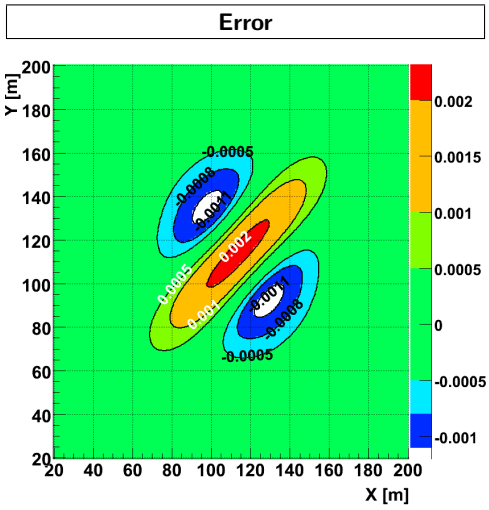

Figure 3.13: Difference between the analytical and numerical (*vector-like rotation*) solutions, for the pulse release after 400 time steps, $\alpha = 45°$

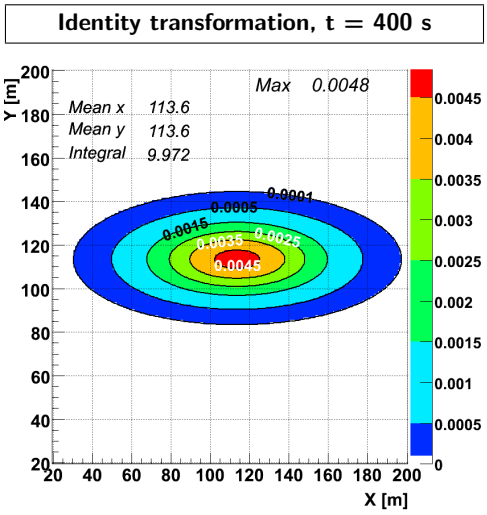

Figure 3.14: Numerical solution by means of *identity transformation* method for the pulse release after 400 time steps, $\alpha = 45°$

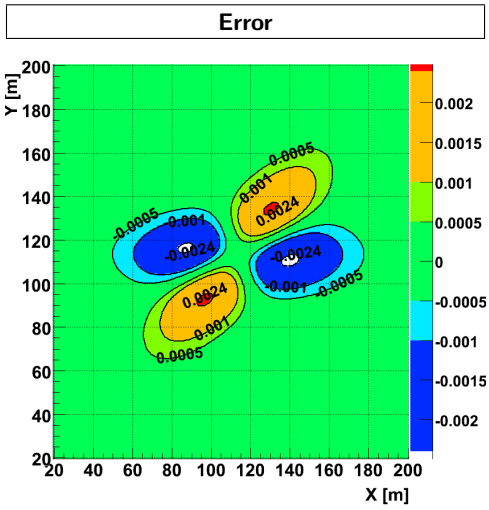

Figure 3.15: Difference between the analytical and numerical (*identity transformation*) solutions, for the pulse release after 400 time steps, $\alpha = 45°$

of small values of concentration lies outside the area presented in the charts. Distributions of concentrations for other angles (0°, 5°, 15°, 30°, 60°, 90°) can be found in Appendix C.

All methods lead to a result identical to that obtained analytically in case when the angle α is equal to 0 or 90 degrees (except for *identity transformation* for the angle of 90 degrees). For all the remaining angles ($0° < \alpha < 90°$) only the *rotation* of the tensor, taking into account the off-diagonal elements gives the same results as the analytical solution. The difference between the numerical solution and the analytical one depends both on the selected method to determine the tensor and the angle α. The maximum values of the obtained errors (Δc) after 400 seconds of simulation as a function of the angle α are presented in figure 3.16.

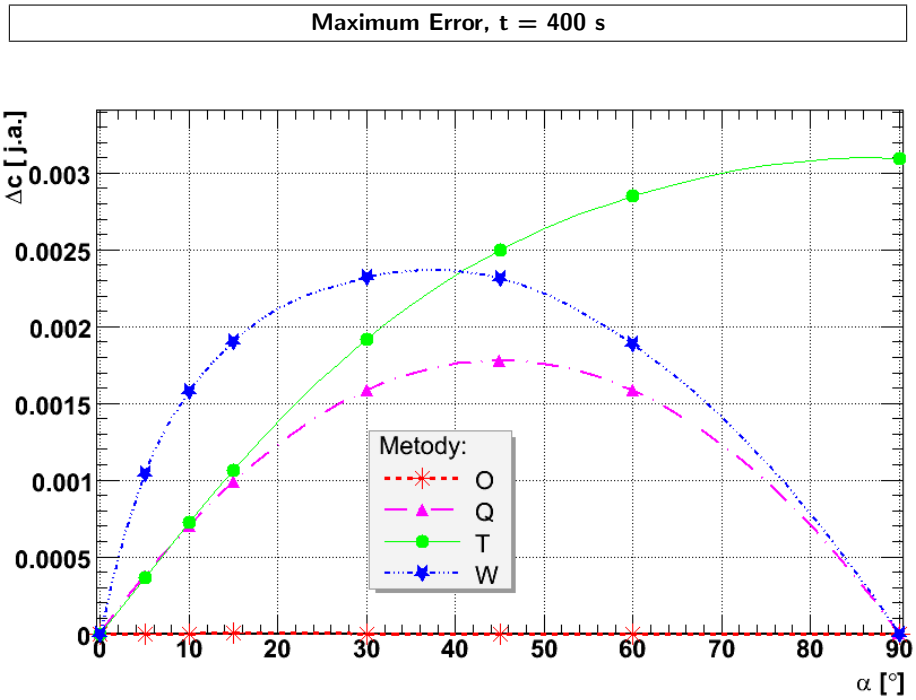

Figure 3.16: Maximum difference (Δc) between the analytical and the numerical solutions for the discussed methods of determining the dispersion tensor after 400 seconds of simulation in case of pulse release; the difference is plotted as a function of angle α

In case of *identity transformation* the error grows with growing the value of angle α. For *quasi rotation* the error is symmetrical against the 45 degrees angle and decreases when the angle gets close to 0 or 90 degrees. *Vector-like rotation* causes large differences in the solutions and they significantly decrease when α approaches 0 or 90 degrees. In this case the maximum error occurs for the angle of $(45° - \beta)$, where β is the angle between the $D_V = [D_L, D_T]$ vector and the flow direction. For *vector-like rotation* in considered case, the maximum error will be obtained for the angle of ca. 38 degrees. In case of full tensor *rotation*, the maximum error is very small, of 10^{-5} – 10^{-6} order of magnitude. It is not visible in the presented figure 3.16.

In case of spreading of the pollutants in rivers and open channels, it is important to know the maximum concentration values for pollutants. This measure may be the key one in the decision making process in case of a possible contamination. Figure 3.17(a) shows the maximum concentration values (c_{max}) after 400 seconds of simulation, depending on the angle α. It is worth noting that the maximum of concentration distribution transfers correctly (in the same way as the maximum of the analytical solution) for all discussed methods, as indicated by the values describing its location: "*Mean x*" and "*Mean y*" (see figs. 3.8, 3.10, 3.14, 3.12 and 3.7). The maximum values, however, depend strongly on the selected method and the angle α. They are correctly defined by the *identity transformation* and *rotation*. The small discrepancies visible in zoomed view in figure 3.17(b) are a numerical effect. In case of *quasi rotation* and *vector-like rotation*, the maximum concentration value error may reach as much as 35.55% and 47.93%, respectively (see table 3.3). The error is defined as the difference between the maximum concentration value in analytical solution (c_{max}^{anal}) and the numerical one (c_{max}^{num}), and normalised to the first one (c_{max}^{anal}):

$$\frac{c_{max}^{anal} - c_{max}^{num}}{c_{max}^{anal}},$$

where the maximum value in case of analytical solution in considered situation was $c_{max}^{anal} = 0.00484$ a.u. (see fig. 3.7).

Observations demonstrate that if in the discussed situation the information on the maximum concentration is the most important one, then solving the simplified equation (2.8) with *identity transformation* we will obtain equally good results as in case of solving the full transport equation (2.9) with *rotation*. It must be kept in mind, however, that simplified methods do not allow to obtain correct forms of concentration distributions.

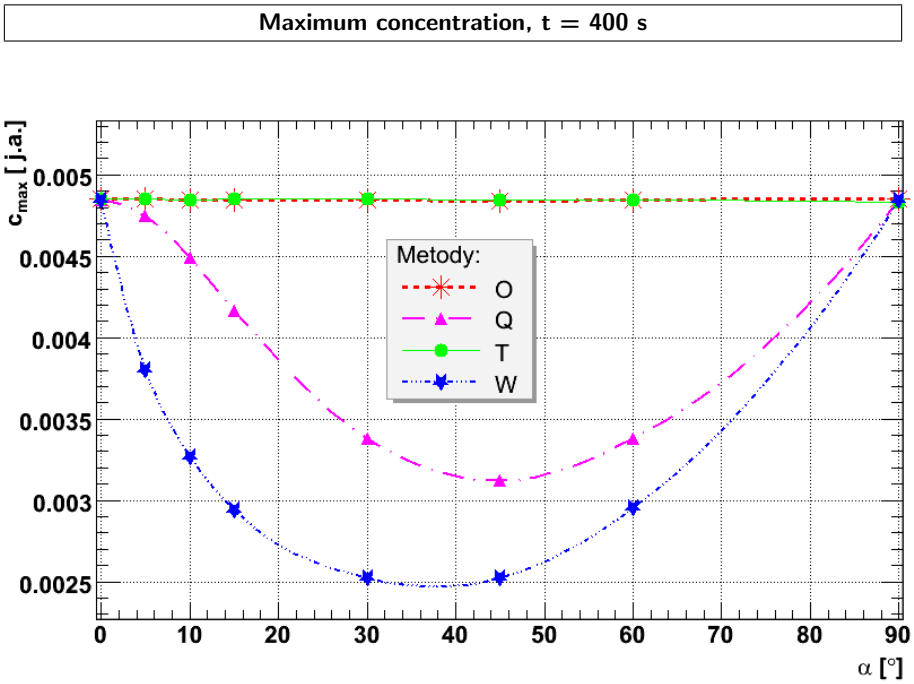

(a)

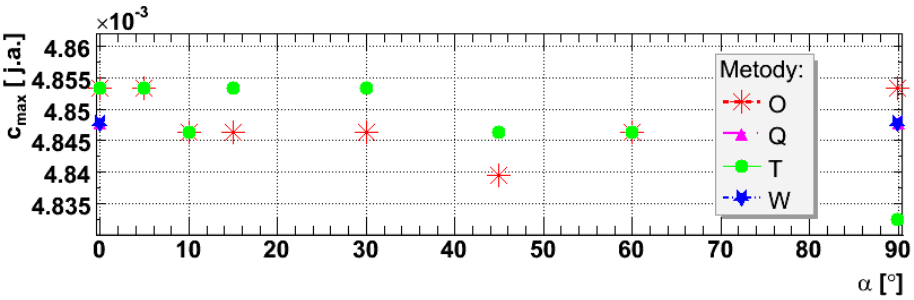

(b) Zoom on the area visible on chart (a) from $c_{max} = 0.00483$ a.u. to $c_{max} = 0.00486$ a.u.

Figure 3.17: Maximum concentration (c_{max}) after 400 seconds of simulation, depending on the angle α in case of pulse release

Table 3.3: Maximum concentration value error expressed in percents defined as $(c_{max}^{anal} - c_{max}^{num})/c_{max}^{anal}$, where c_{max}^{anal} is the maximum concentration value in the analytical solution, and c_{max}^{num} in the numerical one; maximum errors for individual methods are in bold, and the highest obtained errors are underlined

α	Rotation	Quasi rotation	Vector-like rotation	Identity transformation
0°	0.10 %	0.10%	0.10%	**0.10 %**
5°	0.07%	1.99%	21.50%	0.07%
10°	0.05%	7.30%	32.54%	0.05%
15°	0.04%	13.93%	39.19%	0.09%
30°	0.06%	30.24%	**47.93 %**	0.07%
45°	**0.11 %**	**35.55%**	47.89%	0.01%
60°	0.06%	30.24%	39.01%	0.04%

3.3.2 Continuous inflow of solute

In case of continuous inflow of solute, the initial and boundary conditions were set in such a way as to obtain continuous inflow of solute with the discharge of 1 arbitrary unit per second. The source was situated at point $x_0 = 100\,\mathrm{m}$, $y_0 = 100\,\mathrm{m}$. In the discussed situation, it is not easy to obtain an analytic solution, and therefore all simplified methods of determination of the tensor were compared with the correct method, that is the *rotation*. Below, like in the case of instantaneous release, the results for the most extreme situation are presented, when the angle α is equal to 45 degrees. Figures 3.18, 3.19, 3.21, 3.23 illustrate numerical solutions after 1000 seconds since the commencement of continuous discharge. It is easy to notice that the simplified methods cause bigger "spread" of the patch of pollutants. In case of *identity transformation* the distribution of concentration is additionally strongly sloped towards the right-hand bank (see fig. 3.23). Figures 3.20, 3.22 and 3.24 present the differences between the solutions obtained with the application of the *rotation* method and the solutions obtained with the application of individual simplified methods.

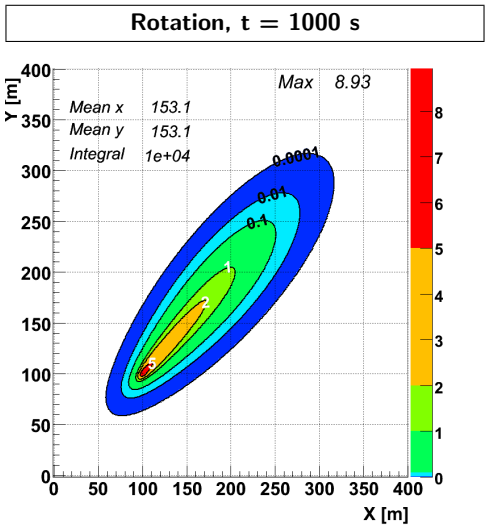

Figure 3.18: Numerical solution by means of *rotation* method for the continuous release after 1000 time steps, $\alpha = 45°$

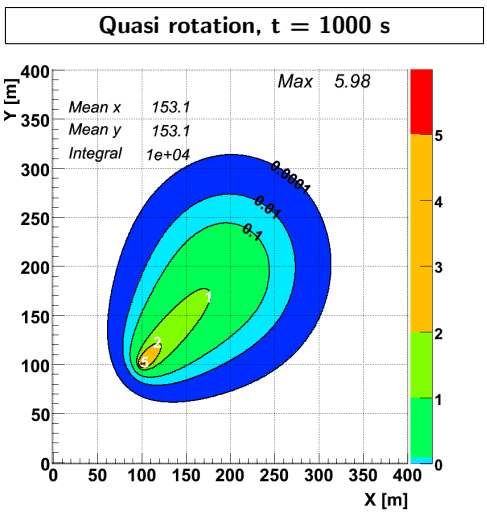

Figure 3.19: Numerical solution by means of *quasi rotation* method for the continuous release after 1000 time steps, $\alpha = 45°$

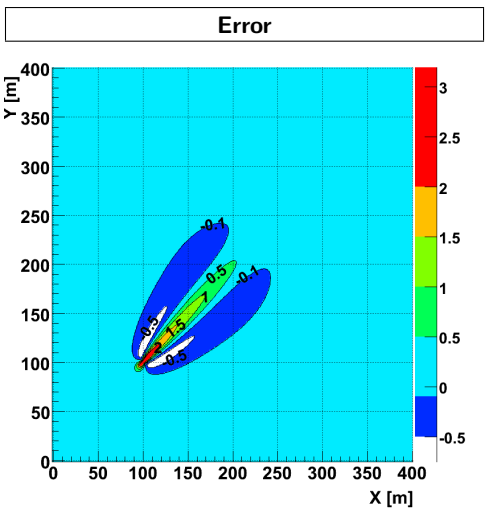

Figure 3.20: Difference between the solution by means of *rotation* and the solution by means of *quasi rotation*, after 1000 time steps, $\alpha = 45°$

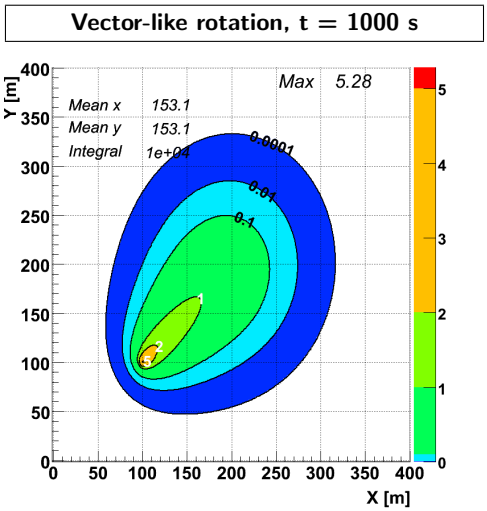

Figure 3.21: Numerical solution by means of *vector-like rotation* method for the continuous release after 1000 time steps, $\alpha = 45°$

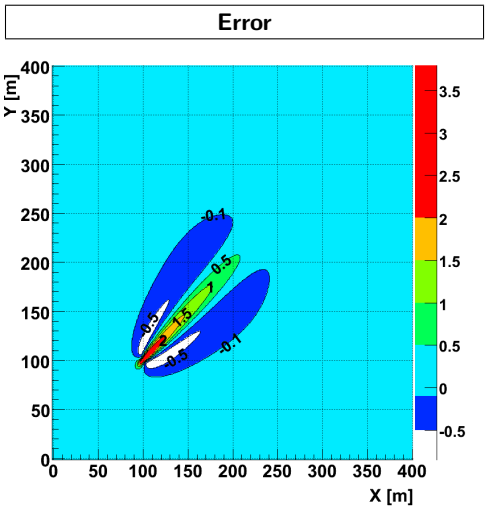

Figure 3.22: Difference between the solution by means of *rotation* and the solution by means of *vector-like rotation*, after 1000 time steps, $\alpha = 45°$

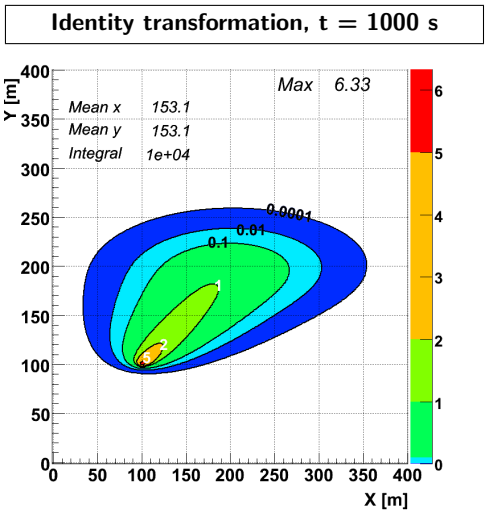

Figure 3.23: Numerical solution by means of *identity transformation* method for the continuous release after 1000 time steps, $\alpha = 45°$

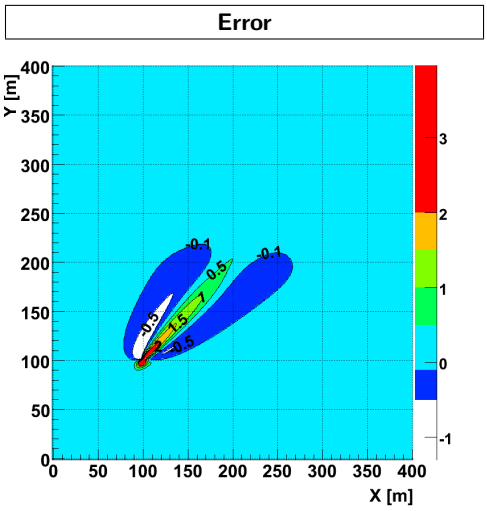

Figure 3.24: Difference between the solution by means of *rotation* and the solution by means of *identity transformation*, after 1000 time steps, $\alpha = 45°$

The maximum difference (Δc) in the function of the angle α is presented in figure 3.25. The results are similar to those of instantaneous release.

Considering the values of maximum concentration ("*Max*" value in figures 3.18, 3.19, 3.21, and 3.23), the variations between the individual methods are clearly visible. Figure 3.26 shows the values of maximum concentration (c_{max}) as functions of the angle α. All the methods predict the proper value of maximum concentration for the angle of 0 and 90 degrees, except for the *identity transformation* in case of $\alpha = 90°$. *Identity transformation* method, unlike in case of instantaneous discharge, wrongly shows the maximum values for all the angles $\alpha > 0°$.

The difference between the obtained value and the correct value increases together with the angle α. In case of *quasi rotation* and *vector-like rotation*, the dependency of maximum concentration on the angle behaves analogically

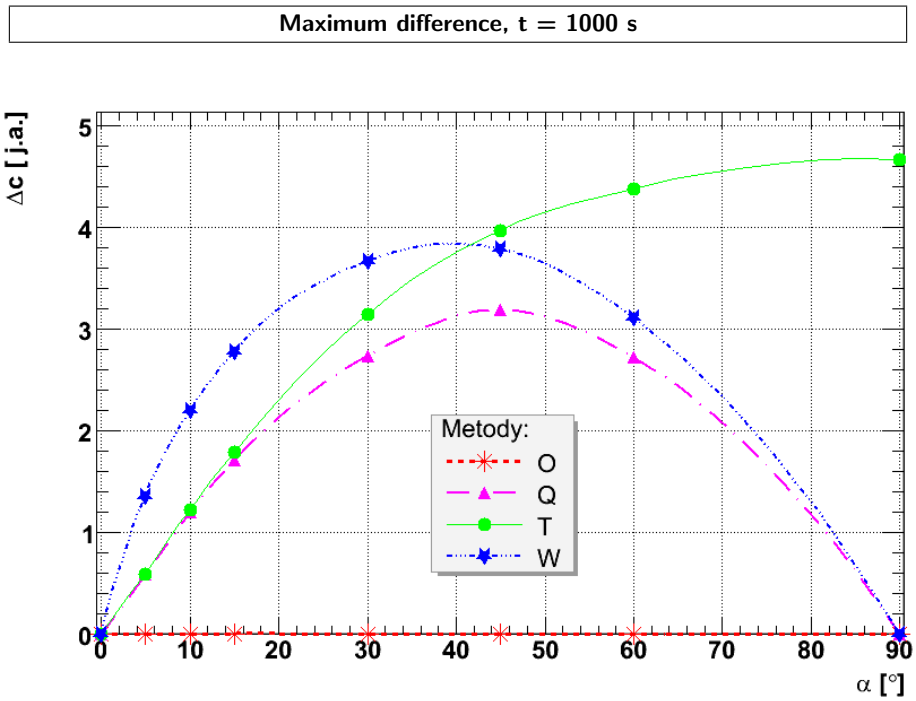

Figure 3.25: Maximum difference (Δc) between the tensor rotation and the other discussed methods of determining the dispersion tensor after 1000 seconds of simulation in case of continuous release; the difference is plotted as a function of the angle α

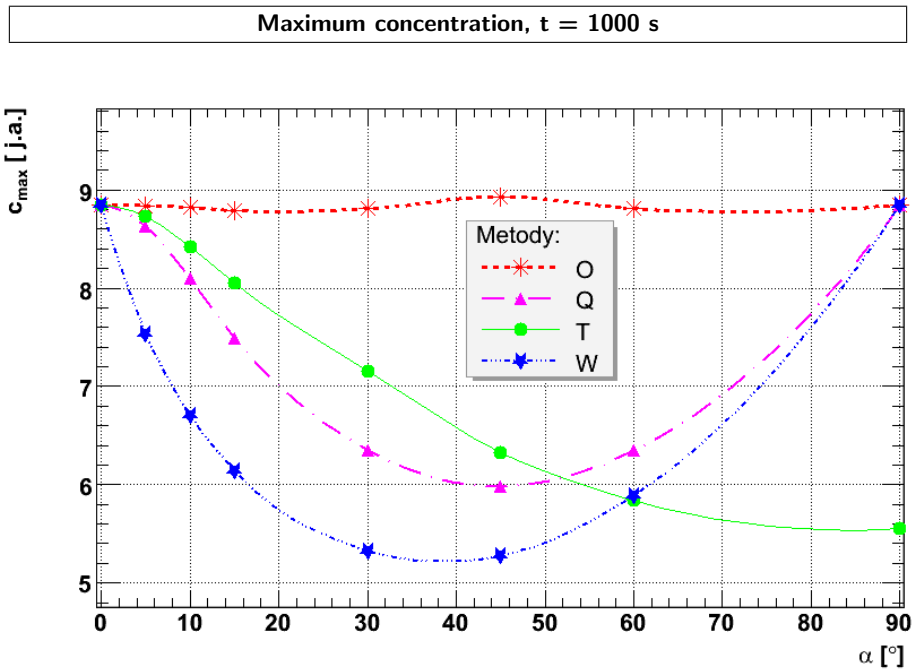

Figure 3.26: Maximum concentration (c_{max}) after 1000 seconds of simulation, depending on the angle α in case of continuous release

to the case of pulse release. Small oscillations of the maximum value visible in case of tensor *rotation* are connected with the method of discretization of the concentration values on the rectangular grid. Each method causes the maximum concentration stabilizes at a different level (fig. 3.27). For the angle of 0 degrees (fig. 3.27(a)) we obtain the same correct values for all methods. For other angles (figs. 3.27(b) – 3.27(f)) the maximum concentration values of the admixture are different and closely depend on the methods applied. The visible differences are the biggest for the angle of 45 degrees (fig. 3.27(d)). The charts demonstrate that in case of continuous release of pollutants, the application of simplified methods causes greater dispersion of the pollutants cloud and by the same, significant lowering of maximum concentration values.

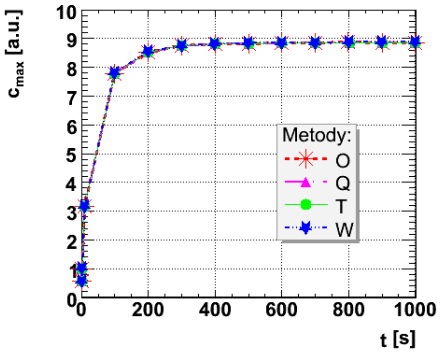

(a) $\alpha = 0°$

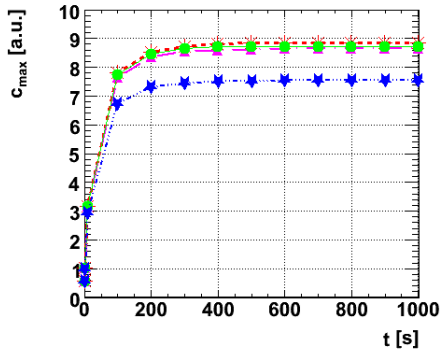

(b) $\alpha = 5°$

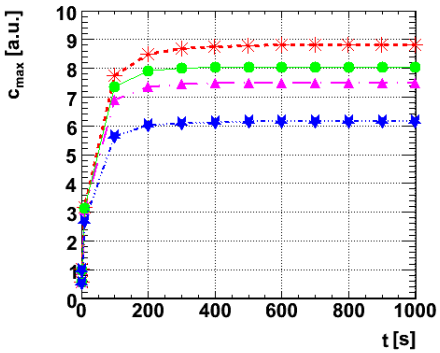

(c) $\alpha = 15°$

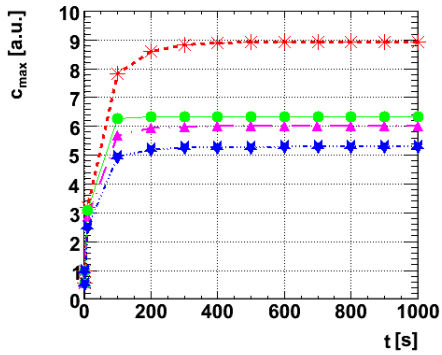

(d) $\alpha = 45°$

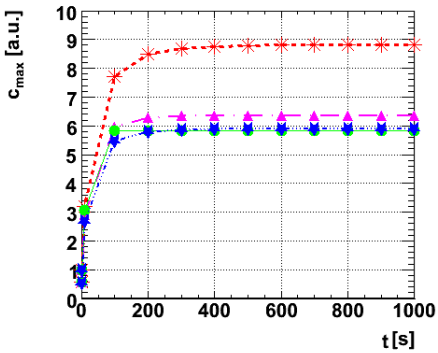

(e) $\alpha = 60°$

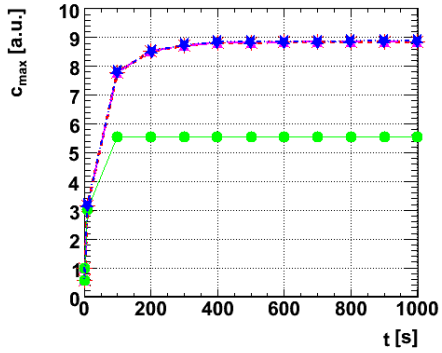

(f) $\alpha = 90°$

Figure 3.27: Maximum concentration values during the simulation of continuous release for various angles α

Chapter 4

Numerical Methods of Solving Two-Dimensional Mass Transport Equation

4.1 Introduction

In natural flow conditions, the transport equation (2.8), with appropriate boundary and initial conditions does not have an analytical solution and has, therefore, to be solved numerically. The development of research concerning transport processes in open channels, and still expanding computational possibilities result in the growth of demands concerning the exactness and effectiveness of solutions, and what follows, continuous need for new and better numerical schemes whose accuracy, stability and speed we are able to determine.

Looking for numerical solutions of partial differential equations, we can specify three basic approaches consisting in transformation of a continuous area, where we are looking for solution, into a discrete area. These are:

- Finite Difference Method (**FDM**),
- Finite Element Method (**FEM**),
- Finite Volume Method (**FVM**).

Finally, we obtain an equation or a system of linear algebraic equations and after solving them we get the information on the searched values in the nodes of the grid. Description of all methods and differences between them could be found, e.g. in (Chung, 2002). In case of open channels, the approaches with

the application of Finite Difference Method and Finite Element Method prevail. The description of the finite element method in application to advection-diffusion equations can be found in (Gresho & Sani, 2000).

The subject of considerations in this book is the Finite Difference Method, the simplest in concept, and what follows – often appropriate. The review of the finite difference methods in application to the one-dimensional advection-diffusion equation was presented, for example, by Fletcher (1991); Islam & Chaudhry (1997); Szymkiewicz (2000); Wang & Hutter (2001). In the case of a two-dimensional equation (without mixed derivatives), various numerical methods are described by, for example, Noye & Tan (1989); Noye (1984).

4.2 Finite Difference Method

The Finite Difference Method was first proposed in the 1920-s by Thom (Thom & Apelt, 1961). It was then called ***square method***, and was later applied in many branches of science, including equations describing processes of transport of solutes in open channels.

The Finite Difference Method consists in direct replacement of a differential equation by an appropriate difference equation (differential operators are replaced with difference operators) whose solution gives an approximate solution to the differential equation (fig. 4.1). The continuous solution domain is replaced with a discrete domain (a one-dimensional case was presented in fig. 4.2), then individual partial derivatives are approximated with the application of the so-called ***difference quotients***. Those quotients result from the function expansion into Taylor series. If a function with one variable $c(x)$ is con-

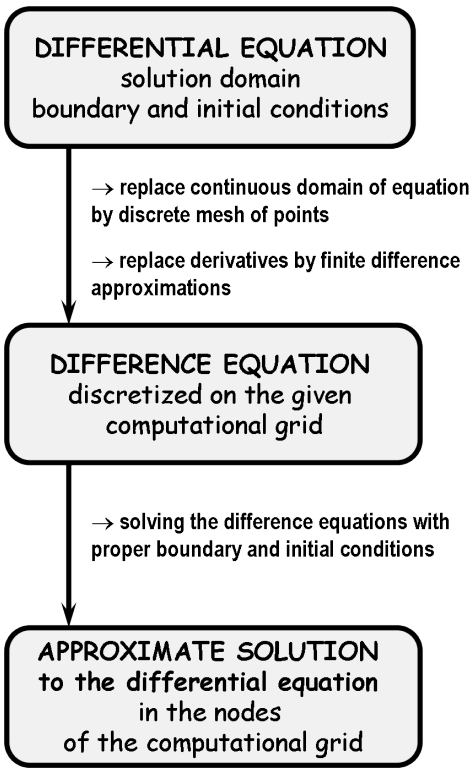

Figure 4.1: Diagram for solving partial differential equation by means of Finite Difference Method

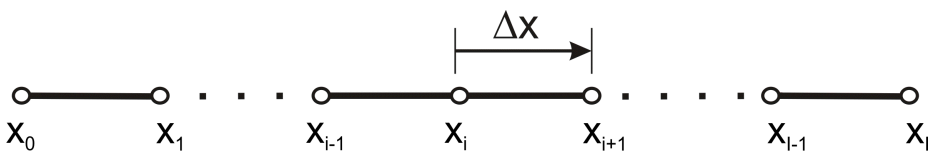

Figure 4.2: One-dimensional, homogenous discretization grid

tinuous and differentiable within the range $\langle x_i, x_i + \Delta x \rangle$, then such a function can be expanded into Taylor series (Bronsztejn & Siemiendiajew, 1997):

$$c(x_i + \Delta x) = c(x_i) + \Delta x \frac{\partial c}{\partial x}\Big|_{x_i} + \frac{\Delta x^2}{2}\frac{\partial^2 c}{\partial x^2}\Big|_{x_i} + \frac{\Delta x^3}{6}\frac{\partial^2 c}{\partial x^2}\Big|_{x_i} + \dots \quad . \tag{4.1}$$

The value of the continuous first derivative $\frac{\partial c}{\partial x}$ in the i-th node of the grid can be approximated by:

- forward difference quotient:

$$\frac{\partial c}{\partial x} = \frac{c_{i+1} - c_i}{\Delta x} + O(\Delta x), \quad (4.2)$$

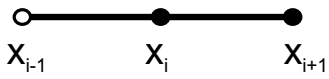

- backward difference quotient:

$$\frac{\partial c}{\partial x} = \frac{c_i - c_{i-1}}{\Delta x} + O(\Delta x), \quad (4.3)$$

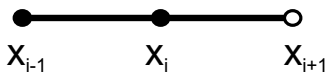

- central difference quotient

$$\frac{\partial c}{\partial x} = \frac{c_{i+1} - c_{i-1}}{2\Delta x} + O(\Delta x^2), \quad (4.4)$$

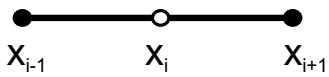

where:

O – denotes order of approximation accuracy;

c_{i-1}, c_i, c_{i+1} – concentration values in points x_{i-1}, x_i, x_{i+1}, respectively.

Table 4.1: Difference quotients applied for the approximation of the first and the second derivative; tables from (a) through (e) include coefficients at the concentration values in the prescribed grid nodes in case of approximation with the following difference quotients: (a) and (c) – forward, (b) and (d) – backward, (e) – central

(a) Forward approximation $O(\Delta x)$

	c_i	c_{i+1}	c_{i+2}
$\Delta x \frac{\partial c}{\partial x}$	-1	1	–
$\Delta x^2 \frac{\partial^2 c}{\partial x^2}$	1	-2	1

(b) Backward approximation $O(\Delta x)$

	c_{i-2}	c_{i-1}	c_i
$\Delta x \frac{\partial c}{\partial x}$	–	1	-1
$\Delta x^2 \frac{\partial^2 c}{\partial x^2}$	1	-2	1

(c) Forward approximation $O(\Delta x^2)$

	c_i	c_{i+1}	c_{i+2}	c_{i+3}
$2\Delta x \frac{\partial c}{\partial x}$	-3	4	-1	–
$\Delta x^2 \frac{\partial^2 c}{\partial x^2}$	2	-5	4	-1

(d) Backward approximation $O(\Delta x^2)$

	c_{i-3}	c_{i-2}	c_{i-1}	c_i
$2\Delta x \frac{\partial c}{\partial x}$	–	1	-4	3
$\Delta x^2 \frac{\partial^2 c}{\partial x^2}$	-1	4	-5	2

(e) Central approximation $O(\Delta x^2)$

	c_{i-1}	c_i	c_{i+1}
$2\Delta x \frac{\partial c}{\partial x}$	-1	0	1
$\Delta x^2 \frac{\partial^2 c}{\partial x^2}$	1	-2	1

The approximation order is connected with the so-called ***truncation error*** in series expansion, occurring during the creation of difference quotients. It can be seen that in case of backward and forward difference quotients (for $\Delta x \to 0$) the error decreases in a linear way with Δx. In case of central quotient, the truncation error decreases with Δx^2. Analogically, the second derivative can be approximated in different ways (see table 4.1). The details concerning the creation of difference quotients can be found in works by, e.g. (Fletcher, 1991; Peyret & Taylor, 1986; Szymkiewicz, 2000, 2003). All difference quotients used in this study are collected in table B.1 in Appendix B.

After the approximation of all partial derivatives, a set of difference equations is obtained, which with appropriate discrete boundary conditions should be solved for the computational grid parameters selected in such a way as to provide for the necessary accuracy and stability as well as possibly low computation costs. The final effect will be an approximate solution to the initial differential equation in the nodes of the given grid. In the study, a rectangular discretization grid on (x, y) plane was used, with the mesh size of $\Delta x \times \Delta y$ (see fig. 4.3).

4.3 Discretization of 2D transport equation

Using a rectangular grid on (x, y) plane (schematically presented on fig. 4.3) we can approximate the partial differential equation (2.13) in the general case by

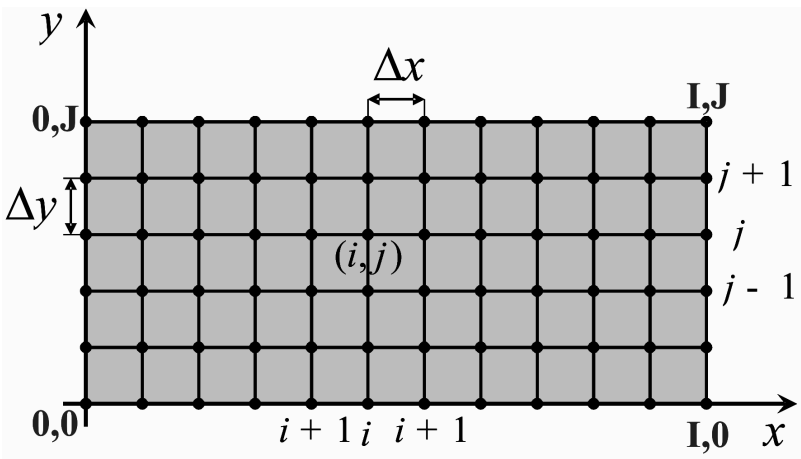

Figure 4.3: Rectangular discretization grid of Δx and Δy unit size on the (x, y) plane

means of the difference equation:

$$\begin{aligned}\frac{c_{i,j}^{n+1}-c_{i,j}^{n}}{\Delta t} &= D_{xx}\left[(1-\theta)\,\delta_x^2 c_{i,j}^{n}+\theta\delta_x^2 c_{i,j}^{n+1}\right]+D_{yy}\left[(1-\theta)\,\delta_y^2 c_{i,j}^{n}+\theta\delta_y^2 c_{i,j}^{n+1}\right]\\ &\quad+2D_{xy}\left[(1-\theta)\,\delta_{xy} c_{i,j}^{n}+\theta\delta_{xy} c_{i,j}^{n+1}\right]\\ &\quad-v_x\left[(1-\theta)\,\Delta_x c_{i,j}^{n}+\theta\Delta_x c_{i,j}^{n+1}\right]-v_y\left[(1-\theta)\,\Delta_y c_{i,j}^{n}+\theta\Delta_y c_{i,j}^{n+1}\right];\end{aligned} \tag{4.5}$$

where:

$\Delta x, \Delta y$ – grid spacing,
Δt – time step,
$\theta \in \langle 0, 1\rangle$ – weighting parameter,
$\delta_x^2 c_{i,j}$, $\delta_y^2 c_{i,j}$, $\delta_{xy} c_{i,j}$, $\Delta_x c_{i,j}$, $\Delta_y c_{i,j}$ – difference operators.

Difference operators for the second-order spatial derivatives have the following form:

$$\delta_x^2 c_{i,j} = \frac{c_{i-1,j}-2c_{i,j}+c_{i+1,j}}{\Delta x^2}, \qquad \delta_y^2 c_{i,j} = \frac{c_{i,j-1}-2c_{i,j}+c_{i,j+1}}{\Delta y^2}. \tag{4.6a}$$

The mixed derivatives and first-order spatial derivatives are discretized as:

$$\delta_{xy} c_{i,j} = \frac{c_{i+1,j+1}-c_{i+1,j-1}-c_{i-1,j+1}+c_{i-1,j-1}}{4\Delta x\Delta y}, \tag{4.6b}$$

$$\begin{aligned}\Delta_x c_{i,j} &= \frac{(1-\alpha_1)c_{i,j}+\alpha_1 c_{i+1,j}-(1-\alpha_1)c_{i-1,j}-\alpha_1 c_{i,j}}{\Delta x},\\ \Delta_y c_{i,j} &= \frac{(1-\alpha_2)c_{i,j}+\alpha_2 c_{i,j+1}-(1-\alpha_2)c_{i,j-1}-\alpha_2 c_{i,j}}{\Delta y},\end{aligned} \tag{4.6c}$$

where:

α_1, α_2 – spatial weighting parameters with values within the range of $\langle 0, 1\rangle$.

The weighting parameter θ present in equation (4.5) determines the averaging in time:

- when $\theta = 0$ – we obtain the explicit scheme;
- when $\theta \in (0, 1\rangle$ – the implicit scheme, particularly for:
  - $\theta = 1$ the Fully Implicit scheme,
  - $\theta = \frac{1}{2}$ the Crank-Nicolson scheme.

Parameters α_i, for $i \in \{1, 2\}$, determine the approximation method of the first space derivative:

- with backward difference quotient (4.3) when $\alpha_i = 0$;
- with central difference quotient (4.4) when $\alpha_i = \frac{1}{2}$;
- with forward difference quotient (4.2) when $\alpha_i = 1$.

In particular, for appropriately selected parameters θ and α_1 and α_2, the following numerical schemes can be obtained:

➤ **Upwind – explicit, forward/backward space scheme**

– when $\theta = 0$, $\alpha_1 = \begin{cases} 0, \text{for } v_x > 0 \\ 1, \text{for } v_x < 0 \end{cases}$ and $\alpha_2 = \begin{cases} 0, \text{for } v_y > 0 \\ 1, \text{for } v_y < 0 \end{cases}$;

➤ **Explicit scheme with central finite difference spatial approximation**

– when $\theta = 0$, $\alpha_1 = \alpha_2 = \frac{1}{2}$;

➤ **Crank-Nicolson scheme with central finite difference spatial approximation**

– when $\theta = \alpha_1 = \alpha_2 = \frac{1}{2}$;

➤ **Alternating Directions Implicit method with central finite difference spatial approximation**

– when $\theta = \alpha_1 = \alpha_2 = \frac{1}{2}$;

➤ **Fully Implicit scheme with central finite difference spatial approximation**

– when $\theta = 1$, $\alpha_1 = \alpha_2 = \frac{1}{2}$.

In the implemented **RivMix** model of spreading of solutes (described further in the book), it is possible to use: Upwind explicit scheme, Crank-Nicolson scheme, and Alternating Directions Implicit Method with central difference quotient. Those methods, collected in table 4.2, are described in detail below.

Table 4.2: Methods implemented in the **RivMix** model

Method		Order of accuracy
Upwind (**UP**)	explicit	$O(\Delta x, \Delta y, \Delta t)$
Crank-Nicolson (**CN**)	implicit	$O(\Delta x^2, \Delta y^2, \Delta t^2)$
Alternating Directions Implicit (**ADI**)	implicit	$O(\Delta x^2, \Delta y^2, \Delta t^2)$
Alternating Directions Implicit version 2 (**ADI2**)	implicit	$O(\Delta x^2, \Delta y^2, \Delta t^2)$

4.3.1 Upwind explicit, forward/backward space scheme

The Upwind scheme is named after the application of the first spatial derivative of the backward (4.3) or forward (4.2) difference quotients for approximation – depending on the sign of velocity in the given point ($\alpha_i = 0$, where the appropriate velocity component is greater than or equal to zero and $\alpha_i = 1$, for a component less than zero). To simplify the notation, this scheme will be referred to as **UP** further on in the book. In the considered case the UP scheme is explicit ($\theta = 0$), which means that in the difference equation there is only one unknown in the $(n+1)$-th time step $c_{i,j}^{n+1}$, which can be directly determined on the basis of concentration values in the previous time step n:

$$c_{i,j}^{n+1} = f\left(c_{i,j}^n,\, c_{i+1,j}^n,\, c_{i-1,j}^n,\, c_{i,j+1}^n,\, c_{i,j-1}^n,\, c_{i+1,j+1}^n,\, c_{i+1,j-1}^n,\, c_{i-1,j+1}^n,\, c_{i-1,j-1}^n\right).$$

The values in $n+1$ time step in the internal nodes of the grid are therefore calculated with the difference equation:

$$c_{i,j}^{n+1} = \left[1 - v_x \Delta t \nabla_x - v_y \Delta t \nabla_y + D_{xx} \Delta t \delta_x^2 + 2 D_{xy} \Delta t \delta_{xy} + D_{yy} \Delta t \delta_y^2\right] c_{i,j}^n\,. \tag{4.7}$$

This equation, after taking into consideration appropriate difference operators, assumes the following form:

$$\begin{aligned} c_{i,j}^{n+1} = c_{i,j}^n &+ \mathcal{C}r_x^d \left[c_{i+1,j}^n - 2c_{i,j}^n + c_{i-1,j}^n\right] + \mathcal{C}r_y^d \left[c_{i,j+1}^n - 2c_{i,j}^n + c_{i,j-1}^n\right] \\ &+ \mathcal{C}r_{xy}^d \left[c_{i+1,j+1}^n - c_{i+1,j-1}^n - c_{i-1,j+1}^n + c_{i-1,j-1}^n\right] \\ &- \mathcal{C}r_x^a \left[(1-2\alpha_1)c_{i,j}^n + \alpha_1 c_{i+1,j}^n - (1-\alpha_1)c_{i-1,j}^n\right] \\ &- \mathcal{C}r_y^a \left[(1-2\alpha_2)c_{i,j}^n + \alpha_2 c_{i,j+1}^n - (1-\alpha_2)c_{i,j-1}^n\right]; \end{aligned} \tag{4.8}$$

where:

$\mathcal{C}r_x^a = \frac{v_x \Delta t}{\Delta x}$, $\mathcal{C}r_y^a = \frac{v_y \Delta t}{\Delta y}$ – advection Courant numbers;

$\mathcal{C}r_x^d = \frac{D_{xx} \Delta t}{\Delta x^2}$, $\mathcal{C}r_{xy}^d = \frac{D_{xy} \Delta t}{4 \Delta x \Delta y}$, $\mathcal{C}r_y^d = \frac{D_{yy} \Delta t}{\Delta y^2}$ – diffusion Courant numbers.

In case of UP scheme after ordering, for $v_x > 0$ and $v_y > 0$ (for other cases – see table 4.3) we obtain:

$$\begin{aligned} c_{i,j}^{n+1} = & \left(1 - \mathcal{C}r_x^a - 2\mathcal{C}r_x^d - \mathcal{C}r_y^a - 2\mathcal{C}r_y^d\right) c_{i,j}^n \\ & + \left(\mathcal{C}r_x^d\right) c_{i+1,j}^n + \left(\mathcal{C}r_x^a + \mathcal{C}r_x^d\right) c_{i-1,j}^n \\ & + \left(\mathcal{C}r_y^d\right) c_{i,j+1}^n + \left(\mathcal{C}r_y^a + \mathcal{C}r_y^d\right) c_{i,j-1}^n \\ & + \left(2\mathcal{C}r_{xy}^d\right) c_{i+1,j+1}^n + \left(-2\mathcal{C}r_{xy}^d\right) c_{i+1,j-1}^n \\ & + \left(-2\mathcal{C}r_{xy}^d\right) c_{i-1,j+1}^n + \left(2\mathcal{C}r_{xy}^d\right) c_{i-1,j-1}^n . \end{aligned} \tag{4.9}$$

The determination of concentration values in points situated at the edges of the calculation grid requires special treatment. The problem is discussed in the further part of the book (Section 4.4). Another example of an explicit scheme is the previously mentioned explicit scheme with central difference approximation. In this scheme, the first spatial derivatives are approximated with central difference quotients (4.4).

Table 4.3: Coefficients in equation (4.9) depending on the signs of velocity components

	Coefficients before:				
	$c_{i,j}^n$	$c_{i+1,j}^n$	$c_{i-1,j}^n$	$c_{i,j+1}^n$	$c_{i,j-1}^n$
$v_x \geqslant 0$ $v_y \geqslant 0$	$1 - \mathcal{C}r_x^a - 2\mathcal{C}r_x^d$ $-\mathcal{C}r_y^a - 2\mathcal{C}r_y^d$	$\mathcal{C}r_x^d$	$\mathcal{C}r_x^a + \mathcal{C}r_x^d$	$\mathcal{C}r_y^d$	$\mathcal{C}r_y^a + \mathcal{C}r_y^d$
$v_x \geqslant 0$ $v_y < 0$	$1 - \mathcal{C}r_x^a - 2\mathcal{C}r_x^d$ $+\mathcal{C}r_y^a - 2\mathcal{C}r_y^d$	$\mathcal{C}r_x^d$	$\mathcal{C}r_x^a + \mathcal{C}r_x^d$	$-\mathcal{C}r_y^a + \mathcal{C}r_y^d$	$\mathcal{C}r_y^d$
$v_x < 0$ $v_y \geqslant 0$	$1 + \mathcal{C}r_x^a - 2\mathcal{C}r_x^d$ $-\mathcal{C}r_y^a - 2\mathcal{C}r_y^d$	$-\mathcal{C}r_x^a + \mathcal{C}r_x^d$	$\mathcal{C}r_x^d$	$\mathcal{C}r_y^d$	$\mathcal{C}r_y^a + \mathcal{C}r_y^d$
$v_x < 0$ $v_y < 0$	$1 + \mathcal{C}r_x^a - 2\mathcal{C}r_x^d$ $+\mathcal{C}r_y^a - 2\mathcal{C}r_y^d$	$-\mathcal{C}r_x^a + \mathcal{C}r_x^d$	$\mathcal{C}r_x^d$	$-\mathcal{C}r_y^a + \mathcal{C}r_y^d$	$\mathcal{C}r_y^d$

Coefficients in front of: $c_{i+1,j+1}^n$, $c_{i+1,j-1}^n$, $c_{i-1,j+1}^n$ and $c_{i-1,j-1}^n$ do not depend on velocity sign

4.3.2 Crank-Nicolson scheme with central finite difference spatial approximation

The Crank-Nicolson scheme (**CN**) proposed in 1947 (Crank & Nicolson, 1947) is an example of an implicit scheme. An implicit formula is obtained when the weighting parameter θ is other than 0. If $\theta = 1$ we will obtain a Fully Implicit (**FI**) – scheme:

$$\left[1 + v_x \Delta t \nabla_x + v_y \Delta t \nabla_y - D_{xx} \Delta t \delta_x^2 + \ -2D_{xy} \Delta t \delta_{xy} - D_{yy} \Delta t \delta_y^2\right] c_{i,j}^{n+1} = c_{i,j}^n \,.$$

The Crank-Nicolson scheme is obtained for parameter $\theta = \frac{1}{2}$. In this case the difference equation for internal points of the grid assumes the following form:

$$\begin{aligned} &\left[1 + \frac{v_x \Delta t}{2} \nabla_x + \frac{v_y \Delta t}{2} \nabla_y - \frac{D_{xx} \Delta t}{2} \delta_x^2 - D_{xy} \Delta t \delta_{xy} - \frac{D_{yy} \Delta t}{2} \delta_y^2\right] c_{i,j}^{n+1} = \\ &= \left[1 - \frac{v_x \Delta t}{2} \nabla_x - \frac{v_y \Delta t}{2} \nabla_y + \frac{D_{xx} \Delta t}{2} \delta_x^2 + D_{xy} \Delta t \delta_{xy} + \frac{D_{yy} \Delta t}{2} \delta_y^2\right] c_{i,j}^n \,. \end{aligned} \tag{4.10}$$

After taking into consideration appropriate difference quotients and ordering, the following equation is obtained for each internal point:

$$\begin{aligned} c_{i,j}^{n+1} \left(1 + \mathcal{C}r_x^d + \mathcal{C}r_y^d\right) + c_{i+1,j}^{n+1} \left(\frac{\mathcal{C}r_x^a}{4} - \frac{\mathcal{C}r_x^d}{2}\right) + c_{i-1,j}^{n+1} \left(-\frac{\mathcal{C}r_x^a}{4} - \frac{\mathcal{C}r_x^d}{2}\right) \\ + c_{i,j+1}^{n+1} \left(\frac{\mathcal{C}r_y^a}{4} - \frac{\mathcal{C}r_y^d}{2}\right) + c_{i,j-1}^{n+1} \left(-\frac{\mathcal{C}r_y^a}{4} - \frac{\mathcal{C}r_y^d}{2}\right) \\ + c_{i+1,j+1}^{n+1} \left(-\mathcal{C}r_{xy}^d\right) + c_{i+1,j-1}^{n+1} \left(\mathcal{C}r_{xy}^d\right) + c_{i-1,j+1}^{n+1} \left(\mathcal{C}r_{xy}^d\right) + c_{i-1,j-1}^{n+1} \left(-\mathcal{C}r_{xy}^d\right) \\ = \left.\begin{aligned} c_{i,j}^n \left(1 - \mathcal{C}r_x^d - \mathcal{C}r_y^d\right) + c_{i+1,j}^n \left(-\frac{\mathcal{C}r_x^a}{4} + \frac{\mathcal{C}r_x^d}{2}\right) + c_{i-1,j}^n \left(\frac{\mathcal{C}r_x^a}{4} + \frac{\mathcal{C}r_x^d}{2}\right) \\ + c_{i,j+1}^n \left(-\frac{\mathcal{C}r_y^a}{4} + \frac{\mathcal{C}r_y^d}{2}\right) + c_{i,j-1}^n \left(\frac{\mathcal{C}r_y^a}{4} + \frac{\mathcal{C}r_y^d}{2}\right) \\ + c_{i+1,j+1}^n \left(\mathcal{C}r_{xy}^d\right) + c_{i+1,j-1}^n \left(-\mathcal{C}r_{xy}^d\right) \\ + c_{i-1,j+1}^n \left(-\mathcal{C}r_{xy}^d\right) + c_{i-1,j-1}^n \left(\mathcal{C}r_{xy}^d\right) \end{aligned}\right\} F_{i,j} \end{aligned} \tag{4.11}$$

where:

$F_{i,j}$ – the value calculated on the basis of known concentration values in the n-th time step.

We can observe that concentration values in the $(n+1)$-th time step ($c_{i,j}^{n+1}$) depend both on concentration values in the previous, the n-th step, and on those in the $(n+1)$-th time step in question. The determination of values in the $(n+1)$-th time step is therefore more difficult than in case of explicit schemes and requires solution of a system of linear equations.

For simplification, equation (4.11) can be written in the following form:

$$\begin{aligned} ac_{i,j}^{n+1} + bc_{i+1,j}^{n+1} + cc_{i-1,j}^{n+1} + dc_{i,j+1}^{n+1} + ec_{i,j-1}^{n+1} \\ + fc_{i+1,j+1}^{n+1} + gc_{i+1,j-1}^{n+1} + hc_{i-1,j+1}^{n+1} + ic_{i-1,j-1}^{n+1} = F_{i,j}\,; \end{aligned} \tag{4.12}$$

where the coefficients assume the form of:

$$\begin{aligned} a &= 1 + Cr_x^d + Cr_y^d, & d &= \frac{Cr_y^a}{4} - \frac{Cr_y^d}{2}, & g &= Cr_{xy}^d, \\ b &= \frac{Cr_x^a}{4} - \frac{Cr_x^d}{2}, & e &= -\frac{Cr_y^a}{4} - \frac{Cr_y^d}{2}, & h &= Cr_{xy}^d, \\ c &= -\frac{Cr_x^a}{4} - \frac{Cr_x^d}{2}, & f &= -Cr_{xy}^d, & i &= -Cr_{xy}^d. \end{aligned}$$

Assigning numbers to the nodes of the grid in the way shown in figure 4.4, where a pair of integers (i,j) is replaced with the number of the node, we can note the searched concentration value vector in the $(n+1)$-th time step in the form of:

$$\mathbf{X} = (c_0, c_1, c_2, \cdots, c_m)^T,$$

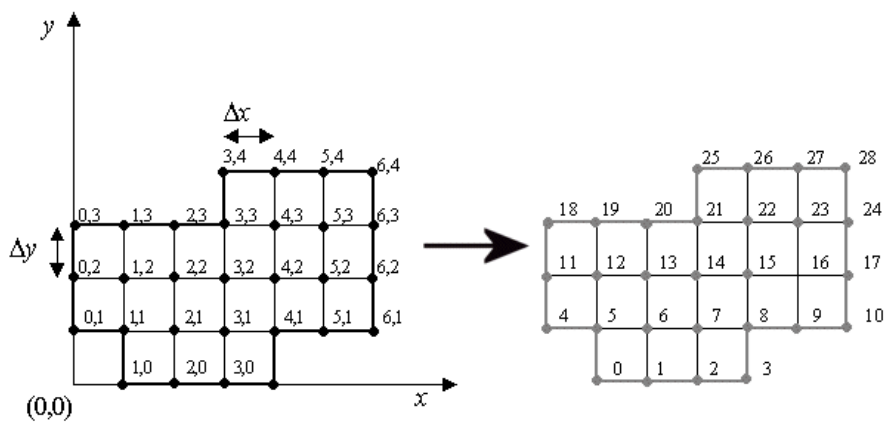

Figure 4.4: Example of transformation of coordinates of a point in the grid into its number (only the inner points from the discretization grid are taken into consideration)

and the $F_{i,j}$ values, respectively, as a vector:

$$\mathbf{F} = (F_0, F_1, F_2, \cdots, F_m);$$

where:

$(m+1)$ – the number of the grid nodes.

The equation system to be solved assumes the following form:

$$\mathbf{A}\,\mathbf{X} = \mathbf{F};$$

where:

$\mathbf{A}$ – band matrix of coefficients in the system (see fig. 4.5).

The matrix $\mathbf{A}$ has the structure as shown in figure 4.5 in which all elements not shown are zero.

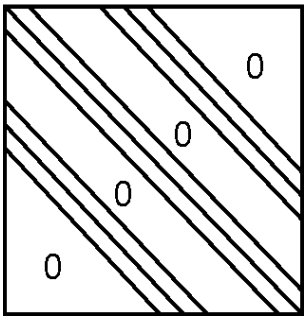

Figure 4.5: Schematic representation of the matrix of coefficients for the equation system obtained after the application of CN scheme.

There are two types of solution methods for the obtained system of linear algebraic equations: the direct ones, such as ***Gauss elimination*** method or the iterative ones, such as ***Jacobi*** method. In case of a large number of grid nodes that we usually encounter, the solution of the obtained equation system in each time step, using the direct methods, results in high computation costs. Then, in practice, iterative methods are applied to solve it. These methods start from the initial approximation ($\mathbf{X}^0$), and then the approximation is gradually improved (a series of consecutive approximations is created: $\mathbf{X}^1$, $\mathbf{X}^2, \cdots$), until the stopping condition is fulfilled (the difference between the iterations becomes small). Below, the implemented methods (Jacobi, Gauss-Seidel and Successive Over Relaxation) are presented:

- **Jacobi method (J)**

$$c_p^{k+1} = \frac{-\sum\limits_{q=1, p\neq q}^{m} a_{p,q} c_q^k + F_p}{a_{p,p}}; \tag{4.13}$$

- **Gauss-Seidel method (GS)**

$$c_p^{k+1} = \frac{\overbrace{-\sum_{q=1}^{p-1} a_{p,q} c_q^{k+1}}^{\substack{\text{points for which} \\ \text{the values in } k+1 \text{ iteration} \\ \text{have already been determined}}} \overbrace{-\sum_{q=p+1}^{m} a_{p,q} c_q^{k}}^{\substack{\text{points for which} \\ \text{we do not know} \\ \text{values in } k+1 \text{ iteration}}} + F_p}{a_{p,p}}; \tag{4.14}$$

- **Successive Over Relaxation method (SOR)**

$$c_p^{k+1} = c_p^k + \omega r_p^k;$$

$$r_p^k = \frac{-\sum_{q=1}^{p-1} a_{p,q} c_q^{k+1} - \sum_{q=p}^{m} a_{p,q} c_q^{k} + F_p}{a_{p,p}}; \tag{4.15}$$

where:

k – iteration number;
$p, q = \{0, 1, 2, \cdots, m\}$;
$0 < \omega < 2$ – relaxation parameter (for $\omega = 1$ we obtain the GS method);
c_p^0 – initial approximation, e.g.: $c_p^0 = 0$.

The detailed description of those methods could be found, e.g. in (Björc & Dahlquist, 1987).

The simplest iterative method is the Jacobi method (4.13); this method, however, is not sufficiently quickly convergent. In order to obtain a result with the required accuracy, a vast number of iterations is required. Therefore, the Gauss-Seidel method (4.14) or the Successful Over Relaxation method (4.15) are usually used. Table 4.4 presents the number of iterations in a single time step for two example sets of parameters, necessary for obtaining a solution with the prescribed accuracy with the application of various iteration methods. The calculations were carried out until the sum of absolute values $|\delta_p|$ was less than 10^{-15}:

$$\sum_{p=0}^{m} |\delta_p| < 10^{-15}, \qquad \text{where:} \quad \delta_p = c_p^{k+1} - c_p^k. \tag{4.16}$$

Table 4.4: The number of iterations in a single time step while solving the equation system obtained in CN scheme for example simulation parameters; in both cases: $\Delta x = \Delta y = 1\,\mathrm{m}$, $\Delta t = 0.5\,\mathrm{s}$ and $m = 62500$ nodes, the number of iterations with the optimal relaxation parameter ω is displayed in bold letters; the quoted iteration number was stable after a few time steps

Method:	J	GS	SOR					
Relaxation parameter	-	1	1.1	1.15	1.2	1.5	1.7	1.8
Number of iterations: $v_x = v_y = 0.2\,\frac{\mathrm{m}}{\mathrm{s}}$ $D_L = 0.5\,\frac{\mathrm{m}^2}{\mathrm{s}}$ $D_T = 0.5\,\frac{\mathrm{m}^2}{\mathrm{s}}$	29	18	12	**9**	12	39	99	>200
Number of iterations: $v_x = v_y = 0.11\,\frac{\mathrm{m}}{\mathrm{s}}$ $D_L = 0.75\,\frac{\mathrm{m}^2}{\mathrm{s}}$ $D_T = 0.1\,\frac{\mathrm{m}^2}{\mathrm{s}}$	27-31	16-20	**11-27**	13-31	15-35	47-79	143-179	>200

The SOR method allows to obtain the solution with a relatively small number of iterations, but it requires the specification of the so-called relaxation parameter which, when wrongly selected, may significantly prolong the calculation time. The method is convergent only when $0 < \omega < 2$. The desired result is obtained in a smaller number of iterations than with the application of GS method only when $\omega > 1$. A special method was implemented in the **RivMix** model (described in Chapter 6) which selects the relaxation parameter which according to the tests carried out depends not only on the size of the calculation grid but also on the other parameters of the simulation. For example sets of parameters the smallest number of iterations obtained with appropriately selected ω is displayed in bold in table 4.4.

4.3.3 Alternating Direction Implicit method with central finite difference spatial approximation

Despite application of iteration methods for solution of equation systems obtained in CN method, receiving a solution is a time consuming process (see Section 5.3). A significant acceleration of the whole calculation process without

any loss of accuracy can be obtained with the application of the Alternating Directions Implicit method (**ADI**) with central finite difference spatial approximation.

The ADI method was first proposed by Douglas (1955) and Peaceman & Rachford (1955) for solving a two-dimensional heat transport equation. The basis of the method is solving an equation with the application of an implicit formula in two steps. The division into steps is made in such a way that each stage is implicit only in one spatial direction (fig. 4.6).

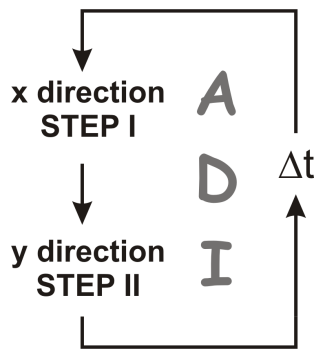

Figure 4.6: Schematically presented ADI method

In the case discussed in this volume, the ADI method is based on the implicit Crank-Nicolson scheme. This scheme, after necessary modifications allowing for the splitting of the solution into two steps, can be written down in the form (McKee *et al.*, 1996):

$$\left[1+\frac{v_x\Delta t}{2}\nabla_x-\frac{D_{xx}\Delta t}{2}\delta_x^2\right]\left[1+\frac{v_y\Delta t}{2}\nabla_y-\frac{D_{yy}\Delta t}{2}\delta_y^2\right]c_{i,j}^{n+1}$$
$$=\left\{\left[1-\frac{v_x\Delta t}{2}\nabla_x+\frac{D_{xx}\Delta t}{2}\delta_x^2\right]\left[1-\frac{v_y\Delta t}{2}\nabla_y+\frac{D_{yy}\Delta t}{2}\delta_y^2\right]+2D_{xy}\Delta t\delta_{xy}\right\}c_{i,j}^{n}\,. \tag{4.17}$$

Applying the ADI method following the Douglas-Rachford algorithm (Douglas & Rachford, 1956), the equation can be divided into two steps in the following way:

STEP I – implicit in x direction, explicit in y direction:

$$\left[1+\frac{v_x\Delta t}{2}\Delta_x-\frac{D_{xx}\Delta t}{2}\delta_x^2\right]c_{i,j}^{n+\frac{1}{2}}$$
$$=\left[1-v_y\Delta t\Delta_y+D_{yy}\Delta t\delta y^2-\frac{v_x\Delta t}{2}\Delta_x+\frac{D_{xx}\Delta t}{2}\delta_x^2+D_{xy}\Delta t\delta_{xy}\right]c_{i,j}^{n}\,; \tag{4.18}$$

STEP II – explicit in x direction, implicit in y direction:

$$\left[1+\frac{v_y\Delta t}{2}\Delta_y-\frac{D_{yy}\Delta t}{2}\delta_y^2\right]c_{i,j}^{n+1}=c_{i,j}^{n+\frac{1}{2}}-\left[-\frac{v_y\Delta t}{2}\Delta_y+\frac{D_{yy}\Delta t}{2}\delta y^2\right]c_{i,j}^{n}\,. \tag{4.19}$$

It may be shown that formulae (4.18) and (4.19) are equivalent to the initial one (4.17). Other ways of splitting the equation into two steps may also be found in the literature, described mainly in case of diffusion equation (e.g. McKee & Mitchell, 1970, 1971). In the implemented model it is also possible to apply the ADI method in the second version, called here **ADI2** in short. The splitting way here is similar to that presented in the work by Smith & Yongming (2001) for the solution to the two-dimensional advection-diffusion equation with the source term and the reaction term. The approximation formula, after adapting it to the two-dimensional advection-diffusion equation considered herein (2.13), assumes the following form:

$$\begin{aligned}&\left[1+\frac{v_x\Delta t}{2}\nabla_x-\frac{D_{xx}\Delta t}{2}\delta_x^2\right]\left[1+\frac{v_y\Delta t}{2}\nabla_y-\frac{D_{yy}\Delta t}{2}\delta_y^2\right]c_{i,j}^{n+1}\\&=\left\{\left[1-\frac{v_x\Delta t}{2}\nabla_x+\frac{D_{xx}\Delta t}{2}\delta_x^2\right]\left[1-\frac{v_y\Delta t}{2}\nabla_y+\frac{D_{yy}\Delta t}{2}\delta_y^2\right]\right.\\&\qquad\left.+2D_{xy}\Delta t\left[\left(\nabla_x-\frac{v_x\Delta t}{2}\delta_x^2\right)\left(\nabla_y-\frac{v_y\Delta t}{2}\delta_y^2\right)\right]\right\}c_{i,j}^{n}\,.\end{aligned} \tag{4.20}$$

The splitting into two stages is done in the following way:

STEP I – implicit in x direction, explicit in y direction:

$$\begin{aligned}&\left[1+\frac{v_x\Delta t}{2}\Delta_x-\frac{D_{xx}\Delta t}{2}\delta_x^2\right]C_{i,j}^{n+\frac{1}{2}}\\&=\left\{\left[1-\frac{v_x\Delta t}{2}\nabla_x+\frac{D_{xx}\Delta t}{2}\delta_x^2\right]\left[1-\frac{v_y\Delta t}{2}\nabla_y+\frac{D_{yy}\Delta t}{2}\delta_y^2\right]\right.\\&\qquad\left.+2D_{xy}\Delta t\left[\left(\nabla_x-\frac{v_x\Delta t}{2}\delta_x^2\right)\left(\nabla_y-\frac{v_y\Delta t}{2}\delta_y^2\right)\right]\right\}c_{i,j}^{n}\,;\end{aligned} \tag{4.21}$$

STEP II – explicit in x direction, implicit in y direction:

$$\left[1+\frac{v_y\Delta t}{2}\Delta_y-\frac{D_{yy}\Delta t}{2}\delta_y^2\right]C_{i,j}^{n+1}=C_{i,j}^{n+\frac{1}{2}}\,. \tag{4.22}$$

Due to absence of significant differences in solutions obtained with the application of ADI and ADI2 methods respectively (see fig. 4.7), the first of the two methods is further analysed in this book (equation 4.17).
Formulae (4.18) and (4.19) can be written down as:

STEP I :

$$c_{i,j}^{n+\frac{1}{2}}\left(1+\mathcal{C}r_x^d\right)+c_{i+1,j}^{n+\frac{1}{2}}\left(\frac{\mathcal{C}r_x^a}{4}-\frac{\mathcal{C}r_x^d}{2}\right)+c_{i-1,j}^{n+\frac{1}{2}}\left(-\frac{\mathcal{C}r_x^a}{4}-\frac{\mathcal{C}r_x^d}{2}\right)$$

$$\left.\begin{aligned}=c_{i,j}^{n}\left(1-\mathcal{C}r_x^d-2\mathcal{C}r_y^d\right)+c_{i+1,j}^{n}\left(-\frac{\mathcal{C}r_x^a}{4}+\frac{\mathcal{C}r_x^d}{2}\right)+c_{i-1,j}^{n}\left(\frac{\mathcal{C}r_x^a}{4}+\frac{\mathcal{C}r_x^d}{2}\right)\\ +c_{i,j+1}^{n}\left(-\frac{\mathcal{C}r_y^a}{4}+\mathcal{C}r_y^d\right)+c_{i,j-1}^{n}\left(\frac{\mathcal{C}r_y^a}{4}+\mathcal{C}r_y^d\right)\\ +c_{i+1,j+1}^{n}\left(\mathcal{C}r_{xy}^d\right)+c_{i+1,j-1}^{n}\left(-\mathcal{C}r_{xy}^d\right)\\ +c_{i-1,j+1}^{n}\left(-\mathcal{C}r_{xy}^d\right)+c_{i-1,j-1}^{n}\left(\mathcal{C}r_{xy}^d\right)\end{aligned}\right\}F_{i,j}^{I} \tag{4.23}$$

STEP II :

$$c_{i,j}^{n+1}\left(1+\mathcal{C}r_y^d\right)+c_{i,j+1}^{n+1}\left(\frac{\mathcal{C}r_y^a}{4}-\frac{\mathcal{C}r_y^d}{2}\right)+c_{i,j-1}^{n+1}\left(-\frac{\mathcal{C}r_y^a}{4}-\frac{\mathcal{C}r_y^d}{2}\right)=$$

$$=c_{i,j}^{n+\frac{1}{2}}+\underbrace{c_{i,j}^{n}\left(\mathcal{C}r_y^d\right)+c_{i,j+1}^{n}\left(\frac{\mathcal{C}r_y^a}{4}-\frac{\mathcal{C}r_y^d}{2}\right)+c_{i,j-1}^{n}\left(-\frac{\mathcal{C}r_y^a}{4}-\frac{\mathcal{C}r_y^d}{2}\right)}_{F_{i,j}^{II}} \tag{4.24}$$

where:

$F_{i,j}^{I}$ and $F_{i,j}^{II}$ – value calculated on the basis of the known concentration values in the n-th time step.

Instead of one big equation system like for CN scheme, in case of ADI method we obtain two systems which can be solved much faster. The matrices of coefficients of the equation systems obtained at both stages were schematically presented in figure 4.8. Due to their specific tridiagonal arrangement, we can apply the special analytical Thomas method to solve the systems of equations.

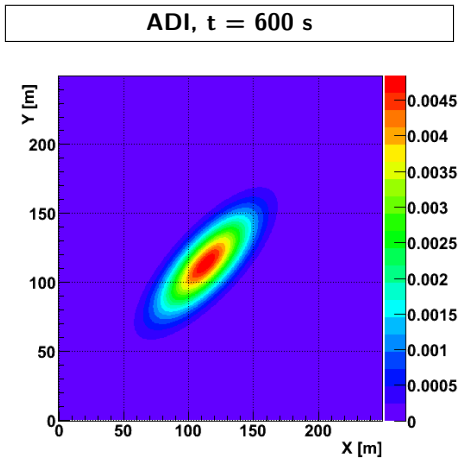

(a) Numerical solution, scheme ADI

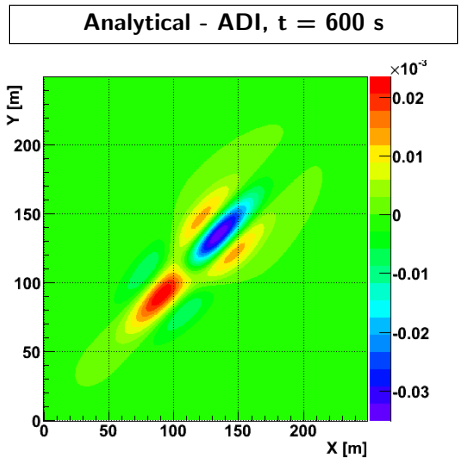

(b) Difference between the analytical and numerical solutions with the application of ADI scheme

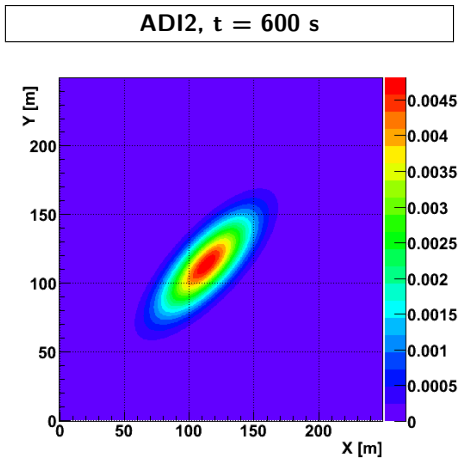

(c) Numerical solution, scheme ADI2

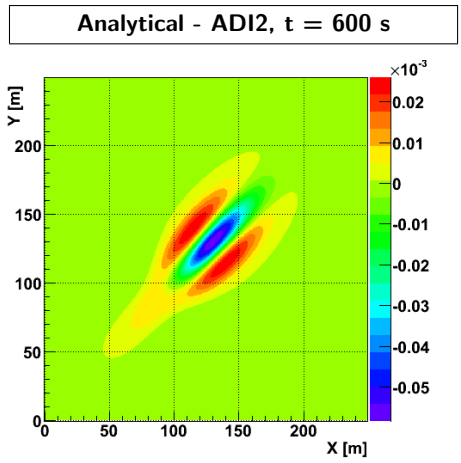

(d) Difference between the analytical and numerical solutions with the application of ADI2 scheme

Figure 4.7: The numerical solution with the application of the ADI method (a) and ADI2 method (c) after 600 seconds; simulation parameters: $\Delta x = \Delta y = 1\,\mathrm{m}$ and $\Delta t = 0.5\,s$, $v_x = v_y = 0.106\,\frac{\mathrm{m}}{\mathrm{s}}$, $D_{xx} = D_{yy} = 0.425\,\frac{\mathrm{m}^2}{\mathrm{s}}$, $D_{xy} = D_{yx} = 0.325\,\frac{\mathrm{m}^2}{\mathrm{s}}$; mass $M = 10\,\mathrm{a.\,u.}$ was discharged at point $x_0 = 50\,\mathrm{m}$, $y_0 = 50\,\mathrm{m}$ at time $t_0 = 0\,\mathrm{s}$; figures (b) and (d) illustrate the difference between the analytical and the numerical solutions

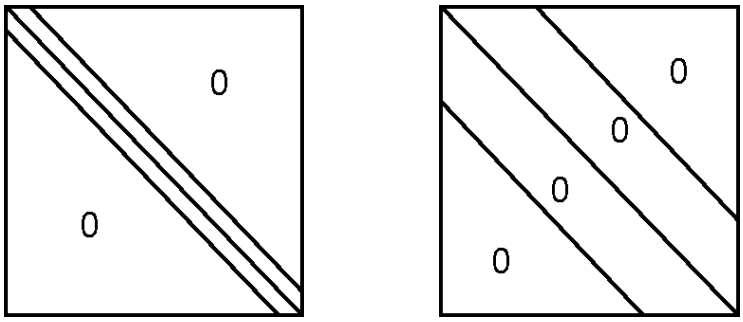

(a) STEP I (b) STEP II

Figure 4.8: Schematically presented matrices of coefficients in the equation systems obtained with the application of ADI scheme

- **Thomas method** (Fletcher, 1991; Szymkiewicz, 2003)

  A tridiagonal matrix **A**:

$$\mathbf{A} = \begin{bmatrix} a_1 & b_1 & 0 & \dots & \dots & \dots & 0 \\ c_2 & a_2 & b_2 & 0 & \dots & \dots & 0 \\ 0 & c_3 & a_3 & b_3 & 0 & \dots & 0 \\ \vdots & \vdots & \vdots & \vdots & \vdots & \vdots & \vdots \\ & & & \dots\dots\dots\dots\dots\dots & & & \\ \vdots & \vdots & \vdots & \vdots & \vdots & \vdots & \vdots \\ 0 & \dots & \dots & 0 & c_{m-1} & a_{m-1} & b_{m-1} \\ 0 & \dots & \dots & \dots & 0 & c_m & a_m \end{bmatrix} \tag{4.25}$$

  is decomposed into two matrices – upper triangular matrix **U** (has elements only on the diagonal and above) and lower triangular matrix **L** (has elements only on the diagonal and below):

$$\mathbf{A} = \mathbf{LU}; \tag{4.26}$$

$$\mathbf{L} = \begin{bmatrix} 1 & 0 & \dots & \dots & \dots & 0 \\ l_2 & 1 & 0 & \dots & \dots & 0 \\ 0 & l_3 & 1 & 0 & \dots & 0 \\ \vdots & \vdots & \vdots & \vdots & \vdots & \vdots \\ & & \dots\dots\dots\dots & & & \\ \vdots & \vdots & \vdots & \vdots & \vdots & \vdots \\ 0 & \dots & 0 & l_{m-1} & 1 & 0 \\ 0 & \dots & \dots & 0 & l_m & 1 \end{bmatrix}, \tag{4.27}$$

$$\mathbf{U} = \begin{bmatrix} u_1 & b_1 & 0 & \dots & \dots & \dots & 0 \\ 0 & u_2 & b_2 & 0 & \dots & \dots & 0 \\ 0 & 0 & u_3 & b_3 & 0 & \dots & 0 \\ \vdots & \vdots & \vdots & \vdots & \vdots & \vdots & \vdots \\ & & & \dots\dots\dots\dots\dots\dots & & & \\ \vdots & \vdots & \vdots & \vdots & \vdots & \vdots & \vdots \\ 0 & \dots & \dots & 0 & 0 & u_{m-1} & b_{m-1} \\ 0 & \dots & \dots & \dots & 0 & 0 & u_m \end{bmatrix}; \tag{4.28}$$

where:

$$\begin{aligned} u_1 &= a_1, \\ l_p &= \frac{c_p}{u_{p-1}}, \\ u_p &= a_p - l_p b_{p-1}, \quad p = 2, 3, \cdots, m\,. \end{aligned} \tag{4.29}$$

The obtained system:

$$\mathbf{LUX} = \mathbf{F}, \tag{4.30}$$

is equivalent to two systems:

$$\begin{aligned} \mathbf{LY} &= \mathbf{F}, \\ \mathbf{UX} &= \mathbf{Y}; \end{aligned} \tag{4.31}$$

which are solved with the application of the following recurrent formulae:

$$\begin{aligned} y_1 &= F_1; \\ y_p &= F_p - l_p y_{p-1}; \qquad p = 2, 3, \cdots, m; \\ c_m &= \frac{y_m}{u_m}; \\ c_p &= \frac{y_p - b_p c_{p+1}}{u_p}; \qquad p = m-1, m-2, \cdots, 1\,. \end{aligned} \tag{4.32}$$

Performing a small number of arithmetical operations, namely, $3(m-1)$ additions and multiplications and $(2m-1)$ divisions (Szymkiewicz, 2003), we obtain exact solution to both equation systems. Therefore, the algorithm is very fast in comparison to iteration methods used in case of CN scheme. Comparison of example calculation times is presented in Section 5.3.

4.4 Initial and boundary conditions

The difference equation being solved must be supplemented with boundary and initial conditions.

The ***initial conditions*** define the values assigned to all system variables at the "start time" and depend on the considered situation. Usually at time $t = 0$ for each grid point, we will have to set the concentration at a given point to some value:

$$c(x, y, 0) = c^0(x, y)\,; \tag{4.33}$$

where:

$c^0(x, y)$ – initial concentration value at a given point (x, y).

The ***boundary conditions*** are specified at each moment in time for all boundary points and depend on the kind of the considered banks. In cases described in this volume in situations when there is water inflow at the edge of the grid (at the boundary point), the value of concentration is prescribed to this point at each moment in time. It is the so-called Dirichlet boundary condition (Fletcher, 1991; Szymkiewicz, 2000), and can be written as follows:

$$c(x_B, y_B, t) = c^B_{x_B, y_B}(t)\,; \tag{4.34}$$

where:

x_B, y_B – the boundary point coordinates,

$c^B_{x_B,y_B}(t)$ – the concentration value at a given boundary point x_B, y_B in time t.

In the outflow situation, it is assumed that the concentration gradient on the bank is constant (the so-called Neumann boundary conditions):

$$\left.\frac{\partial c}{\partial n}\right|_{x_B,y_B} = const\,, \tag{4.35}$$

so, for example, in case when the outflow is situated on the right bank (parallel to y axis):

$$c_{B,j} = 2c_{B-1,j} - c_{B-2,j}\,, \tag{4.36}$$

where:
B – has been used here to denote the point index (see fig. 4.4).

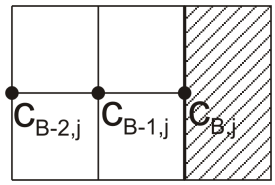

Figure 4.9: Schematic representation of the right-hand border edge of the calculation grid

In case of physical banks, assuming that we deal with impermeable banks, the values at the edges of the grid would be calculated with the application of coefficients presented in Appendix D in tables: D.1 (for UP scheme); D.2, D.3 (for CN) and D.4, D.5 (for ADI). In the numerical tests carried out, also periodic boundary conditions were applied in some cases. In case of continuous release it was also necessary to setup the so-called ***inner boundary conditions***, defining the concentration value at the source point (or points) in each time step.

Chapter 5

Properties of Considered Numerical Schemes

5.1 Introduction

Nowadays, when the computer sciences are much developed, the numerical simulation could be used to support the expensive laboratory and field experiments. Such simulations are cheaper and faster and first of all they can simulate situations and physical phenomena which cannot be done experimentally or analytically. Therefore, numerical methods are often used in many branches of science including hydrodynamics, but using them we have to remember that they give us not the exact solution but approximate one (often good enough for our purposes). It is not always easy to choose the proper method for our case. When applying numerical methods, we can encounter many problems, such as:

- numerical diffusion and numerical dispersion,
- limitation of computation time and disc space,
- instability of the schemes used.

These problems make the selection of the method appropriate for solving a given equation even more difficult. First of all, the required accuracy and computation costs must be taken into account, and the main attention in this chapter is paid to this issue. It is of extreme importance for the interpretation of the results, as it may happen that values treated as physical were only the result of numerical errors.

5.2 Accuracy – truncation error

The accuracy of the solution is a very important element during numerical solution of the initial-boundary issue. Ferziger (1988) wrote "Knowledge of the accuracy of any procedure is essential to successful use of the method. This is especially true of numerical methods for solving partial differential equations (...)" in a special note concerning numerical accuracy.

The root of the finite difference methods are difference quotients created on the basis of expansions of the function into Taylor series (see Section 4.2). Due to the fact that not all elements of the series may be taken into account, truncated series are used for the construction of numerical schemes, which is the source of dissipation and dispersion errors influencing the obtained solution. The dissipation error can cause excessive smoothing of the solution, while the dispersion error creates oscillations of non-physical nature (Fletcher, 1991; Szymkiewicz, 2006; Thomas, 1995). Understanding the truncation error is therefore necessary for finding out the accuracy of the method and selecting the appropriate numerical scheme.

Most discussions in the literature state only the approximation order of a numerical method, which does not provide any information on the value and the nature of the error. However, detailed analyses concerning numerical errors in finite difference methods used to solve advection-diffusion equations are usually carried out for one-dimensional problems (like in case of works by: Ataie-Ashtiani *et al.*, 1996, 1999; Dehghan, 2004; Karahan, 2006). Comprehensive compilation of numerical schemes used to one-dimensional advection-diffusion equation, together with the determined truncation errors is presented by Fletcher (1991). In a two-dimensional case, the truncation errors were determined for the equations disregarding mixed derivatives (e.g. Noye & Tan, 1989), which limits the discussion to certain specific situations (as demonstrated in Chapter 3). At this point, attention should be paid to the latest analyses by Ataie-Ashtiani & Hosseini (2005a,b), where full 2D advection-diffusion including additional terms is discussed. The authors, however, focus only on the numerical diffusion error (dissipation error, if only second-order derivatives are taken into account in error analysis, is often called the numerical diffusion error). Numerical dispersion – also connected with the truncation of Taylor series – is also an unwanted effect present at the application of numerical schemes used in hydromechanics. Both kinds of errors are discussed in works of: Bielecka-Kieloch (1998); Szymkiewicz (2006) for two-dimensional advection equation.

Much attention was paid in this study to determination of numerical diffusion and numerical dispersion errors, in case of full 2D advection-diffusion

equation (including mixed derivatives). The determination method and analysis of the errors referred to the above will, therefore, be the subject of further discussion.

5.2.1 Modified Equation Approach

The accuracy of difference methods used for solving a transport equation can be determined by means of ***Modified Equation Approach*** – **MEA**. This method, presented in 1974 by Warming & Hyett, allows to determine the error resulting from truncation of Taylor series during the discretization of the equation. The error is, in fact, the difference between the real solution and the one obtained after the approximation of the equation with the given numerical scheme. MEA was used in hydromechanics by Abbott & Basco (1989); Fischer *et al.* (1979); Peyret & Taylor (1986); Szymkiewicz (2006), among others. If we label differential equation (4.5) as $E_{Dys} = 0$, and T is the truncation error, then the ***modified equation*** (which we solve in practice) can be defined as:

$$E_{Mod} = E_{Dys} + T = 0\,. \tag{5.1}$$

In order to create a modified equation for the schemes discussed in this study, the procedure presented in figure 5.1 has to be completed. Before commencing

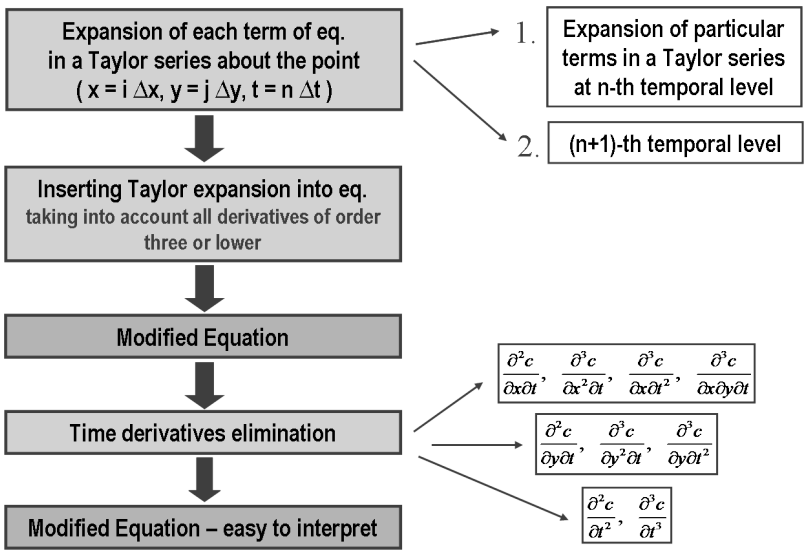

Figure 5.1: Modified Equation Approach – diagram

the construction of E_{Mod} equation (4.5) can be written down in the following form, for simplicity:

$$\begin{aligned} & b_0 c_{i,j}^{n+1} + b_1 c_{i+1,j}^{n+1} + b_2 c_{i-1,j}^{n+1} + b_3 c_{i,j+1}^{n+1} + b_4 c_{i,j-1}^{n+1} \\ & + b_5 c_{i+1,j+1}^{n+1} + b_6 c_{i+1,j-1}^{n+1} + b_7 c_{i-1,j+1}^{n+1} + b_8 c_{i-1,j-1}^{n+1} \\ & = a_0 c_{i,j}^{n} + a_1 c_{i+1,j}^{n} + a_2 c_{i-1,j}^{n} + a_3 c_{i,j+1}^{n} + a_4 c_{i,j-1}^{n} \\ & + a_5 c_{i+1,j+1}^{n} + a_6 c_{i+1,j-1}^{n} + a_7 c_{i-1,j+1}^{n} + a_8 c_{i-1,j-1}^{n} \,. \end{aligned} \tag{5.2}$$

The coefficients of this equation are, respectively:

$$\begin{aligned} b_0 &= 1 + \theta \left[2 \left(\mathcal{C}r_x^d + \mathcal{C}r_y^d \right) + \mathcal{C}r_x^a \left(1 - 2\alpha_1\right) + \mathcal{C}r_y^a \left(1 - 2\alpha_2\right) \right] , \\ a_0 &= 1 + (1-\theta) \left[-2 \left(\mathcal{C}r_x^d + \mathcal{C}r_y^d \right) + \mathcal{C}r_x^a \left(2\alpha_1 - 1\right) + \mathcal{C}r_y^a \left(2\alpha_2 - 1\right) \right] , \\ b_1 &= \theta \left(-\mathcal{C}r_x^d + \alpha_1 \mathcal{C}r_x^a \right) , \\ a_1 &= (1-\theta) \left(\mathcal{C}r_x^d - \alpha_1 \mathcal{C}r_x^a \right) , \\ b_2 &= \theta \left(-\mathcal{C}r_x^d - (1-\alpha_1) \mathcal{C}r_x^a \right) , \\ a_2 &= (1-\theta) \left[\mathcal{C}r_x^d + (1-\alpha_1) \mathcal{C}r_x^a \right] , \\ b_3 &= \theta \left(-\mathcal{C}r_y^d + \alpha_2 \mathcal{C}r_y^a \right) , \\ a_3 &= (1-\theta) \left(\mathcal{C}r_y^d - \alpha_2 \mathcal{C}r_y^a \right) , \\ b_4 &= \theta \left(-\mathcal{C}r_y^d - (1-\alpha_2) \mathcal{C}r_y^a \right) , \\ a_4 &= (1-\theta) \left[\mathcal{C}r_y^d + (1-\alpha_2) \mathcal{C}r_y^a \right] , \\ b_5 &= -2\theta \mathcal{C}r_{xy}^d \,, & a_5 &= 2\,(1-\theta)\, \mathcal{C}r_{xy}^d \,, \\ b_6 &= 2\theta \mathcal{C}r_{xy}^d \,, & a_6 &= -2\,(1-\theta)\, \mathcal{C}r_{xy}^d \,, \\ b_7 &= 2\theta \mathcal{C}r_{xy}^d \,, & a_7 &= -2\,(1-\theta)\, \mathcal{C}r_{xy}^d \,, \\ b_8 &= -2\theta \mathcal{C}r_{xy}^d \,, & a_8 &= 2\,(1-\theta)\, \mathcal{C}r_{xy}^d \,. \end{aligned} \tag{5.3}$$

The whole procedure starts with replacing each term of equation (5.2) by its expansion in Taylor series about the point ($x = i\Delta x$, $y = j\Delta y$, $t = n\Delta t$). We assume at the same time the existence of a continuous and differentiable function $c(x, y, t)$, which is equal to the solution to equation (2.13) in the grid nodes (Warming & Hyett, 1974).

The expansions of individual terms into Taylor series in the n-th time step can be written down in the following way:

$$c^n_{i\pm1,j} = c^n_{i,j} \pm \Delta x \frac{\partial c}{\partial x} + \frac{\Delta x^2}{2}\frac{\partial^2 c}{\partial x^2} \pm \frac{\Delta x^3}{6}\frac{\partial^3 c}{\partial x^3} + \dots , \tag{5.4a}$$

$$c^n_{i,j\pm1} = c^n_{i,j} \pm \Delta y \frac{\partial c}{\partial y} + \frac{\Delta y^2}{2}\frac{\partial^2 c}{\partial y^2} \pm \frac{\Delta y^3}{6}\frac{\partial^3 c}{\partial y^3} + \dots , \tag{5.4b}$$

$$\begin{aligned} c^n_{i\pm1,j\pm1} = c^n_{i,j} &\pm \Delta x \frac{\partial c}{\partial x} \pm \Delta y \frac{\partial c}{\partial y} + \frac{\Delta x^2}{2}\frac{\partial^2 c}{\partial x^2} + (\pm\Delta x)(\pm\Delta y)\frac{\partial^2 c}{\partial x \partial y} + \frac{\Delta y^2}{2}\frac{\partial^2 c}{\partial y^2} \\ &\pm \frac{\Delta x^3}{6}\frac{\partial^3 c}{\partial x^3} \pm \frac{\Delta x^2 \Delta y}{2}\frac{\partial^3 c}{\partial x^2 \partial y} \pm \frac{\Delta x \Delta y^2}{2}\frac{\partial^3 c}{\partial x \partial y^2} \pm \frac{\Delta y^3}{6}\frac{\partial^3 c}{\partial y^3} + \dots . \end{aligned} \tag{5.4c}$$

In the $(n+1)$-th time step they assume the following form:

$$c^{n+1}_{i,j} = c^n_{i,j} + \Delta t \frac{\partial c}{\partial t} + \frac{\Delta t^2}{2}\frac{\partial^2 c}{\partial t^2} + \frac{\Delta t^3}{6}\frac{\partial^3 c}{\partial t^3} + \dots , \tag{5.5a}$$

$$\begin{aligned} c^{n+1}_{i\pm1,j} = c^n_{i,j} &+ \Delta t \frac{\partial c}{\partial t} \pm \Delta x \frac{\partial c}{\partial x} + \frac{\Delta t^2}{2}\frac{\partial^2 c}{\partial t^2} \pm \Delta t \Delta x \frac{\partial^2 c}{\partial x \partial t} + \frac{\Delta x^2}{2}\frac{\partial^2 c}{\partial x^2} \\ &+ \frac{\Delta t^3}{6}\frac{\partial^3 c}{\partial t^3} \pm \frac{\Delta t^2 \Delta x}{2}\frac{\partial^3 c}{\partial x \partial t^2} + \frac{\Delta t \Delta x^2}{2}\frac{\partial^3 c}{\partial x^2 \partial t} \pm \frac{\Delta x^3}{6}\frac{\partial^3 c}{\partial x^3} + \dots , \end{aligned} \tag{5.5b}$$

$$\begin{aligned} c^{n+1}_{i,j\pm1} = c^n_{i,j} &+ \Delta t \frac{\partial c}{\partial t} \pm \Delta y \frac{\partial c}{\partial y} + \frac{\Delta t^2}{2}\frac{\partial^2 c}{\partial t^2} \pm \Delta t \Delta y \frac{\partial^2 c}{\partial y \partial t} + \frac{\Delta y^2}{2}\frac{\partial^2 c}{\partial y^2} \\ &+ \frac{\Delta t^3}{6}\frac{\partial^3 c}{\partial t^3} \pm \frac{\Delta t^2 \Delta y}{2}\frac{\partial^3 c}{\partial y \partial t^2} + \frac{\Delta t \Delta y^2}{2}\frac{\partial^3 c}{\partial y^2 \partial t} \pm \frac{\Delta y^3}{6}\frac{\partial^3 c}{\partial y^3} + \dots , \end{aligned} \tag{5.5c}$$

$$\begin{aligned} c^{n+1}_{i\pm1,j\pm1} = c^n_{i,j} &+ \Delta t \frac{\partial c}{\partial t} \pm \Delta x \frac{\partial c}{\partial x} \pm \Delta y \frac{\partial c}{\partial y} + \frac{\Delta t^2}{2}\frac{\partial^2 c}{\partial t^2} + \frac{\Delta x^2}{2}\frac{\partial^2 c}{\partial x^2} + \frac{\Delta y^2}{2}\frac{\partial^2 c}{\partial y^2} \\ &+ (\pm\Delta x)(\pm\Delta y)\frac{\partial^2 c}{\partial x \partial y} \pm \Delta x \Delta t \frac{\partial^2 c}{\partial x \partial t} \pm \Delta y \Delta t \frac{\partial^2 c}{\partial y \partial t} \\ &+ \frac{\Delta t^3}{6}\frac{\partial^3 c}{\partial t^3} \pm \frac{\Delta x^3}{6}\frac{\partial^3 c}{\partial x^3} \pm \frac{\Delta y^3}{6}\frac{\partial^3 c}{\partial y^3} + \Delta t(\pm\Delta x)(\pm\Delta y)\frac{\partial^3 c}{\partial x \partial y \partial t} \\ &\pm \frac{\Delta x^2 \Delta y}{2}\frac{\partial^3 c}{\partial x^2 \partial y} \pm \frac{\Delta x \Delta y^2}{2}\frac{\partial^3 c}{\partial x \partial y^2} + \frac{\Delta t \Delta x^2}{2}\frac{\partial^3 c}{\partial x^2 \partial t} \\ &+ \frac{\Delta t \Delta y^2}{2}\frac{\partial^3 c}{\partial y^2 \partial t} \pm \frac{\Delta t^2 \Delta x}{2}\frac{\partial^3 c}{\partial x \partial t^2} \pm \frac{\Delta t^2 \Delta y}{2}\frac{\partial^3 c}{\partial y \partial t^2} + \dots . \end{aligned} \tag{5.5d}$$

Inserting expansions (5.4) and (5.5) to the equation (5.2), after the reduction we obtain:

$$\begin{aligned}
&\frac{\partial c}{\partial t} + v_x \frac{\partial c}{\partial x} + v_y \frac{\partial c}{\partial y} + \frac{\Delta t}{2}\frac{\partial^2 c}{\partial t^2} \\
&\quad + \left[-D_{xx} + (2\alpha_1 - 1)\,\frac{v_x \Delta x}{2}\right]\frac{\partial^2 c}{\partial x^2} + \left[-D_{yy} + (2\alpha_2 - 1)\,\frac{v_y \Delta y}{2}\right]\frac{\partial^2 c}{\partial y^2} \\
&\qquad - 2D_{xy}\frac{\partial^2 c}{\partial x \partial y} + \theta v_x \Delta t \frac{\partial^2 c}{\partial x \partial t} + \theta v_y \Delta t \frac{\partial^2 c}{\partial y \partial t} \\
&\qquad + \frac{\Delta t^2}{6}\frac{\partial^3 c}{\partial t^3} + \frac{v_x \Delta x^2}{6}\frac{\partial^3 c}{\partial x^3} + \frac{v_y \Delta y^2}{6}\frac{\partial^3 c}{\partial y^3} \\
&\quad - 2\theta D_{xy}\Delta t \frac{\partial^3 c}{\partial x \partial y \partial t} + \theta \Delta t \left[-2D_{xx} + (2\alpha_1 - 1)\,\frac{v_x \Delta x}{2}\right]\frac{\partial^3 c}{\partial x^2 \partial t} \\
&\qquad + \theta \Delta t \left[-2D_{yy} + (2\alpha_2 - 1)\,\frac{v_y \Delta y}{2}\right]\frac{\partial^3 c}{\partial y^2 \partial t} \\
&\qquad + \theta \frac{v_x \Delta t^2}{2}\frac{\partial^3 c}{\partial x \partial t^2} + \theta \frac{v_y \Delta t^2}{2}\frac{\partial^3 c}{\partial y \partial t^2} = 0\,. \qquad (5.6)
\end{aligned}$$

During the transformations, the derivatives of the fourth-order and higher were omitted. For the details of the derivation of equation (5.6) and the proposed table facilitating transformations, see Appendix E. The obtained equation is the sought modified equation (E_{Mod}). For the simplicity of notation, the following symbols were introduced for coefficients before the respective partial derivatives:

$$\begin{aligned}
a &= \frac{v_x \Delta x^2}{6}, & l &= \theta v_x \Delta t, \\
b &= \frac{v_y \Delta y^2}{6}, & m &= \theta v_y \Delta t, \\
d &= v_x, & n &= \frac{\Delta t^2}{6}, \\
e &= v_y, & o &= -2\theta D_{xy}\Delta t, \\
f &= \frac{\Delta t}{2}, & p &= \theta \Delta t \left(-2D_{xx} + (2\alpha_1 - 1)\frac{v_x \Delta x}{2}\right), \qquad (5.7) \\
g &= -D_{xx} + (2\alpha_1 - 1)\frac{v_x \Delta x}{2}, & q &= \theta \Delta t \left(-2D_{yy} + (2\alpha_2 - 1)\frac{v_y \Delta y}{2}\right), \\
h &= -D_{yy} + (2\alpha_2 - 1)\frac{v_y \Delta y}{2}, & r &= \theta \frac{v_x \Delta t^2}{2}, \\
k &= -2D_{xy}, & z &= \theta \frac{v_y \Delta t^2}{2}.
\end{aligned}$$

The modified equation (5.6) assumes then the following form:

$$\frac{\partial c}{\partial t} + d\frac{\partial c}{\partial x} + e\frac{\partial c}{\partial y} + f\frac{\partial^2 c}{\partial t^2} + g\frac{\partial^2 c}{\partial x^2} + h\frac{\partial^2 c}{\partial y^2} + k\frac{\partial^2 c}{\partial x \partial y} + l\frac{\partial^2 c}{\partial x \partial t} + m\frac{\partial^2 c}{\partial y \partial t}$$
$$+ n\frac{\partial^3 c}{\partial t^3} + a\frac{\partial^3 c}{\partial x^3} + b\frac{\partial^3 c}{\partial y^3} + o\frac{\partial^3 c}{\partial x \partial y \partial t} + p\frac{\partial^3 c}{\partial x^2 \partial t} + q\frac{\partial^3 c}{\partial y^2 \partial t} + r\frac{\partial^3 c}{\partial x \partial t^2} + z\frac{\partial^3 c}{\partial y \partial t^2} = 0\,. \tag{5.8}$$

The next key point is the elimination of higher order time derivatives:

$$\frac{\partial^2 c}{\partial t^2}, \frac{\partial^3 c}{\partial t^3}, \frac{\partial^2 c}{\partial x \partial t}, \frac{\partial^3 c}{\partial x^2 \partial t}, \frac{\partial^3 c}{\partial x \partial t^2}, \frac{\partial^2 c}{\partial y \partial t}, \frac{\partial^3 c}{\partial y^2 \partial t}, \frac{\partial^3 c}{\partial y \partial t^2}, \text{ and } \frac{\partial^3 c}{\partial x \partial y \partial t}\,. \tag{5.9}$$

This operation, leading to leaving only the first derivative $\frac{\partial c}{\partial t}$ and space derivatives, will allow to interpret the truncation error. In order to obtain appropriate expressions for time derivatives, appropriate differentiation operations must be performed on the modified equation (Thomas, 1995). In order to replace the terms:

$$\frac{\partial^2 c}{\partial x \partial t}, \frac{\partial^3 c}{\partial x^2 \partial t}, \frac{\partial^3 c}{\partial x \partial t^2}, \frac{\partial^3 c}{\partial x \partial y \partial t} \tag{5.10}$$

we differentiate equation (5.6) successively with respect to:

$$\frac{\partial}{\partial x}, \frac{\partial^2}{\partial x^2}, \frac{\partial^2}{\partial x \partial t}, \frac{\partial^2}{\partial x \partial y}. \tag{5.11}$$

We proceed analogically to obtain the terms:

$$\frac{\partial^2 c}{\partial y \partial t}, \frac{\partial^3 c}{\partial y^2 \partial t}, \frac{\partial^3 c}{\partial y \partial t^2}. \tag{5.12}$$

In order to find relevant expressions for:

$$\frac{\partial^2 c}{\partial t^2}, \frac{\partial^3 c}{\partial t^3} \tag{5.13}$$

we differentiate equation (5.6) with respect to:

$$\frac{\partial}{\partial t}, \frac{\partial^2}{\partial t^2}. \tag{5.14}$$

After appropriate transformation and taking into consideration third-order derivatives, we obtain:

$$\begin{aligned}\frac{\partial^2 c}{\partial t^2} &= d^2\frac{\partial^2 c}{\partial x^2} + e^2\frac{\partial^2 c}{\partial y^2} + 2de\frac{\partial^2 c}{\partial x\partial y} + 2d(fd^2+g-ld)\frac{\partial^3 c}{\partial x^3}+\\ &+ 2e(fe^2+h-em)\frac{\partial^3 c}{\partial y^3} + 2(3d^2ef+kd-2dle-md^2+eg)\frac{\partial^3 c}{\partial x^2\partial y}+\\ &+ 2(3fde^2+hd-2emd+kd-le^2)\frac{\partial^3 c}{\partial x\partial y^2},\end{aligned} \tag{5.15a}$$

$$\frac{\partial^3 c}{\partial t^3} = -d^3\frac{\partial^3 c}{\partial x^3} - e^3\frac{\partial^3 c}{\partial y^3} - 3d^2e\frac{\partial^3 c}{\partial x^2\partial y} - 3de^2\frac{\partial^3 c}{\partial x\partial y^2}, \tag{5.15b}$$

$$\begin{aligned}\frac{\partial^2 c}{\partial x\partial t} &= -d\frac{\partial^2 c}{\partial x^2} - e\frac{\partial^2 c}{\partial x\partial y} + (-fd^2-g+ld)\frac{\partial^3 c}{\partial x^3}+\\ &+ (-2def-k+le+dm)\frac{\partial^3 c}{\partial x^2\partial y} + (-fe^2-h+em)\frac{\partial^3 c}{\partial x\partial y^2},\end{aligned} \tag{5.15c}$$

$$\frac{\partial^3 c}{\partial x^2\partial t} = -d\frac{\partial^3 c}{\partial x^3} - e\frac{\partial^3 c}{\partial x^2\partial y}, \tag{5.15d}$$

$$\frac{\partial^3 c}{\partial x\partial t^2} = d^2\frac{\partial^3 c}{\partial x^3} + 2de\frac{\partial^3 c}{\partial x^2\partial y} + e^2\frac{\partial^3 c}{\partial x\partial y^2}, \tag{5.15e}$$

$$\begin{aligned}\frac{\partial^2 c}{\partial y\partial t} &= -d\frac{\partial^2 c}{\partial x\partial y} - e\frac{\partial^2 c}{\partial y^2} + (-fd^2-g+dl)\frac{\partial^3 c}{\partial x^2\partial y}+\\ &+ (-2def-k+le+md)\frac{\partial^3 c}{\partial x\partial y^2} + (-fe^2-h+em)\frac{\partial^3 c}{\partial y^3},\end{aligned} \tag{5.15f}$$

$$\frac{\partial^3 c}{\partial y^2\partial t} = -d\frac{\partial^3 c}{\partial x\partial y^2} - e\frac{\partial^3 c}{\partial y^3}, \tag{5.15g}$$

$$\frac{\partial^3 c}{\partial y\partial t^2} = d^2\frac{\partial^3 c}{\partial x^2\partial y} + 2de\frac{\partial^3 c}{\partial x\partial y^2} + e^2\frac{\partial^3 c}{\partial y^3}, \tag{5.15h}$$

$$\frac{\partial^3 c}{\partial x\partial y\partial t} = -d\frac{\partial^3 c}{\partial x^2\partial y} - e\frac{\partial^3 c}{\partial x\partial y^2}. \tag{5.15i}$$

In various analyses, an error often occurs which Thomas (1995) pays his attention to, and it consists in the application of elimination of time derivatives of the solved original equation (in the discussed situation, equation (2.13)), instead of the modified equation (here equation (5.6)). It may also happen that in some cases the result will be the same – irrespective of the equation applied by us. Often, however, as in case of the analysed two-dimensional advection-diffusion equation, this leads to neglecting some terms in formulae (5.15), and as a result – modification of the truncation error which is the aim of the discussion. For the considered equation, in case of the second derivative in time $\frac{\partial^2 c}{\partial t^2}$, differentiating the initial equation (2.13) with respect to $\frac{\partial}{\partial t}$, instead of the modified equation (5.6), the following relation may be obtained erroneously:

$$\begin{aligned}
\frac{\partial^2 c}{\partial t^2} &= (-2D_{xx}v_x)\frac{\partial^3 c}{\partial x^3} + (-2D_{yy}v_y)\frac{\partial^3 c}{\partial y^3} \\
&+ (-2D_{xx}v_y - 4D_{xy}v_x)\frac{\partial^3 c}{\partial x^2 \partial y} \\
&+ (-2D_{yy}v_x - 4D_{xy}v_y)\frac{\partial^3 c}{\partial x \partial y^2} \\
&+ v_x^2\frac{\partial^2 c}{\partial x^2} + 2v_x v_y \frac{\partial^2 c}{\partial x \partial y} + v_y^2 \frac{\partial^2 c}{\partial y^2};
\end{aligned} \tag{5.16}$$

instead of relation (5.15a). In case of mixed derivatives, one obtains the relations

$$\frac{\partial^2 c}{\partial x \partial t} = D_{xx}\frac{\partial^3 c}{\partial x^3} + D_{yy}\frac{\partial^3 c}{\partial x \partial y^2} + 2D_{xy}\frac{\partial^3 c}{\partial x^2 \partial y} - v_x\frac{\partial^2 c}{\partial x^2} - v_y\frac{\partial^2 c}{\partial x \partial y}; \tag{5.17}$$

$$\frac{\partial^2 c}{\partial y \partial t} = D_{xx}\frac{\partial^3 c}{\partial x^2 \partial y} + D_{yy}\frac{\partial^3 c}{\partial y^3} + 2D_{xy}\frac{\partial^3 c}{\partial x \partial y^2} - v_x\frac{\partial^2 c}{\partial x \partial y} - v_y\frac{\partial^2 c}{\partial y^2}; \tag{5.18}$$

instead of (5.15c) and (5.15f). The expressions (5.16), (5.17) and (5.18) are true only for equation (2.13) and not for the considered modified equation (5.6) (Thomas, 1995). Differences occur in the obtained coefficients before the third-order spatial derivatives.

After inserting the appropriate expressions (5.15) to the modified equation (5.6), the equation assumes the form:

$$
\begin{aligned}
&\frac{\partial c}{\partial t} + v_x \frac{\partial c}{\partial x} + v_y \frac{\partial c}{\partial y} - 2D_{xy}\frac{\partial^2 c}{\partial x \partial y} - D_{xx}\frac{\partial^2 c}{\partial x^2} - D_{yy}\frac{\partial^2 c}{\partial y^2} \\
&\qquad = 2\left[v_x v_y \Delta t \left(\theta - \frac{1}{2}\right)\right]\frac{\partial^2 c}{\partial x \partial y} \\
&\qquad + \left[v_x^2 \Delta t \left(\theta - \frac{1}{2}\right) - \frac{v_x \Delta x}{2}\left(2\alpha_1 - 1\right)\right]\frac{\partial^2 c}{\partial x^2} \\
&\qquad + \left[v_y^2 \Delta t \left(\theta - \frac{1}{2}\right) - \frac{v_y \Delta y}{2}\left(2\alpha_2 - 1\right)\right]\frac{\partial^2 c}{\partial y^2} \\
&- \left[+\frac{v_x^3 \Delta t^2}{3}\eta - v_x^2 \Delta t \Delta x \left(\theta - \frac{1}{2}\right)\left(2\alpha_1 - 1\right) + \frac{v_x \Delta x^2}{6} + v_x \Delta t D_{xx}\xi\right]\frac{\partial^3 c}{\partial x^3} \\
&- \left[+\frac{v_y^3 \Delta t^2}{3}\eta - v_y^2 \Delta t \Delta y \left(\theta - \frac{1}{2}\right)\left(2\alpha_2 - 1\right) + \frac{v_y \Delta y^2}{6} + v_y \Delta t D_{yy}\xi\right]\frac{\partial^3 c}{\partial y^3} \\
&\qquad - \left[+v_x^2 v_y \Delta t^2 \eta - v_x v_y \Delta t \Delta x \left(\theta - \frac{1}{2}\right)\left(2\alpha_1 - 1\right)\right. \\
&\qquad\qquad \left. + v_y \Delta t D_{xx}\xi + 4 v_x \Delta t D_{xy}\left(\theta - \frac{1}{2}\right)\right]\frac{\partial^3 c}{\partial x^2 \partial y} \\
&\qquad - \left[+v_x v_y^2 \Delta t^2 \eta - v_x v_y \Delta t \Delta y \left(\theta - \frac{1}{2}\right)\left(2\alpha_2 - 1\right)\right. \\
&\qquad\qquad \left. + v_x \Delta t D_{yy}\xi + 4 v_y \Delta t D_{xy}\left(\theta - \frac{1}{2}\right)\right]\frac{\partial^3 c}{\partial x \partial y^2}\,; \qquad (5.19)
\end{aligned}
$$

where:

$$\eta = \left(1 - 3\theta + 3\theta^2\right),\ \xi = \left(3\theta - 1\right).$$

It is easy to notice additional expressions that do not appear in the solved original equation (2.13). Those expressions represent the terms that have been neglected in the process of discretization of the original equation, that is the truncation error sought. Even terms relate to the ***dissipation*** error while the odd terms relate to the ***dispersion*** (Fletcher, 1991). For smooth functions, the value of the truncation error is determined by the value of the first expression of the truncated part of the series (Szymkiewicz, 2006), therefore, we can limit our discussion to the lowest orders of even and odd derivatives occurring in

the truncation error. The error related to the second-order derivatives is called ***numerical diffusion***, and the error related to the third-order derivatives is called ***numerical dispersion***, which in the two-dimensional case assume the tensor form (Szymkiewicz, 2006).

Writing down equation (5.19) in vector-like form, analogously to equation (2.6), we obtain:

$$\begin{aligned}&\frac{\partial c(\mathbf{x},t)}{\partial t} + \mathbf{v}(\mathbf{x},t)\cdot\nabla c(\mathbf{x},t) - \nabla\Big[\mathbf{D}(\mathbf{x},t)\cdot\nabla c(\mathbf{x},t)\Big]\\ &= \nabla\left[\mathbf{D^N}(\mathbf{x},t)\cdot\nabla c(\mathbf{x},t)\right] + \nabla\left[\mathbf{T^N}(\mathbf{x},t)\cdot\Delta c(\mathbf{x},t)\right];\end{aligned} \tag{5.20}$$

where:

$$\underset{\textit{dispersion tensor}}{\mathbf{D} = \begin{bmatrix} D_{xx} & D_{xy} \\ D_{yx} & D_{yy} \end{bmatrix}}, \quad \underset{\textit{numerical diffusion tensor}}{\mathbf{D^N} = \begin{bmatrix} D^N_{11} & D^N_{12} \\ D^N_{21} & D^N_{22} \end{bmatrix}}, \quad \underset{\textit{numerical dispersion tensor}}{\mathbf{T^N} = \begin{bmatrix} T^N_{11} & T^N_{12} \\ T^N_{21} & T^N_{22} \end{bmatrix}}.$$

Now, the errors of numerical diffusion and dispersion can be easily compared for the numerical schemes discussed in the study. In the general case for the advection-diffusion equation (2.6) the coefficients of numerical diffusion and dispersion tensors are:

$$D^N_{11} = v_x\Delta x\left[\mathcal{C}r^a_x\left(\theta - \frac{1}{2}\right) - \left(\alpha_1 - \frac{1}{2}\right)\right], \tag{5.21a}$$

$$D^N_{12} = v_x v_y \Delta t\left(\theta - \frac{1}{2}\right), \tag{5.21b}$$

$$D^N_{21} = v_x v_y \Delta t\left(\theta - \frac{1}{2}\right), \tag{5.21c}$$

$$D^N_{22} = v_y\Delta y\left[\mathcal{C}r^a_y\left(\theta - \frac{1}{2}\right) - \left(\alpha_2 - \frac{1}{2}\right)\right], \tag{5.21d}$$

$$T_{11}^N = v_x \Delta x^2 \left[-\frac{(\mathcal{C}r_x^a)^2}{3}\eta + \mathcal{C}r_x^a \left(\theta - \frac{1}{2}\right)(2\alpha_1 - 1) - \frac{1}{6} - \mathcal{C}r_x^d \xi \right], \tag{5.21e}$$

$$\begin{aligned} T_{12}^N = v_y \Delta x^2 \Bigg[& -(\mathcal{C}r_x^a)^2 \eta + \mathcal{C}r_x^a \left(\theta - \frac{1}{2}\right)(2\alpha_1 - 1) \\ & -\mathcal{C}r_x^d \xi - 16 \frac{\mathcal{C}r_x^a \mathcal{C}r_{xy}^d}{\mathcal{C}r_y^a} \left(\theta - \frac{1}{2}\right) \Bigg], \end{aligned} \tag{5.21f}$$

$$\begin{aligned} T_{21}^N = v_x \Delta y^2 \Bigg[& -(\mathcal{C}r_y^a)^2 \eta + \mathcal{C}r_y^a \left(\theta - \frac{1}{2}\right)(2\alpha_2 - 1) \\ & -\mathcal{C}r_y^d \xi - 16 \frac{\mathcal{C}r_y^a \mathcal{C}r_{xy}^d}{\mathcal{C}r_x^a} \left(\theta - \frac{1}{2}\right) \Bigg], \end{aligned} \tag{5.21g}$$

$$T_{22}^N = v_y \Delta y^2 \left[-\frac{(\mathcal{C}r_y^a)^2}{3}\eta + \mathcal{C}r_y^a \left(\theta - \frac{1}{2}\right)(2\alpha_2 - 1) - \frac{1}{6} - \mathcal{C}r_y^d \xi \right]. \tag{5.21h}$$

Assuming appropriate values of weighting parameters, the values of errors for the schemes in question can be easily calculated and they have been collected in tables 5.1 (UP) and 5.2 (CN, FI).

As expected, only in case of Crank-Nicolson scheme, we can avoid the serious problem of numerical diffusion. Nevertheless, with inappropriate selection of simulation parameters, non-physical oscillations can occur in the solution due to the numerical dispersion error. In case of Upwind and Fully Implicit schemes, both numerical diffusion and numerical dispersion tensors are different from zero.

For illustration, in a straight channel for which the analytical solution can be obtained, simulations with the application of Crank-Nicolson and Upwind schemes were carried out. Figure 5.2 presents the results of the simulations after 1150 seconds for selected parameters, with the application of the UP (fig. 5.2(b)) and CN (fig. 5.2(c)) methods, respectively, and the analytical solution (fig. 5.2(a)). In case of the CN scheme, there is no visible difference between the numerical and the analytical solutions, whereas the difference is conspicuous for the UP scheme. The maximum of concentration is situated at the same point, but its value and the shape of concentration distribution differ significantly from the analytical solution and the solution with the application of the Crank-Nicolson scheme. Numerical diffusion is the reason of the above.

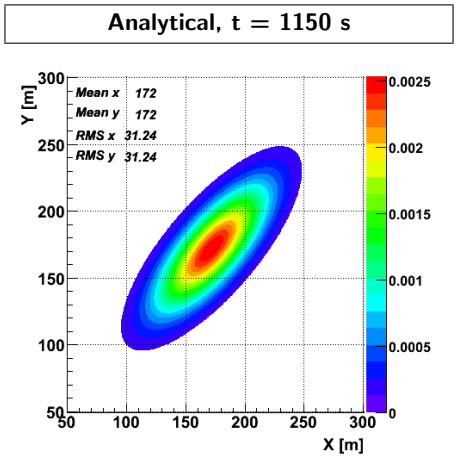

(a) Analytical solution

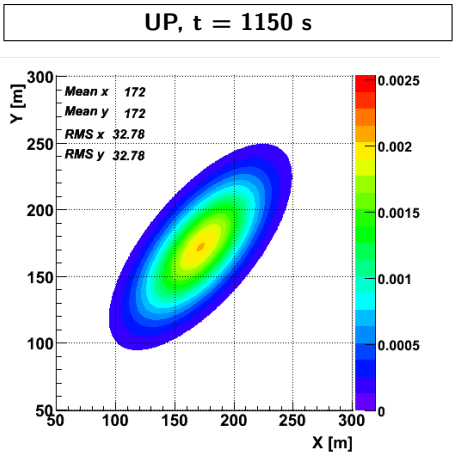

(b) Numerical solution, scheme UP

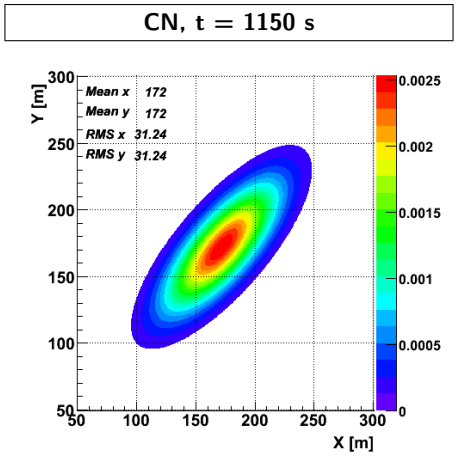

(c) Numerical solution, scheme CN

Figure 5.2: Analytical (a) and numerical solution with the application of UP scheme (b) and CN scheme (c) after 1150 seconds; simulation parameters: $\Delta x = \Delta y = 1\,\mathrm{m}$ and $\Delta t = 0.5\,\mathrm{s}$, $v_x = v_y = 0.106\,\frac{\mathrm{m}}{\mathrm{s}}$, $D_{xx} = D_{yy} = 0.425\,\frac{\mathrm{m}^2}{\mathrm{s}}$, $D_{xy} = D_{yx} = 0.325\,\frac{\mathrm{m}^2}{\mathrm{s}}$; mass $M = 10\,\mathrm{a.u.}$ was discharged at point $x_0 = 50\,\mathrm{m}$, $y_0 = 50\,\mathrm{m}$ at time $t_0 = 0\,\mathrm{s}$

Table 5.1: Values of coefficients of numerical diffusion and dispersion tensors for UP scheme

	UP
D_{11}^N	$-v_x \Delta x \left[\frac{\mathcal{C}r_x^a}{2} + \left(\alpha_1 - \frac{1}{2}\right)\right]$
D_{12}^N	$-\frac{v_x v_y \Delta t}{2}$
D_{21}^N	$-\frac{v_x v_y \Delta t}{2}$
D_{22}^N	$-v_y \Delta y \left[\frac{\mathcal{C}r_y^a}{2} + \left(\alpha_2 - \frac{1}{2}\right)\right]$
T_{11}^N	$v_x \Delta x^2 \left[-\frac{(\mathcal{C}r_x^a)^2}{3} - \mathcal{C}r_x^a \left(\alpha_1 - \frac{1}{2}\right) - \frac{1}{6} + \mathcal{C}r_x^d\right]$
T_{12}^N	$v_y \Delta x^2 \left[-(\mathcal{C}r_x^a)^2 - \mathcal{C}r_x^a \left(\alpha_1 - \frac{1}{2}\right) + \mathcal{C}r_x^d + 8\frac{\mathcal{C}r_x^a \mathcal{C}r_{xy}^d}{\mathcal{C}r_y^a}\right]$
T_{21}^N	$v_x \Delta y^2 \left[-(\mathcal{C}r_y^a)^2 - \mathcal{C}r_y^a \left(\alpha_2 - \frac{1}{2}\right) + \mathcal{C}r_y^d + 8\frac{\mathcal{C}r_y^a \mathcal{C}r_{xy}^d}{\mathcal{C}r_x^a}\right]$
T_{22}^N	$v_y \Delta y^2 \left[-\frac{(\mathcal{C}r_y^a)^2}{3} - \mathcal{C}r_y^a \left(\alpha_2 - \frac{1}{2}\right) - \frac{1}{6} + \mathcal{C}r_y^d\right]$

Using the Upwind scheme, we solve the advection-diffusion equation with a greater diffusion coefficient effectively:

$$D_{i,j}^{Res} = D_{i,j} + D_{i,j}^N, \text{ for } i \in \{1, 2\}; \tag{5.22}$$

where:
$D_{i,j}$ – actual dispersion coefficient,
$D_{i,j}^N$ – numerical diffusion coefficient,
$D_{i,j}^{Res}$ – resultant (effective) diffusion coefficient.

Table 5.2: Values of coefficients of numerical diffusion and dispersion tensors for CN and FI schemes

	CN	**FI**
D_{11}^N	0	$\frac{v_x^2 \Delta t}{2}$
D_{12}^N	0	$\frac{v_x v_y \Delta t}{2}$
D_{21}^N	0	$\frac{v_x v_y \Delta t}{2}$
D_{22}^N	0	$\frac{v_y^2 \Delta t}{2}$
T_{11}^N	$-\frac{v_x \Delta x^2}{2}\left[\frac{(\mathcal{C}r_x^a)^2}{6}+\frac{1}{3}+\mathcal{C}r_x^d\right]$	$-v_x \Delta x^2\left[\frac{(\mathcal{C}r_x^a)^2}{3}+\frac{1}{6}+2\mathcal{C}r_x^d\right]$
T_{12}^N	$-\frac{v_y \Delta x^2}{2}\left[\frac{(\mathcal{C}r_x^a)^2}{2}+\mathcal{C}r_x^d\right]$	$-v_y \Delta x^2\left[(\mathcal{C}r_x^a)^2+2\mathcal{C}r_x^d+8\frac{\mathcal{C}r_x^a \mathcal{C}r_{xy}^d}{\mathcal{C}r_y^a}\right]$
T_{21}^N	$-\frac{v_x \Delta y^2}{2}\left[\frac{(\mathcal{C}r_y^a)^2}{2}+\mathcal{C}r_y^d\right]$	$-v_x \Delta y^2\left[(\mathcal{C}r_y^a)^2+2\mathcal{C}r_y^d+8\frac{\mathcal{C}r_y^a \mathcal{C}r_{xy}^d}{\mathcal{C}r_x^a}\right]$
T_{22}^N	$-\frac{v_y \Delta y^2}{2}\left[\frac{(\mathcal{C}r_y^a)^2}{6}+\frac{1}{3}+\mathcal{C}r_y^d\right]$	$-v_y \Delta y^2\left[\frac{(\mathcal{C}r_y^a)^2}{3}+\frac{1}{6}+2\mathcal{C}r_y^d\right]$

In the example in question, the resultant diffusion tensor is:

$$\underset{\textit{effective diffusion tensor}}{\mathbf{D}^{\mathbf{Res}} = \begin{bmatrix} 0.475 & 0.322 \\ 0.322 & 0.475 \end{bmatrix}} = \underset{\textit{actual dispersion tensor}}{\begin{bmatrix} 0.425 & 0.325 \\ 0.325 & 0.425 \end{bmatrix}} + \underset{\textit{numerical diffusion tensor}}{\begin{bmatrix} 0.05 & -0.003 \\ -0.003 & 0.05 \end{bmatrix}}.$$

For detailed comparison of both (UP and CN) schemes with analytical solution, see Chapter 7.

It can be verified that the value of numerical diffusion coefficient resulting from calculations based on MEA is the same as the value of numerical diffusion coefficient obtained during the simulation. For simplification, let us consider the situation where:

$$v_x > 0, \quad v_y = 0, \quad D_{xy} = D_{yx} = 0 \quad \text{and} \quad D_{yy} = 0. \tag{5.23}$$

Then the components of numerical diffusion and numerical dispersion tensors are, respectively:

$$\mathbf{D^N} = \begin{bmatrix} -\dfrac{v_x}{2}\left(v_x \Delta t - \Delta x\right) & 0 \\ \\ 0 & 0 \end{bmatrix},$$

$$\mathbf{T^N} = \begin{bmatrix} v_x \left[D_{xx}\Delta t - \dfrac{1}{6}\left(\Delta x^2 - \Delta t^2 v_x^2\right)\right] & 0 \\ \\ 0 & 0 \end{bmatrix}.$$

The simulation parameters have been selected in such a way that all the components of the numerical dispersion tensor be equal 0, for $v_x \neq 0$, i.e. we demand that:

$$v_x \left[D_{xx}\Delta t - \frac{1}{6}\left(\Delta x^2 - \Delta t^2 v_x^2\right)\right] = 0 \tag{5.24}$$

$$\Updownarrow v_x \neq 0 \tag{5.25}$$

$$D_{xx} = \frac{1}{6}\left(\frac{\Delta x^2}{\Delta t} - \Delta t v_x^2\right), \tag{5.26}$$

that is, for example:

$$\Delta x = 1,\ \Delta t = 1 \Rightarrow\ D_{xx} = \frac{1}{6}\left(1 - v_x^2\right); \tag{5.27}$$

$$\text{for} \quad v_x = 0.15 \ \Rightarrow\ D_{xx} = 0.163\,. \tag{5.28}$$

Table 5.3: Comparison of numerical diffusion error calculated using modified equation approach and determined based on the simulation; UP scheme

Δt	Δx	v_x	D_{xx}	$\mathcal{C}r_x^a$	$\mathcal{C}r_x^d$	D_{11}^N	D_{xx}^{Res}	No of time steps	σ_A	σ_S	σ_N
1	1	0.15	0.163	0.15	0.163	0.064	0.227	100	5.71 ± 0.13	6.73 ± 0.15	6.733
								500	12.77 ± 0.28	15.05 ± 0.34	15.055
1	1	0.001	0.1667	0.001	0.1667	0.0005	0.1672	100	5.77 ± 0.12	5.78 ± 0.12	5.782
								500	12.91 ± 0.29	12.93 ± 0.29	12.93
1	1	0.001	0.0167	0.001	0.0167	0.0005	0.0172	500	4.082 ± 0.091	4.141 ± 0.095	4.143
0.5	1	0.15	0.33	0.075	0.166	0.069	0.401	100	6.76 ± 0.13	6.33 ± 0.14	6.33
1	2	0.15	0.64	0.075	0.161	0.14	0.78	100	5.67 ± 0.13	6.26 ± 0.14	6.256
								500	12.69 ± 0.29	13.99 ± 0.31	13.99

σ_S – standard deviation from Gauss distribution adjusted to the results of the simulation
σ_A – standard deviation of the analytical solution
σ_N – standard deviation determined for the resultant diffusion coefficient taking into account the calculated numerical diffusion error

The comparison of the results obtained on the basis of theoretical discussion and computer simulations is presented in table 5.3. For simulation results after 100 or 500 time steps the Gauss distribution was adjusted, and then the standard deviation σ_S was read out. In the same way the standard deviation σ_A was read out for the analytical solution, i.e. solution not affected by the numerical diffusion error. Standard deviation resulting from the theoretically determined numerical diffusion coefficient σ_N was determined on the basis of the known relation:

$$\sigma_N = \sqrt{2D_{xx}^{Res}t}\,. \tag{5.29}$$

When $\Delta x \neq 1$ and $\Delta t \neq 1$, the above equation reads:

$$\sigma_N = \sqrt{2\frac{D_{xx}^{Res}}{\Delta x^2}n\Delta t}\,; \tag{5.30}$$

where:

n – number of time steps.

The values of σ_N are in agreement with the values of σ_S and, as expexted, are higher than the values of σ_A resulting from analytical solution, not affected by the numerical diffusion error.

5.2.2 Truncation error for Alternating Direction Implicit method

In case of Alternating Direction Implicit method (ADI), the calculations are carried out in two stages: (4.18) and (4.19). In order to determine the truncation error, we need to step back to the formula equivalent to both equations (4.17), which, for the sake of simplification, (like in case of equation (4.5)) we shall note as:

$$\begin{aligned} &b_0c_{i,j}^{n+1} + b_1c_{i+1,j}^{n+1} + b_2c_{i-1,j}^{n+1} + b_3c_{i,j+1}^{n+1} + b_4c_{i,j-1}^{n+1} \\ &+b_5c_{i+1,j+1}^{n+1} + b_6c_{i+1,j-1}^{n+1} + b_7c_{i-1,j+1}^{n+1} + b_8c_{i-1,j-1}^{n+1} \\ &= a_0c_{i,j}^{n} + a_1c_{i+1,j}^{n} + a_2c_{i-1,j}^{n} + a_3c_{i,j+1}^{n} + a_4c_{i,j-1}^{n} \\ &+a_5c_{i+1,j+1}^{n} + a_6c_{i+1,j-1}^{n} + a_7c_{i-1,j+1}^{n} + a_8c_{i-1,j-1}^{n}\,. \end{aligned} \tag{5.31}$$

The coefficients are, in this case, respectively:

$$
\begin{aligned}
b_0 &= 1 + \mathcal{C}r_y^d + \mathcal{C}r_x^d + \mathcal{C}r_x^d \mathcal{C}r_y^d, \\
b_1 &= \frac{\mathcal{C}r_x^a}{4} - \frac{\mathcal{C}r_x^d}{2} + \frac{\mathcal{C}r_x^a \mathcal{C}r_y^d}{4} - \frac{\mathcal{C}r_x^d \mathcal{C}r_y^d}{2}, \\
b_2 &= -\frac{\mathcal{C}r_x^a}{4} - \frac{\mathcal{C}r_x^d}{2} - \frac{\mathcal{C}r_x^a \mathcal{C}r_y^d}{4} - \frac{\mathcal{C}r_x^d \mathcal{C}r_y^d}{2}, \\
b_3 &= \frac{\mathcal{C}r_y^a}{4} - \frac{\mathcal{C}r_y^d}{2} + \frac{\mathcal{C}r_y^a \mathcal{C}r_x^d}{4} - \frac{\mathcal{C}r_x^d \mathcal{C}r_y^d}{2}, \\
b_4 &= -\frac{\mathcal{C}r_y^a}{4} - \frac{\mathcal{C}r_y^d}{2} - \frac{\mathcal{C}r_y^a \mathcal{C}r_x^d}{4} - \frac{\mathcal{C}r_x^d \mathcal{C}r_y^d}{2}, \\
b_5 &= \frac{\mathcal{C}r_x^a \mathcal{C}r_y^a}{16} - \frac{\mathcal{C}r_x^a \mathcal{C}r_y^d}{8} - \frac{\mathcal{C}r_y^a \mathcal{C}r_x^d}{8} + \frac{\mathcal{C}r_x^d \mathcal{C}r_y^d}{4}, \\
b_6 &= -\frac{\mathcal{C}r_x^a \mathcal{C}r_y^a}{16} - \frac{\mathcal{C}r_x^a \mathcal{C}r_y^d}{8} + \frac{\mathcal{C}r_y^a \mathcal{C}r_x^d}{8} + \frac{\mathcal{C}r_x^d \mathcal{C}r_y^d}{4}, \\
b_7 &= -\frac{\mathcal{C}r_x^a \mathcal{C}r_y^a}{16} + \frac{\mathcal{C}r_x^a \mathcal{C}r_y^d}{8} - \frac{\mathcal{C}r_y^a \mathcal{C}r_x^d}{8} + \frac{\mathcal{C}r_x^d \mathcal{C}r_y^d}{4}, \\
b_8 &= \frac{\mathcal{C}r_x^a \mathcal{C}r_y^a}{16} + \frac{\mathcal{C}r_x^a \mathcal{C}r_y^d}{8} + \frac{\mathcal{C}r_y^a \mathcal{C}r_x^d}{8} + \frac{\mathcal{C}r_x^d \mathcal{C}r_y^d}{4}, \\
a_0 &= 1 - \mathcal{C}r_y^d - \mathcal{C}r_x^d + \mathcal{C}r_x^d \mathcal{C}r_y^d, \\
a_1 &= -\frac{\mathcal{C}r_x^a}{4} + \frac{\mathcal{C}r_x^d}{2} + \frac{\mathcal{C}r_x^a \mathcal{C}r_y^d}{4} - \frac{\mathcal{C}r_x^d \mathcal{C}r_y^d}{2}, \\
a_2 &= \frac{\mathcal{C}r_x^a}{4} + \frac{\mathcal{C}r_x^d}{2} - \frac{\mathcal{C}r_x^a \mathcal{C}r_y^d}{4} - \frac{\mathcal{C}r_x^d \mathcal{C}r_y^d}{2}, \\
a_3 &= -\frac{\mathcal{C}r_y^a}{4} + \frac{\mathcal{C}r_y^d}{2} + \frac{\mathcal{C}r_y^a \mathcal{C}r_x^d}{4} - \frac{\mathcal{C}r_x^d \mathcal{C}r_y^d}{2}, \\
a_4 &= \frac{\mathcal{C}r_y^a}{4} + \frac{\mathcal{C}r_y^d}{2} - \frac{\mathcal{C}r_y^a \mathcal{C}r_x^d}{4} - \frac{\mathcal{C}r_x^d \mathcal{C}r_y^d}{2}, \\
a_5 &= \frac{\mathcal{C}r_x^a \mathcal{C}r_y^a}{16} - \frac{\mathcal{C}r_x^a \mathcal{C}r_y^d}{8} - \frac{\mathcal{C}r_y^a \mathcal{C}r_x^d}{8} + \frac{\mathcal{C}r_x^d \mathcal{C}r_y^d}{4} + 2\mathcal{C}r_{xy}^d, \\
a_6 &= -\frac{\mathcal{C}r_x^a \mathcal{C}r_y^a}{16} - \frac{\mathcal{C}r_x^a \mathcal{C}r_y^d}{8} + \frac{\mathcal{C}r_y^a \mathcal{C}r_x^d}{8} + \frac{\mathcal{C}r_x^d \mathcal{C}r_y^d}{4} - 2\mathcal{C}r_{xy}^d, \\
a_7 &= -\frac{\mathcal{C}r_x^a \mathcal{C}r_y^a}{16} + \frac{\mathcal{C}r_x^a \mathcal{C}r_y^d}{8} - \frac{\mathcal{C}r_y^a \mathcal{C}r_x^d}{8} + \frac{\mathcal{C}r_x^d \mathcal{C}r_y^d}{4} - 2\mathcal{C}r_{xy}^d, \\
a_8 &= \frac{\mathcal{C}r_x^a \mathcal{C}r_y^a}{16} + \frac{\mathcal{C}r_x^a \mathcal{C}r_y^d}{8} + \frac{\mathcal{C}r_y^a \mathcal{C}r_x^d}{8} + \frac{\mathcal{C}r_x^d \mathcal{C}r_y^d}{4} + 2\mathcal{C}r_{xy}^d.
\end{aligned}
\tag{5.32}
$$

We perform subsequent stages in the same way as in case of general discretization, i.e. at the beginning, each term of equation (5.31) is substituted with its expansion into Taylor series.

Applying (5.4) and (5.5), after simplification, we obtain a modified equation for the ADI method:

$$\frac{\partial c}{\partial t} + v_x \frac{\partial c}{\partial x} + v_y \frac{\partial c}{\partial y} + \frac{\Delta t}{2}\frac{\partial^2 c}{\partial t^2} - D_{xx}\frac{\partial^2 c}{\partial x^2} - D_{yy}\frac{\partial^2 c}{\partial y^2} - 2D_{xy}\frac{\partial^2 c}{\partial x \partial y}$$
$$+\frac{v_x \Delta t}{2}\frac{\partial^2 c}{\partial x \partial t} + \frac{v_y \Delta t}{2}\frac{\partial^2 c}{\partial y \partial t} + \frac{\Delta t^2}{6}\frac{\partial^3 c}{\partial t^3} + \frac{v_x \Delta x^2}{6}\frac{\partial^3 c}{\partial x^3} + \frac{v_y \Delta y^2}{6}\frac{\partial^3 c}{\partial y^3} + \frac{v_x v_y \Delta t^2}{4}\frac{\partial^3 c}{\partial x \partial y \partial t}$$
$$-\frac{D_{xx}\Delta t}{2}\frac{\partial^3 c}{\partial x^2 \partial t} - \frac{D_{yy}\Delta t}{2}\frac{\partial^3 c}{\partial y^2 \partial t} + \frac{v_x \Delta t^2}{4}\frac{\partial^3 c}{\partial x \partial t^2} + \frac{v_y \Delta t^2}{4}\frac{\partial^3 c}{\partial y \partial t^2} = 0\,. \quad (5.33)$$

The equation can be also written in the same form as equation (5.8), but this time the coefficients are:

$$\begin{aligned}
a &= \frac{v_x \Delta x^2}{6}, & l &= \frac{v_x \Delta t}{2},\\
b &= \frac{v_y \Delta y^2}{6}, & m &= \frac{v_y \Delta t}{2},\\
d &= v_x, & n &= \frac{\Delta t^2}{6},\\
e &= v_y, & o &= \frac{v_x v_y \Delta t^2}{4},\\
f &= \frac{\Delta t}{2}, & p &= -\frac{D_{xx}\Delta t}{2},\\
g &= -D_{xx}, & q &= -\frac{D_{yy}\Delta t}{2},\\
h &= -D_{yy}, & r &= \frac{v_x \Delta t^2}{4},\\
k &= -2D_{xy}, & z &= \frac{v_y \Delta t^2}{4}.
\end{aligned} \quad (5.34)$$

After the elimination of time derivatives, replaced with the formulae (5.15) determined in the previous section (remembering about different values of coefficients a, b, ..., z), after transformations taking into account third-order derivatives, we obtain a modified equation in the form enabling the interpretation of truncation error:

$$\frac{\partial c}{\partial t} + v_x \frac{\partial c}{\partial x} + v_y \frac{\partial c}{\partial y} - 2D_{xy}\frac{\partial^2 c}{\partial x \partial y} - D_{xx}\frac{\partial^2 c}{\partial x^2} - D_{yy}\frac{\partial^2 c}{\partial y^2}$$
$$= -\left[\frac{v_x^3 \Delta t^2}{12} + \frac{v_x \Delta x^2}{6}\right]\frac{\partial^3 c}{\partial x^3} - \left[\frac{v_y^3 \Delta t^2}{12} + \frac{v_y \Delta y^2}{6}\right]\frac{\partial^3 c}{\partial y^3}$$
$$+ v_x \Delta t D_{xy}\frac{\partial^3 c}{\partial x^2 \partial y} + v_y \Delta t D_{xy}\frac{\partial^3 c}{\partial x \partial y^2}\,. \quad (5.35)$$

The components of numerical diffusion and dispersion tensors are presented in table 5.4. Analogically to the CN scheme, in case of ADI approach, the components of numerical diffusion tensor are zero, while the numerical dispersion coefficients remain non-zero, which, like in case of CN, can cause non-physical oscillations. Similarly, there is no visible difference between the analytical solution and the numerical one (see fig. 5.3).

Exact comparison of the numerical solution with the analytical one and with the other schemes is presented in Chapter 7.

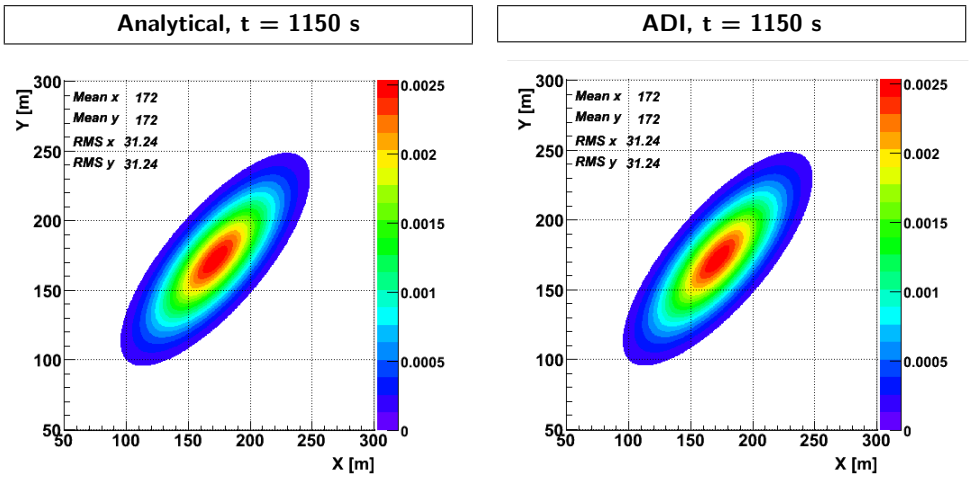

(a) Analytical solution

(b) Numerical solution, ADI method

Figure 5.3: Analytical solution (a) and numerical one with the application of ADI method (b) after 1150 seconds; simulation parameters: $v_x = v_y = 0.106\,\frac{\mathrm{m}}{\mathrm{s}}$, $D_{xx} = D_{yy} = 0.425\,\frac{\mathrm{m}^2}{\mathrm{s}}$, $D_{xy} = D_{yx} = 0.325\,\frac{\mathrm{m}^2}{\mathrm{s}}$, $\Delta x = \Delta y = 1\,\mathrm{m}$ and $\Delta t = 0.5\,\mathrm{s}$; mass $M = 10\,\mathrm{a.\,u.}$ was discharged at point $x_0 = 50\,\mathrm{m}$, $y_0 = 50\,\mathrm{m}$ at time $t_0 = 0\,\mathrm{s}$

Table 5.4: Values of the coefficients of numerical diffusion and dispersion tensors for the ADI method

	ADI
D_{11}^N	0
D_{12}^N	0
D_{21}^N	0
D_{22}^N	0
T_{11}^N	$-\frac{v_x \Delta x^2}{2}\left[\frac{(\mathcal{C}r_x^a)^2}{6}+\frac{1}{3}\right]$
T_{12}^N	$-v_x D_{xy}\Delta t$
T_{21}^N	$-v_y D_{xy}\Delta t$
T_{22}^N	$-\frac{v_y \Delta y^2}{2}\left[\frac{(\mathcal{C}r_y^a)^2}{6}+\frac{1}{3}\right]$

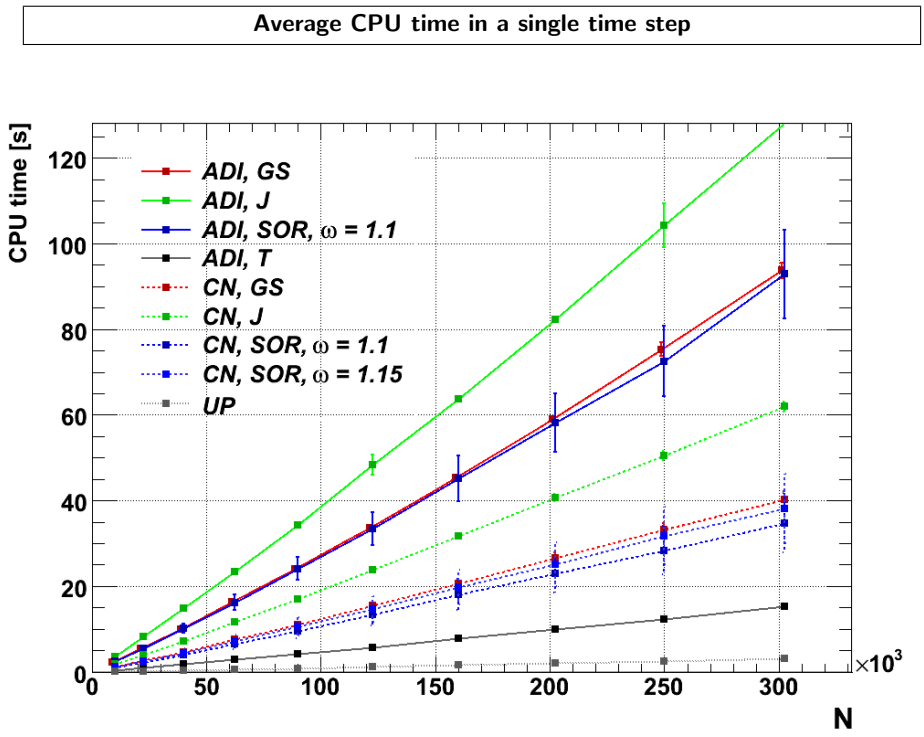

Figure 5.4: Average CPU time in a single time step; processor: Intel(R) Pentium(R) 4 – 2.60 GHz, RAM: 1024 MB; the average was calculated from 100 measurements of CPU time consumption in a single time step; N – number of nodes in the grid

5.3 Computation speed and stability

An important, from the practical point of view, aspect in numerical solving of equations is the speed of computations. Especially in an emergency situation (e.g. sudden catastrophic release of pollutants), we are interested in obtaining the results determining the predicted distribution of concentrations as soon as possible. The speed is of crucial importance when the computations are carried out for large and geometrically complex objects or when the simulations have to be repeated many times. Table 5.5 illustrates the average ***CPU*** (Central Processing Unit) ***time*** and ***real time*** in a single time step, for example, simulation parameters with the application of various approaches. The calculations were performed on a PC computer with Intel(R) Pentium(R) 4 – 2.60 GHz processor. The bigger the number of nodes of the computation grid (see fig. 5.4), the more visible the differences between the methods.

The fastest is the explicit UP scheme, which on the other hand is not an accurate method. It may generate large numerical diffusion, as presented above. Apart from that, the method is conditionally stable, which imposes limitations on the selected time step. The stability means here the ability of the numerical scheme to attenuate incidental interferences to the solution during computation (Szymkiewicz, 2000, 2003). Such interferences can be, for example, round-off errors connected with the finite representation of numbers in the computer. We can generally divide the numerical schemes into:

➤ **absolutely stable** – schemes which are always stable, irrespective of the selected parameters of computation grid; they do not create rapid increase in errors during computation;

Table 5.5: Average CPU time and real time in a single time step in case of various schemes, for exemplary simulation parameters: $v_x = v_y = 0.2\,\frac{\mathrm{m}}{\mathrm{s}}$, $D_L = D_T = 0.5\,\frac{\mathrm{m}^2}{\mathrm{s}}$, $\Delta t = 0.5\,\mathrm{s}$, $\Delta x = \Delta y = 1.0\,\mathrm{m}$; the average CPU time and real time for a single step was normalized to the average time in case of the fastest method, UP; the tests were carried out on a computer with the Intel(R) Pentium(R) 4 processor – 2.60 GHz, and RAM: 1024 MB

Numerical scheme	Method of solving the set of equations	Average simulation time in a single step	
		wall clock (real) time	CPU (processor) time
UP	–	1	1
CN	J	19.98	18.72
CN	G-S	12.98	12.29
CN	SOR ω=1.1	9.24	8.56
CN	SOR ω=1.15 *	6.97	6.55
ADI	J	41.40	38.03
ADI	G-S	28.41	26.82
ADI	SOR ω=1.1*	20.02	18.79
ADI	T	4.57	4.30

* – optimum relaxation parameter for the given formula and simulation parameters;

- **absolutely unstable** – schemes which we always obtain unstable solutions with, irrespective of the selected size of the computation grid mesh;
- **conditionally stable** – schemes providing stable solutions for appropriately selected parameters; the conditions to be met by those parameters are called stability criteria.

Stable solutions, in case of the UP scheme, are obtained when the following condition (Dehghan, 2004; Noye & Tan, 1989) is met:

$$\mathcal{C}r_x^a + \mathcal{C}r_y^a + 2\left(\mathcal{C}r_x^d + \mathcal{C}r_y^d\right) \leqslant 1. \tag{5.36}$$

Table 5.6 comprises examples when the UP formula gives stable or unstable solutions, depending on the selected time step Δt and other parameters unaltered. The examples are illustrated in figure 5.5, showing simulation results after 100 time steps. In order to eliminate additional errors related to the high gradient of concentration values on the computation grid, the initial concentration was prescribed with Gauss distribution.

Applying the CN or ADI method, the prescribed time step Δt may be significantly greater than in case of UP, which, in practice, means obtaining the solution quicker. In the case of UP scheme (fig. 5.6(a)) and for the time step

Table 5.6: Stability of schemes for exemplary parameters; stability was determined on the basis of simulations carried out for: $v_x = v_y = 0.106\ \frac{\mathrm{m}}{\mathrm{s}}$ and $D_L = 0.75\ \frac{\mathrm{m}^2}{\mathrm{s}}$, $D_T = 0.1\ \frac{\mathrm{m}^2}{\mathrm{s}}$; results of simulation after 100 time steps are illustrated in figure 5.7

	Parameters		Stability criteria, UP		Stability		
Lp.	$\Delta x = \Delta y\ [m]$	$\Delta t\ [s]$	$\mathcal{C}r_x^a + \mathcal{C}r_y^a$	$\mathcal{C}r_x^d + \mathcal{C}r_y^d$	UP	CN	ADI
1.	1	0.5	0.106	0.425	stable	stable	stable
2.	1	0.6	0.127	0.510	unstable	stable	stable
3.	1	0.65	0.138	0.552	unstable	stable	stable
4.	1	0.7	0.148	0.595	unstable	stable	stable
5.	1	0.8	0.170	0.680	unstable	stable	stable
6.	1	1	0.212	0.850	unstable	stable	stable

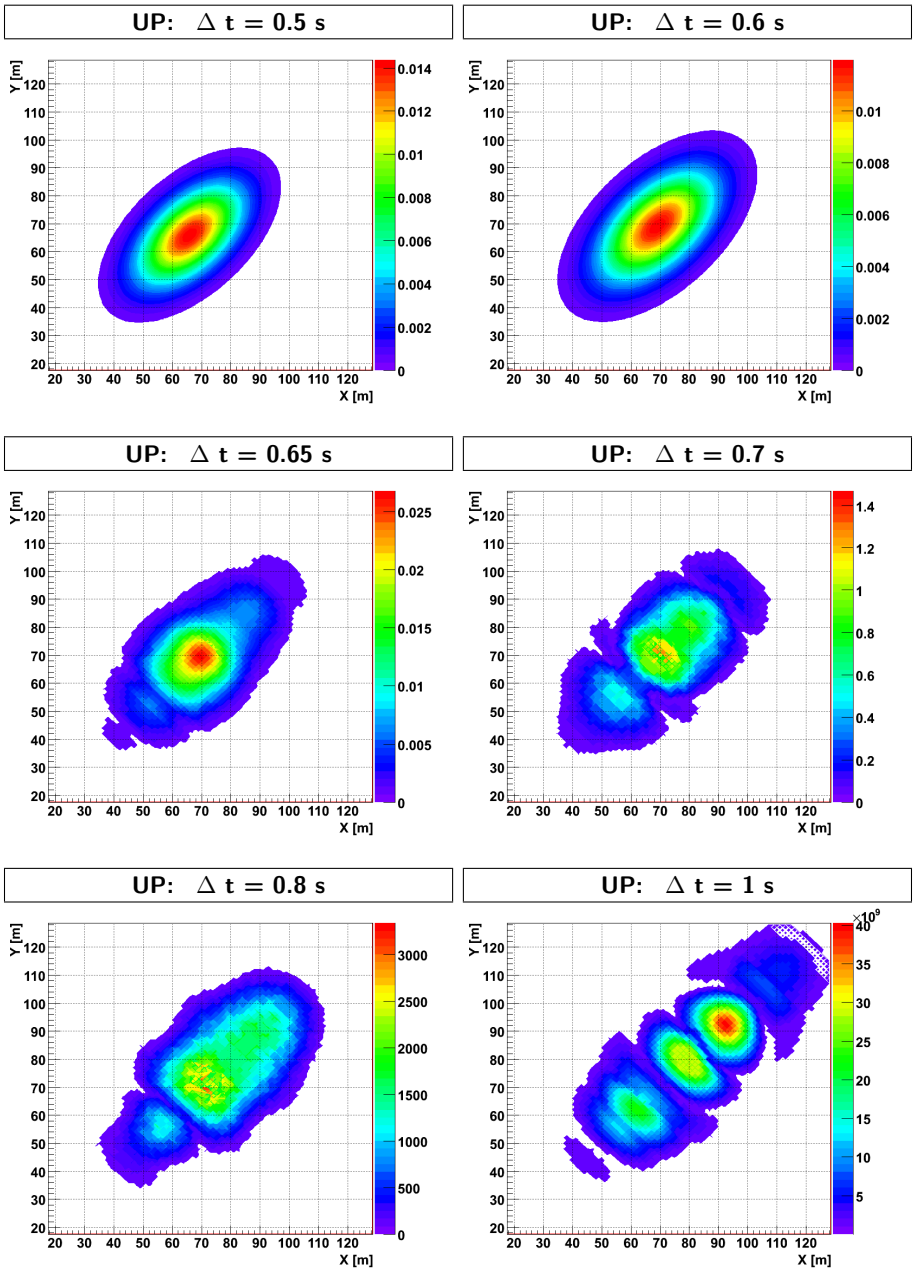

Figure 5.5: Results of simulation with the application of the UP scheme after 100 time steps for various values of time step; simulation parameters: $v_x = v_y = 0.106\,\frac{\mathrm{m}}{\mathrm{s}}$ $D_L = 0.75\,\frac{\mathrm{m}^2}{\mathrm{s}}$, $D_T = 0.1\,\frac{\mathrm{m}^2}{\mathrm{s}}$, $\Delta x = \Delta y = 1\,\mathrm{m}$

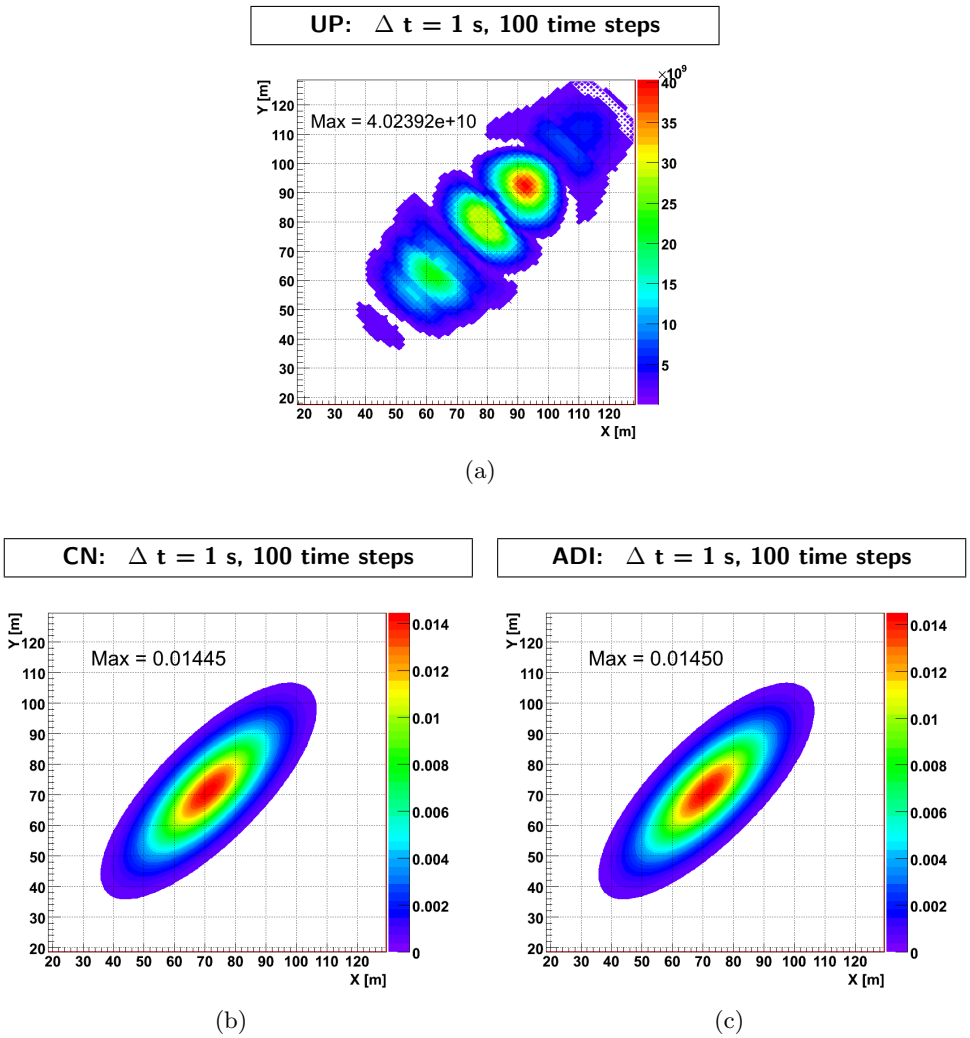

Figure 5.6: Results of simulation with the application of UP (a), CN (b) and ADI (c) schemes after 100 time steps for $\Delta t = 1\,\mathrm{s}$; simulation parameters: $v_x = v_y = 0.106\ \frac{\mathrm{m}}{\mathrm{s}}$ and $D_L = 0.75\ \frac{\mathrm{m}^2}{\mathrm{s}}$, $D_T = 0.1\ \frac{\mathrm{m}^2}{\mathrm{s}}$, $\Delta x = \Delta y = 1$ m

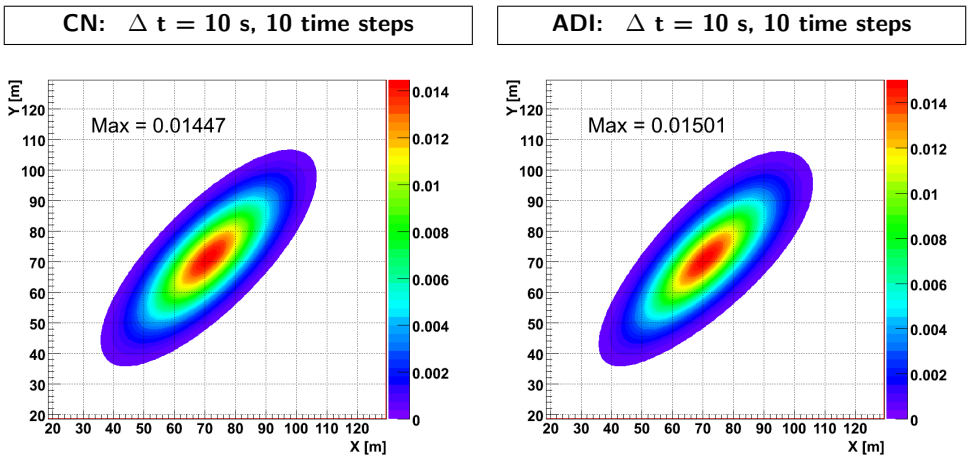

(a) (b)

Figure 5.7: Results of simulation with the application of the CN (a) and ADI (b) schemes after 10 time steps for $\Delta t = 10\,\mathrm{s}$; simulation parameters: $v_x = v_y = 0.106\,\frac{\mathrm{m}}{\mathrm{s}}$ and $D_L = 0.75\,\frac{\mathrm{m}^2}{\mathrm{s}}$, $D_T = 0.1\,\frac{\mathrm{m}^2}{\mathrm{s}}$, $\Delta x = \Delta y = 1\,\mathrm{m}$

of $\Delta t = 1$ s we obtain unstable solution, in case of CN (fig. 5.6(b)) and ADI (fig. 5.6(c)) we obtain relatively accurate solution for the same parameters. Increasing the time step to $\Delta t = 10$ s, we still obtain high accuracy solutions, but performing only 10 time steps instead of 100 (fig. 5.7). Therefore, the solution required after 100 seconds is obtained 10 times faster. This is possible, because both methods, CN and ADI, are unconditionally stable (Fletcher, 1991; McKee *et al.*, 1996; Noye & Tan, 1989), and as was demonstrated above, they do not generate numerical diffusion. Since they are implicit methods, it is necessary to solve a system of linear equations, as mentioned above, in order to reach the solution, which can be time consuming with a high number of grid nodes. Figure 5.5 illustrates that application of the ADI method leading to two tri-diagonal equation systems, which can be solved with analytical Thomas method, enables reaching the solution relatively quickly. Additionally, the selected time step can be significantly larger than in case of the UP scheme. However, non-physical oscillations may occur here due to the numerical dispersion discussed earlier. The problem appears together with the increase of the so-called ***Peclet number*** (fig. 5.8). Peclet number (Pe) defines the proportion of the advection term to the diffusion term in the transport equation (Szymkiewicz, 2000):

$$Pe = \frac{U \Delta x}{D}\,, \tag{5.37}$$

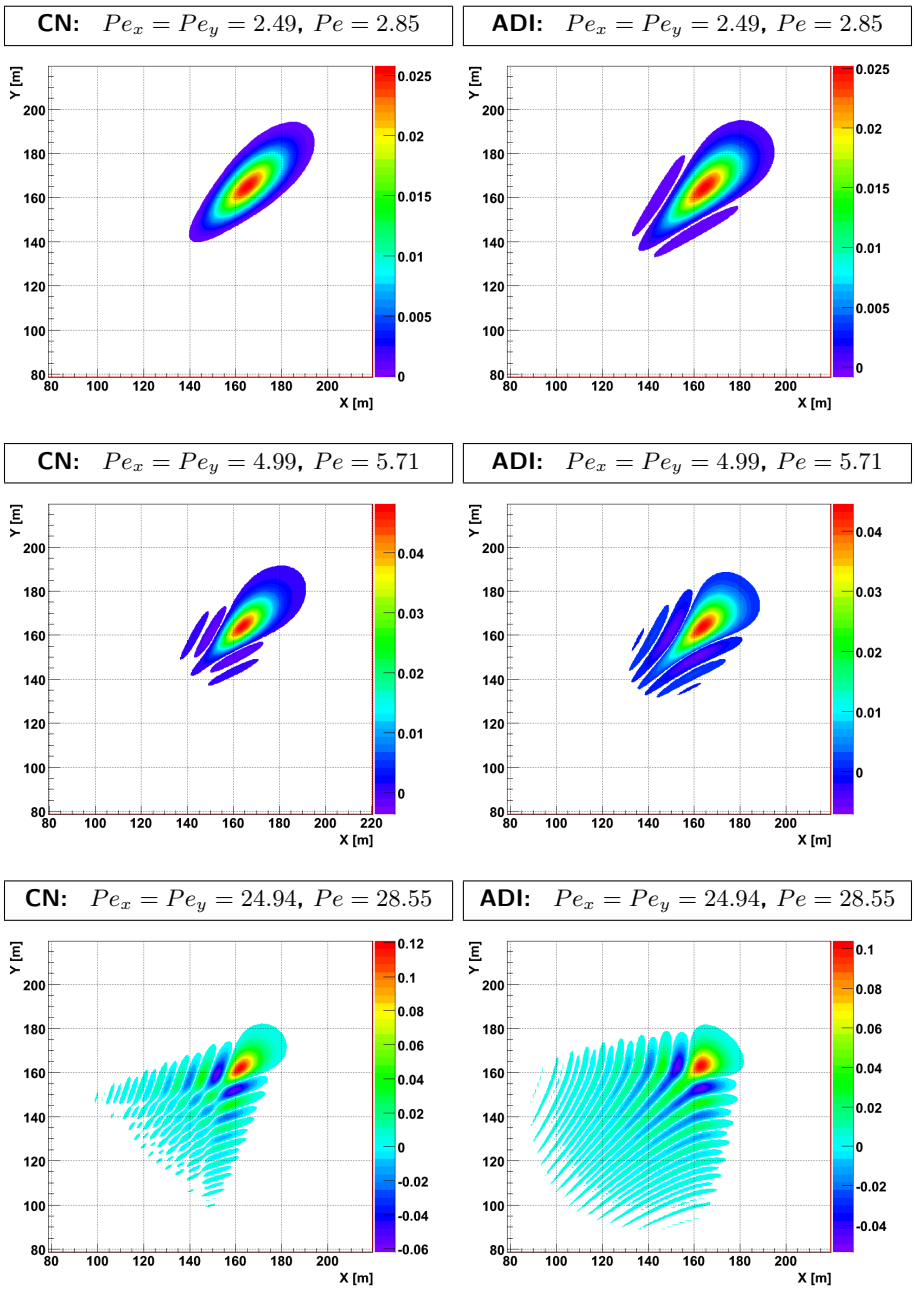

Figure 5.8: Non-physical oscillations of the solution; results of simulation with the application of CN and ADI schemes after 100 time steps, for various Peclet number values; $\Delta x = \Delta y = 1\,\mathrm{m}$, $\Delta t = 1\,\mathrm{s}$

where:

U – average flow velocity,
D – diffusion coefficient.

We can write it, in two dimensions, as:

$$Pe_x = \frac{v_x \Delta x}{D_{xx}}, \qquad Pe_y = \frac{v_y \Delta y}{D_{yy}}. \tag{5.38}$$

The definition of Peclet number in the following form is also encountered (Fabritz, 1995):

$$Pe = \frac{\sqrt{(v_x/\Delta x)^2 + (v_y/\Delta y)^2}}{(D_{xx}/\Delta x^2) + (D_{yy}/\Delta y^2) - (D_{xy}/(\Delta x \Delta y))}. \tag{5.39}$$

In case of two-dimensional transport equation discussed in this book, dispersion coefficients in the equation are so big that the diffusion term has a smoothing effect and attenuates oscillations. The problem of oscillations can also be reduced by decreasing space steps. In case when the advection term in the equation is the dominant term, other numerical schemes should be used, like QUICKEST (*Quadratic Upstream Interpolation for Convective Kinematics with Estimated Streaming Terms*), ULTIMATE QUICKEST, TVE (*Total Variation Diminishing*), ADI-QUICK (*Quadratic Upstream Interpolation for Convective Kinematics*) (for details concerning the schemes see: Balzano, 1999; Guan & Zhang, 2005; Szymkiewicz, 2000; Wu & Falconer, 1998), or improved UP method where the diffusion term in the equation is corrected on the basis of the numerical diffusion error determined at each time step.

Chapter 6

Description of RivMix Model

6.1 Introduction

Two-dimensional numerical model of spreading of pollutants in surface flowing waters – River Mixing Model (**RivMix** for short) was implemented with the application of C++ language under Linux operating system. ROOT (Object Oriented Data Analysis Framework), a data analysis package created in the European Organization for Nuclear Research – CERN (Brun & Rademakers, 1997) was used for visualization of results. The data analysis package is written in C++ programming language, which provides for easy integration with the numerical model code.

Below, the parameters controlling the course of simulation (Section 6.2), the structure and the algorithm of the program (Section 6.3) are described in detail. Those description should help particularly those readers who would like to use **RivMix** model or would like to build alike model on their own.

6.2 Simulation parameters

The course of simulation is controlled by a number of parameters loaded from configuration files. This way, the shape of the flow area, time and grid spacing and the numerical scheme are prescribed, among others. The basic parameters are contained in the `param.txt` file:

`param.txt` file format			
`flag`			
`t`	Δx	Δy	Δt
`Sch`	`tensor`		
v_x	v_y		
D_L	D_T		

- `flag` – parameter determining the format of the input file specifying the computation grid with proper parameters:

  ➤ `flag = 0` – the simulation starts for constant velocity field and constant transverse and longitudinal dispersion coefficients (constant values are read from the `param.txt` file); grid nodes are read from `grid.txt` file;

  `grid.txt` file format

x	y

  x, y – grid nodes indices

  ➤ `flag = 1` – simulation for constant coefficients of transverse and longitudinal dispersion; velocity field and grid nodes are read from `v.txt` file;

  `v.txt` file format

x	y	$\mathbf{v_x}$	$\mathbf{v_y}$

  v_x, v_y – velocity components

  ➤ `flag = 2` – the velocity field, the dispersion tensor (D_{xx}, D_{xy}, D_{yy}) and the grid nodes are read from `data.txt` file;

  `data.txt` file format

x	y	$\mathbf{v_x}$	$\mathbf{v_y}$	$\mathbf{D_{xx}}$	$\mathbf{D_{xy}}$	$\mathbf{D_{yy}}$

  D_{xx}, D_{xy}, D_{yy} – dispersion tensor coefficients

  ➤ `flag = 3` – simulation for constant velocity field; grid nodes and dispersion tensor are read from `d.txt` file;

  `d.txt` file format

x	y	$\mathbf{D_{xx}}$	$\mathbf{D_{xy}}$	$\mathbf{D_{yy}}$

- `t` – number of time steps for which the simulation is to be carried out;
- `Sch` – numerical scheme which will be used for calculation; possible values: "`cn`", "`up`", "`adi`" or "`adi2`", referring to Crank-Nicolson, Upwind and Alternate Direction Implicit method in two variants;
- $\mathbf{\Delta t}$ – time step [s];
- $\mathbf{\Delta x}$ and $\mathbf{\Delta y}$ – spatial steps defining the size of the mesh of the calculation grid [m];

- $\mathbf{v_x}$ and $\mathbf{v_y}$ – values of velocity components $\left[\frac{\mathrm{m}}{\mathrm{s}}\right]$ (valid when these values are constant over the whole computation grid parameter, `flag` is 0 or 3);
- $\mathbf{D_L}$ and $\mathbf{D_T}$ – values of dispersion coefficients $\left[\frac{\mathrm{m}^2}{\mathrm{s}}\right]$ (valid when these values are constant over the whole computation grid, parameter `flag` is 0 or 1);
- `tensor` – method of determining the components of the dispersion tensor (D_{xx}, D_{xy}, D_{yy}) on the basis of D_L and D_T coefficients (*rotation*, *quasi-rotation*, *vector-like rotation* or *identity transformation*, see Chapter 3);
- `M`, ω – method to solve the system of equations and relaxation parameter; read from an additional input file `method.txt` if necessary.

`method.txt` file format	
`M`	ω

6.3 Algorithm

The algorithm of the program is presented in diagrams in figures 6.3, 6.4 and 6.5. Its individual stages are described below:

1. **Initialization of simulation parameters**
   At the first stage, the following simulation parameters are initialized: `flag`, number of time steps `t`, $\mathbf{\Delta t}$, $\mathbf{\Delta x}$, $\mathbf{\Delta y}$, scheme `Sch`, method of calculation of the dispersion tensor `tensor`, $\mathbf{v_x}$, $\mathbf{v_y}$, $\mathbf{D_L}$, $\mathbf{D_T}$.

2. **Preparation of the computation grid**
   The computation grid is constructed on the basis of the input files `grid.txt`, `v.txt`, `data.txt`, or `d.txt`, and then stored in the container from C++ Standard Template Library (STL). The kind of the grid is represented with the application of the object inheritance mechanism available in C++ programming language. The inheritance pattern is presented in figure 6.1. If the program were started with `flag` parameter equal to `0` or `1` the dispersion tensor components would also be determined.

3. **Formulation of initial and boundary conditions**
   Boundary points are selected. The areas where inflow or outflow occurs are defined on the basis of an additional file `InOut.txt`. At this stage all initial concentration values are initialized. Also the maximum values for

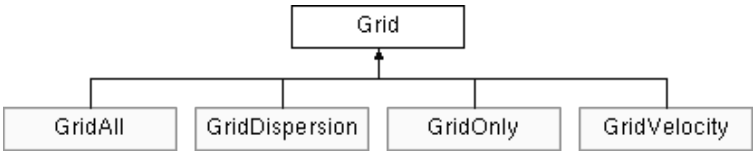

Figure 6.1: Inheritance pattern diagram for classes representing the computation grid

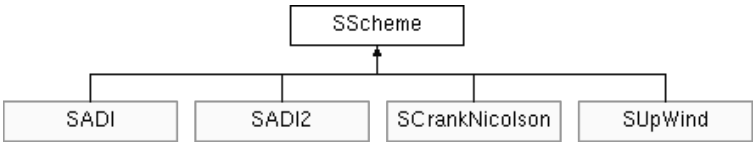

Figure 6.2: Inheritance diagram for classes representing the discussed numerical approaches

Courant and Peclet numbers are calculated, whose values are helpful at checking the stability condition or the possibility of occurrence of non-physical oscillations (see Chapter 5).

`InOut.txt` file format				
kind	$\mathbf{x_1}$	$\mathbf{x_2}$	$\mathbf{y_1}$	$\mathbf{y_2}$
kind – defines the input kind; possible values: „in" or „out" x_1, x_2, y_1, y_2 – x and y coordinates of the initial and boundary points for the given input				

4. **Recording initial concentration in a file**

   Initial concentration is recorded in a text file `grid_Conc_Sch_0.txt`, where "`Sch`" assumes the value of the applied numerical formula, e.g. "`cn`".

`grid_Conc_Sch_0.txt` file format		
x	**y**	**Conc**
Conc – concentration value		

5. **Calculation of concentration values in the next time step**
   At the next stage, which is performed for the prescribed number of `t`, the concentration in the next time step is determined. This stage depends on the kind of the selected formula and approach to the solution to a system of equations. It is presented in detail in figure 6.4. Like in the case of the computation grid – the numerical formula for solving the transport equation is specified by the inheritance (fig. 6.2) and polymorphism mechanisms (Stroustrup, 2000).

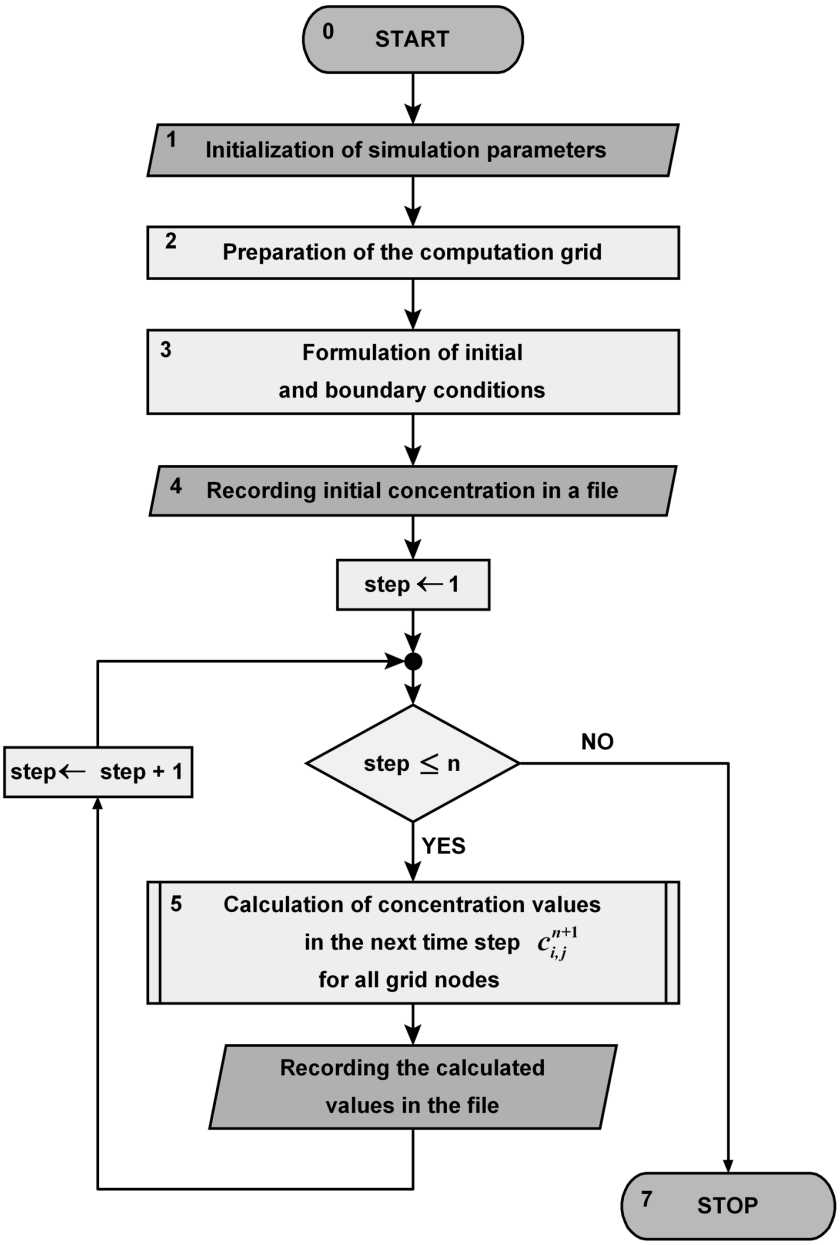

Figure 6.3: Block diagram of the **RivMix** model – main program; individual stages are discussed in Section 6.3; procedure block 5 – *Calculation of concentration values in the next time step* – is illustrated in figure 6.4

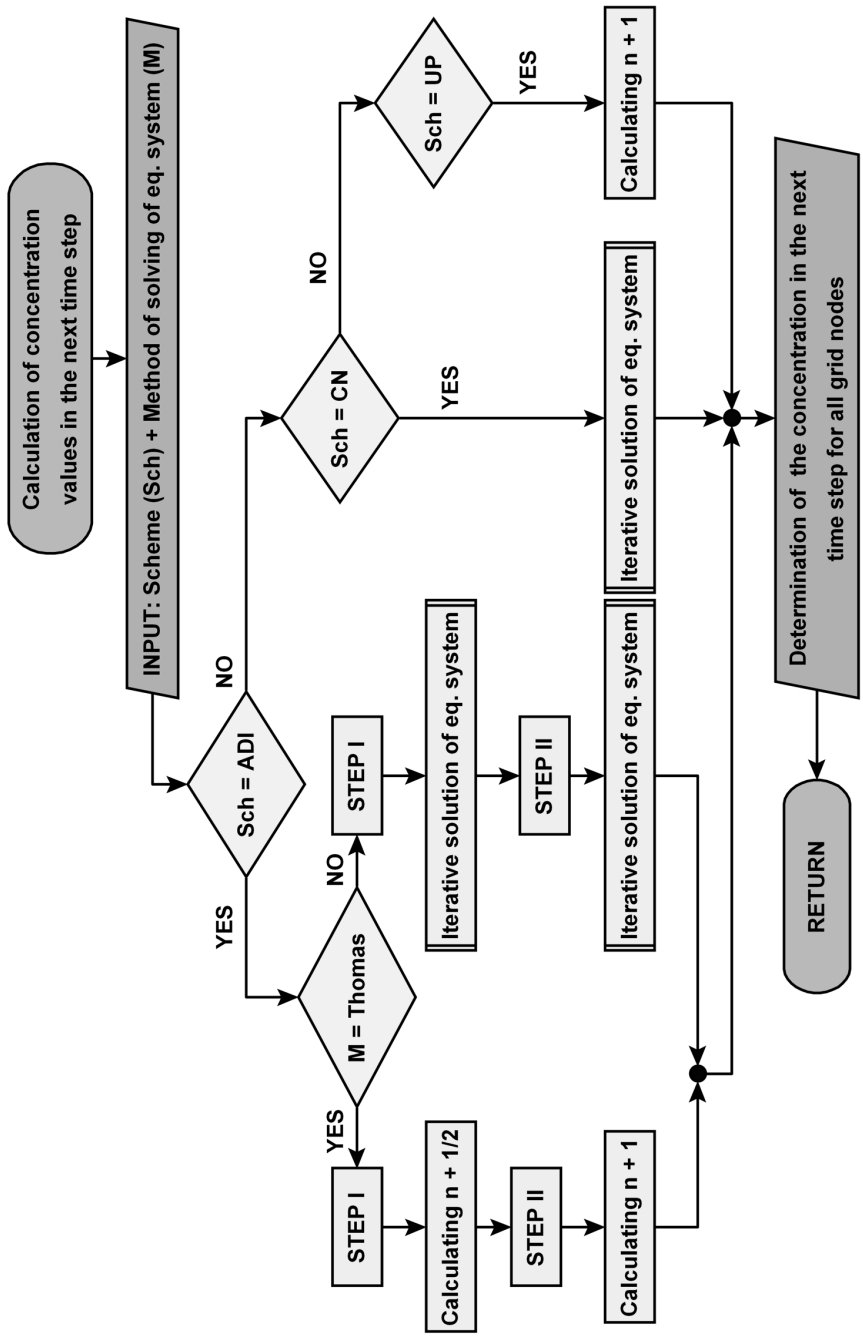

Figure 6.4: Block diagram of the **RivMix** model – *Calculation of concentration values in the next time step*; for description of numerical schemes see Chapter 4; procedure block *Iterative solving of the equation system* is presented in figure 6.5

Depending on the numerical formula selected for calculations:

- **ADI or ADI2** – concentration values at $(n+1)$-th time step are determined in two stages, depending on the selected method, resultant equation systems are solved with the application of Thomas algorithm or iteratively (fig. 6.5) with the over-relaxation, Gauss-Seidel or Jacobi approach;
- **CN** – concentration values in $(n+1)$-th time step are determined with the application of the selected iterative method (fig. 6.5) of successive over-relaxation, Gauss-Seidel or Jacobi, to solve the resultant set of equation system;
- **UP** – values in $(n+1)$-th time step are determined directly on the basis of the previous step.

If the successive over-relaxation method is applied, and the relaxation parameter is not specified in the input file, function selecting an optimal parameter for the given simulation setup and the size of the computation grid will be called. A number of simulations are carried out for various values of the relaxation parameter ω in the first time step. The parameter for which the smallest number of iterations was performed to reach the result with the desired accuracy is selected as the optimal one.

6. **Recording the calculated values in the file**
The concentration values calculated in the next time step are recorded in a text file. It is possible to record all or only selected time steps in one or multiple files. The x, y coordinates of the point, and the concentration value at this point are recorded.
Also the component values of velocity and dispersion tensor for each node of the grid can be recorded.

`grid_Conc_Sch_t.txt` file format; option I

x	**y**	**Conc**

`grid_Conc_Sch_t.txt` file format; option II

x	**y**	$\mathbf{v_x}$	$\mathbf{v_y}$	$\mathbf{D_{xx}}$	$\mathbf{D_{xy}}$	$\mathbf{D_{yy}}$	**Conc**

It has to be kept in mind, however, that for large size grids the resulting files may be very big (e.g. for a grid of 250×250, the size of the file with the concentration values in a single time step is ca. 1 – 2 MB).

7. **STOP**
The program stops after performing the prescribed number of time steps `t`.

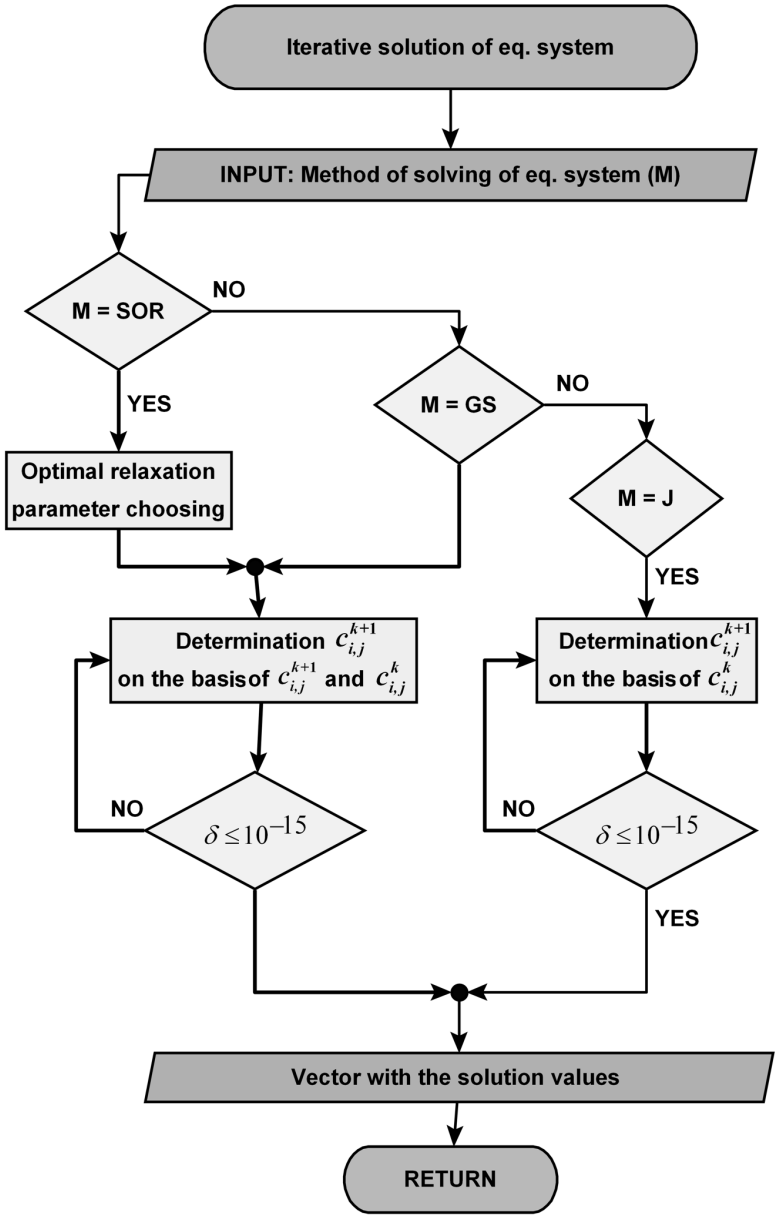

Figure 6.5: Block diagram of the **RivMix** model – *Iterative solving of equation system*; $k + 1$ denotes the next iteration during solving the equation system at a given time step n; for the description of iterative methods, see Section 4.3.2

Chapter 7

Model Verification

7.1 Introduction

The operation of the implemented **RivMix** model, and different numerical schemes which could be used in it, was verified by comparing the obtained simulation results with the analytical solution, in case when such solution could be reached (Section 7.2). Also, the simulation results were compared with concentration distributions obtained during a tracer test in the laboratory compound channel (Section 7.3). In the first case, the analysis was carried out with the application of various implemented numerical schemes: UP, CN, and ADIfor instantaneous and continuous discharge of pollutants. In case of the laboratory channel with continuous inflow of the tracer, the most effective scheme, ADI, was used. Apart from the tests presented in this chapter, the operation of the model is illustrated by the test carried out in Chapter 3, where special emphasis was put on various methods of determination of the dispersion tensor. In that chapter, situations of instantaneous and continuous discharge of pollutants in case of a straight channel situated at various angles in relation to x axis of the coordinate system is described. Like in the case of the laboratory channel, the fastest method, ADI, was applied.

7.2 Wide rectangular channel

A wide rectangular channel was selected for the tests, for which it is possible to reach the analytical solution. The channel was described in Chapter 3 and schematically presented in figure 3.5. In order to use the analytical solution (defined by equation 2.16) the calculations were carried out far away from the banks (boundary conditions at infinity) for constant values of dispersion coef-

Table 7.1: Simulation parameters used in the tests carried out

Velocity components		Dispersion coefficients		Grid spacing		Time step
$v_x \left[\frac{\mathrm{m}}{\mathrm{s}}\right]$	$v_y \left[\frac{\mathrm{m}}{\mathrm{s}}\right]$	$D_L \left[\frac{\mathrm{m}^2}{\mathrm{s}}\right]$	$D_T \left[\frac{\mathrm{m}^2}{\mathrm{s}}\right]$	Δx[m]	Δy[m]	Δt[s]
0.106	0.106	0.75	0.1	1	1	0.5

ficients, constant velocity field, and constant depth of the channel. Simulation parameters are presented in table 7.1. The values of flow parameters and longitudinal dispersion parameters were selected so that they remain in the real range of those values. In the case in question, they reflect the values determined in a tracer experiment for the Upper Narew river in its initial section – 5.75 kilometres away from the discharge point. The data were taken from works by (Rowiński *et al.*, 2003a,b). The time and spatial steps were selected in such a way that the discussed schemes be stable and no non-physical oscillations occur. In particular, in order for the UP scheme to be stable, a time step of $\Delta t = 0.5\,\mathrm{s}$ had to be accepted. The initial concentration was preset in such a way that it does not influence the accuracy of the obtained results, so that there occur no large concentration gradients in the computation grid (which appear when the initial concentration is preset in one point with Dirac delta).

A number of simulations were carried out for so selected set of parameters with the application of the numerical scheme under discussion: UP, CN, and ADI. In case of instantaneous and continuous discharge, 2000 and 5000 time steps, respectively, were carried out for each discussed scheme. The size of the computation grid was 400×400 points in both cases. For instantaneous discharge of pollutants, the results obtained with different numerical schemes were compared with the analytical solution. In case of continuous discharge, the results for different schemes were compared with each other.

7.2.1 Instantaneous discharge of pollutants

In case of instantaneous discharge of pollutants, which can occur in an emergency situation, a discharge of mass $M = 10$ a.u. at point $x_0 = y_0 = 50\,\mathrm{m}$ was considered. The initial concentration was prescribed with the application of the analytical solution determined after 150 seconds for the same parameters as the simulation parameters. The initial concentration distribution is illustrated in figure 7.1.

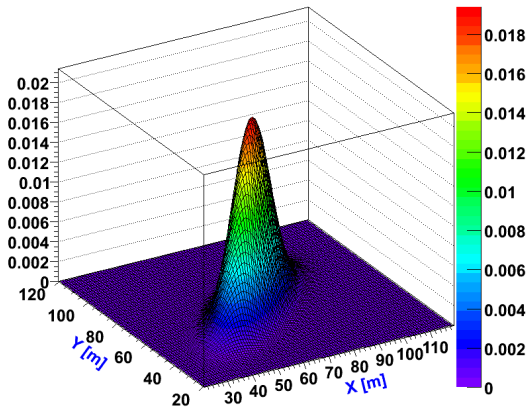

(a)

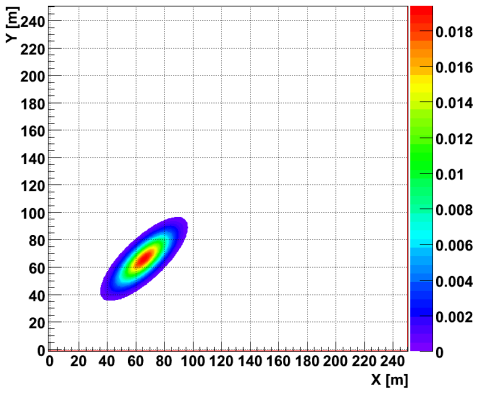

(b)

Figure 7.1: Initial concentration in the tests carried out with instantaneous discharge of pollutants (analytical solution after 150 seconds after discharge)

Figures 7.2 – 7.4 present the results of simulation (figs. 7.2(a), 7.3(a) and 7.4(a)) and the analytical solution (fig. 7.5) after 750 seconds from the release. The charts present two-dimensional concentration distributions $c(x, y)$, the maximum of which is indicated by values "*Mean x*" and "*Mean y*". "*RMS x*" and "*RMS y*" denote standard deviation of projection of concentration distribution on x and y axis, respectively. The value of the "*Integral*" variable is the total mass on computational grid, which does not change during simulation time (equals the initially discharged value of 10 arbitrary units) as illustrated

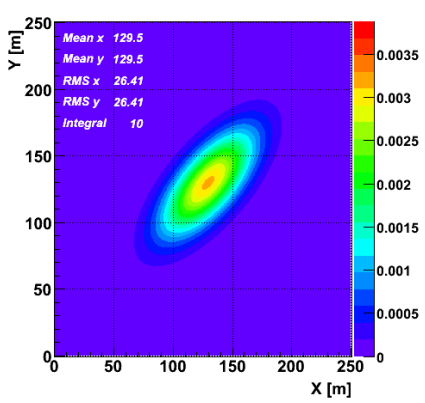

(a) Numerical solution after 750 seconds, UP scheme

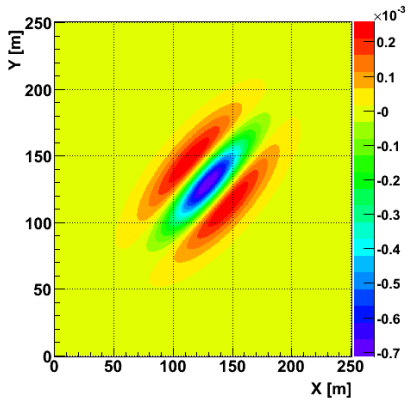

(b) Difference between the analytical solution and the numerical one, UP scheme

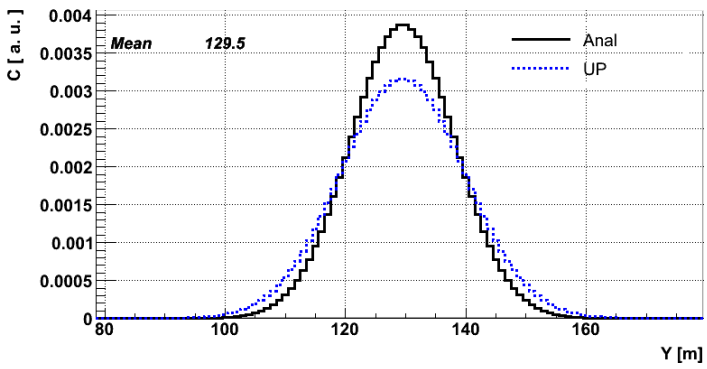

(c) Projection of the solution on the straight line perpendicular to $y = x$ and crossing the point (*Mean x*, *Mean y*)

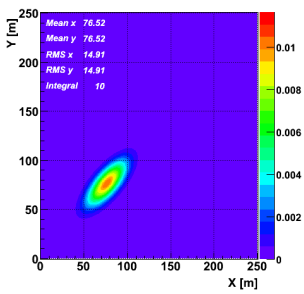

(d) 250 s

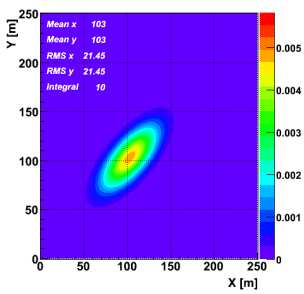

(e) 500 s

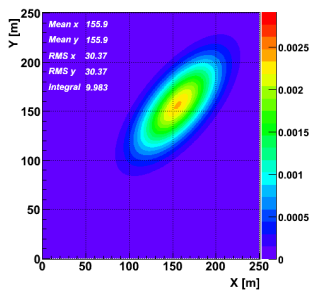

(f) 1000 s

Figure 7.2: Results of simulation with the application of the UP scheme after 750 seconds – figs. (a), (b), (c), and figs. (d), (e), (f) illustrating the course of the simulation in time

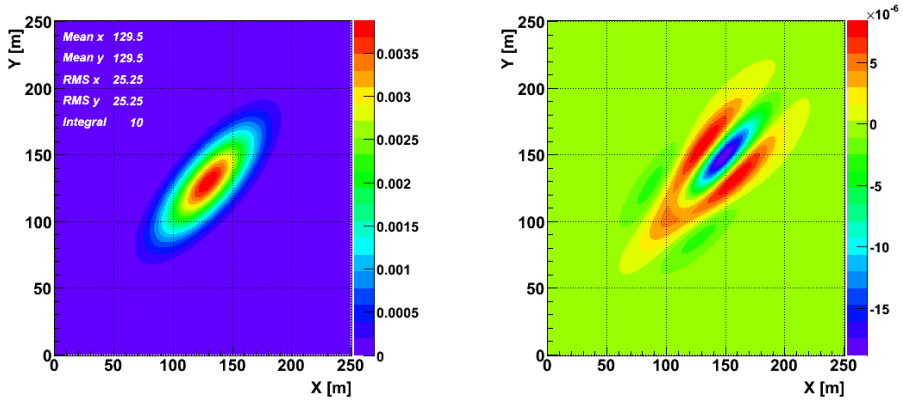

(a) Numerical solution after 750 seconds, CN scheme

(b) Difference between the analytical solution and the numerical one, CN scheme

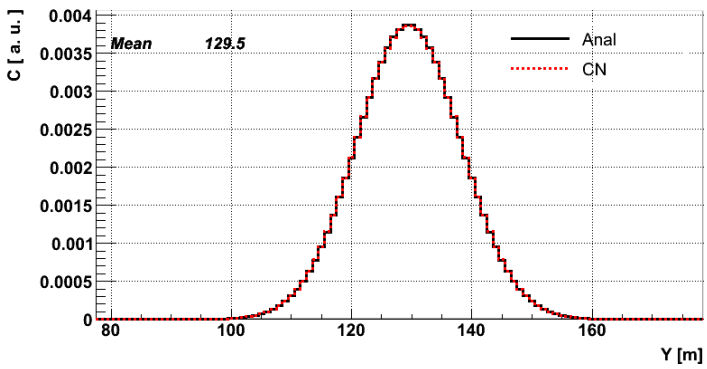

(c) Projection of the solution on the straight line perpendicular to $y = x$ and crossing the point (*Mean x*, *Mean y*)

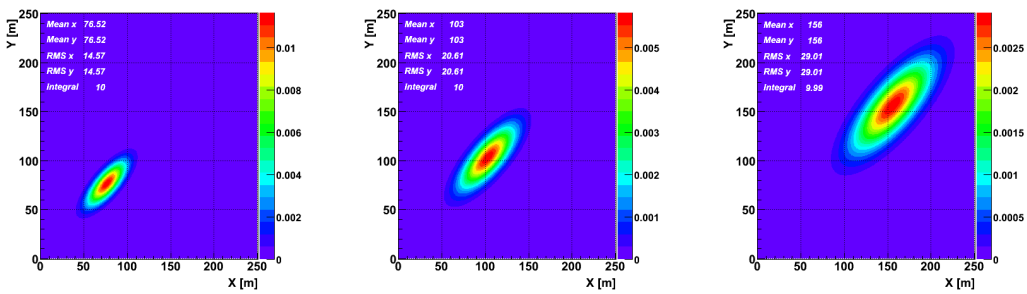

(d) 250 s

(e) 500 s

(f) 1000 s

Figure 7.3: Results of simulation with the application of the CN scheme after 750 seconds – figs. (a), (b), (c), and figs. (d), (e), (f) illustrating the course of the simulation in time

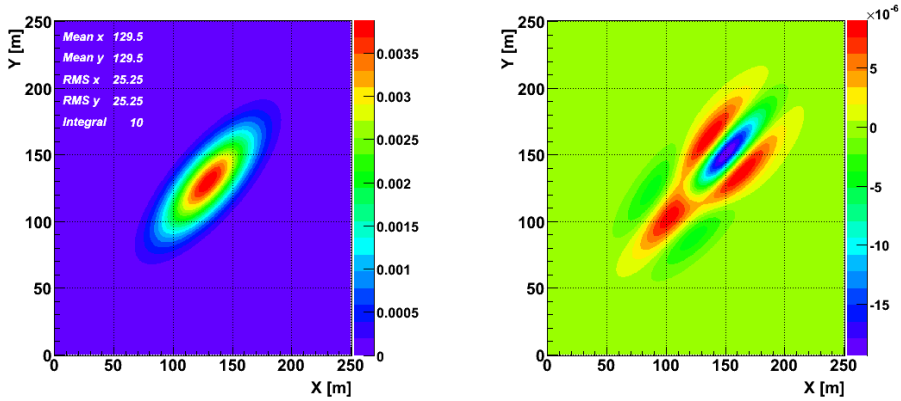

(a) Numerical solution after 750 seconds, ADI scheme

(b) Difference between the analytical solution and the numerical one, ADI scheme

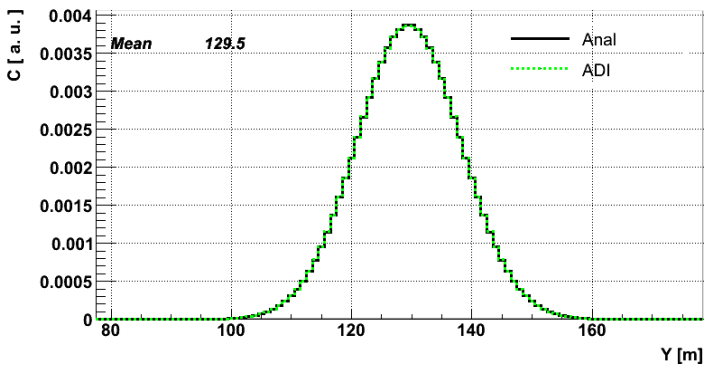

(c) Projection of the solution on the straight line perpendicular to $y = x$ and crossing the point (*Mean x*, *Mean y*)

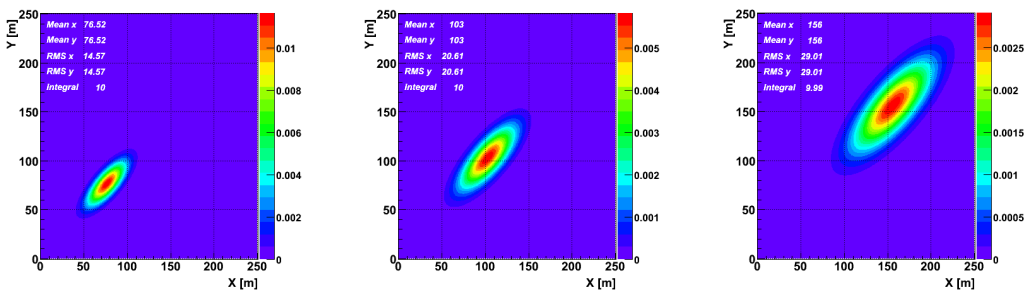

(d) 250 s

(e) 500 s

(f) 1000 s

Figure 7.4: Results of simulation with the application of the ADI scheme after 750 seconds – figs. (a), (b), (c), and figs. (d), (e), (f) illustrating the course of the simulation in time

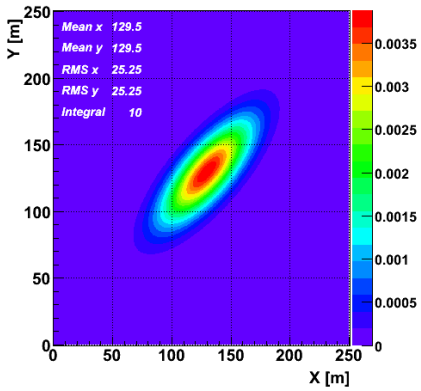

Figure 7.5: Analytical solution after 750 seconds

in figures 7.2(d) – 7.2(f), 7.3(d) – 7.3(f) and 7.4(d) – 7.4(f), indicating that the discussed numerical schemes preserve mass. Each concentration distribution – for a given numerical scheme – is accompanied by a histogram with the difference between the analytical solution and the numerical one (figs. 7.2(b), 7.3(b) and 7.4(b)), which gives information on the order of magnitude of the obtained errors.

In figures 7.2(c), 7.3(c) and 7.4(c) we can see the cross-section of the solution along the straight line perpendicular to $y = x$ and crossing the point representing the maximum concentration value at a given moment in time. For comparison, each figure stores both numerical and analytical solutions.

The differences between the analytical solution and the numerical one with the Upwind scheme are evident. The difference in both the shape and the value of maximum concentration is very well visible. The maximum difference after 750 seconds (fig. 7.2(b)) equals around 10 % of the maximum concentration in the analytical solution. In case of Crank-Nicolson and Alternating Direction Implicit method it is difficult to notice the difference between the obtained numerical solutions and the analytical one. The maximum difference is in both cases about 0.5 % of the maximum concentration value in the analytical solution. In projections 7.3(c) and 7.4(c) we can see a perfect agreement with the analytical solution. In case of the UP scheme 7.2(c) we can observe the effect of faster spreading of the pollution cloud, which is the result of the numerical diffusion described in Chapter 5. The difference between the analytical solution and the numerical one increases with the time of simulation (see fig. 7.6).

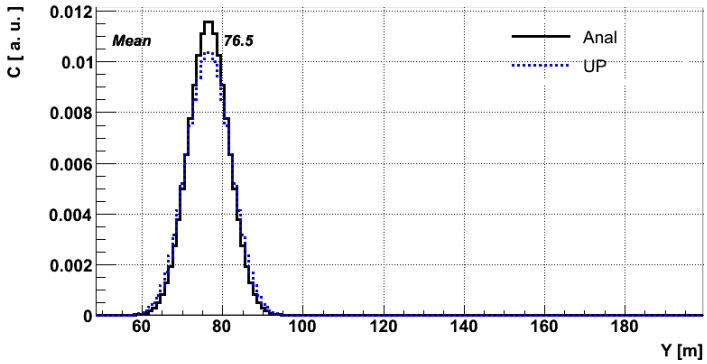

(a) 250 seconds – after 200 time steps of the simulation

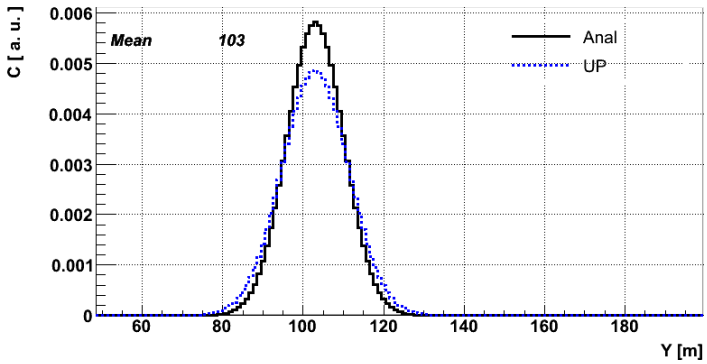

(b) 500 seconds – after 700 time steps of the simulation

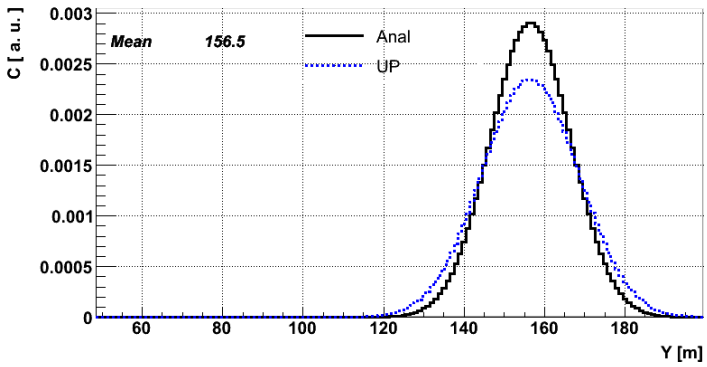

(c) 1000 seconds – after 1700 time steps of the simulation

Figure 7.6: Projection of the numerical solution and the analytical one on the straight line perpendicular to $y = x$ and crossing the point with the maximum concentration at a given moment in time

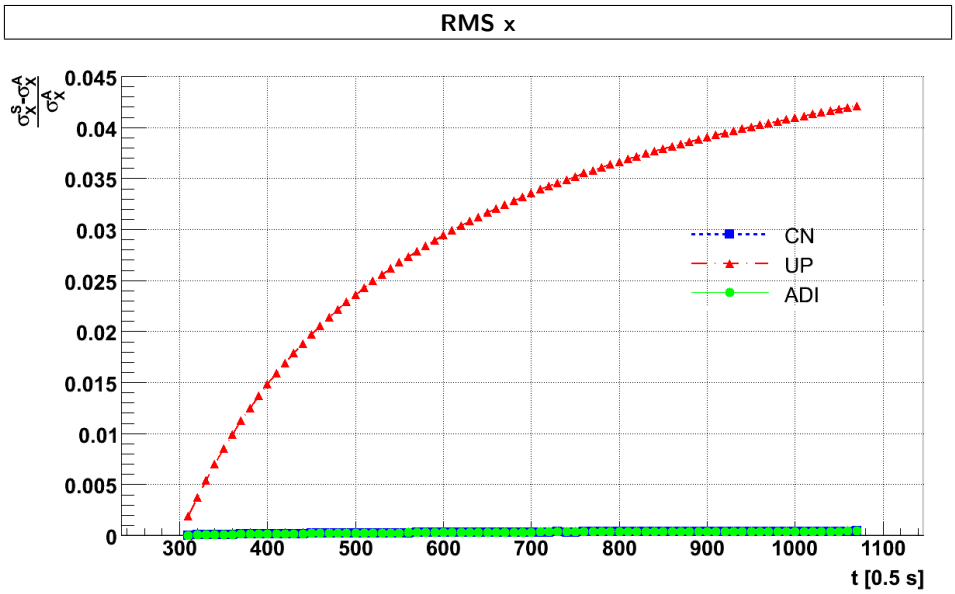

Figure 7.7: Difference between the standard deviation of the projection of the numerical solution σ_X^S and the analytical one σ_X^A upon the x axis in consecutive time steps, normalized by σ_X^A

The spread of the pollution clouds during the simulation can be determined by observing, for example, the values of standard deviation of concentration distribution projections upon x and y axes denoted in the figures by "*RMS x*" and "*RMS y*". Figure 7.7 illustrates the difference between the value of standard deviation obtained in each time step during the simulation (σ_X^S) and standard deviation in the analytical solution (σ_X^A). The difference was normalized by the value of standard deviation for the analytical solution (σ_X^A). The values of "*RMS y*" behave in a similar way. For the CN and ADI schemes, the difference is close to zero, while in case of the UP it increases with the number of time steps performed.

7.2.2 Continuous inflow of pollutants

Another situation for which numerical tests were carried out is a continuous inflow of pollutants occurring, for example, at discharge of thermal pollutants into rivers by heat-and-power plants. Continuous inflow of pollutants was simulated by increasing the mass by 10 arbitrary units at each time step. The source

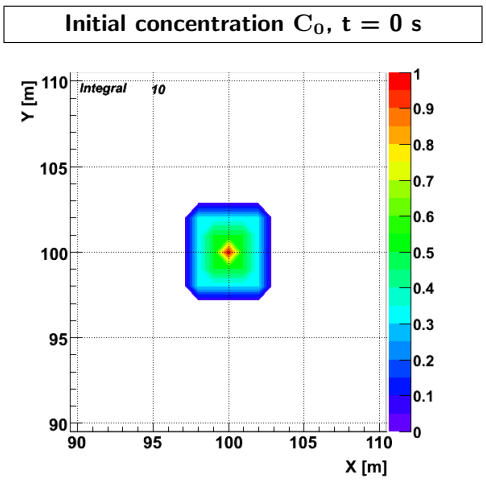

Figure 7.8: Initial concentration distribution $\mathbf{C_0}$ at time $t = 0\,\mathrm{s}$ used in the tests with continuous inflow of pollutants

– like in case of instantaneous discharge – is not situated in one point, but, in order to avoid high concentration gradients in the computational grid, was distributed over a number of adjacent points. At each time step the concentration increases at the appropriate nodes of the grid by a preset value „*val*”:

- $val = 1$ a.u. at point $x = 100$, $y = 100$;
- $val = 0.5$ a.u. at 8 points surrounding $(x,\, y) = (100, 100)$;
- $val = 0.3125$ a.u. in 16 points.

The distribution of concentration at the initial moment is illustrated in figure 7.8.

In figure 7.9 we can see the results of simulation after 3000 time steps of simulation for CN (fig. 7.9(a)), ADI (fig. 7.9(b)) and UP (fig. 7.9(c)). The charts in figure 7.10 comprise cross-sections along the $y = x$ axis (fig. 7.10(a)) and along a straight line perpendicular to it and running across the middle of the channel (fig. 7.10(b)). Like in case of instantaneous discharge, we observe a faster spreading of the pollutant cloud in case of the UP scheme. The maximum value of concentration establishes at a different level than in case of ADI and CN schemes for which we obtain almost identical solutions. The pollutant cloud reaches the cross-section along the middle of the channel faster in case of UP scheme than in case of CN and ADI schemes.

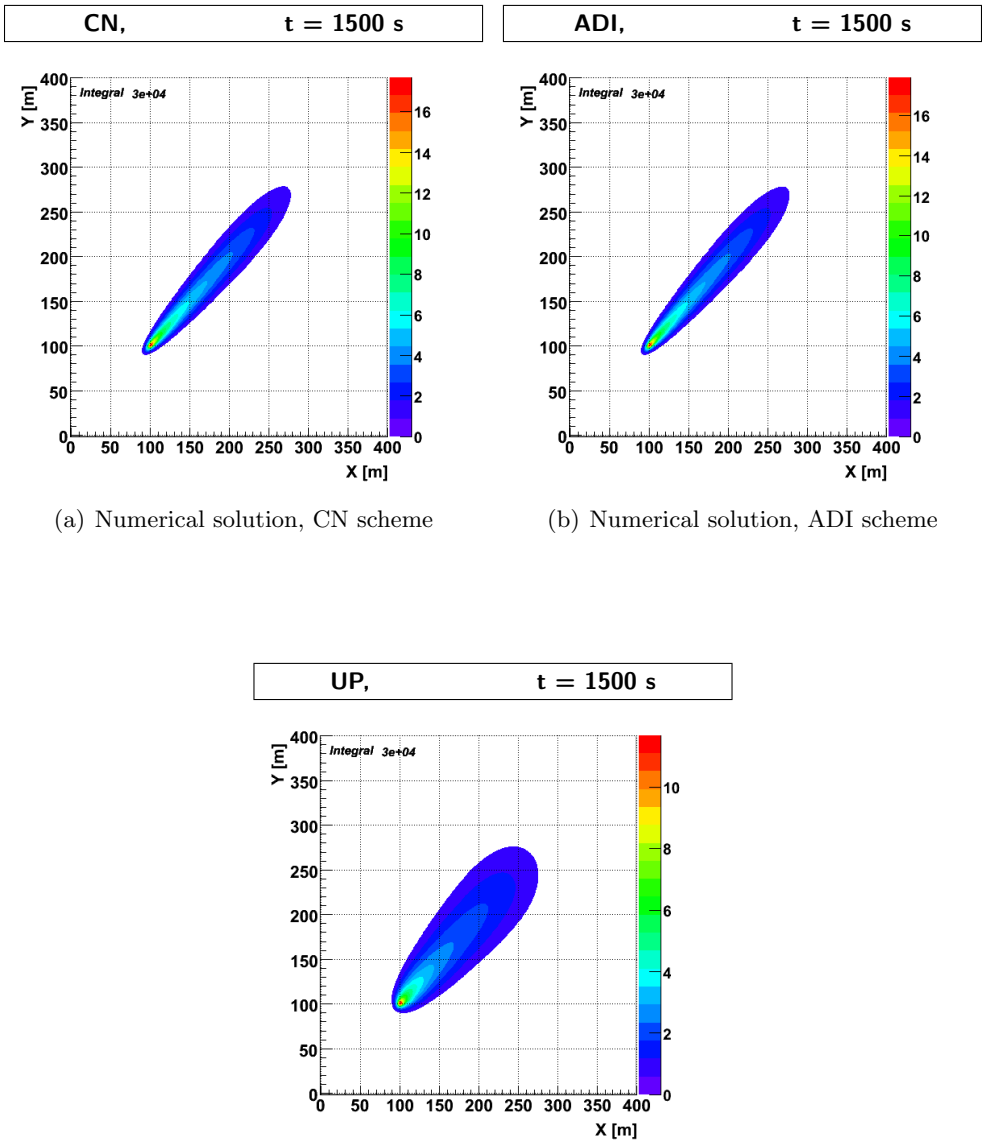

(a) Numerical solution, CN scheme

(b) Numerical solution, ADI scheme

(c) Numerical solution, UP scheme

Figure 7.9: Results of simulation for continuous discharge of pollutants after 1500 seconds for the discussed schemes

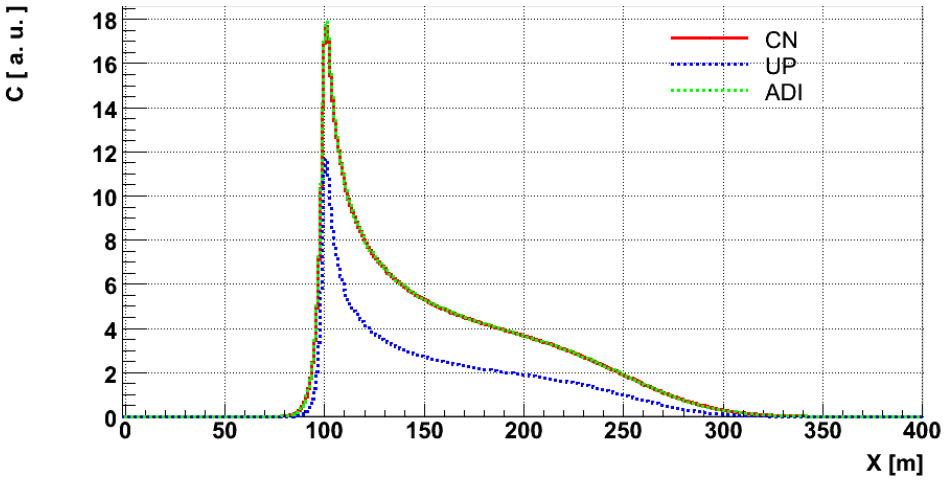

(a)

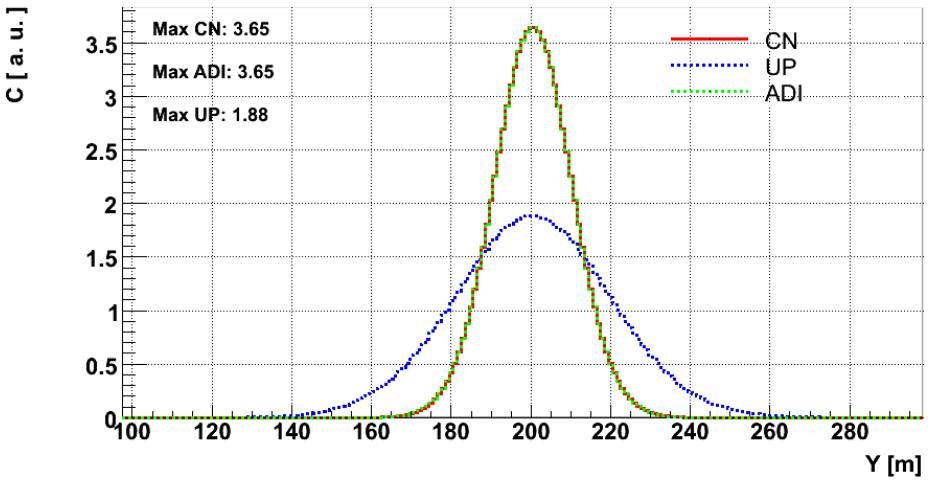

(b)

Figure 7.10: Projection of the numerical solution with the application of various schemes: (a) – on the straight line $y = x$; (b) – on the straight line perpendicular to $y = x$, crossing the middle of the channel

7.3 Laboratory compound channel

Obtaining real-life data for verification of a model requires accurate measurements of the velocity field and carrying out a two-dimensional tracer experiment. In practice, it is an expensive undertaking, requiring application of special equipment. The complexity of such experiments is confirmed by the scarce amount of experimental data concerning the two-dimensional problem of mass transport in open channels. In order to perform a qualitative verification of the model for realistic values of velocity field and dispersion coefficients, the data obtained in a compound laboratory channel at Sheffield Hallam University was used. A tracer experiment with the application of fluorescent tracer – Rhodamine WT [1], whose concentration was measured with Turner Designs fluorometer, was carried out in the channel. The velocity of water was measured with a LDA (Laser Doppler Anemometry). The obtained data comprise (Guymer, 2006):

- information concerning the geometry of the channel;
- depth-averaged velocity field;
- transverse mixing coefficients determined on the basis of experimental data;
- values of concentration of the tracer in prescribed profiles.

The discussed laboratory channel consisting of two parts, the main channel and floodplains, is presented schematically in figure 7.11. The width of the channel is $B = 1.2\,\mathrm{m}$, with the width of the main channel $b = 0.196\,\mathrm{m}$. The walls of the main channel are inclined at 45°. The tracer experiment was carried out for a steady flow $Q = 17.2\,\frac{\mathrm{l}}{\mathrm{s}}$. The average velocity of the water in the channel was $U = 0.478\,\frac{\mathrm{m}}{\mathrm{s}}$, the depth in the main channel $H = 0.0972\,\mathrm{m}$, and $h = 0.0318\,\mathrm{m}$ over the floodplains. The profile of the bottom of the channel is drawn in figure 7.12. The broken lines denote the start and the end, respectively, of the section of variable depth between the main channel and the floodplains. The depth-averaged velocity fields for the whole channel and the distribution D_{yy}, being input data for the simulations carried out are presented in figures 7.13 and 7.14 respectively.

The velocity field and the transverse mixing coefficients were used as input data for the simulations carried out, and the concentration values in the

[1] A tracer often used during the experiments in rivers (see, e.g. Rowiński *et al.*, 2003a, 2007), with color range from red to light-pink – depending on concentration

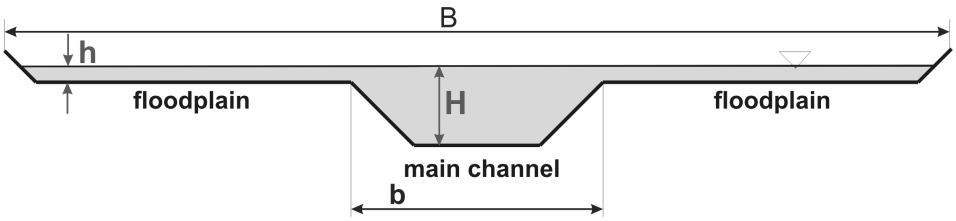

Figure 7.11: Schematic representation of the laboratory channel for which the simulations were carried out

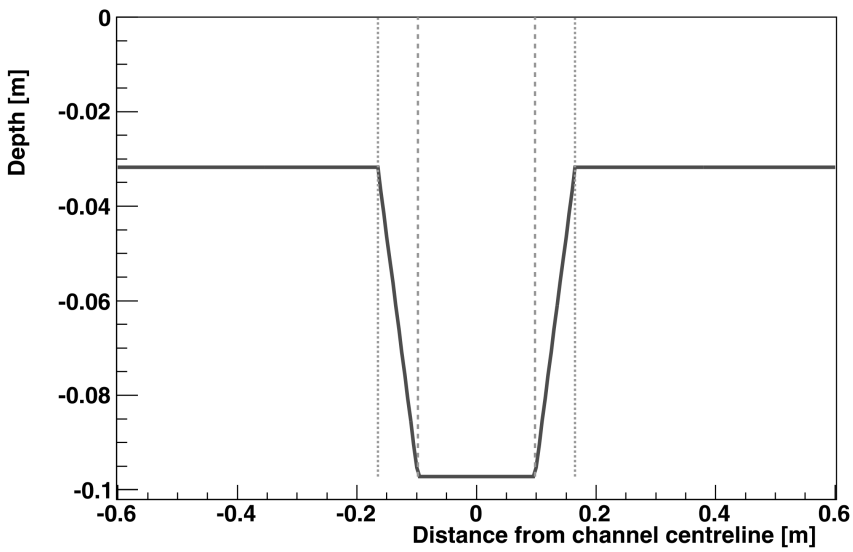

Figure 7.12: Profile of the bottom of the channel

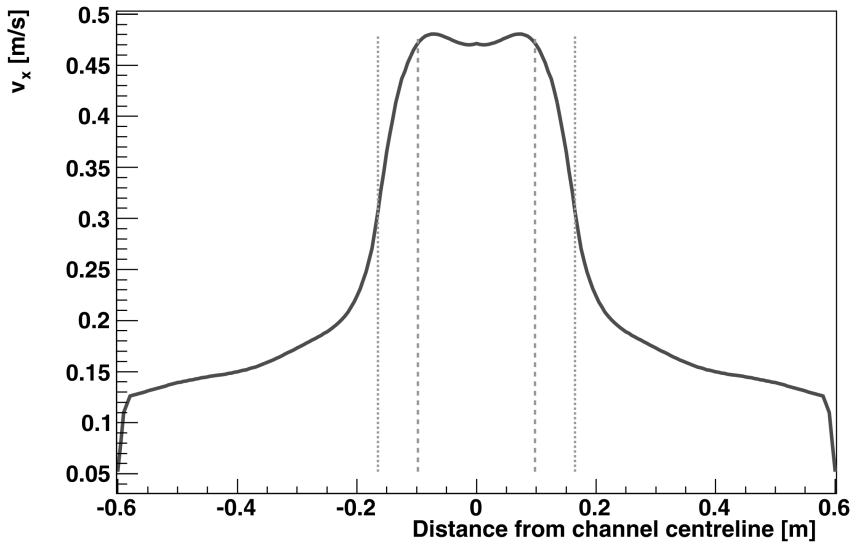

Figure 7.13: Depth-averaged (mean velocity) v_x distribution in the discussed channel

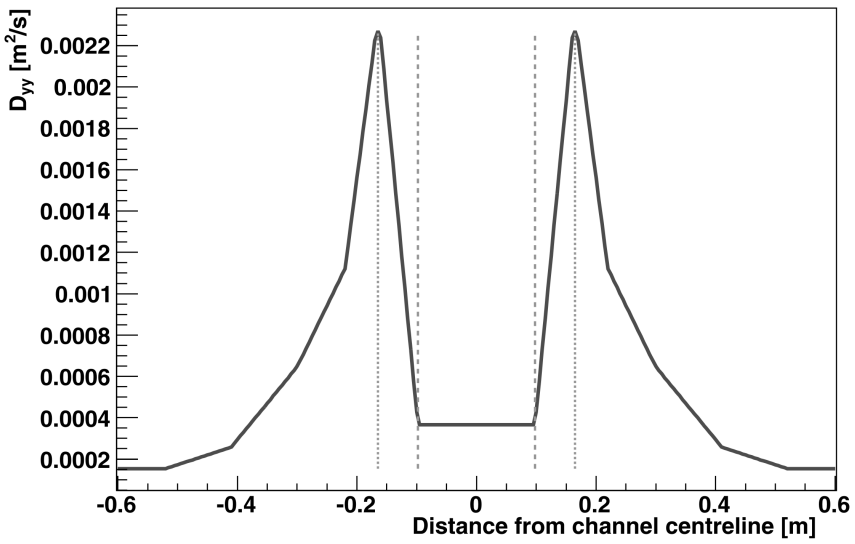

Figure 7.14: Transverse dispersion coefficient D_{yy} distribution in the channel

measured profiles – for verification of the results. It has to be stressed at the beginning, however, that in case of the tracer experiment carried in the channel in question, the concentration was measured at one depth, in the first version at $z = 2.11\,\mathrm{cm}$ (measured from the water surface), in the second (used here) – at the bottom of the channel. In case of measurements at one depth, we cannot speak about depth-averaged concentration values, and it is an obvious oversimplification at the basis of the model. The transverse mixing coefficients determined in the laboratory in Sheffield on the basis of measured concentration distributions with the application of the modified momentum method (Holley *et al.*, 1972), may also be encumbered with error. Therefore, the discussion presented in this chapter may be treated only as qualitative checking of the operation of the **RivMix** model on experimental data with variable velocity field and variable dispersion coefficients. In order to carry out reliable quantitative tests, the tracer experiment should comprise measurements of a larger number of depth-averaged concentration distribution profiles, which would allow for determination of vertically-averaged concentration values.

The simulation was carried out using the fastest method, ADI, the simulation parameters are presented in table 7.2. The value of the D_L coefficient (equal D_{xx} in the case in question) was determined on the basis of the empirical relationship (Elder, 1959):

$$D_{xx} = 5.93 h u_*, \tag{7.1}$$

where:

u_* – friction velocity;
h – depth.

In the calculations, the values of u_* determined at Sheffield Hallam University were used:

- $u_* = 0.0219\,\frac{\mathrm{m}}{\mathrm{s}}$ – for the main channel,
- $u_* = 0.0138\,\frac{\mathrm{m}}{\mathrm{s}}$ – for floodplains.

The distribution of longitudinal dispersion coefficient D_L is illustrated in figure 7.15. This relationship is one of the simplest empirical formulae used for determining of D_L available in the literature (Section 2.4), but its selection turned out to have insignificant influence upon the obtained distribution of tracer concentrations.

In the tracer experiment, continuous inflow of pollutants was taken into consideration, with the source situated in the middle of the channel over the

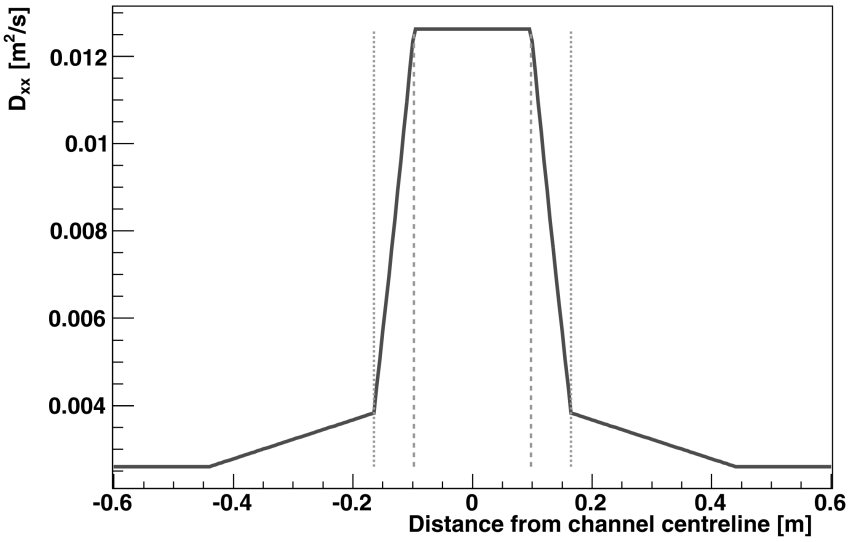

Figure 7.15: Longitudinal dispersion coefficient distribution in the channel

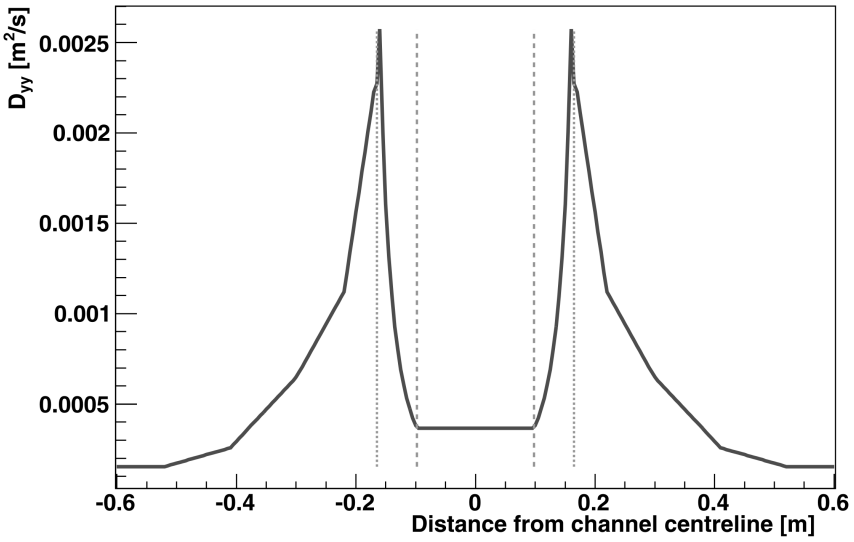

Figure 7.16: Transverse dispersion coefficient distribution in the channel

Table 7.2: Simulation parameters used in the tests carried out

Grid spacing		Time step
Δx[m]	Δy[m]	Δt[s]
0.01	0.005	0.1

surface of the water. The source in the numerical tests was simulated with the application of Gauss distribution (with standard deviation of $\sigma_x = \sqrt{3}\Delta x, \sigma_y = \sqrt{3}\Delta y$), increasing the concentration value by 10 arbitrary units at the point representing the situation of the source in each time step.

In the analysis leading to the determination of D_{yy} coefficient, a triangular distribution of dispersion coefficient as a function of the distance from the axis of the channel was assumed. This dependency was smoothed in the model in order to avoid numerical problems connected with large variations of the coefficient between consecutive nodes of the grid (fig. 7.16).

The results of the simulation after 50 time steps are illustrated in figure 7.17. Numerical tests demonstrated that the distribution of concentration in space can be considered fixed after 100 time steps, as presented in figure 7.18.

Because the first series of measurements was carried out close to the source (at distances of 0.112 m, 0.182 m, 0.252 m, 0.322 m and 0.392 m from the source), where the pollutant cloud is not yet mixed over the channel depth, it was disregarded. Such a situation should be modeled with the application of a three-dimensional equation, see Chapter 2. The second series of measurements was done at a distance of 1.89 m, 2.14 m and $2,64$ m from the source. In this case, vertical mixing can be assumed (see table 2.2) and the depth-averaged two-dimensional advection-diffusion equation (2.6) could be used. For such a situation, the three profiles given, the results of simulation and the results of measurements were plotted in figures 7.19, 7.21 and 7.23.

Note that the results of simulations were scaled in such a way that the maximum concentration value from the simulations be equal to the maximum value measured in the given profile. Because common normalization for all three profiles did not bring about desired results, each profile was normalized separately in individual profiles. The shapes obtained as a result of the simulation are characterized with high similarity to the shapes of distribution obtained during the experiment. The fact that the sides of the distribution are close to the expected ones (figs. 7.20, 7.22 and 7.24) requires special attention. Obviously, in

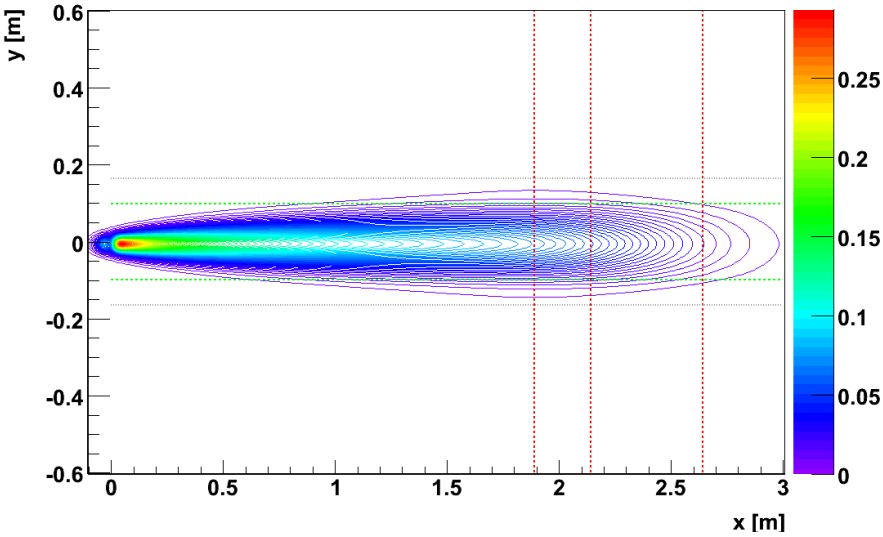

Figure 7.17: Concentration distribution $c(x, y)$ after 50 time steps

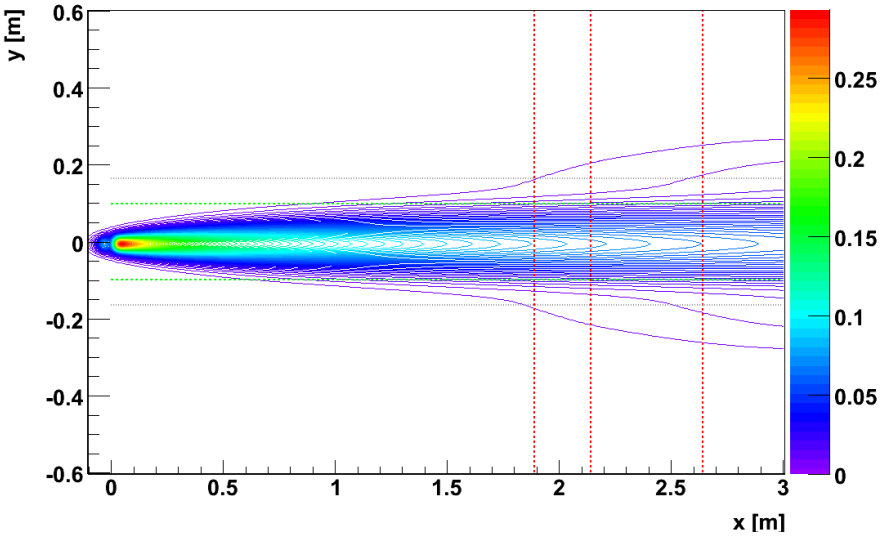

Figure 7.18: Concentration distribution $c(x, y)$ after 100 time steps

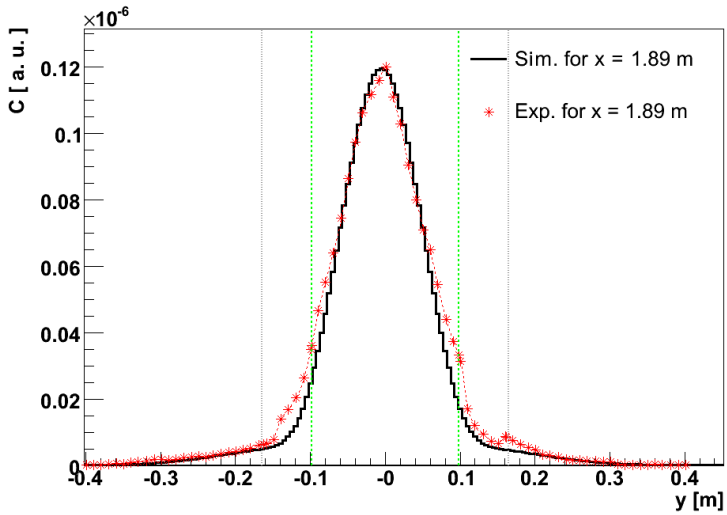

Figure 7.19: Concentration distribution after 100 time steps at the distance of 1.89 m from the source – comparison of simulated and experimental results

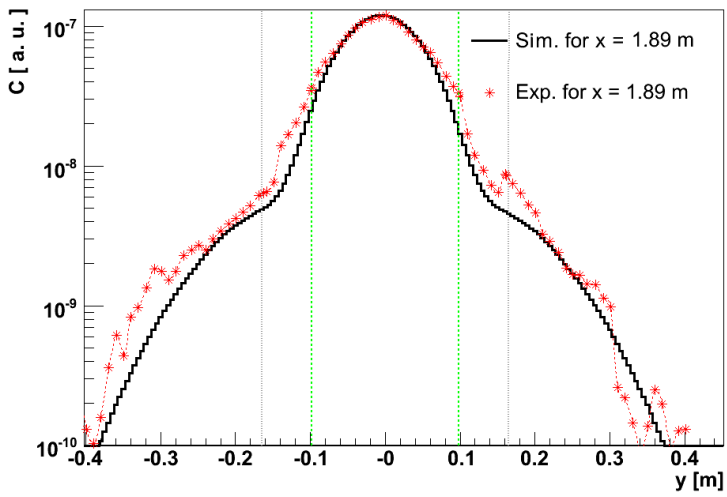

Figure 7.20: Concentration distribution after 100 time steps at the distance of 1.89 m from the source – comparison of simulated and experimental results; logarithmic scale

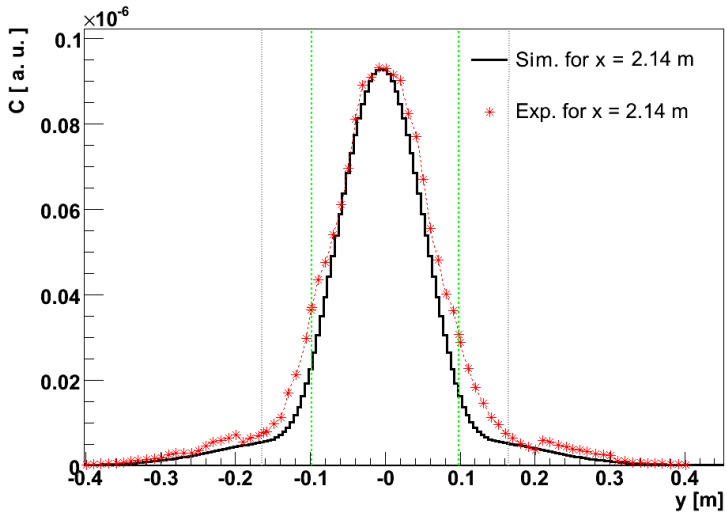

Figure 7.21: Concentration distribution after 100 time steps at the distance of 2.14 m from the source – comparison of simulated and experimental results

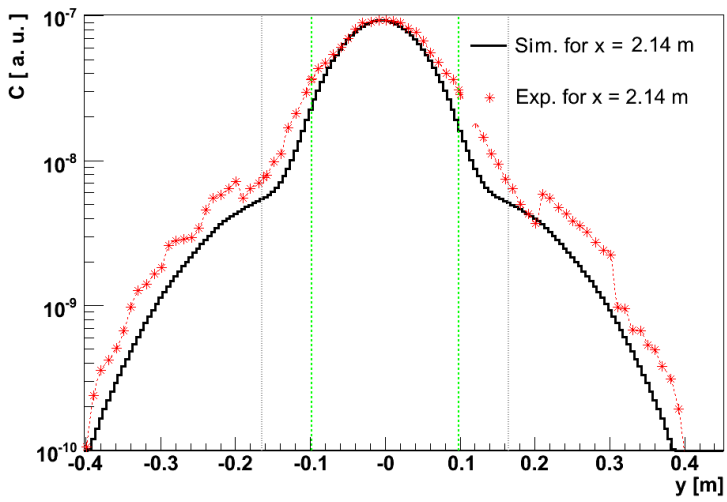

Figure 7.22: Concentration distribution after 100 time steps at the distance of 2.14 m from the source – comparison of simulated and experimental results; logarithmic scale

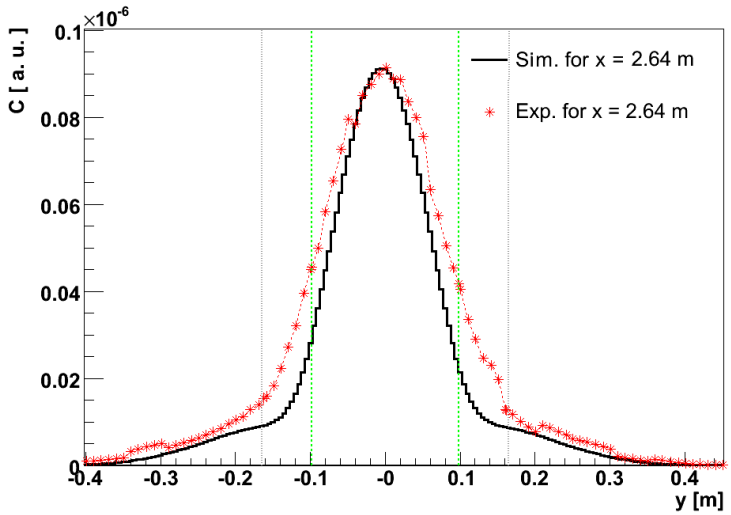

Figure 7.23: Concentration distribution after 100 time steps at the distance of 2.64 m from the source – comparison of simulated and experimental results

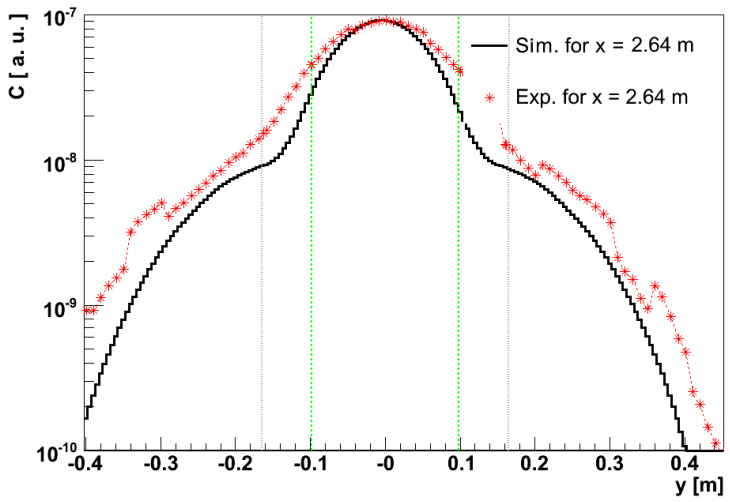

Figure 7.24: Concentration distribution after 100 time steps at the distance of 2.64 m from the source – comparison of simulated and experimental results; logarithmic scale

ideal situation we would like the maximum values of concentrations obtained during the simulation to agree with the data, which could not be obtained without assessing possible systematic errors in the collected data and derived D_{yy} coefficients. The basic problem here is the fact that the concentrations in the experiment (measured at the bottom of the channel) may not be representative for the averaged concentration values, and we obtain such data as a result of the simulations carried out. The next reason for partial disagreement of the simulation results with the data may be the uncertainty in the determination of the D_{yy} coefficient connected with the momentum method and the assumed triangular distribution of the dispersion coefficient in the function of distance from the axis of the channel. The attempts can be made to solve the problem by independent determination of D_{xx} and D_{yy} coefficients, which is in turn a separate and complex problem which whole volumes are devoted to (e.g. Beak, 2004; Boxall, 2000).

Chapter 8

Concluding remarks

A computer model (River Mixing Model – **RivMix**) of transport of passive solutes, described in the book, can be used for analyses of two-dimensional spreading of pollutants in rivers and be an effective tool to carry out the assessment of the impact on the environment. The **RivMix** model enables selection of one of the four implemented numerical schemes: Upwind (UP), Crank-Nicolson (CN), and the Alternating Direction Implicit method in two variations marked as (ADI) and (ADI2). The analysis of properties and speed of the schemes in question, presented in the book, and first of all the determined accuracy and comparison of the implemented methods with the analytical solution for a straight channel will be useful for the model users. They allow to evaluate the usefulness of individual methods and the results obtained with them, and the selection of the appropriate method depending on the demands of the specific problem. The analyses can also be useful for people solving numerical advection-diffusion equation with mixed derivatives, not necessarily applied to the transport of pollutants in open channels, especially since the number of publications in which mixed derivatives in two-dimensional advection-diffusion equation are taken into consideration is small.

Solving the transport equation numerically, attention has to be paid first of all to the accuracy of the applied method, and, what follows, the obtained results. What is also often important is the computing cost; the numerical tests carried out demonstrated that the implicit UP scheme is the fastest of all the discussed ones. Using it, however, one has to be aware of the numerical diffusion significantly influencing the exactness of the obtained results. The error magnitude can be estimated using the equations derived in the book. Nevertheless, in case of an emergency, e.g. instantaneous discharge of pollutants into a river, the UP scheme can provide us with information on the situation of the maxi-

mum concentration, and therefore the possibility to take up necessary measures quickly. In order to obtain an exact solution not affected with the numerical diffusion error, the ADI method has to be used, which is based on the implicit CN scheme, with the Thomas analytical method for solving the equation systems. The method is stable and relatively fast. Carrying out numerical calculations, one has to remember about appropriate selection of simulation parameters – time step and the size of the mesh in the computation grid. In case of the UP scheme, attention has to be paid that the scheme be stable, and in case of ADI and CN that no non-physical oscillations occur. Due to the limitations of the time step in case of the UP scheme, in some situations, when we are not interested in high resolution of results, the ADI method may turn out faster since the time step used in it can be bigger.

While modeling spreading of pollutants, mixed derivatives are often disregarded, due to the (not always right) assumption that the dispersion tensor present in the equation is diagonal. The tests of various methods of simplification of a non-diagonal dispersion tensor, carried out in this work, demonstrate that such assumption can have significant influence upon the obtained solution. The presented computation tests demonstrate unambiguously that using the simplified two-dimensional transport equation, the correct solution can be obtained only in very specific cases. The error will not be big for simple geometry if the slope of the axis of the channel changes insignificantly along the length considered. Only in some situations, e.g. when we are interested in the location with the maximum concentration of solute, disregarding mixed derivatives will not influence the expected result – irrespective of the geometry of the channel in question. When we consider instantaneous discharge of admixture, all methods correctly indicate the position of maximum concentration, and identity transformations, additionally, maximum concentration value. In other situations we obtain results divergent from reality. The obtained results can be helpful in conscious application of simplified versions of dispersion tensor.

The verification of the model carried out with the application of the analytical solution demonstrates that solutions with high accuracy can be obtained for CN and ADI schemes, which is confirmed by the preceding analysis of truncation error. With the application of the UP scheme, the obtained results are affected by numerical diffusion error. Verification with experimental data confirmed, on the other hand, the qualitative performance of the model which properly reflexes the shapes of concentration distributions in individual profiles. Reliable qualitative analyses require that an appropriate tracer experiment be carried out, comprising measurements of the appropriated number of profiles of concentration distributions along the depth, in order to determine vertically-averaged

concentration values. Carrying out such an experiment shall be the purpose of further research. The experiments should be carried out for channels with various geometries.

Appendix A

2D Transport Equation for Constant and Variable Depth

The two-dimensional depth-averaged transport equation:

$$h\left(\frac{\partial c}{\partial t}+v_x\frac{\partial c}{\partial x}+v_y\frac{\partial c}{\partial y}\right) = \frac{\partial}{\partial x}\left(hD_{xx}\frac{\partial c}{\partial x}+hD_{xy}\frac{\partial c}{\partial y}\right)+\frac{\partial}{\partial y}\left(hD_{yy}\frac{\partial c}{\partial y}+hD_{yx}\frac{\partial c}{\partial x}\right), \quad \text{(A.1)}$$

after differentiating the right side of the equation, becomes:

$$\frac{\partial c}{\partial t}+v_x\frac{\partial c}{\partial x}+v_y\frac{\partial c}{\partial y} = \frac{1}{h}\left(\frac{\partial(hD_{xx})}{\partial x}\frac{\partial c}{\partial x}+hD_{xx}\frac{\partial^2 c}{\partial x^2}+\frac{\partial(hD_{xy})}{\partial x}\frac{\partial c}{\partial y}+hD_{xy}\frac{\partial^2 c}{\partial x\partial y} + \frac{\partial(hD_{yx})}{\partial y}\frac{\partial c}{\partial x}+hD_{yx}\frac{\partial^2 c}{\partial x\partial y}+\frac{\partial(hD_{yy})}{\partial y}\frac{\partial c}{\partial y}+hD_{yy}\frac{\partial^2 c}{\partial y^2}\right). \quad \text{(A.2)}$$

After regrouping one obtains:

$$\frac{\partial c}{\partial t} + \frac{\partial c}{\partial x}\underbrace{\left(v_x - \frac{1}{h}\frac{\partial(hD_{xx})}{\partial x} - \frac{1}{h}\frac{\partial(hD_{xy})}{\partial y}\right)}_{v_x^{'}} + \frac{\partial c}{\partial y}\underbrace{\left(v_y - \frac{1}{h}\frac{\partial(hD_{xy})}{\partial x} - \frac{1}{h}\frac{\partial(hD_{yy})}{\partial y}\right)}_{v_y^{'}} = D_{xx}\frac{\partial^2 c}{\partial x^2} + 2D_{xy}\frac{\partial^2 c}{\partial x \partial y} + D_{yy}\frac{\partial^2 c}{\partial y^2}. \quad \text{(A.3)}$$

For the constant depth and constant dispersion coefficients or when the variations of those between the grid nodes are small we can assume that:

$$v_x = v_x^{'},$$
$$v_y = v_y^{'}.$$

In other case values $v_x^{'}$ and $v_y^{'}$ must be calculated numerically, e.g. using central difference quotient (4.4).

Appendix B

Difference Operators Used in the Book

Table B.1 contains all difference operators used in the book. Aside the differential operators the symbols used to mark difference operators and order of accuracy for particular difference quotients have been written.

Table B.1: Collection of all difference quotients used in the book

Differential operator	Difference operator	Applied difference quotients	Approximation order
$\frac{\partial c}{\partial x}$	$\nabla_x C_{i,j}$	$\frac{c_{i,j} - c_{i-1,j}}{\Delta x}$	$O(\Delta x)$
$\frac{\partial c}{\partial x}$	$\nabla_x C_{i,j}$	$\frac{c_{i+1,j} - c_{i,j}}{\Delta x}$	$O(\Delta x)$
$\frac{\partial c}{\partial x}$	$\nabla_x C_{i,j}$	$\frac{c_{i+1,j} - c_{i-1,j}}{2\Delta x}$	$O(\Delta x^2)$
$\frac{\partial^2 c}{\partial x^2}$	$\delta_x^2 C_{i,j}$	$\frac{c_{i-1,j} - 2c_{i,j} + c_{i+1,j}}{\Delta x^2}$	$O(\Delta x^2)$
$\frac{\partial^2 c}{\partial x \partial y}$	$\delta_{xy} C_{i,j}$	$\frac{c_{i+1,j+1} - c_{i+1,j-1} - c_{i-1,j+1} + c_{i-1,j-1}}{4\Delta x \Delta y}$	$O(\Delta x^2, \Delta y^2)$
$\frac{\partial c}{\partial x}\frac{\partial c}{\partial y}$	$\nabla_x \nabla_y C_{i,j}$	$\frac{c_{i+1,j+1} - c_{i+1,j-1} - c_{i-1,j+1} + c_{i-1,j-1}}{4\Delta x \Delta y}$	$O(\Delta x^2, \Delta y^2)$
$\frac{\partial c}{\partial x}\frac{\partial^2 c}{\partial y^2}$	$\nabla_x \delta_y^2 C_{i,j}$	$\frac{-c_{i-1,j-1} + 2c_{i-1,j} - c_{i-1,j+1} + c_{i+1,j-1} - 2c_{i+1,j} + c_{i-1,j-1}}{2\Delta x \Delta y^2}$	$O(\Delta x^2, \Delta y^2)$
$\frac{\partial c}{\partial y}\frac{\partial^2 c}{\partial x^2}$	$\nabla_y \delta_x^2 C_{i,j}$	$\frac{-c_{i-1,j-1} + c_{i-1,j+1} + 2c_{i,j-1} - 2c_{i,j+1} - c_{i+1,j-1} + c_{i-1,j-1}}{2\Delta x^2 \Delta y}$	$O(\Delta x^2, \Delta y^2)$
$\frac{\partial^2 c}{\partial x^2}\frac{\partial^2 c}{\partial y^2}$	$\delta_x^2 \delta_y^2 C_{i,j}$	$\frac{4c_{i,j} - 2c_{i+1,j} - 2c_{i-1,j} - c_{i,j+1} - 2c_{i,j-1}}{\Delta x^2 \Delta y^2}$ $+\frac{c_{i+1,j+1} + c_{i+1,j-1} + c_{i-1,j+1} + c_{i-1,j-1}}{\Delta x^2 \Delta y^2}$	$O(\Delta x^2, \Delta y^2)$

Appendix C

Dispersion Tensor Simplifications for Different Angles α

In this appendix the simulation results for tests of different methods of dispersion tensor simplification described in Chapter 3, for angles α: 0°, 5°, 15°, 30° and 60° have been collected.

C.1 Instantaneous release of solute

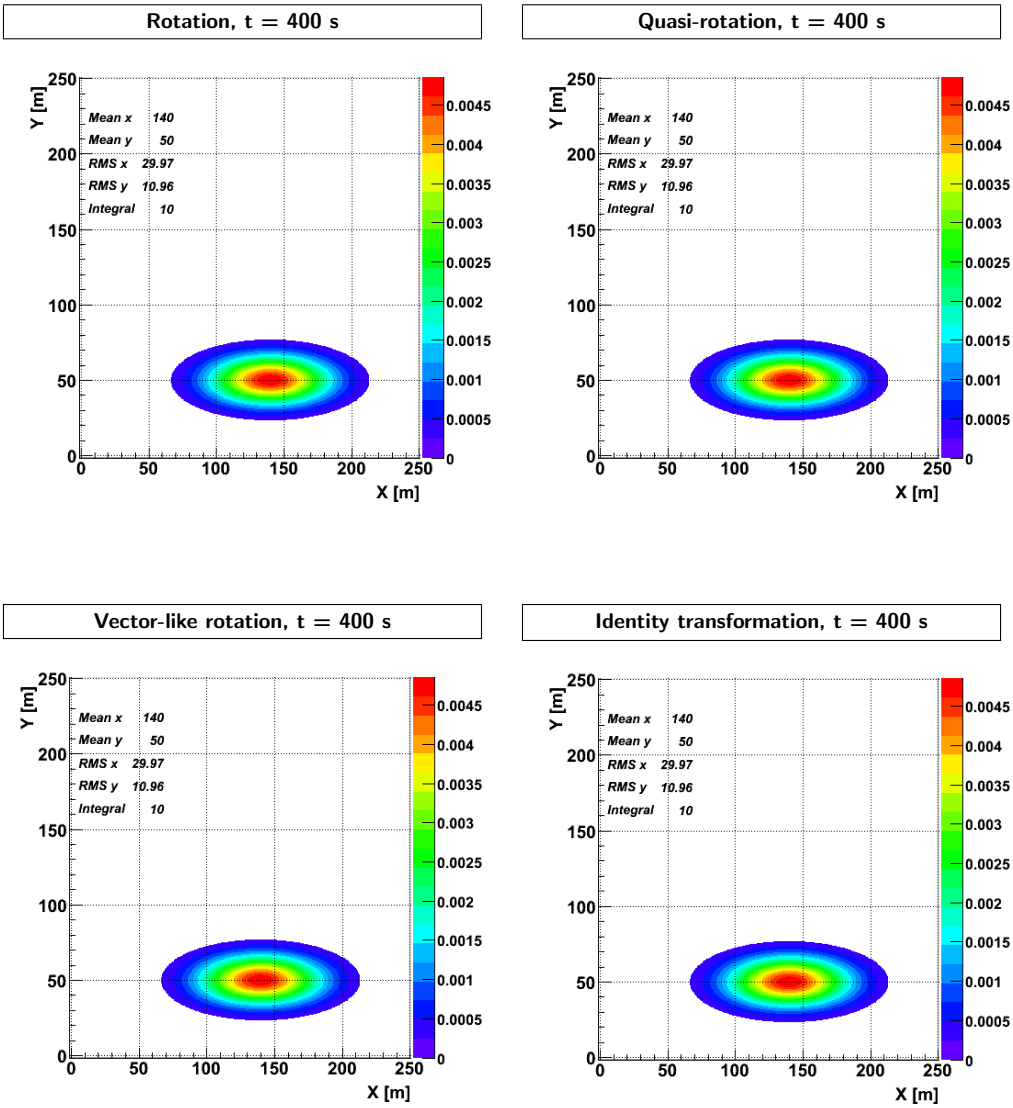

Figure C.1: Numerical solution with application of different methods of dispersion tensor transformation for the pulse release after 400 time steps, $\alpha = 0°$

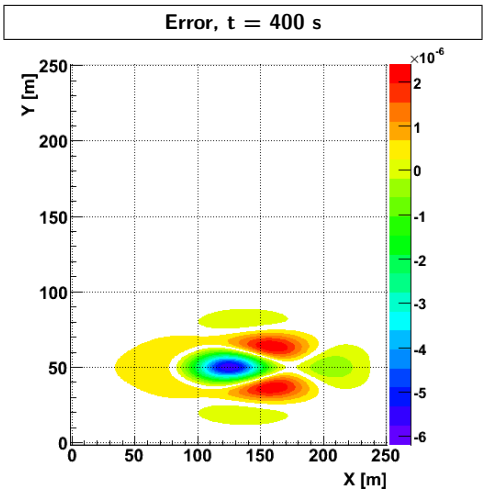

Figure C.2: Difference between the numerical solution and analytical one for the pulse release after 400 time steps, $\alpha = 0°$; the difference is the same for all methods of dispersion tensor transformation

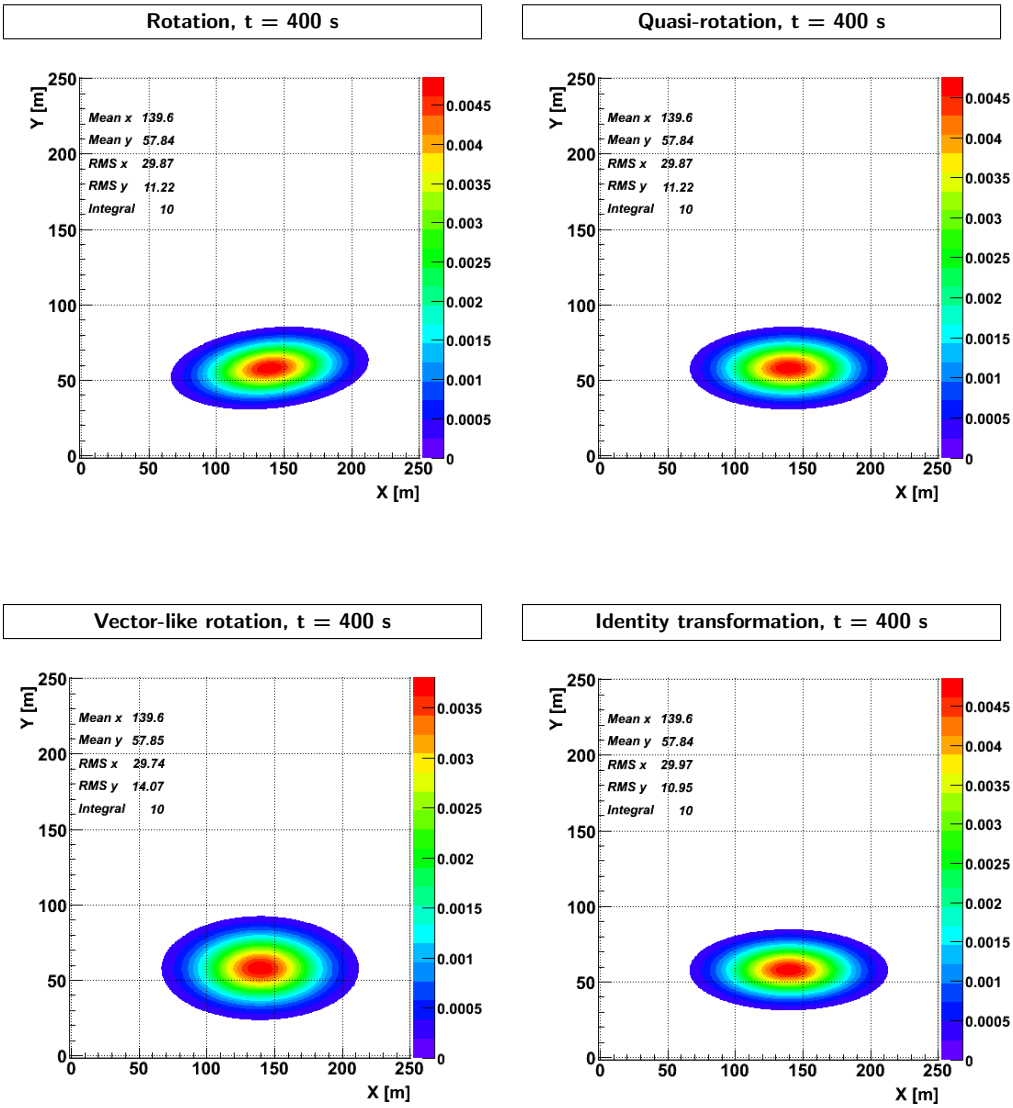

Figure C.3: Numerical solution with application of different methods of dispersion tensor transformation for the pulse release after 400 time steps, $\alpha = 5°$

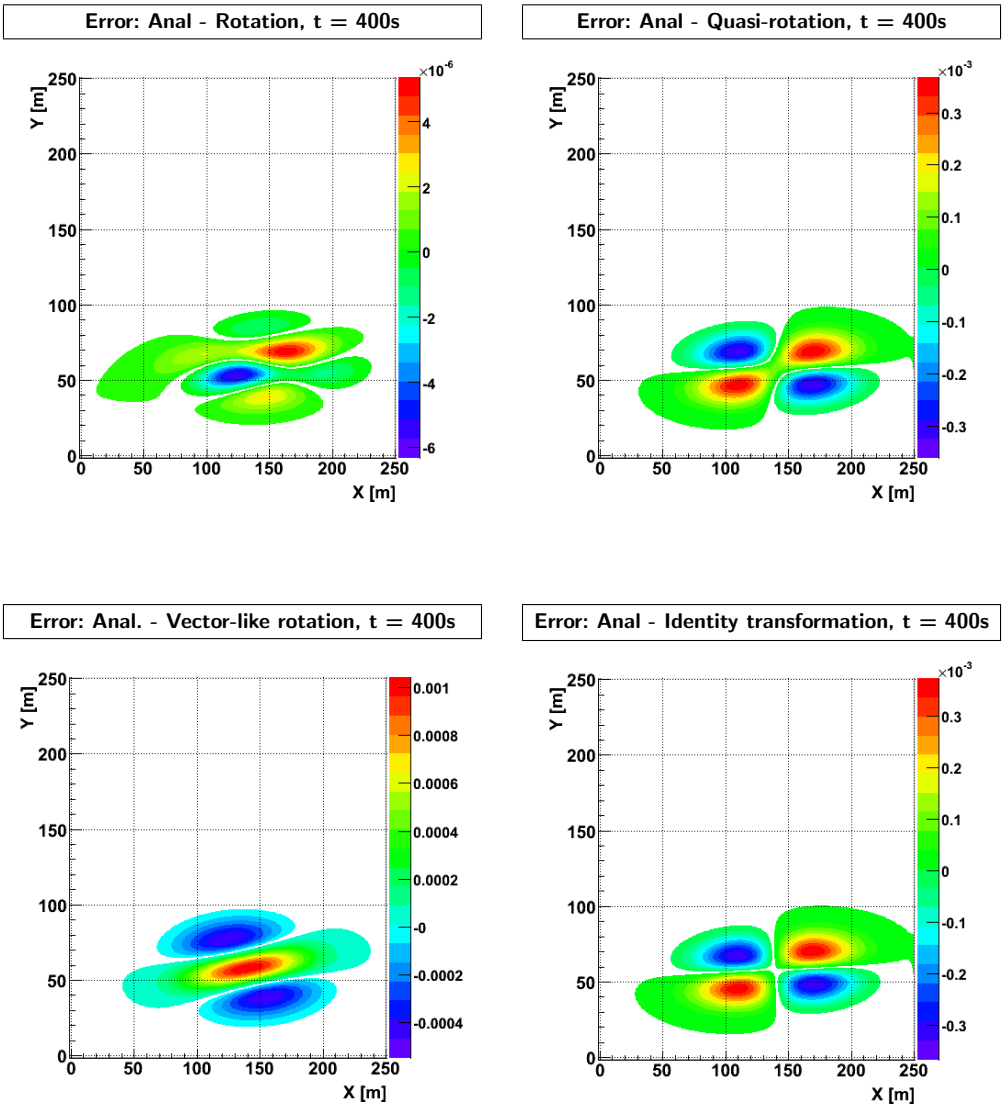

Figure C.4: Difference between the numerical solution and analytical one for different methods of dispersion tensor transformation for the pulse release after 400 time steps, $\alpha = 5°$

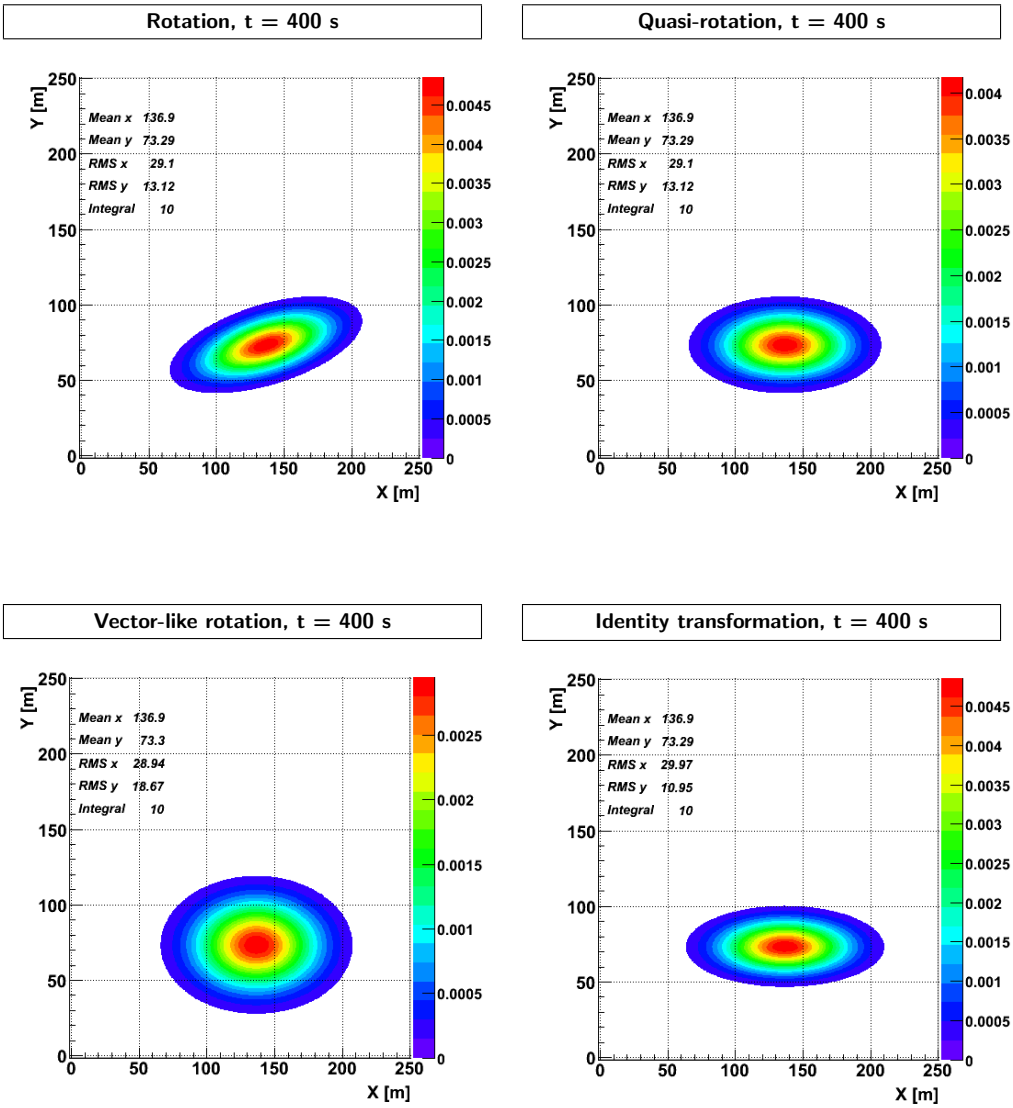

Figure C.5: Numerical solution with application of different methods of dispersion tensor transformation for the pulse release after 400 time steps, $\alpha = 15°$

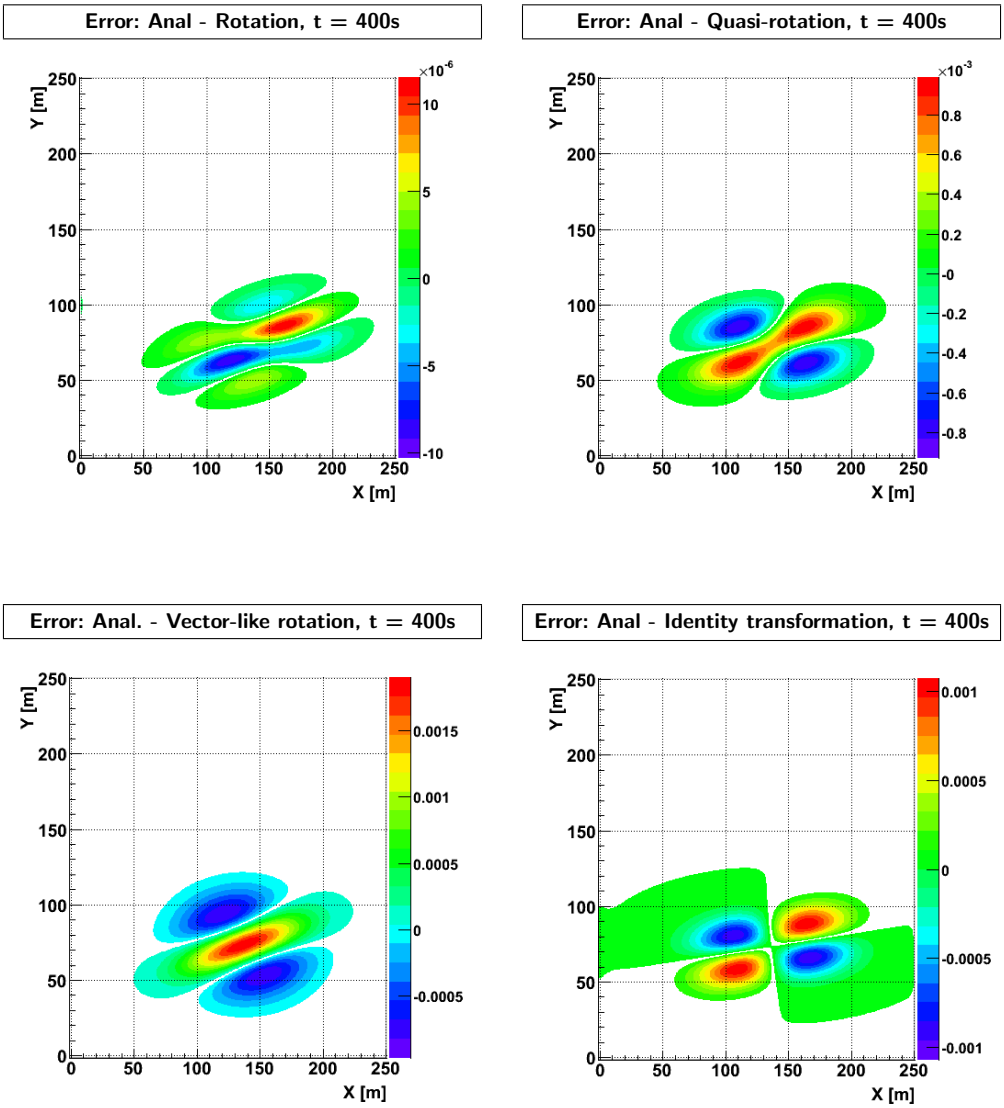

Figure C.6: Difference between the numerical solution and analytical one for different methods of dispersion tensor transformation for the pulse release after 400 time steps, $\alpha = 15°$

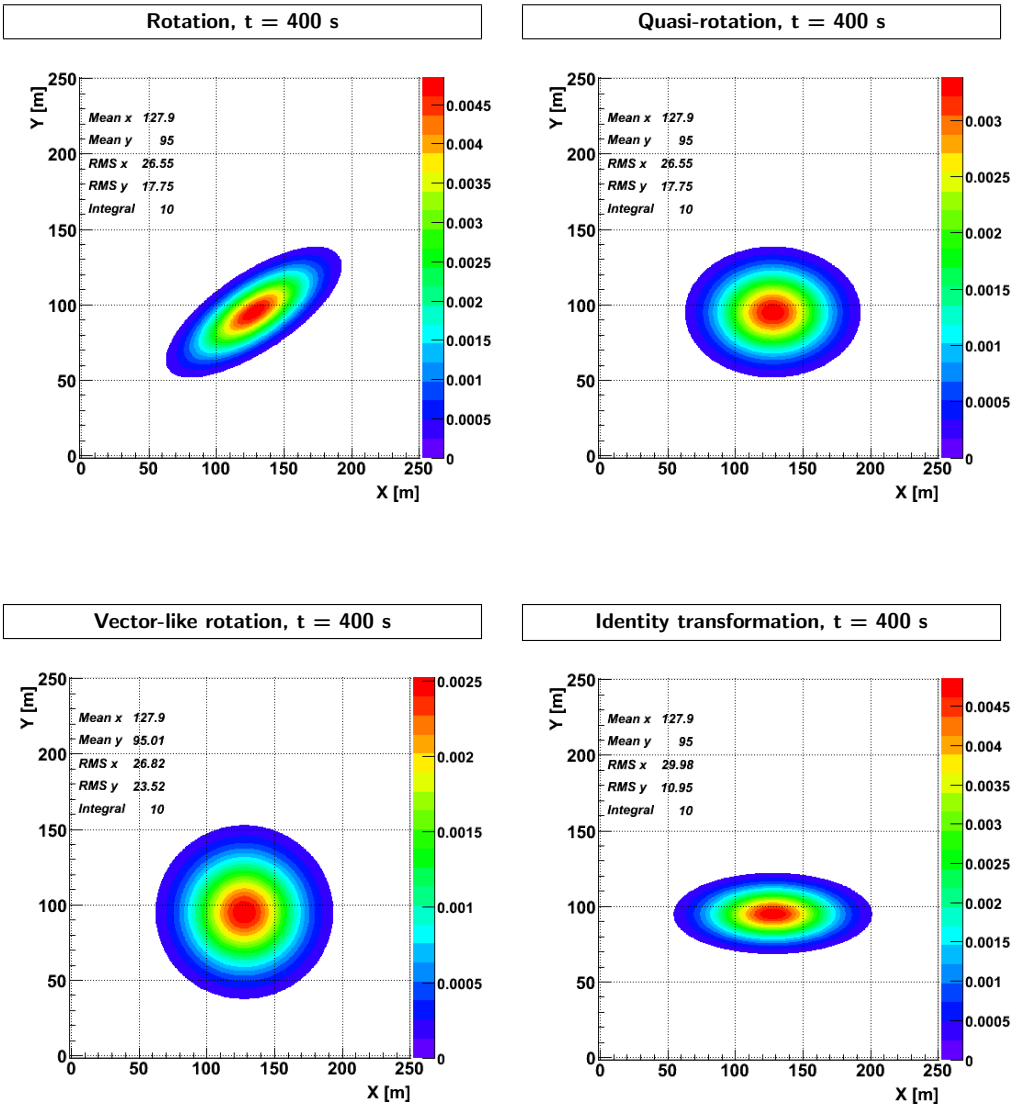

Figure C.7: Numerical solution with application of different methods of dispersion tensor transformation for the pulse release after 400 time steps, $\alpha = 30°$

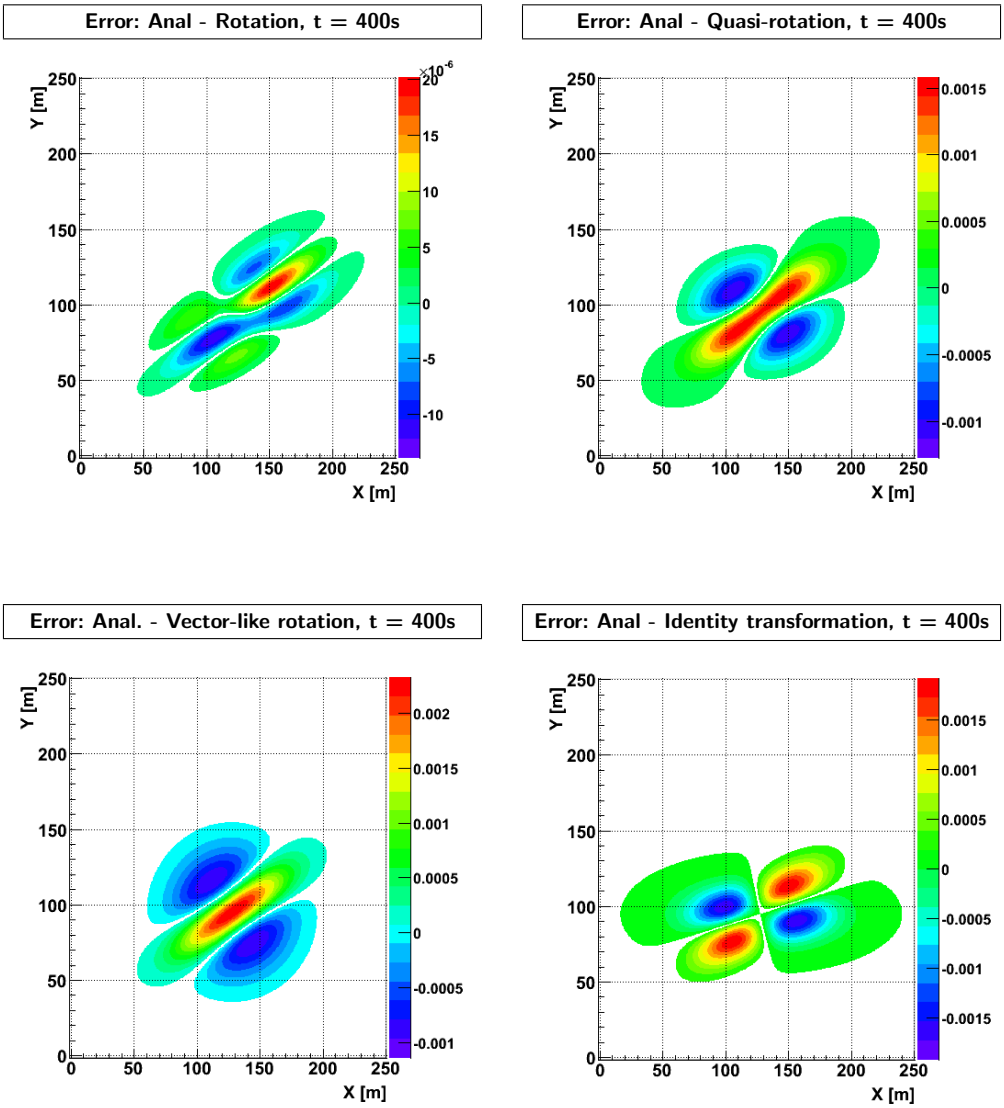

Figure C.8: Difference between the numerical solution and analytical one for different methods of dispersion tensor transformation for the pulse release after 400 time steps, $\alpha = 30°$

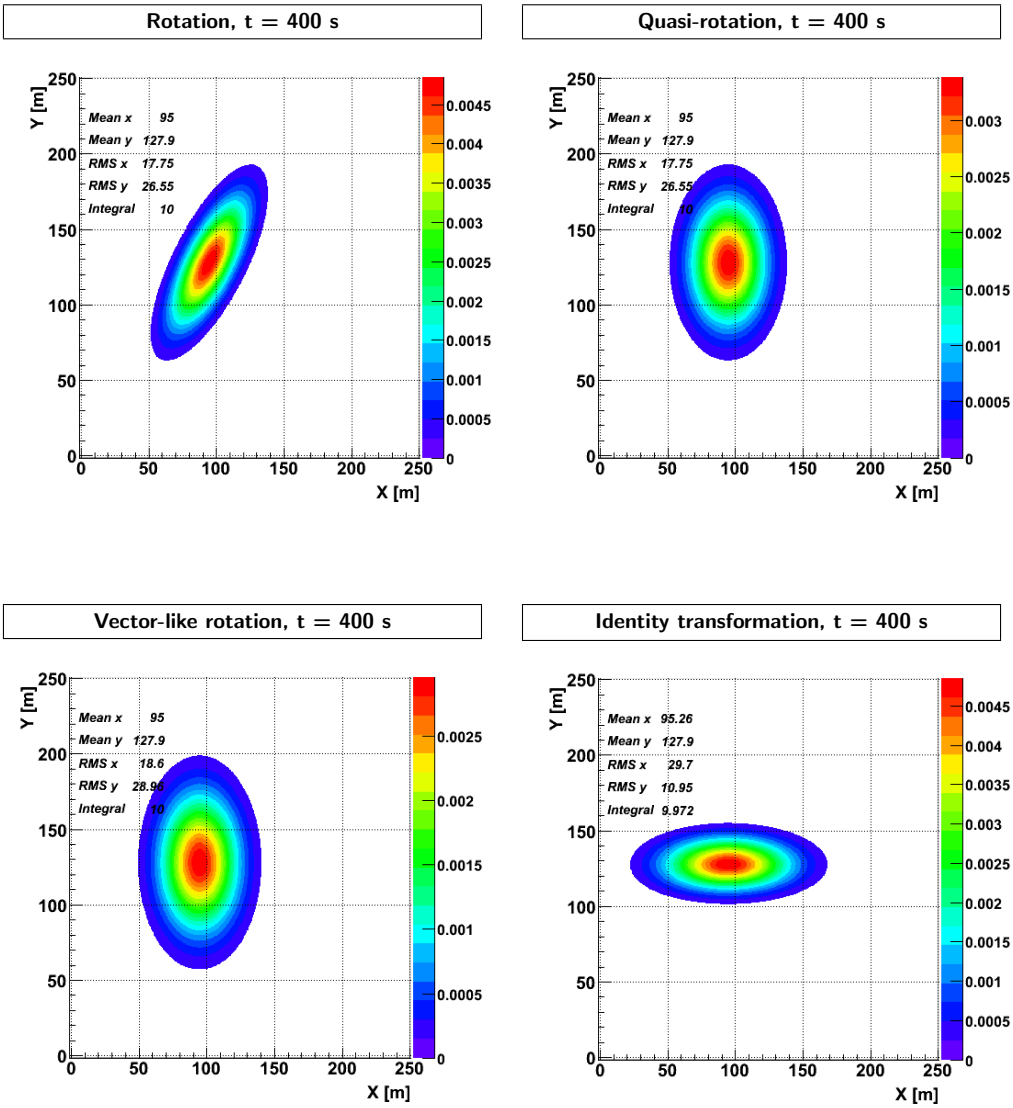

Figure C.9: Numerical solution with application of different methods of dispersion tensor transformation for the pulse release after 400 time steps, $\alpha = 60°$

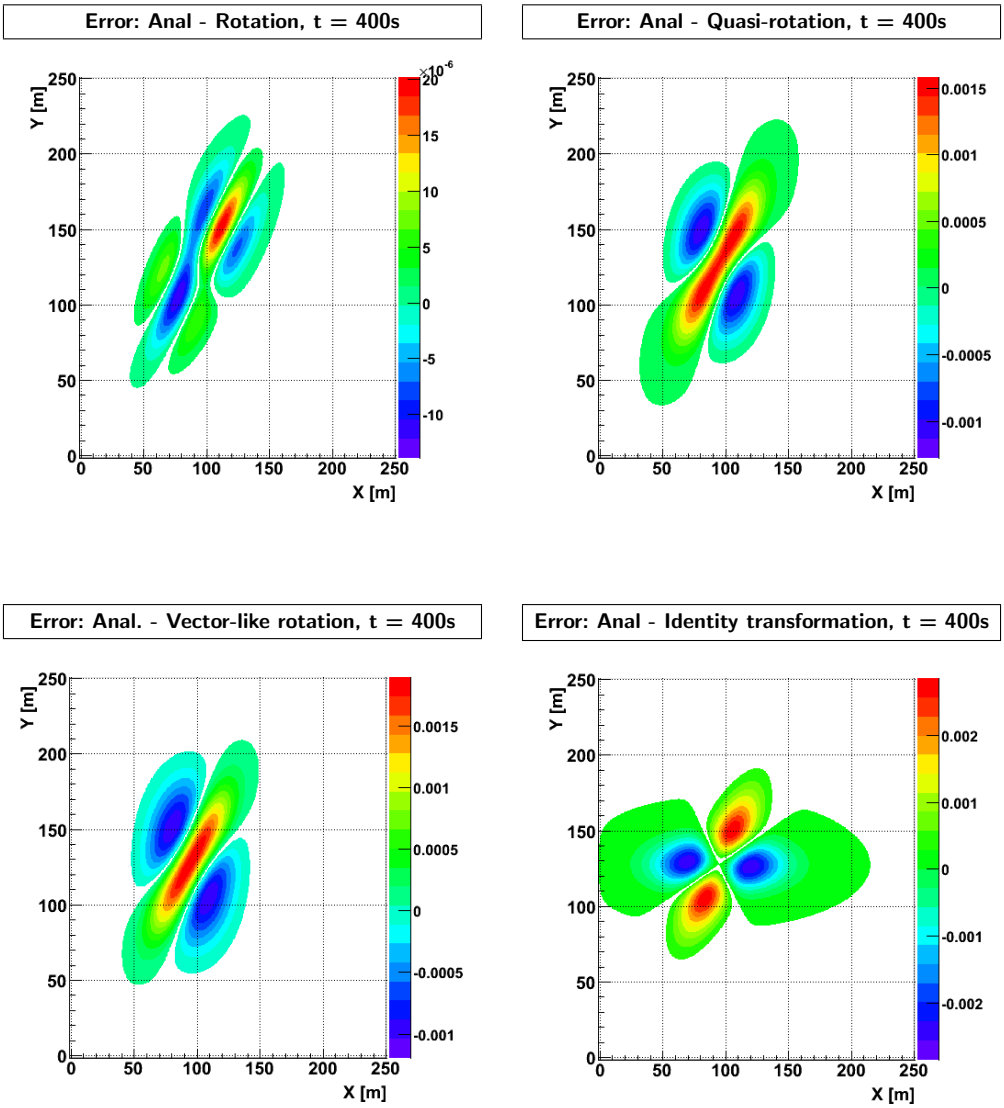

Figure C.10: Difference between the numerical solution and analytical one for different methods of dispersion tensor transformation for the pulse release after 400 time steps, $\alpha = 60°$

C.2 Continuous inflow of solute

In case of $\alpha = 0°$ there is no difference between the solution by means of *rotation* and the solution with application of one of different methods of dispersion tensor simplifications, therefore, in this case the difference hasn't been plotted.

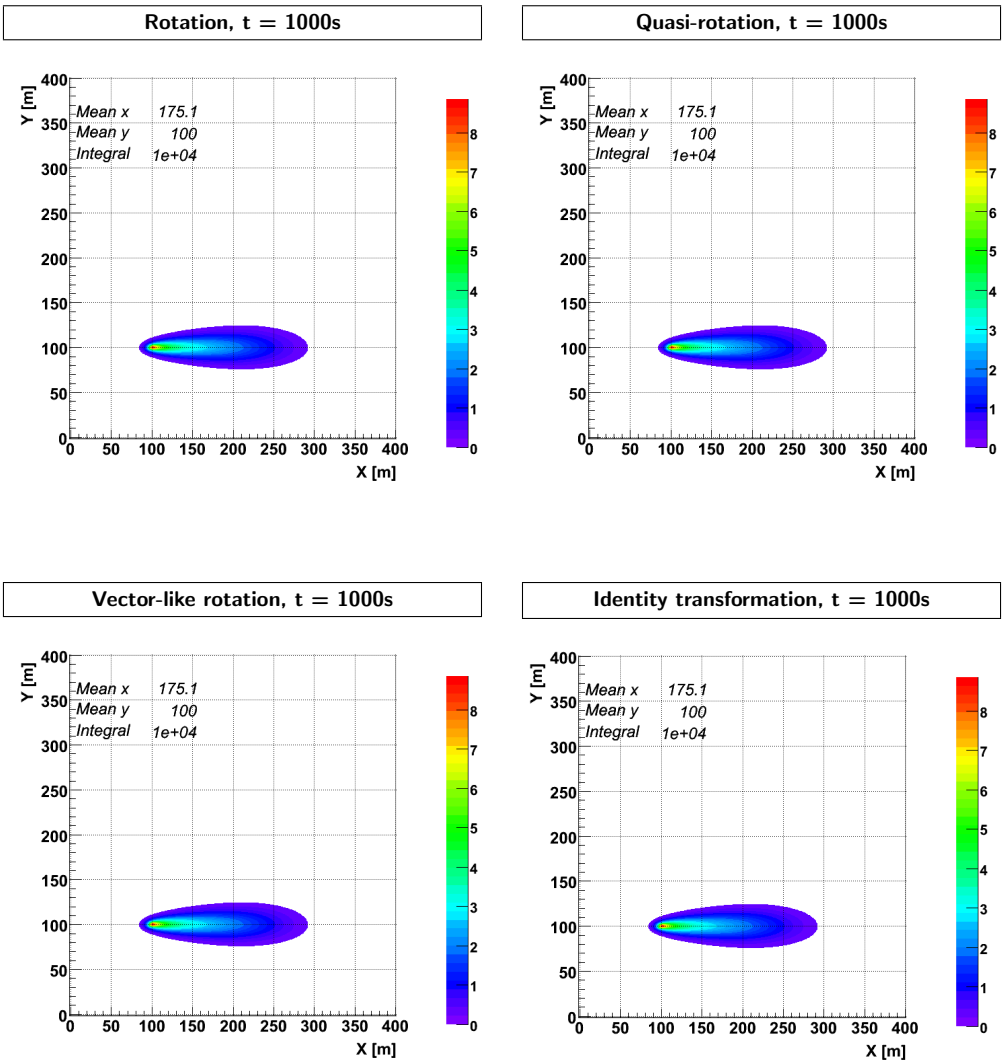

Figure C.11: Numerical solution with application of different methods of dispersion tensor transformation for the continuous release after 1000 time steps, $\alpha = 0°$

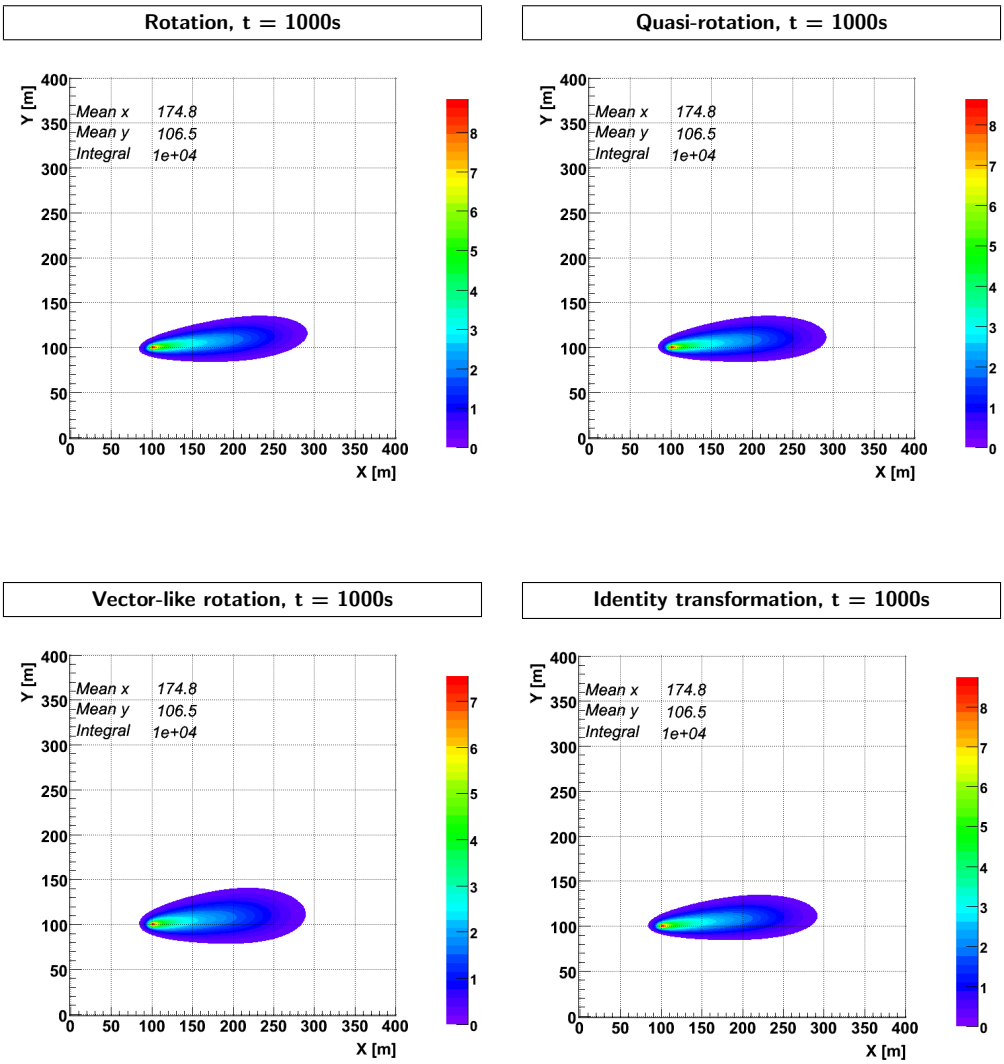

Figure C.12: Numerical solution with application of different methods of dispersion tensor transformation for the continuous release after 1000 time steps, $\alpha = 5°$

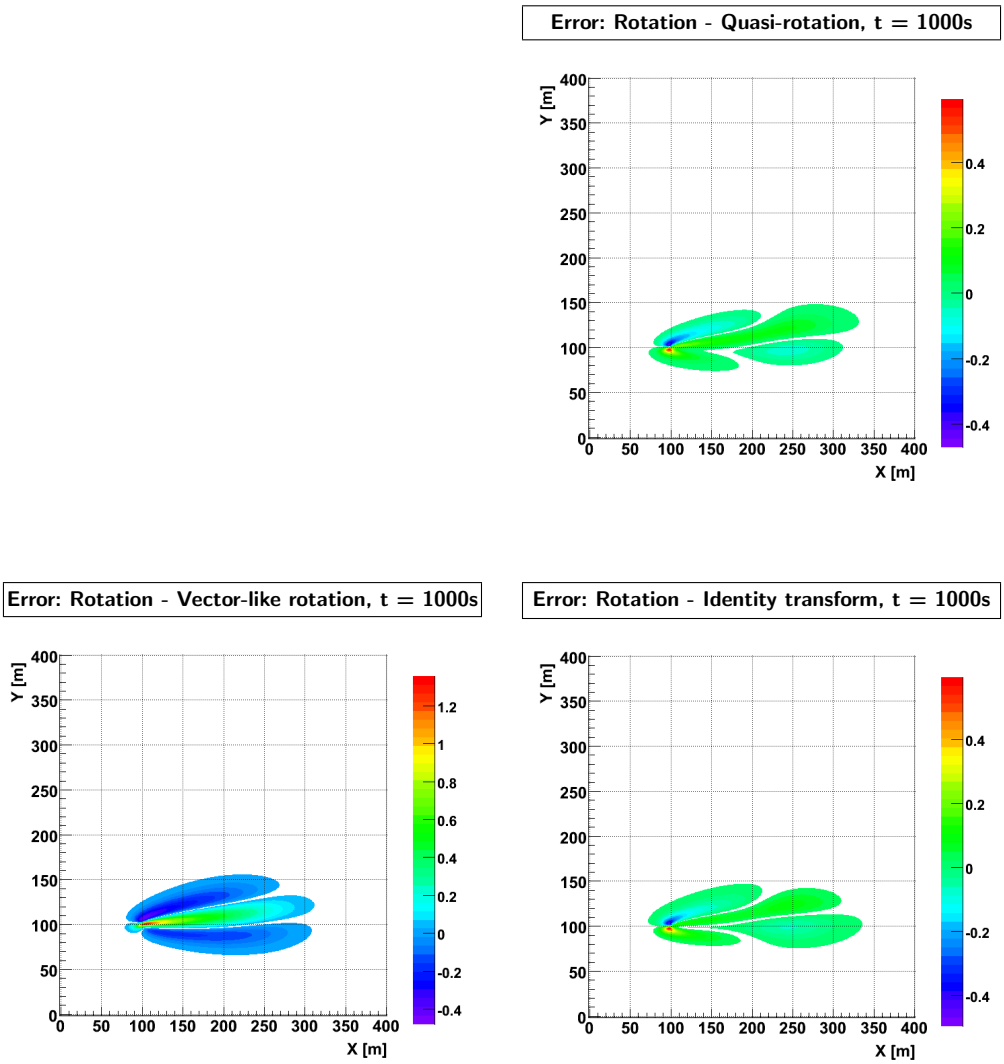

Figure C.13: Difference between the solution by means of *rotation* and the solution with application of one of different methods of dispersion tensor transformation, after 1000 time steps, $\alpha = 5°$

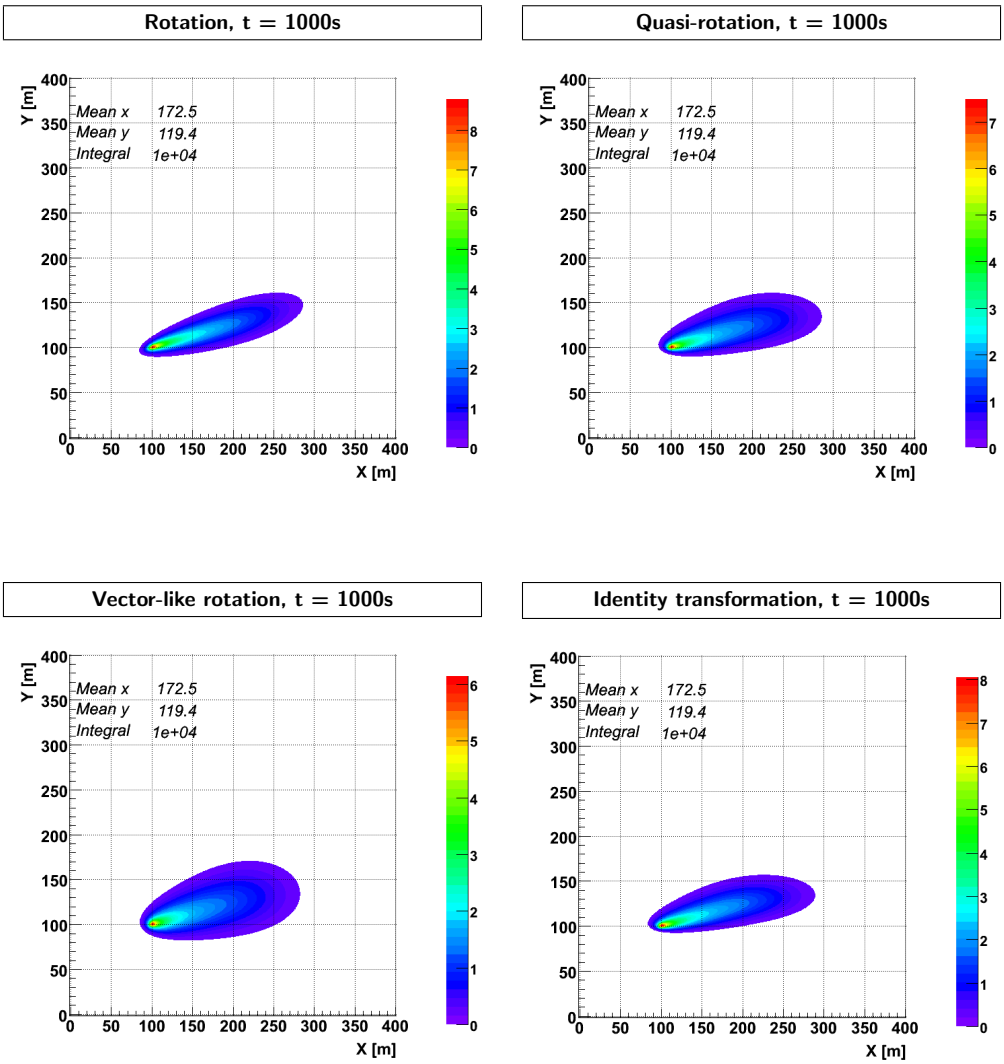

Figure C.14: Numerical solution with application of different methods of dispersion tensor transformation for the continuous release after 1000 time steps, $\alpha = 15°$

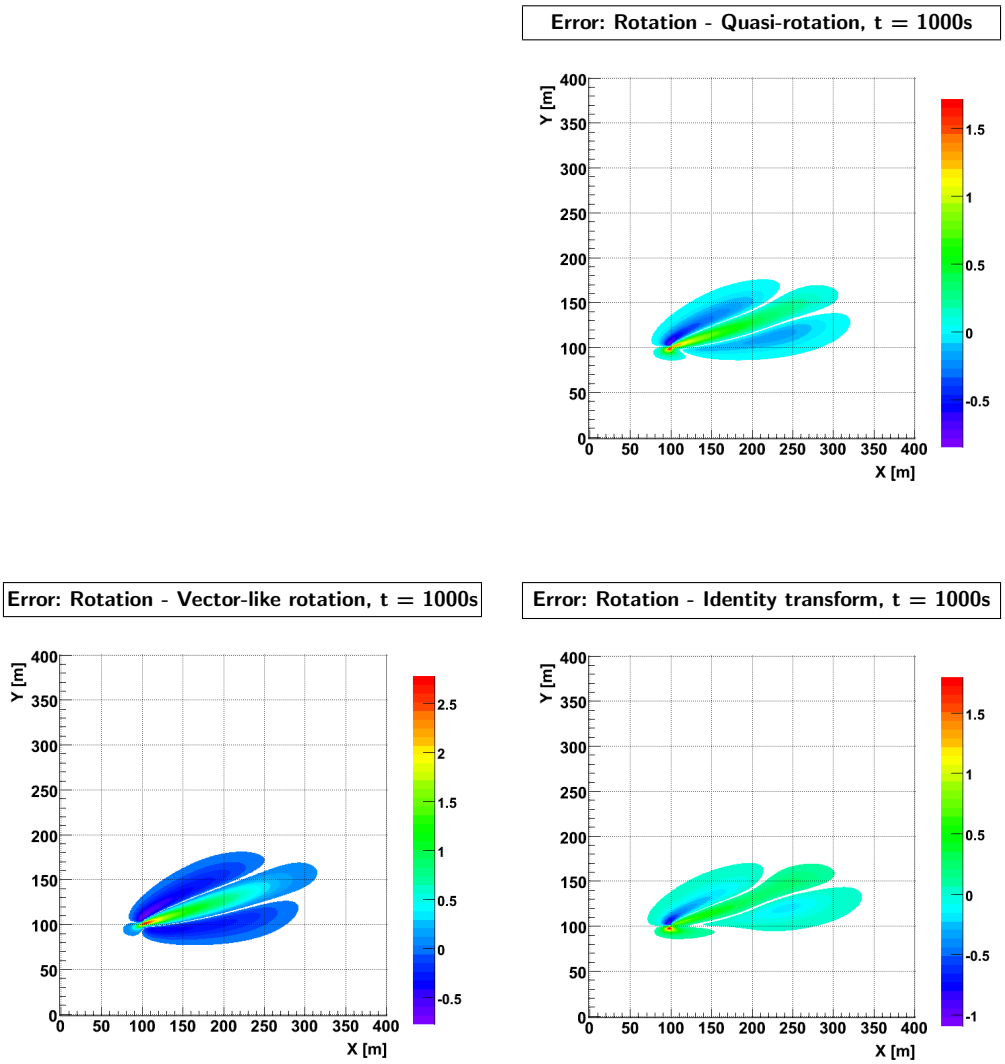

Figure C.15: Difference between the solution by means of *rotation* and the solution with application of one of different methods of dispersion tensor transformation, after 1000 time steps, $\alpha = 15°$

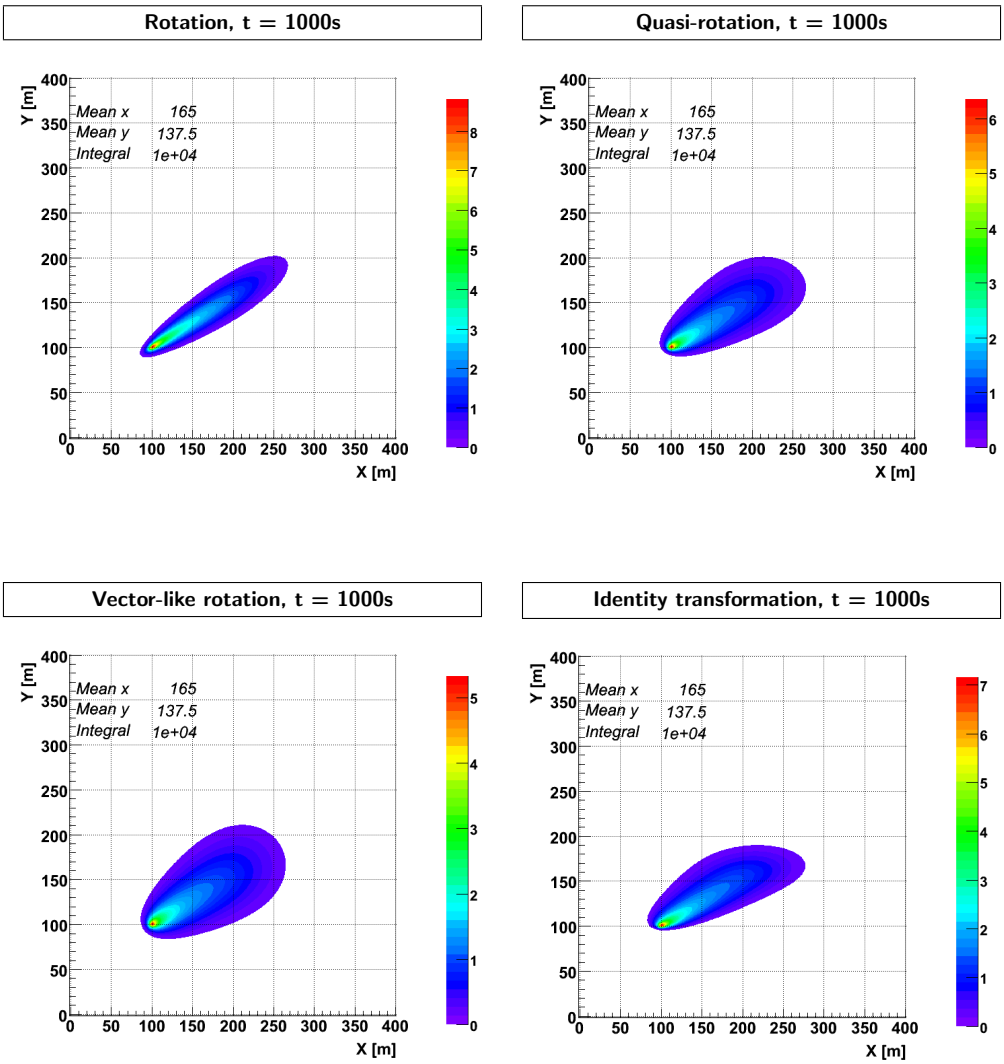

Figure C.16: Numerical solution with application of different methods of dispersion tensor transformation for the continuous release after 1000 time steps, $\alpha = 30°$

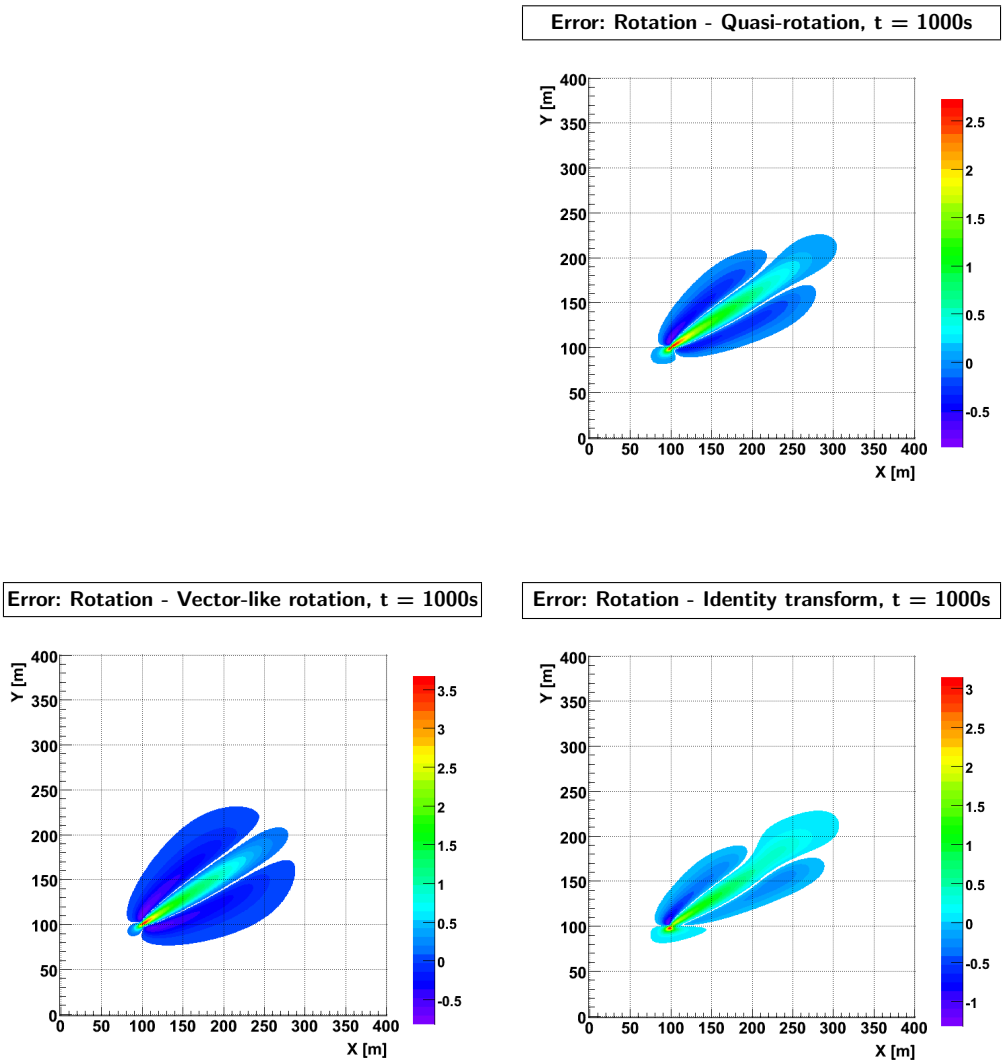

Figure C.17: Difference between the solution by means of *rotation* and the solution with application of one of different methods of dispersion tensor transformation, after 1000 time steps, $\alpha = 30°$

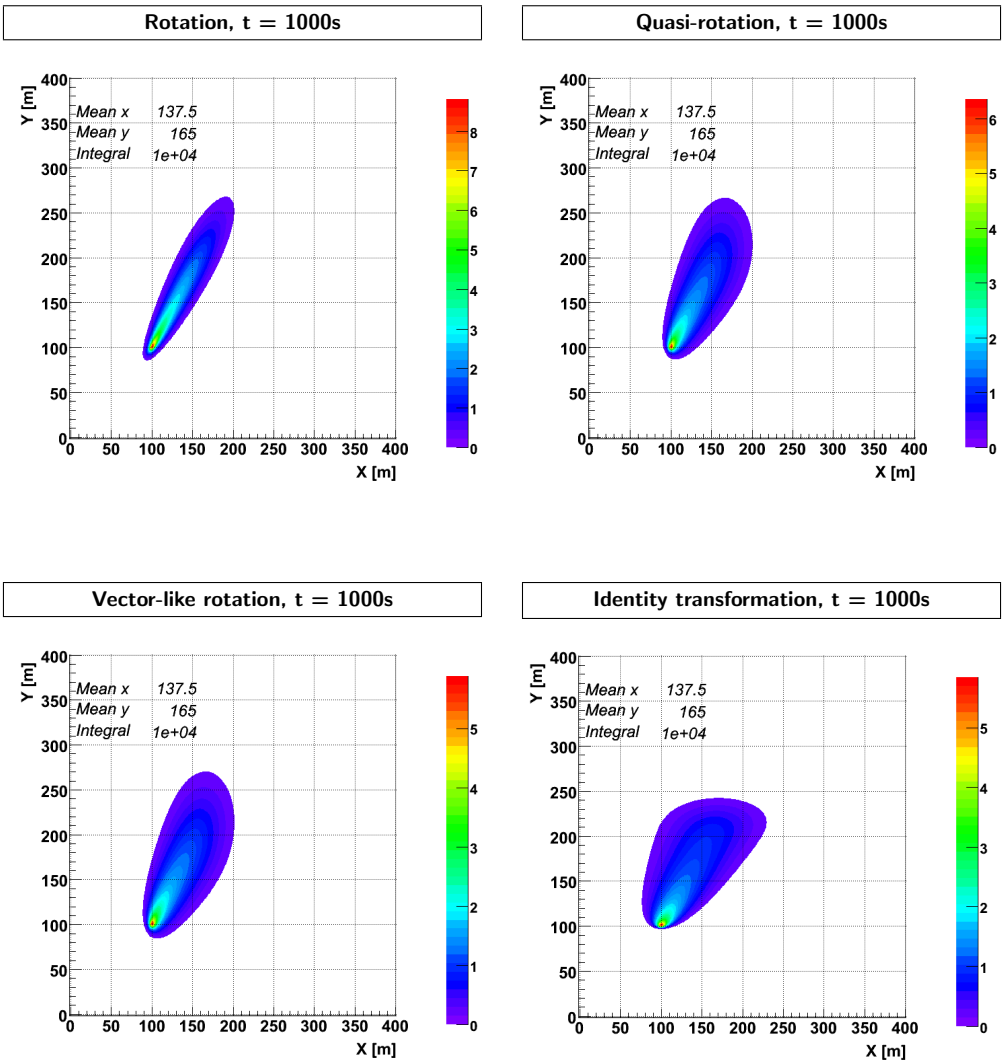

Figure C.18: Numerical solution with application of different methods of dispersion tensor transformation for the continuous release after 1000 time steps, $\alpha = 60°$

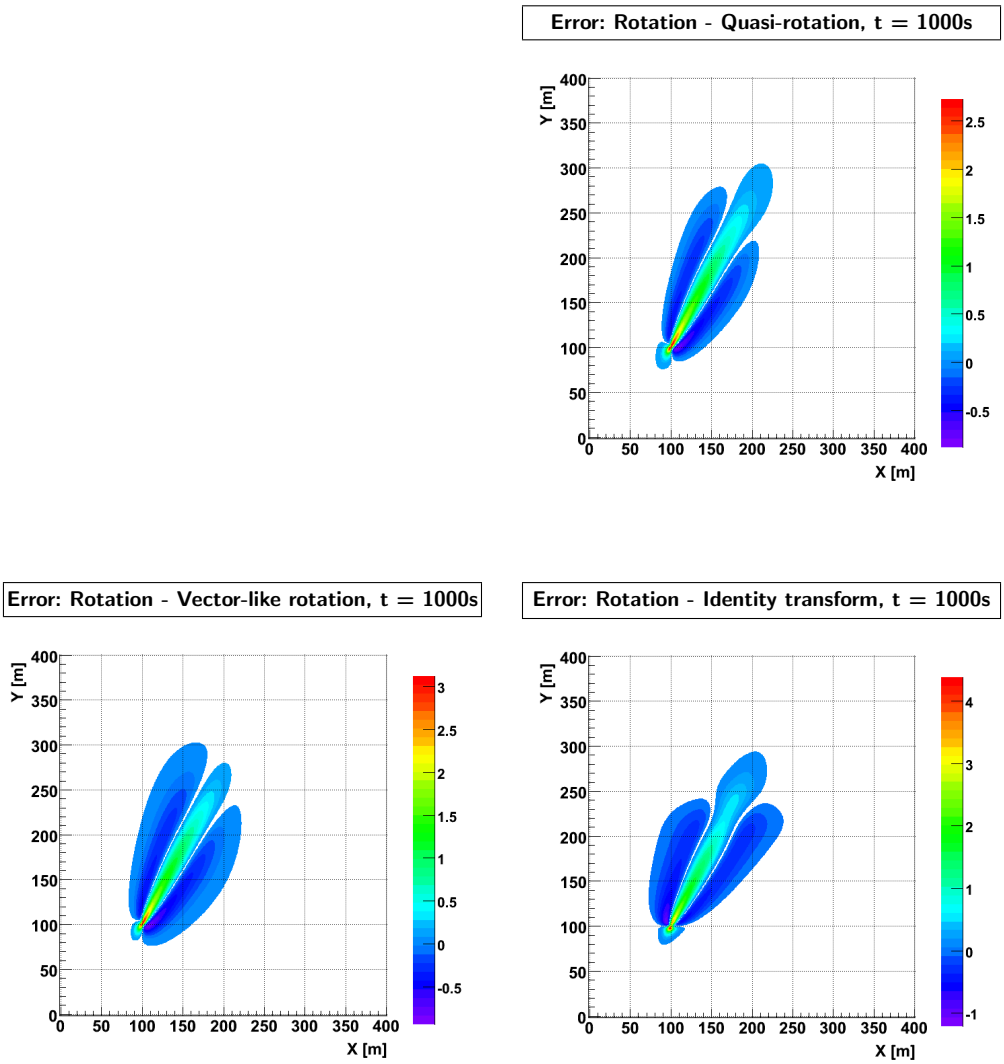

Figure C.19: Difference between the solution by means of *rotation* and the solution with application of one of different methods of dispersion tensor transformation, after 1000 time steps, $\alpha = 60°$

Appendix D

Boundary Conditions

The appendix presents the concentration coefficients used in difference equations at the boundary points for all described schemes: UP (eq. 4.9) – table D.1, CN (eq. 4.11) – tables D.2, D.3 and ADI (eq. 4.23 and 4.24) – tables D.4 and D.5. Table D.6 applies for all schemes.

The following symbols were used to mark the different types of boundaries:

- $\cdot$ – point inside the flow area;
- $\uparrow$ – top boundary;
- $\downarrow$ – bottom boundary;
- $\leftarrow$ – left boundary;
- $\rightarrow$ – right boundary;
- $\nwarrow$ – top-left corner;
- $\nearrow$ – top-right corner;
- $\swarrow$ – bottom-left corner;
- $\searrow$ – bottom-right corner;
- $\lrcorner$ – top-left edge;
- $\llcorner$ – top-right edge;
- $\urcorner$ – bottom-left edge;
- $\ulcorner$ – bottom-right edge.

Table D.1: UP scheme; concentration coefficients in equation (4.9) depending on the velocity sign

		Coefficients before:				
		$c^n_{i,j}$	$c^n_{i+1,j}$	$c^n_{i-1,j}$	$c^n_{i,j+1}$	$c^n_{i,j-1}$
	$v_x \geqslant 0; v_y \geqslant 0$	$1 - \mathcal{C}r^a_x - 2\mathcal{C}r^d_x - \mathcal{C}r^d_y - 2\mathcal{C}r^d_y$	$\mathcal{C}r^d_x$	$\mathcal{C}r^a_x + \mathcal{C}r^d_x$	$\mathcal{C}r^d_y$	$\mathcal{C}r^a_y + \mathcal{C}r^d_y$
·	$v_x \geqslant 0; v_y < 0$	$1 - \mathcal{C}r^a_x - 2\mathcal{C}r^d_x + \mathcal{C}r^a_y - 2\mathcal{C}r^d_y$	$\mathcal{C}r^d_x$	$\mathcal{C}r^a_x + \mathcal{C}r^d_x$	$-\mathcal{C}r^a_y + \mathcal{C}r^d_y$	$\mathcal{C}r^d_y$
	$v_x < 0; v_y \geqslant 0$	$1 + \mathcal{C}r^a_x - 2\mathcal{C}r^d_x - \mathcal{C}r^a_y - 2\mathcal{C}r^d_y$	$-\mathcal{C}r^a_x + \mathcal{C}r^d_x$	$\mathcal{C}r^d_x$	$\mathcal{C}r^d_y$	$\mathcal{C}r^a_y + \mathcal{C}r^d_y$
	$v_x < 0; v_y < 0$	$1 + \mathcal{C}r^a_x - 2\mathcal{C}r^d_x + \mathcal{C}r^a_y - 2\mathcal{C}r^d_y$	$-\mathcal{C}r^a_x + \mathcal{C}r^d_x$	$\mathcal{C}r^d_x$	$-\mathcal{C}r^a_y + \mathcal{C}r^d_y$	$\mathcal{C}r^d_y$

Continuation on the next page ...

Table D.1: UP scheme; concentration coefficients in equation (4.9) depending on the velocity sign

... continued from the previous page

		Coefficients before:				
		$c^n_{i,j}$	$c^n_{i+1,j}$	$c^n_{i-1,j}$	$c^n_{i,j+1}$	$c^n_{i,j-1}$
$\uparrow$	$v_x \geqslant 0; v_y \geqslant 0$	$1 - \mathcal{C}r^a_x - 2\mathcal{C}r^d_x - \mathcal{C}r^d_y$	$\mathcal{C}r^d_x$	$\mathcal{C}r^a_x + \mathcal{C}r^d_x$	0	$\mathcal{C}r^a_y + \mathcal{C}r^d_y$
	$v_x \geqslant 0; v_y < 0$	$1 - \mathcal{C}r^a_x + \mathcal{C}r^a_y - 2\mathcal{C}r^d_x - \mathcal{C}r^d_y$	$\mathcal{C}r^d_x$	$\mathcal{C}r^a_x + \mathcal{C}r^d_x$	0	$\mathcal{C}r^d_y$
	$v_x < 0; v_y \geqslant 0$	$1 + \mathcal{C}r^a_x - 2\mathcal{C}r^d_x - \mathcal{C}r^d_y$	$-\mathcal{C}r^a_x + \mathcal{C}r^d_x$	$\mathcal{C}r^d_x$	0	$\mathcal{C}r^a_y + \mathcal{C}r^d_y$
	$v_x < 0; v_y < 0$	$1 + \mathcal{C}r^a_x + \mathcal{C}r^a_y - 2\mathcal{C}r^d_x - \mathcal{C}r^d_y$	$-\mathcal{C}r^a_x + \mathcal{C}r^d_x$	$\mathcal{C}r^d_x$	0	$\mathcal{C}r^d_y$
$\downarrow$	$v_x \geqslant 0; v_y \geqslant 0$	$1 - \mathcal{C}r^a_x - \mathcal{C}r^a_y - 2\mathcal{C}r^d_x - \mathcal{C}r^d_y$	$\mathcal{C}r^d_x$	$\mathcal{C}r^a_x + \mathcal{C}r^d_x$	$\mathcal{C}r^d_y$	0
	$v_x \geqslant 0; v_y < 0$	$1 - \mathcal{C}r^a_x - 2\mathcal{C}r^d_x - \mathcal{C}r^d_y$	$\mathcal{C}r^d_x$	$\mathcal{C}r^a_x + \mathcal{C}r^d_x$	$-\mathcal{C}r^a_y + \mathcal{C}r^d_y$	0
	$v_x < 0; v_y \geqslant 0$	$1 + \mathcal{C}r^a_x - \mathcal{C}r^a_y - 2\mathcal{C}r^d_x - \mathcal{C}r^d_y$	$-\mathcal{C}r^a_x + \mathcal{C}r^d_x$	$\mathcal{C}r^d_x$	$\mathcal{C}r^d_y$	0
	$v_x < 0; v_y < 0$	$1 + \mathcal{C}r^a_x - 2\mathcal{C}r^d_x - \mathcal{C}r^d_y$	$-\mathcal{C}r^a_x + \mathcal{C}r^d_x$	$\mathcal{C}r^d_x$	$-\mathcal{C}r^a_y + \mathcal{C}r^d_y$	0
$\leftarrow$	$v_x \geqslant 0; v_y \geqslant 0$	$1 - \mathcal{C}r^a_x - \mathcal{C}r^a_y - \mathcal{C}r^d_x - 2\mathcal{C}r^d_y$	$\mathcal{C}r^d_x$	0	$\mathcal{C}r^d_y$	$\mathcal{C}r^a_y + \mathcal{C}r^d_y$
	$v_x \geqslant 0; v_y < 0$	$1 - \mathcal{C}r^a_x + \mathcal{C}r^a_y - \mathcal{C}r^d_y - 2\mathcal{C}r^d_y$	$\mathcal{C}r^d_x$	0	$-\mathcal{C}r^a_y + \mathcal{C}r^d_y$	$\mathcal{C}r^d_y$
	$v_x < 0; v_y \geqslant 0$	$1 + -\mathcal{C}r^a_y - \mathcal{C}r^d_x - 2\mathcal{C}r^d_y$	$-\mathcal{C}r^a_x + \mathcal{C}r^d_x$	0	$\mathcal{C}r^d_y$	$\mathcal{C}r^a_y + \mathcal{C}r^d_y$
	$v_x < 0; v_y < 0$	$1 + \mathcal{C}r^a_y - \mathcal{C}r^d_x - 2\mathcal{C}r^d_y$	$-\mathcal{C}r^a_x + \mathcal{C}r^d_x$	0	$-\mathcal{C}r^a_y + \mathcal{C}r^d_y$	$\mathcal{C}r^d_y$
$\rightarrow$	$v_x \geqslant 0; v_y \geqslant 0$	$1 - \mathcal{C}r^a_y - \mathcal{C}r^d_x - 2\mathcal{C}r^d_y$	0	$\mathcal{C}r^a_x + \mathcal{C}r^d_x$	$\mathcal{C}r^d_y$	$\mathcal{C}r^a_y + \mathcal{C}r^d_y$
	$v_x \geqslant 0; v_y < 0$	$1 + \mathcal{C}r^a_y + \mathcal{C}r^a_y - \mathcal{C}r^d_x - 2\mathcal{C}r^d_y$	0	$\mathcal{C}r^a_x + \mathcal{C}r^d_x$	$-\mathcal{C}r^a_y + \mathcal{C}r^d_y$	$\mathcal{C}r^d_y$
	$v_x < 0; v_y \geqslant 0$	$1 + \mathcal{C}r^a_x - \mathcal{C}r^a_y - \mathcal{C}r^d_x - 2\mathcal{C}r^d_y$	0	$\mathcal{C}r^d_x$	$\mathcal{C}r^d_y$	$\mathcal{C}r^a_y + \mathcal{C}r^d_y$
	$v_x < 0; v_y < 0$	$1 + \mathcal{C}r^a_x + \mathcal{C}r^a_y - \mathcal{C}r^d_x - 2\mathcal{C}r^d_y$	0	$\mathcal{C}r^d_x$	$-\mathcal{C}r^a_y + \mathcal{C}r^d_y$	$\mathcal{C}r^d_y$

Continuation on the next page ...

Table D.1: UP scheme; concentration coefficients in equation (4.9) depending on the velocity sign

... continued from the previous page

		Coefficients before:				
		$c^n_{i,j}$	$c^n_{i+1,j}$	$c^n_{i-1,j}$	$c^n_{i,j+1}$	$c^n_{i,j-1}$
$\nwarrow$	$v_x \geqslant 0; v_y \geqslant 0$	$1 - \mathcal{C}r^a_x - \mathcal{C}r^d_x - \mathcal{C}r^d_y + 2\mathcal{C}r^d_{xy}$	$\mathcal{C}r^d_x$	0	0	$\mathcal{C}r^a_y + \mathcal{C}r^d_y$
	$v_x \geqslant 0; v_y < 0$	$1 - \mathcal{C}r^a_x + \mathcal{C}r^a_y - \mathcal{C}r^d_x - \mathcal{C}r^d_y + 2\mathcal{C}r^d_{xy}$	$\mathcal{C}r^d_x$	0	0	$\mathcal{C}r^d_y$
	$v_x < 0; v_y \geqslant 0$	$1 - \mathcal{C}r^d_x - \mathcal{C}r^d_y + 2\mathcal{C}r^d_{xy}$	$-\mathcal{C}r^a_x + \mathcal{C}r^d_x$	0	0	$\mathcal{C}r^a_y + \mathcal{C}r^d_y$
	$v_x < 0; v_y < 0$	$1 + \mathcal{C}r^a_y - \mathcal{C}r^d_x - \mathcal{C}r^d_y + 2\mathcal{C}r^d_{xy}$	$-\mathcal{C}r^a_x + \mathcal{C}r^d_y$	0	0	$\mathcal{C}r^d_y$
$\nearrow$	$v_x \geqslant 0; v_y \geqslant 0$	$1 - \mathcal{C}r^d_x - \mathcal{C}r^d_y - 2\mathcal{C}r^d_{xy}$	0	$\mathcal{C}r^a_x + \mathcal{C}r^d_x$	0	$\mathcal{C}r^a_y + \mathcal{C}r^d_y$
	$v_x \geqslant 0; v_y < 0$	$1 - \mathcal{C}r^a_y - \mathcal{C}r^d_x - \mathcal{C}r^d_y - 2\mathcal{C}r^d_{xy}$	0	$\mathcal{C}r^a_x + \mathcal{C}r^d_x$	0	$\mathcal{C}r^d_y$
	$v_x < 0; v_y \geqslant 0$	$1 + \mathcal{C}r^a_x - \mathcal{C}r^d_x - \mathcal{C}r^d_y - 2\mathcal{C}r^d_{xy}$	0	$\mathcal{C}r^d_x$	0	$\mathcal{C}r^a_y + \mathcal{C}r^d_y$
	$v_x < 0; v_y < 0$	$1 + \mathcal{C}r^a_x + \mathcal{C}r^a_y - \mathcal{C}r^d_x - \mathcal{C}r^d_y - 2\mathcal{C}r^d_{xy}$	0	$\mathcal{C}r^d_x$	0	$\mathcal{C}r^d_y$
$\swarrow$	$v_x \geqslant 0; v_y \geqslant 0$	$1 - \mathcal{C}r^a_x - \mathcal{C}r^a_y - \mathcal{C}r^d_x - \mathcal{C}r^d_y - 2\mathcal{C}r^d_{xy}$	$\mathcal{C}r^d_x$	0	$\mathcal{C}r^d_y$	0
	$v_x \geqslant 0; v_y < 0$	$1 - \mathcal{C}r^a_x - \mathcal{C}r^d_x - \mathcal{C}r^d_y - 2\mathcal{C}r^d_{xy}$	$\mathcal{C}r^d_x$	0	$-\mathcal{C}r^a_y + \mathcal{C}r^d_y$	0
	$v_x < 0; v_y \geqslant 0$	$1 + \mathcal{C}r^a_x - \mathcal{C}r^d_x - \mathcal{C}r^d_y - 2\mathcal{C}r^d_{xy}$	$-\mathcal{C}r^a_x + \mathcal{C}r^d_x$	0	$\mathcal{C}r^d_y$	0
	$v_x < 0; v_y < 0$	$1 - \mathcal{C}r^d_x - \mathcal{C}r^d_y - 2\mathcal{C}r^d_{xy}$	$-\mathcal{C}r^a_x + \mathcal{C}r^d_x$	0	$-\mathcal{C}r^a_y + \mathcal{C}r^d_y$	0
$\searrow$	$v_x \geqslant 0; v_y \geqslant 0$	$1 - \mathcal{C}r^a_y - \mathcal{C}r^d_x - \mathcal{C}r^d_y + 2\mathcal{C}r^d_{xy}$	0	$\mathcal{C}r^a_x + \mathcal{C}r^d_x$	$\mathcal{C}r^d_y$	0
	$v_x \geqslant 0; v_y < 0$	$1 - \mathcal{C}r^d_x - \mathcal{C}r^d_y + 2\mathcal{C}r^d_{xy}$	0	$\mathcal{C}r^a_x + \mathcal{C}r^d_x$	$-\mathcal{C}r^a_y + \mathcal{C}r^d_y$	0
	$v_x < 0; v_y \geqslant 0$	$1 + \mathcal{C}r^a_x - \mathcal{C}r^a_y - \mathcal{C}r^d_x - \mathcal{C}r^d_y + 2\mathcal{C}r^d_{xy}$	0	$\mathcal{C}r^d_x$	$\mathcal{C}r^d_y$	0
	$v_x < 0; v_y < 0$	$1 + \mathcal{C}r^a_x - \mathcal{C}r^d_x - \mathcal{C}r^d_y + 2\mathcal{C}r^d_{xy}$	0	$\mathcal{C}r^d_x$	$-\mathcal{C}r^a_y + \mathcal{C}r^d_y$	0

Continuation on the next page ...

Table D.1: UP scheme; concentration coefficients in equation (4.9) depending on the velocity sign

... continued from the previous page

		Coefficients before:				
		$c^n_{i,j}$	$c^n_{i+1,j}$	$c^n_{i-1,j}$	$c^n_{i,j+1}$	$c^n_{i,j-1}$
⌟	$v_x \geqslant 0; v_y \geqslant 0$	$1 - \mathcal{C}r^a_x - 2\mathcal{C}r^d_x - \mathcal{C}r^d_y - 2\mathcal{C}r^d_y - 2\mathcal{C}r^d_{xy}$	$\mathcal{C}r^d_x$	$\mathcal{C}r^a_x + \mathcal{C}r^d_x$	$\mathcal{C}r^d_y$	$\mathcal{C}r^a_y + \mathcal{C}r^d_y$
	$v_x \geqslant 0; v_y < 0$	$1 - \mathcal{C}r^a_x - 2\mathcal{C}r^d_x + \mathcal{C}r^a_y - 2\mathcal{C}r^d_y - 2\mathcal{C}r^d_{xy}$	$\mathcal{C}r^d_x$	$\mathcal{C}r^a_x + \mathcal{C}r^d_x$	$-\mathcal{C}r^a_y + \mathcal{C}r^d_y$	$\mathcal{C}r^d_y$
	$v_x < 0; v_y \geqslant 0$	$1 + \mathcal{C}r^a_x - 2\mathcal{C}r^d_x - \mathcal{C}r^a_y - 2\mathcal{C}r^d_y - 2\mathcal{C}r^d_{xy}$	$-\mathcal{C}r^a_x + \mathcal{C}r^d_x$	$\mathcal{C}r^d_x$	$\mathcal{C}r^d_y$	$\mathcal{C}r^a_y + \mathcal{C}r^d_y$
	$v_x < 0; v_y < 0$	$1 + \mathcal{C}r^a_x - 2\mathcal{C}r^d_x + \mathcal{C}r^a_y - 2\mathcal{C}r^d_y - 2\mathcal{C}r^d_{xy}$	$-\mathcal{C}r^a_x + \mathcal{C}r^d_x$	$\mathcal{C}r^d_x$	$-\mathcal{C}r^a_y + \mathcal{C}r^d_y$	$\mathcal{C}r^d_y$
⌞	$v_x \geqslant 0; v_y \geqslant 0$	$1 - \mathcal{C}r^a_x - 2\mathcal{C}r^d_x - \mathcal{C}r^d_y - 2\mathcal{C}r^d_y + 2\mathcal{C}r^d_{xy}$	$\mathcal{C}r^d_x$	$\mathcal{C}r^a_x + \mathcal{C}r^d_x$	$\mathcal{C}r^d_y$	$\mathcal{C}r^a_y + \mathcal{C}r^d_y$
	$v_x \geqslant 0; v_y < 0$	$1 - \mathcal{C}r^a_x - 2\mathcal{C}r^d_x + \mathcal{C}r^a_y - 2\mathcal{C}r^d_y + 2\mathcal{C}r^d_{xy}$	$\mathcal{C}r^d_x$	$\mathcal{C}r^a_x + \mathcal{C}r^d_x$	$-\mathcal{C}r^a_y + \mathcal{C}r^d_y$	$\mathcal{C}r^d_y$
	$v_x < 0; v_y \geqslant 0$	$1 + \mathcal{C}r^a_x - 2\mathcal{C}r^d_x - \mathcal{C}r^a_y - 2\mathcal{C}r^d_y$	$-\mathcal{C}r^a_x + \mathcal{C}r^d_x + 2\mathcal{C}r^d_{xy}$	$\mathcal{C}r^d_x$	$\mathcal{C}r^d_y$	$\mathcal{C}r^a_y + \mathcal{C}r^d_y$
	$v_x < 0; v_y < 0$	$1 + \mathcal{C}r^a_x - 2\mathcal{C}r^d_x + \mathcal{C}r^a_y - 2\mathcal{C}r^d_y$	$-\mathcal{C}r^a_x + \mathcal{C}r^d_x + 2\mathcal{C}r^d_{xy}$	$\mathcal{C}r^d_x$	$-\mathcal{C}r^a_y + \mathcal{C}r^d_y$	$\mathcal{C}r^d_y$
⌜	$v_x \geqslant 0; v_y \geqslant 0$	$1 - \mathcal{C}r^a_x - 2\mathcal{C}r^d_x - \mathcal{C}r^d_y - 2\mathcal{C}r^d_y + 2\mathcal{C}r^d_{xy}$	$\mathcal{C}r^d_x$	$\mathcal{C}r^a_x + \mathcal{C}r^d_x$	$\mathcal{C}r^d_y$	$\mathcal{C}r^a_y + \mathcal{C}r^d_y$
	$v_x \geqslant 0; v_y < 0$	$1 - \mathcal{C}r^a_x - 2\mathcal{C}r^d_x + \mathcal{C}r^a_y - 2\mathcal{C}r^d_y + 2\mathcal{C}r^d_{xy}$	$\mathcal{C}r^d_x$	$\mathcal{C}r^a_x + \mathcal{C}r^d_x$	$-\mathcal{C}r^a_y + \mathcal{C}r^d_y$	$\mathcal{C}r^d_y$
	$v_x < 0; v_y \geqslant 0$	$1 + \mathcal{C}r^a_x - 2\mathcal{C}r^d_x - \mathcal{C}r^a_y - 2\mathcal{C}r^d_y + 2\mathcal{C}r^d_{xy}$	$-\mathcal{C}r^a_x + \mathcal{C}r^d_x$	$\mathcal{C}r^d_x$	$\mathcal{C}r^d_y$	$\mathcal{C}r^a_y + \mathcal{C}r^d_y$
	$v_x < 0; v_y < 0$	$1 + \mathcal{C}r^a_x - 2\mathcal{C}r^d_x + \mathcal{C}r^a_y - 2\mathcal{C}r^d_y + 2\mathcal{C}r^d_{xy}$	$-\mathcal{C}r^a_x + \mathcal{C}r^d_x$	$\mathcal{C}r^d_x$	$-\mathcal{C}r^a_y + \mathcal{C}r^d_y$	$\mathcal{C}r^d_y$
⌝	$v_x \geqslant 0; v_y \geqslant 0$	$1 - \mathcal{C}r^a_x - 2\mathcal{C}r^d_x - \mathcal{C}r^d_y - 2\mathcal{C}r^d_y - 2\mathcal{C}r^d_{xy}$	$\mathcal{C}r^d_x$	$\mathcal{C}r^a_x + \mathcal{C}r^d_x$	$\mathcal{C}r^d_y$	$\mathcal{C}r^a_y + \mathcal{C}r^d_y$
	$v_x \geqslant 0; v_y < 0$	$1 - \mathcal{C}r^a_x - 2\mathcal{C}r^d_x + \mathcal{C}r^a_y - 2\mathcal{C}r^d_y - 2\mathcal{C}r^d_{xy}$	$\mathcal{C}r^d_x$	$\mathcal{C}r^a_x + \mathcal{C}r^d_x$	$-\mathcal{C}r^a_y + \mathcal{C}r^d_y$	$\mathcal{C}r^d_y$
	$v_x < 0; v_y \geqslant 0$	$1 + \mathcal{C}r^a_x - 2\mathcal{C}r^d_x - \mathcal{C}r^a_y - 2\mathcal{C}r^d_y - 2\mathcal{C}r^d_{xy}$	$-\mathcal{C}r^a_x + \mathcal{C}r^d_x$	$\mathcal{C}r^d_x$	$\mathcal{C}r^d_y$	$\mathcal{C}r^a_y + \mathcal{C}r^d_y$
	$v_x < 0; v_y < 0$	$1 + \mathcal{C}r^a_x - 2\mathcal{C}r^d_x + \mathcal{C}r^a_y - 2\mathcal{C}r^d_y - 2\mathcal{C}r^d_{xy}$	$-\mathcal{C}r^a_x + \mathcal{C}r^d_x$	$\mathcal{C}r^d_x$	$-\mathcal{C}r^a_y + \mathcal{C}r^d_y$	$\mathcal{C}r^d_y$

Table D.2: CN scheme; concentration coefficients in equation (4.11) in the n-th time step for different boundary types

	Coefficients before:				
	$c^n_{i,j}$	$c^n_{i+1,j}$	$c^n_{i-1,j}$	$c^n_{i,j+1}$	$c^n_{i,j-1}$
$\cdot$	$1 - \mathcal{C}r^d_x - \mathcal{C}r^d_y$	$-\mathcal{C}r^a_x/4 + \mathcal{C}r^d_x/2$	$\mathcal{C}r^a_x/4 + \mathcal{C}r^d_x/2$	$-\mathcal{C}r^a_y/4 + \mathcal{C}r^d_y/2$	$\mathcal{C}r^a_y/4 + \mathcal{C}r^d_y/2$
$\uparrow$	$1 - \mathcal{C}r^d_x - \mathcal{C}r^d_y/2 + \mathcal{C}r^a_y/4$	$-\mathcal{C}r^a_x/4 + \mathcal{C}r^d_x/2$	$\mathcal{C}r^a_x/4 + \mathcal{C}r^d_x/2$	0	$\mathcal{C}r^a_y/4 + \mathcal{C}r^d_y/2$
$\downarrow$	$1 - \mathcal{C}r^d_x - \mathcal{C}r^d_y/2 - \mathcal{C}r^a_y/4$	$-\mathcal{C}r^a_x/4 + \mathcal{C}r^d_x/2$	$\mathcal{C}r^a_x/4 + \mathcal{C}r^d_x/2$	$-\mathcal{C}r^a_y/4 + \mathcal{C}r^d_y/2$	0
$\leftarrow$	$1 - \mathcal{C}r^d_x/2 - \mathcal{C}r^d_y - \mathcal{C}r^a_x/4$	$-\mathcal{C}r^a_x/4 + \mathcal{C}r^d_x/2$	0	$-\mathcal{C}r^a_y/4 + \mathcal{C}r^d_y/2$	$\mathcal{C}r^a_y/4 + \mathcal{C}r^d_y/2$
$\rightarrow$	$1 - \mathcal{C}r^d_x/2 - \mathcal{C}r^d_y + \mathcal{C}r^a_x/4$	0	$\mathcal{C}r^a_x/4 + \mathcal{C}r^d_x/2$	$-\mathcal{C}r^a_y/4 + \mathcal{C}r^d_y/2$	$\mathcal{C}r^a_y/4 + \mathcal{C}r^d_y/2$
$\nwarrow$	$1 - \mathcal{C}r^d_x/2 - \mathcal{C}r^d_y/2$	$-\mathcal{C}r^a_x/4 + \mathcal{C}r^d_x/2$	0	0	$\mathcal{C}r^a_y/4 + \mathcal{C}r^d_y/2$
$\nearrow$	$1 - \mathcal{C}r^d_x/2 - \mathcal{C}r^d_y/2$	0	$\mathcal{C}r^a_x/4 + \mathcal{C}r^d_x/2$	0	$\mathcal{C}r^a_y/4 + \mathcal{C}r^d_y/2$
$\swarrow$	$1 - \mathcal{C}r^d_x/2 - \mathcal{C}r^d_y/2$	$-\mathcal{C}r^a_x/4 + \mathcal{C}r^d_x/2$	0	$-\mathcal{C}r^a_y/4 + \mathcal{C}r^d_y/2$	0
$\searrow$	$1 - \mathcal{C}r^d_x/2 - \mathcal{C}r^d_y/2$	0	$\mathcal{C}r^a_x/4 + \mathcal{C}r^d_y/2$	$-\mathcal{C}r^a_y/4 + \mathcal{C}r^d_y/2$	0
$\lrcorner$	$1 - \mathcal{C}r^d_x - \mathcal{C}r^d_y - \mathcal{C}r^d_{xy}$	$-\mathcal{C}r^a_x/4 + \mathcal{C}r^d_x/2$	$\mathcal{C}r^a_x/4 + \mathcal{C}r^d_x/2$	$-\mathcal{C}r^a_y/4 + \mathcal{C}r^d_y/2$	$\mathcal{C}r^a_y/4 + \mathcal{C}r^d_y/2$
$\llcorner$	$1 - \mathcal{C}r^d_x - \mathcal{C}r^d_y + \mathcal{C}r^d_{xy}$	$-\mathcal{C}r^a_x/4 + \mathcal{C}r^d_x/2$	$\mathcal{C}r^a_x/4 + \mathcal{C}r^d_x/2$	$-\mathcal{C}r^a_y/4 + \mathcal{C}r^d_y/2$	$\mathcal{C}r^a_y/4 + \mathcal{C}r^d_y/2$
$\urcorner$	$1 - \mathcal{C}r^d_x - \mathcal{C}r^d_y + \mathcal{C}r^d_{xy}$	$-\mathcal{C}r^a_x/4 + \mathcal{C}r^d_x/2$	$\mathcal{C}r^a_x/4 + \mathcal{C}r^d_x/2$	$-\mathcal{C}r^a_y/4 + \mathcal{C}r^d_y/2$	$\mathcal{C}r^a_y/4 + \mathcal{C}r^d_y/2$
$\ulcorner$	$1 - \mathcal{C}r^d_x - \mathcal{C}r^d_y - \mathcal{C}r^d_{xy}$	$-\mathcal{C}r^a_x/4 + \mathcal{C}r^d_x/2$	$\mathcal{C}r^a_x/4 + \mathcal{C}r^d_x/2$	$-\mathcal{C}r^a_y/4 + \mathcal{C}r^d_y/2$	$\mathcal{C}r^a_y/4 + \mathcal{C}r^d_y/2$

Table D.3: CN scheme; concentration coefficients in equation (4.11) in the $(n+1)$-th time step for different boundary types

	Coefficients before:				
	$c_{i,j}^{n+1}$	$c_{i+1,j}^{n+1}$	$c_{i-1,j}^{n+1}$	$c_{i,j+1}^{n+1}$	$c_{i,j-1}^{n+1}$
$\cdot$	$1+\mathcal{C}r_x^d+\mathcal{C}r_y^d$	$\mathcal{C}r_x^a/4-\mathcal{C}r_x^d/2$	$-\mathcal{C}r_x^a/4-\mathcal{C}r_x^d/2$	$\mathcal{C}r_y^a/4-\mathcal{C}r_y^d/2$	$-\mathcal{C}r_y^a/4-\mathcal{C}r_y^d/2$
$\uparrow$	$1+\mathcal{C}r_x^d+\mathcal{C}r_y^d/2-\mathcal{C}r_y^a/4$	$\mathcal{C}r_x^a/4-\mathcal{C}r_x^d/2$	$-\mathcal{C}r_x^a/4-\mathcal{C}r_x^d/2$	0	$-\mathcal{C}r_y^a/4-\mathcal{C}r_y^d/2$
$\downarrow$	$1+\mathcal{C}r_x^d+\mathcal{C}r_y^d/2+\mathcal{C}r_y^a/4$	$\mathcal{C}r_x^a/4-\mathcal{C}r_x^d/2$	$-\mathcal{C}r_x^a/4-\mathcal{C}r_x^d/2$	$\mathcal{C}r_y^a/4-\mathcal{C}r_y^d/2$	0
$\leftarrow$	$1+\mathcal{C}r_x^d/2+\mathcal{C}r_y^d+\mathcal{C}r_x^a/4$	$\mathcal{C}r_x^a/4-\mathcal{C}r_x^d/2$	0	$\mathcal{C}r_y^a/4-\mathcal{C}r_y^d/2$	$-\mathcal{C}r_y^a/4-\mathcal{C}r_y^d/2$
$\rightarrow$	$1+\mathcal{C}r_x^d/2+\mathcal{C}r_y^d-\mathcal{C}r_x^a/4$	0	$-\mathcal{C}r_x^a/4-\mathcal{C}r_x^d/2$	$\mathcal{C}r_y^a/4-\mathcal{C}r_y^d/2$	$-\mathcal{C}r_y^a/4-\mathcal{C}r_y^d/2$
$\nwarrow$	$1+\mathcal{C}r_x^d/2+\mathcal{C}r_y^d/2$	$\mathcal{C}r_x^a/4-\mathcal{C}r_x^d/2$	0	0	$-\mathcal{C}r_y^a/4-\mathcal{C}r_y^d/2$
$\nearrow$	$1+\mathcal{C}r_x^d/2+\mathcal{C}r_y^d/2$	0	$-\mathcal{C}r_x^a/4-\mathcal{C}r_x^d/2$	0	$-\mathcal{C}r_y^a/4-\mathcal{C}r_y^d/2$
$\swarrow$	$1+\mathcal{C}r_x^d/2+\mathcal{C}r_y^d/2$	$\mathcal{C}r_x^a/4-\mathcal{C}r_x^d/2$	0	$\mathcal{C}r_y^a/4-\mathcal{C}r_y^d/2$	0
$\searrow$	$1+\mathcal{C}r_x^d/2+\mathcal{C}r_y^d/2$	0	$-\mathcal{C}r_x^a/4-\mathcal{C}r_y^d/2$	$\mathcal{C}r_y^a/4-\mathcal{C}r_y^d/2$	0
$\lrcorner$	$1+\mathcal{C}r_x^d+\mathcal{C}r_y^d+\mathcal{C}r_{xy}^d$	$\mathcal{C}r_x^a/4-\mathcal{C}r_x^d/2$	$-\mathcal{C}r_x^a/4-\mathcal{C}r_x^d/2$	$\mathcal{C}r_y^a/4-\mathcal{C}r_y^d/2$	$-\mathcal{C}r_y^a/4-\mathcal{C}r_y^d/2$
$\llcorner$	$1+\mathcal{C}r_x^d+\mathcal{C}r_y^d-\mathcal{C}r_{xy}^d$	$\mathcal{C}r_x^a/4-\mathcal{C}r_x^d/2$	$-\mathcal{C}r_x^a/4-\mathcal{C}r_x^d/2$	$\mathcal{C}r_y^a/4-\mathcal{C}r_y^d/2$	$-\mathcal{C}r_y^a/4-\mathcal{C}r_y^d/2$
$\urcorner$	$1+\mathcal{C}r_x^d+\mathcal{C}r_y^d-\mathcal{C}r_{xy}^d$	$\mathcal{C}r_x^a/4-\mathcal{C}r_x^d/2$	$-\mathcal{C}r_x^a/4-\mathcal{C}r_x^d/2$	$\mathcal{C}r_y^a/4-\mathcal{C}r_y^d/2$	$-\mathcal{C}r_y^a/4-\mathcal{C}r_y^d/2$
$\ulcorner$	$1+\mathcal{C}r_x^d+\mathcal{C}r_y^d+\mathcal{C}r_{xy}^d$	$\mathcal{C}r_x^a/4-\mathcal{C}r_x^d/2$	$-\mathcal{C}r_x^a/4-\mathcal{C}r_x^d/2$	$\mathcal{C}r_y^a/4-\mathcal{C}r_y^d/2$	$-\mathcal{C}r_y^a/4-\mathcal{C}r_y^d/2$

Table D.4: ADI scheme, STEP I; concentration coefficients in equation (4.23) for different boundary types

	Coefficients before:							
	$c^n_{i,j}$	$c^n_{i+1,j}$	$c^n_{i-1,j}$	$c^n_{i,j+1}$	$c^n_{i,j-1}$	$c^{n+\frac{1}{2}}_{i,j}$	$c^{n+\frac{1}{2}}_{i+1,j}$	$c^{n+\frac{1}{2}}_{i-1,j}$
$\cdot$	$1-\mathcal{C}r^d_x-2\mathcal{C}r^d_y$	$-\mathcal{C}r^a_x/4+\mathcal{C}r^d_x/2$	$\mathcal{C}r^a_x/4+\mathcal{C}r^d_x/2$	$-\mathcal{C}r^a_y/2+\mathcal{C}r^d_y$	$\mathcal{C}r^a_y/2+\mathcal{C}r^d_y$	$1+\mathcal{C}r^d_x$	$\mathcal{C}r^a_x/4-\mathcal{C}r^d_x/2$	$-\mathcal{C}r^a_x/4-\mathcal{C}r^d_x/2$
$\uparrow$	$1-\mathcal{C}r^d_x-\mathcal{C}r^d_y$ $+\mathcal{C}r^a_y/2$	$-\mathcal{C}r^a_x/4+\mathcal{C}r^d_x/2$	$\mathcal{C}r^a_x/4+\mathcal{C}r^d_x/2$	0	$\mathcal{C}r^a_y/2+\mathcal{C}r^d_y$	$1+\mathcal{C}r^d_x$	$\mathcal{C}r^a_x/4-\mathcal{C}r^d_x/2$	$-\mathcal{C}r^a_x/4-\mathcal{C}r^d_x/2$
$\downarrow$	$1-\mathcal{C}r^d_x-\mathcal{C}r^d_y$ $-\mathcal{C}r^a_y/2$	$-\mathcal{C}r^a_x/4+\mathcal{C}r^d_x/2$	$\mathcal{C}r^a_x/4+\mathcal{C}r^d_x/2$	$-\mathcal{C}r^a_y/2+\mathcal{C}r^d_y$	0	$1+\mathcal{C}r^d_x$	$\mathcal{C}r^a_x/4-\mathcal{C}r^d_x/2$	$-\mathcal{C}r^a_x/4-\mathcal{C}r^d_x/2$
$\leftarrow$	$1-\mathcal{C}r^d_x/2-2\mathcal{C}r^d_y$ $-\mathcal{C}r^a_x/4$	$-\mathcal{C}r^a_x/4+\mathcal{C}r^d_x/2$	0	$-\mathcal{C}r^a_y/2+\mathcal{C}r^d_y$	$\mathcal{C}r^a_y/2+\mathcal{C}r^d_y$	$1+\mathcal{C}r^d_x/2$ $+\mathcal{C}r^a_x/4$	$\mathcal{C}r^a_x/4-\mathcal{C}r^d_x/2$	0
$\rightarrow$	$1-\mathcal{C}r^d_x/2-2\mathcal{C}r^d_y$ $+\mathcal{C}r^a_x/4$	0	$\mathcal{C}r^a_x/4+\mathcal{C}r^d_x/2$	$-\mathcal{C}r^a_y/2+\mathcal{C}r^d_y$	$\mathcal{C}r^a_y/2+\mathcal{C}r^d_y$	$1+\mathcal{C}r^d_x/2$ $-\mathcal{C}r^a_x/4$	0	$-\mathcal{C}r^a_x/4-\mathcal{C}r^d_x/2$
$\nwarrow$	$-\mathcal{C}r^a_x/4+\mathcal{C}r^a_y/2$ $-\mathcal{C}r^a_x/4+\mathcal{C}r^a_y/2$	$-\mathcal{C}r^a_x/4+\mathcal{C}r^d_x/2$	0	0	$\mathcal{C}r^a_y/2+\mathcal{C}r^d_y$	$1+\mathcal{C}r^d_x/2$ $+\mathcal{C}r^a_x/4$	$\mathcal{C}r^a_x/4-\mathcal{C}r^d_x/2$	0
$\nearrow$	$1-\mathcal{C}r^d_x/2-\mathcal{C}r^d_y$ $+\mathcal{C}r^a_x/4+\mathcal{C}r^a_y/2$	0	$\mathcal{C}r^a_x/4+\mathcal{C}r^d_x/2$	0	$\mathcal{C}r^a_y/2+\mathcal{C}r^d_y$	$1+\mathcal{C}r^d_x/2$ $-\mathcal{C}r^a_x/4$	0	$-\mathcal{C}r^a_x/4-\mathcal{C}r^d_x/2$

Continuation on the next page ...

Table D.4: ADI scheme, STEP I; concentration coefficients in equation (4.23) for different boundary types

... continued from the previous page

	Coefficients before:							
	$c^n_{i,j}$	$c^n_{i+1,j}$	$c^n_{i-1,j}$	$c^n_{i,j+1}$	$c^n_{i,j-1}$	$c^{n+\frac{1}{2}}_{i,j}$	$c^{n+\frac{1}{2}}_{i+1,j}$	$c^{n+\frac{1}{2}}_{i-1,j}$
↙	$1-\mathcal{C}r^d_x/2-\mathcal{C}r^d_y$ $-\mathcal{C}r^a_x/4-\mathcal{C}r^a_y/2$	$-\mathcal{C}r^a_x/4+\mathcal{C}r^d_x/2$	0	$-\mathcal{C}r^a_y/2+\mathcal{C}r^d_y$	0	$1+\mathcal{C}r^d_x/2$ $+\mathcal{C}r^a_x/4$	$\mathcal{C}r^a_x/4-\mathcal{C}r^d_x/2$	0
↘	$1-\mathcal{C}r^d_x/2-\mathcal{C}r^d_y$ $+\mathcal{C}r^a_x/4-\mathcal{C}r^a_y/2$	0	$\mathcal{C}r^a_x/4+\mathcal{C}r^d_x/2$	$-\mathcal{C}r^a_y/2+\mathcal{C}r^d_y$	0	$1+\mathcal{C}r^d_x/2$ $-\mathcal{C}r^a_x/4$	0	$-\mathcal{C}r^a_x/4-\mathcal{C}r^d_x/2$
⌟	$1-\mathcal{C}r^d_x-2\mathcal{C}r^d_y$ $-2\mathcal{C}r^d_{xy}$	$-\mathcal{C}r^a_x/4+\mathcal{C}r^d_x/2$	$\mathcal{C}r^a_x/4+\mathcal{C}r^d_x/2$	$-\mathcal{C}r^a_y/2+\mathcal{C}r^d_y$	$\mathcal{C}r^a_y/2+\mathcal{C}r^d_y$	$1+\mathcal{C}r^d_x$	$\mathcal{C}r^a_x/4-\mathcal{C}r^d_x/2$	$-\mathcal{C}r^a_x/4-\mathcal{C}r^d_x/2$
⌞	$1-\mathcal{C}r^d_x-2\mathcal{C}r^d_y$ $+2\mathcal{C}r^d_{xy}$	$-\mathcal{C}r^a_x/4+\mathcal{C}r^d_x/2$	$\mathcal{C}r^a_x/4+\mathcal{C}r^d_x/2$	$-\mathcal{C}r^a_y/2+\mathcal{C}r^d_y$	$\mathcal{C}r^a_y/2+\mathcal{C}r^d_y$	$1+\mathcal{C}r^d_x$	$\mathcal{C}r^a_x/4-\mathcal{C}r^d_x/2$	$-\mathcal{C}r^a_x/4-\mathcal{C}r^d_x/2$
⌝	$1-\mathcal{C}r^d_x-2\mathcal{C}r^d_y$ $+\mathcal{C}r^d_{xy}$	$-\mathcal{C}r^a_x/4+\mathcal{C}r^d_x/2$	$\mathcal{C}r^a_x/4+\mathcal{C}r^d_x/2$	$-\mathcal{C}r^a_y/2+\mathcal{C}r^d_y$	$\mathcal{C}r^a_y/2+\mathcal{C}r^d_y$	$1+\mathcal{C}r^d_x$	$\mathcal{C}r^a_x/4-\mathcal{C}r^d_x/2$	$-\mathcal{C}r^a_x/4-\mathcal{C}r^d_x/2$
⌜	$1-\mathcal{C}r^d_x-2\mathcal{C}r^d_y$ $-\mathcal{C}r^d_{xy}$	$-\mathcal{C}r^a_x/4+\mathcal{C}r^d_x/2$	$\mathcal{C}r^a_x/4+\mathcal{C}r^d_x/2$	$-\mathcal{C}r^a_y/2+\mathcal{C}r^d_y$	$\mathcal{C}r^a_y/2+\mathcal{C}r^d_y$	$1+\mathcal{C}r^d_x$	$\mathcal{C}r^a_x/4-\mathcal{C}r^d_x/2$	$-\mathcal{C}r^a_x/4-\mathcal{C}r^d_x/2$

Table D.5: ADI scheme, STEP II; concentration coefficients in equation (4.24) for different boundary types

	Coefficients before:					
	$c^n_{i,j}$	$c^n_{i,j+1}$	$c^n_{i,j-1}$	$c^{n+1}_{i,j}$	$c^{n+1}_{i,j+1}$	$c^{n+1}_{i,j-1}$
$\cdot$	$\mathcal{C}r^d_y$	$\mathcal{C}r^a_y/4 - \mathcal{C}r^d_y/2$	$-\mathcal{C}r^a_y/4 - \mathcal{C}r^d_y/2$	$1 + \mathcal{C}r^d_y$	$\mathcal{C}r^a_y/4 - \mathcal{C}r^d_y/2$	$-\mathcal{C}r^a_y/4 - \mathcal{C}r^d_y/2$
$\uparrow$	$\mathcal{C}r^d_y/2 - \mathcal{C}r^a_y/4$	0	$-\mathcal{C}r^a_y/4 - \mathcal{C}r^d_y/2$	$1 + \mathcal{C}r^d_y/2 - \mathcal{C}r^a_y/4$	0	$-\mathcal{C}r^a_y/4 - \mathcal{C}r^d_y/2$
$\downarrow$	$\mathcal{C}r^d_y/2 + \mathcal{C}r^a_y/4$	$\mathcal{C}r^a_y/4 - \mathcal{C}r^d_y/2$	0	$1 + \mathcal{C}r^d_y/2 + \mathcal{C}r^a_y/4$	$\mathcal{C}r^a_y/4 - \mathcal{C}r^d_y/2$	0
$\leftarrow$	$\mathcal{C}r^d_y$	$\mathcal{C}r^a_y/4 - \mathcal{C}r^d_y/2$	$-\mathcal{C}r^a_y/4 - \mathcal{C}r^d_y/2$	$1 + \mathcal{C}r^d_y$	$\mathcal{C}r^a_y/4 - \mathcal{C}r^d_y/2$	$-\mathcal{C}r^a_y/4 - \mathcal{C}r^d_y/2$
$\rightarrow$	$\mathcal{C}r^d_y$	$\mathcal{C}r^a_y/4 - \mathcal{C}r^d_y/2$	$-\mathcal{C}r^a_y/4 - \mathcal{C}r^d_y/2$	$1 + \mathcal{C}r^d_y$	$\mathcal{C}r^a_y/4 - \mathcal{C}r^d_y/2$	$-\mathcal{C}r^a_y/4 - \mathcal{C}r^d_y/2$
$\nwarrow$	$\mathcal{C}r^d_y/2 - \mathcal{C}r^a_y/4$	0	$-\mathcal{C}r^a_y/4 - \mathcal{C}r^d_y/2$	$1 + \mathcal{C}r^d_y/2 - \mathcal{C}r^a_y/4$	0	$-\mathcal{C}r^a_y/4 - \mathcal{C}r^d_y/2$
$\nearrow$	$\mathcal{C}r^d_y/2 - \mathcal{C}r^a_y/4$	0	$-\mathcal{C}r^a_y/4 + \mathcal{C}r^d_y/2$	$1 + \mathcal{C}r^d_y/2 - \mathcal{C}r^a_y/4$	0	$-\mathcal{C}r^a_y/4 - \mathcal{C}r^d_y/2$
$\swarrow$	$\mathcal{C}r^d_y/2 + \mathcal{C}r^a_y/4$	$\mathcal{C}r^a_y/4 - \mathcal{C}r^d_y/2$	0	$1 + \mathcal{C}r^d_y/2 + \mathcal{C}r^a_y/4$	$\mathcal{C}r^a_y/4 - \mathcal{C}r^d_y/2$	0
$\searrow$	$\mathcal{C}r^d_y/2 + \mathcal{C}r^a_y/4$	$\mathcal{C}r^a_y/4 - \mathcal{C}r^d_y/2$	0	$1 + \mathcal{C}r^d_y/2 + \mathcal{C}r^a_x/4$	$\mathcal{C}r^a_y/4 - \mathcal{C}r^d_y/2$	0

Table D.6: UP, CN and ADI schemes; concentration coefficients not considered in the previous tables

	Coefficients before:							
	$c^n_{i+1,j+1}$	$c^n_{i+1,j-1}$	$c^n_{i-1,j+1}$	$c^n_{i-1,j-1}$	$c^{n+1}_{i+1,j+1}$	$c^{n+1}_{i+1,j-1}$	$c^{n+1}_{i-1,j+1}$	$c^{n+1}_{i-1,j-1}$
$\cdot$	$a\mathcal{C}r^d_{xy}$	$-a\mathcal{C}r^d_{xy}$	$-a\mathcal{C}r^d_{xy}$	$a\mathcal{C}r^d_{xy}$	$-b\mathcal{C}r^d_{xy}$	$b\mathcal{C}r^d_{xy}$	$b\mathcal{C}r^d_{xy}$	$-b\mathcal{C}r^d_{xy}$
$\uparrow$	0	$-a\mathcal{C}r^d_{xy}$	0	$a\mathcal{C}r^d_{xy}$	0	$b\mathcal{C}r^d_{xy}$	0	$-b\mathcal{C}r^d_{xy}$
$\downarrow$	$a\mathcal{C}r^d_{xy}$	0	$-a\mathcal{C}r^d_{xy}$	0	$-b\mathcal{C}r^d_{xy}$	0	$b\mathcal{C}r^d_{xy}$	0
$\leftarrow$	$a\mathcal{C}r^d_{xy}$	$-a\mathcal{C}r^d_{xy}$	0	0	$-b\mathcal{C}r^d_{xy}$	$b\mathcal{C}r^d_{xy}$	0	0
$\rightarrow$	0	0	$-a\mathcal{C}r^d_{xy}$	$a\mathcal{C}r^d_{xy}$	0	0	$b\mathcal{C}r^d_{xy}$	$-b\mathcal{C}r^d_{xy}$
$\nwarrow$	0	$-a\mathcal{C}r^d_{xy}$	0	0	0	$b\mathcal{C}r^d_{xy}$	0	0
$\nearrow$	0	0	0	$a\mathcal{C}r^d_{xy}$	0	0	0	$-b\mathcal{C}r^d_{xy}$
$\swarrow$	$a\mathcal{C}r^d_{xy}$	0	0	0	$-b\mathcal{C}r^d_{xy}$	0	0	0
$\searrow$	0	0	$-a\mathcal{C}r^d_{xy}$	0	0	0	$b\mathcal{C}r^d_{xy}$	0
$\lrcorner$	$a\mathcal{C}r^d_{xy}$	$-a\mathcal{C}r^d_{xy}$	0	$a\mathcal{C}r^d_{xy}$	$-b\mathcal{C}r^d_{xy}$	$b\mathcal{C}r^d_{xy}$	0	$-b\mathcal{C}r^d_{xy}$
$\llcorner$	0	$-a\mathcal{C}r^d_{xy}$	$-a\mathcal{C}r^d_{xy}$	$a\mathcal{C}r^d_{xy}$	0	$b\mathcal{C}r^d_{xy}$	$b\mathcal{C}r^d_{xy}$	$-b\mathcal{C}r^d_{xy}$
$\urcorner$	$a\mathcal{C}r^d_{xy}$	$-a\mathcal{C}r^d_{xy}$	$-a\mathcal{C}r^d_{xy}$	0	$-b\mathcal{C}r^d_{xy}$	$b\mathcal{C}r^d_{xy}$	$b\mathcal{C}r^d_{xy}$	0
$\ulcorner$	$a\mathcal{C}r^d_{xy}$	0	$-a\mathcal{C}r^d_{xy}$	$a\mathcal{C}r^d_{xy}$	$-b\mathcal{C}r^d_{xy}$	0	$b\mathcal{C}r^d_{xy}$	$-b\mathcal{C}r^d_{xy}$

Coefficient $a = 2$ for the UP and ADI schemes and $a = 1$ for the CN scheme
Coefficient $b = 0$ for the UP and ADI schemes and $b = 1$ for the CN scheme

Appendix E

Modified Equation

The appendix presents the details of construction of the modified equation, described in Chapter 5. Table E.1 has been proposed to simplify the calculation which has to be done during the construction of modified equation. Instructions how to use the table are presented below.

The first column contains all the terms that can appear in the Taylor expansions (5.4) and (5.5). The table header contains all the concentration values in particular points ($c_{i,j}^{n+1}$, $c_{i+1,j}^{n+1}$, ..., $c_{i-1,j-1}^{n+1}$; $c_{i,j}^{n}$, $c_{i+1,j}^{n}$, ..., $c_{i-1,j-1}^{n}$), which appear in equation (5.2). Following the procedure described in Chapter 5 the first step to obtain the modified equation is the expansion of terms of equation (5.2) into Taylor series. The expansions should be put into the table in the following way: if in the expansion around a given point a term from the first column appears, one puts a relevant coefficient from equation (5.2), in the remaining cells one puts „– ” mark. For example for the $c_{i,j}^{n+1}$, the expansion into Taylor series is the following:

$$c_{i,j}^{n+1} = c_{i,j}^{n} + \Delta t \frac{\partial c}{\partial t} + \frac{\Delta t^2}{2}\frac{\partial^2 c}{\partial t^2} + \frac{\Delta t^3}{6}\frac{\partial^3 c}{\partial t^3} + \dots , \tag{E.1}$$

In the table one puts coefficient b_0 for $c_{i,j}^{n}$, $\Delta t \frac{\partial c}{\partial t}$, $\frac{\Delta t^2}{2}\frac{\partial^2 c}{\partial t^2}$ and $\frac{\Delta t^3}{6}\frac{\partial^2 c}{\partial t^2}$, and in remaining cells one puts „–”. Following this procedure for all terms of equation (5.2) one fills the whole table. Next, one summs up all the table rows. At this step many terms reduce. For such terms the table cells were filed with gray color. The remaining summed values should be put into last two columns, with relevant coefficients: (5.3) for the next to last, and (5.32) for the last one. Modified equation for the general case (5.6) will be obtained by summing up products of the first and next to last column. For the ADI method one should sum the products of first and last columns.

Table E.1: The table useful when the Modified Equation is created

	$c_{i,j}^{n+1}$	$c_{i+1,j}^{n+1}$	$c_{i-1,j}^{n+1}$	$c_{i,j+1}^{n+1}$	$c_{i,j-1}^{n+1}$	$c_{i+1,j+1}^{n+1}$	$c_{i+1,j-1}^{n+1}$	$c_{i-1,j+1}^{n+1}$	$c_{i-1,j-1}^{n+1}$	$c_{i,j}^{n}$	$c_{i+1,j}^{n}$	$c_{i-1,j}^{n}$
$c_{i,j}^{n}$	b_0	b_1	b_2	b_3	b_4	b_5	b_6	b_7	b_8	a_0	a_1	a_2
$\Delta t \frac{\partial c}{\partial t}$	b_0	b_1	b_2	b_3	b_4	b_5	b_6	b_7	b_8	-	-	-
$\Delta x \frac{\partial c}{\partial x}$	-	b_1	$-b_2$	-	-	b_5	b_6	$-b_7$	$-b_8$	-	a_1	$-a_2$
$\Delta y \frac{\partial c}{\partial y}$	-	-	-	b_3	$-b_4$	b_5	$-b_6$	b_7	$-b_8$	-	-	-
$\frac{\Delta t^2}{2} \frac{\partial^2 c}{\partial t^2}$	b_0	b_1	b_2	b_3	b_4	b_5	b_6	b_7	b_8	-	-	-
$\frac{\Delta x^2}{2} \frac{\partial^2 c}{\partial x^2}$	-	b_1	b_2	-	-	b_5	b_6	b_7	b_8	-	a_1	a_2
$\frac{\Delta y^2}{2} \frac{\partial^2 c}{\partial y^2}$	-	-	-	b_3	b_4	b_5	b_6	b_7	b_8	-	-	-
$\Delta x \Delta y \frac{\partial^2 c}{\partial x \partial y}$	-	-	-	-	-	b_5	$-b_6$	$-b_7$	b_8	-	-	-
$\Delta x \Delta t \frac{\partial^2 c}{\partial x \partial t}$	-	b_1	$-b_2$	-	-	b_5	b_6	$-b_7$	$-b_8$	-	-	-
$\Delta y \Delta t \frac{\partial^2 c}{\partial y \partial t}$	-	-	-	b_3	$-b_4$	b_5	$-b_6$	b_7	$-b_8$	-	-	-
$\frac{\Delta t^3}{6} \frac{\partial^3 c}{\partial t^3}$	b_0	b_1	b_2	b_3	b_4	b_5	b_6	b_7	b_8	-	-	-
$\frac{\Delta x^3}{6} \frac{\partial^3 c}{\partial x^3}$	-	b_1	$-b_2$	-	-	b_5	b_6	$-b_7$	$-b_8$	-	a_1	$-a_2$
$\frac{\Delta y^3}{6} \frac{\partial^3 c}{\partial y^3}$	-	-	-	b_3	$-b_4$	b_5	$-b_6$	b_7	$-b_8$	-	-	-
$\Delta x \Delta t \Delta y \frac{\partial^3 c}{\partial x \partial y \partial t}$	-	-	-	-	-	b_5	$-b_6$	$-b_7$	b_8	-	-	-
$\frac{\Delta x^2 \Delta y}{2} \frac{\partial^3 c}{\partial x^2 \partial y}$	-	-	-	-	-	b_5	$-b_6$	b_7	$-b_8$	-	-	-
$\frac{\Delta x \Delta y^2}{2} \frac{\partial^3 c}{\partial x \partial y^2}$	-	-	-	-	-	b_5	b_6	$-b_7$	$-b_8$	-	-	-
$\frac{\Delta t \Delta x^2}{2} \frac{\partial^3 c}{\partial x^2 \partial t}$	-	b_1	b_2	-	-	b_5	b_6	b_7	b_8	-	-	-
$\frac{\Delta t \Delta y^2}{2} \frac{\partial^3 c}{\partial y^2 \partial t}$	-	-	-	b_3	b_4	b_5	b_6	b_7	b_8	-	-	-
$\frac{\Delta t^2 \Delta x}{2} \frac{\partial^3 c}{\partial x \partial t^2}$	-	b_1	$-b_2$	-	-	b_5	b_6	$-b_7$	$-b_8$	-	-	-
$\frac{\Delta t^2 \Delta y}{2} \frac{\partial^3 c}{\partial y \partial t^2}$	-	-	-	b_3	$-b_4$	b_5	$-b_6$	b_7	$-b_8$	-	-	-

Table E.1: The table useful when the Modified Equation is created (continued)

	$c^n_{i,j+1}$	$c^n_{i,j-1}$	$c^n_{i+1,j+1}$	$c^n_{i+1,j-1}$	$c^n_{i-1,j+1}$	$c^n_{i-1,j-1}$	general	ADI
$c^n_{i,j}$	a_3	a_4	a_5	a_6	a_7	a_8	0	0
$\Delta t\frac{\partial c}{\partial t}$	-	-	-	-	-	-	1	1
$\Delta x\frac{\partial c}{\partial x}$	-	-	a_5	a_6	$-a_7$	$-a_8$	$\mathcal{C}r^a_x$	$\mathcal{C}r^a_x$
$\Delta y\frac{\partial c}{\partial y}$	a_3	$-a_4$	a_5	$-a_6$	a_7	$-a_8$	$\mathcal{C}r^a_y$	$\mathcal{C}r^a_y$
$\frac{\Delta t^2}{2}\frac{\partial^2 c}{\partial t^2}$	-	-	-	-	-	-	1	1
$\frac{\Delta x^2}{2}\frac{\partial^2 c}{\partial x^2}$	-	-	a_5	a_6	a_7	a_8	$-2\mathcal{C}r^d_x + \mathcal{C}r^a_x(2\alpha_1 - 1)$	$-2\mathcal{C}r^d_x$
$\frac{\Delta y^2}{2}\frac{\partial^2 c}{\partial y^2}$	a_3	a_4	a_5	a_6	a_7	a_8	$-2\mathcal{C}r^d_y + \mathcal{C}r^a_y(2\alpha_2 - 1)$	$-2\mathcal{C}r^d_y$
$\Delta x\Delta y\frac{\partial^2 c}{\partial x\partial y}$	-	-	a_5	$-a_6$	$-a_7$	a_8	$-8\mathcal{C}r^d_{xy}$	$-8\mathcal{C}r^d_{xy}$
$\Delta x\Delta t\frac{\partial^2 c}{\partial x\partial t}$	-	-	-	-	-	-	$\theta\mathcal{C}r^a_x$	$\frac{\mathcal{C}r^a_x}{2}$
$\Delta y\Delta t\frac{\partial^2 c}{\partial y\partial t}$	-	-	-	-	-	-	$\theta\mathcal{C}r^a_y$	$\frac{\mathcal{C}r^a_y}{2}$
$\frac{\Delta t^3}{6}\frac{\partial^3 c}{\partial t^3}$	-	-	-	-	-	-	1	1
$\frac{\Delta x^3}{6}\frac{\partial^3 c}{\partial x^3}$	-	-	a_5	a_6	$-a_7$	$-a_8$	$\mathcal{C}r^a_x$	$\mathcal{C}r^a_x$
$\frac{\Delta y^3}{6}\frac{\partial^3 c}{\partial y^3}$	a_3	$-a_4$	a_5	$-a_6$	a_7	$-a_8$	$\mathcal{C}r^a_y$	$\mathcal{C}r^a_y$
$\Delta x\Delta t\Delta y\frac{\partial^3 c}{\partial x\partial y\partial t}$	-	-	-	-	-	-	$-8\theta\mathcal{C}r^d_{xy}$	$\frac{\mathcal{C}r^a_x\mathcal{C}r^a_y}{4}$
$\frac{\Delta x^2\Delta y}{2}\frac{\partial^3 c}{\partial x^2\partial y}$	-	-	a_5	$-a_6$	a_7	$-a_8$	0	0
$\frac{\Delta x\Delta y^2}{2}\frac{\partial^3 c}{\partial x\partial y^2}$	-	-	a_5	a_6	$-a_7$	$-a_8$	0	0
$\frac{\Delta t\Delta x^2}{2}\frac{\partial^3 c}{\partial x^2\partial t}$	-	-	-	-	-	-	$\theta\left[-2\mathcal{C}r^d_x + \mathcal{C}r^a_x(2\alpha_1 - 1)\right]$	$-\mathcal{C}r^d_x$
$\frac{\Delta t\Delta y^2}{2}\frac{\partial^3 c}{\partial y^2\partial t}$	-	-	-	-	-	-	$\theta\left[-2\mathcal{C}r^d_y + \mathcal{C}r^a_y(2\alpha_2 - 1)\right]$	$-\mathcal{C}r^d_y$
$\frac{\Delta t^2\Delta x}{2}\frac{\partial^3 c}{\partial x\partial t^2}$	-	-	-	-	-	-	$\theta\mathcal{C}r^a_x$	$\frac{\mathcal{C}r^a_x}{2}$
$\frac{\Delta t^2\Delta y}{2}\frac{\partial^3 c}{\partial y\partial t^2}$	-	-	-	-	-	-	$\theta\mathcal{C}r^a_y$	$\frac{\mathcal{C}r^a_y}{2}$

List of symbols

a	dimensionless coefficient
B, b [m]	width of the river or channel
c $\left[kg/m^3\right]$, $[a.u.]$	concentration
$c^n_{i,j}$ $[a.u.]$	concentration value at point (i,j) at n-th time step
$\mathcal{C}r^a_x$, $\mathcal{C}r^a_y$	advection Courant numbers
$\mathcal{C}r^d_x$, $\mathcal{C}r^d_y$, $\mathcal{C}r^d_{xy}$	diffusion Courant numbers
$\mathbf{D}$ $\left[\mathrm{m}^2/\mathrm{s}\right]$	dispersion tensor
$\mathbf{D^{Res}}$ $\left[\mathrm{m}^2/\mathrm{s}\right]$	effective (resultant) diffusion tensor
$\mathbf{D_D}$ $\left[\mathrm{m}^2/\mathrm{s}\right]$	diagonal dispersion tensor
$\mathbf{D_V}$ $\left[\mathrm{m}^2/\mathrm{s}\right]$	vector of dispersion coefficients
D_L $\left[\mathrm{m}^2/\mathrm{s}\right]$	longitudinal dispersion coefficient
$\mathbf{D^N}$ $\left[\mathrm{m}^2/\mathrm{s}\right]$	numerical diffusion tensor
D^N_{11}, D^N_{12}, D^N_{21}, D^N_{22} $\left[\mathrm{m}^2/\mathrm{s}\right]$	coefficients of numerical diffusion tensor

D_T $\left[\mathrm{m}^2/\mathrm{s}\right]$	transverse dispersion coefficient
$D_{xx}, D_{xy}, D_{yx}, D_{yy}$ $\left[\mathrm{m}^2/\mathrm{s}\right]$	elements of dispersion tensor
g $\left[\mathrm{m}/\mathrm{s}^2\right]$	gravitation
H [m]	averaged depth of the river or channel
h [m]	local depth of the river or channel
M [kg] , $[a.u.]$	mass of the solute
Pe	Peclet number
R [m]	hydraulic radius
$\mathbf{R}(\alpha)$	rotation matrix with the angle α
S_0 [%] , [‰]	slope of the channel
t [s]	time
$\mathbf{T^N}$ $\left[\mathrm{m}^3/\mathrm{s}\right]$	numerical dispersion tensor
$T^N_{11}, T^N_{12}, T^N_{21}, T^N_{22}$ $\left[\mathrm{m}^3/\mathrm{s}\right]$	coefficients of numerical dispersion tensor
u_* [m/s]	friction (shear) velocity
V $\left[\mathrm{m}^3\right]$	volume of the liquid
$\mathbf{v}$ [m/s]	velocity vector

v_x [m/s]	x component of velocity vector
v_y [m/s]	y component of velocity vector
x [m]	x-coordinate of the Cartesian system
x_i	i-th point on the discretization grid
y [m]	y-coordinate of the Cartesian system
α [$\circ$]	angle between the flow direction and x axis of coordinate system
α_1, α_2	spatial weighting parameters with the values within the range $\langle 0, 1 \rangle$ determining the approximation method of the first space derivative
$\Delta_x c_{i,j}$, $\Delta_y c_{i,j}$	difference operators
$\delta_x^2 c_{i,j}$, $\delta_y^2 c_{i,j}$, δ_{xy}	difference operators
Δt [s]	time step
Δx [m]	grid spacing in x direction
Δy [m]	grid spacing in y direction
μ_x [m]	x-coordinate of the mean value of the concentration distribution
μ_y [m]	y-coordinate of the mean value of the concentration distribution
ω	relaxation parameter
σ_A [m]	standard deviation of analytical solution of advection-diffusion equation
σ_N [m]	standard deviation determined for the resultant diffusion coefficient taking into account the calculated numerical diffusion error

σ_S [m]	standard deviation of the Gauss distribution fitted to the simulation results
θ	weighting parameter with the values within the range $\langle 0, 1 \rangle$ determining the averaging in time

List of acronyms

ADI	Alternating Direction Implicit method
CN	Crank-Nicolson scheme
FDM	Finite Difference Method
FEM	Finite Element Method
FI	Fully Implicit scheme
FVM	Finite Volume Method
GS	Gauss-Seidel method
J	Jacobi method
MEA	Modified Equation Approach
RivMix	River Mixing Model
SOR	Successive Over Relaxation method
T	Thomas method
UP	Upwind scheme

List of Figures

2.1 Aerial photograph of an industrial discharge located near the middle of the regulated River Rhine . . . 12
2.2 Tracer study of horizontal mixing in Missouri river in USA . . . 13
2.3 Rhodamine dye study of hydrology of stream-lake interactions (Spring Creek) . . . 13
2.4 Tracer test performed in a natural Narew river in the North-East of Poland 14
2.5 Tracer test performed in a small river . . . 14
2.6 Tracer test performed in a natural Narew river in the North-East of Poland 15
2.7 An example of analytical solution . . . 22

3.1 Schematic representation of the dispersion tensor in the Cartesian coordinate system . . . 25
3.2 $\mathbf{D_D}$ tensor rotation by angle α . . . 26
3.3 Diagram representation of $\mathbf{D_V} = [D_L, D_T]$ for a rectangular channel whose main axis is not parallel to the x-axis . . . 28
3.4 Vector $\mathbf{D_V}$ rotation by angle α . . . 28
3.5 Scheme of straight, rectangular channel, used for computations . . . 30
3.6 Dependence of the D_{xy} coefficient on the angle α for the considered methods . . . 32
3.7 Analytical solution for the pulse release of the substance after 400 seconds from t_0 . . . 33
3.8 Numerical solution by means of full tensor *rotation* method for the pulse release after 400 time steps, $\alpha = 45°$ . . . 34
3.9 Difference between the analytical and numerical (*rotation*) solutions, for the pulse release after 400 time steps, $\alpha = 45°$ . . . 34
3.10 Numerical solution by means of *quasi rotation* method for the pulse release after 400 time steps, $\alpha = 45°$ . . . 34
3.11 Difference between the analytical and numerical (*quasi rotation*) solutions, for the pulse release after 400 time steps, $\alpha = 45°$ . . . 34

3.12 Numerical solution by means of *vector-like rotation* method for the pulse release after 400 time steps, $\alpha = 45°$ 35
3.13 Difference between the analytical and numerical (*vector-like rotation*) solutions, for the pulse release after 400 time steps, $\alpha = 45°$ 35
3.14 Numerical solution by means of *identity transformation* method for the pulse release after 400 time steps, $\alpha = 45°$ 35
3.15 Difference between the analytical and numerical (*identity transformation*) solutions, for the pulse release after 400 time steps, $\alpha = 45°$ 35
3.16 Maximum difference (Δc) between the analytical and the numerical solutions for the discussed methods of determining the dispersion tensor after 400 seconds of simulation in case of pulse release; the difference is plotted as a function of angle α 36
3.17 Maximum concentration (c_{max}) after 400 seconds of simulation, depending on the angle α in case of pulse release 38
3.18 Numerical solution by means of *rotation* method for the continuous release after 1000 time steps, $\alpha = 45°$ 40
3.19 Numerical solution by means of *quasi rotation* method for the continuous release after 1000 time steps, $\alpha = 45°$ 40
3.20 Difference between the solution by means of *rotation* and the solution by means of *quasi rotation*, after 1000 time steps, $\alpha = 45°$ 40
3.21 Numerical solution by means of *vector-like rotation* method for the continuous release after 1000 time steps, $\alpha = 45°$ 41
3.22 Difference between the solution by means of *rotation* and the solution by means of *vector-like rotation*, after 1000 time steps, $\alpha = 45°$ 41
3.23 Numerical solution by means of *identity transformation* method for the continuous release after 1000 time steps, $\alpha = 45°$ 41
3.24 Difference between the solution by means of *rotation* and the solution by means of *identity transformation*, after 1000 time steps, $\alpha = 45°$ . . . 41
3.25 Maximum difference (Δc) between the tensor rotation and the other discussed methods of determining the dispersion tensor after 1000 seconds of simulation in case of continuous release; the difference is plotted as a function of the angle α 42
3.26 Maximum concentration (c_{max}) after 1000 seconds of simulation, depending on the angle α in case of continuous release 43
3.27 Maximum concentration values during the simulation of continuous release for various angles α 44

4.1 Diagram for solving partial differential equation by means of Finite Difference Method 46
4.2 One-dimensional, homogenous discretization grid 47
4.3 Rectangular discretization grid of Δx and Δy unit size on the (x, y) plane 49
4.4 Example of transformation of coordinates of a point in the grid into its number (only the inner points from the discretization grid are taken into consideration) 55

4.5 Schematic representation of the matrix of coefficients for the equation system obtained after the application of CN scheme. 56
4.6 Schematically presented ADI method 59
4.7 The numerical solution with the application of the ADI scheme (a) and ADI2 scheme (c) 62
4.8 Schematically presented matrices of coefficients in the equation systems obtained with the application of ADI scheme 63
4.9 Schematic representation of the right-hand border edge of the calculation grid 66

5.1 Modified Equation Approach – diagram 69
5.2 Analytical (a) and numerical solution with the application of UP scheme (b) and CN scheme (c) after 1150 seconds 79
5.3 Analytical solution (a) and numerical one with the application of ADI method (b) after 1150 seconds 87
5.4 Average CPU time in a single time step 89
5.5 Results of simulation with the application of the UP scheme after 100 time steps for various values of time step 92
5.6 Results of simulation with the application of UP (a), CN (b) and ADI (c) schemes after 100 time steps for $\Delta t = 1\,\mathrm{s}$ 93
5.7 Results of simulation with the application of the CN (a) and ADI (b) schemes after 10 time steps for $\Delta t = 10\,\mathrm{s}$ 94
5.8 Non-physical oscillations of the solution 95

6.1 Inheritance pattern diagram for classes representing the computation grid 100
6.2 Inheritance diagram for classes representing the discussed numerical approaches 100
6.3 Block diagram of the **RivMix** model – main program 101
6.4 Block diagram of the **RivMix** model – *Calculation of concentration values in the next time step* 102
6.5 Block diagram of the **RivMix** model – *Iterative solving of equation system* 104

7.1 Initial concentration in the tests carried out with instantaneous discharge of pollutants (analytical solution after 150 seconds after discharge) . . . 107
7.2 Results of simulation with the application of the UP scheme after 750 seconds – figs. (a), (b), (c), and figs. (d), (e), (f) illustrating the course of the simulation in time 108
7.3 Results of simulation with the application of the CN scheme after 750 seconds – figs. (a), (b), (c), and figs. (d), (e), (f) illustrating the course of the simulation in time 109
7.4 Results of simulation with the application of the ADI scheme after 750 seconds – figs. (a), (b), (c), and figs. (d), (e), (f) illustrating the course of the simulation in time 110
7.5 Analytical solution after 750 seconds 111

7.6 Projection of the numerical solution and the analytical one on the straight line perpendicular to $y = x$ and crossing the point with the maximum concentration at a given moment in time 112
7.7 Difference between the standard deviation of the projection of the numerical solution σ_X^S and the analytical one σ_X^A upon the x axis in consecutive time steps, normalized by σ_X^A 113
7.8 Initial concentration distribution $\mathbf{C_0}$ at time $t = 0\,\mathrm{s}$ used in the tests with continuous inflow of pollutants 114
7.9 Results of simulation for continuous discharge of pollutants after 1500 seconds for the discussed schemes 115
7.10 Projection of the numerical solution with the application of various schemes: (a) – on the straight line $y = x$; (b) – on the straight line perpendicular to $y = x$, crossing the middle of the channel 116
7.11 Schematic representation of the laboratory channel for which the simulations were carried out 118
7.12 Profile of the bottom of the channel 118
7.13 Depth-averaged (mean velocity) v_x distribution in the discussed channel 119
7.14 Transverse dispersion coefficient D_{yy} distribution in the channel 119
7.15 Longitudinal dispersion coefficient distribution in the channel 121
7.16 Transverse dispersion coefficient distribution in the channel 121
7.17 Concentration distribution $c(x, y)$ after 50 time steps 123
7.18 Concentration distribution $c(x, y)$ after 100 time steps 123
7.19 Concentration distribution after 100 time steps at the distance of 1.89 m from the source – comparison of simulated and experimental results . . 124
7.20 Concentration distribution after 100 time steps at the distance of 1.89 m from the source – comparison of simulated and experimental results; logarithmic scale 124
7.21 Concentration distribution after 100 time steps at the distance of 2.14 m from the source – comparison of simulated and experimental results . . 125
7.22 Concentration distribution after 100 time steps at the distance of 2.14 m from the source – comparison of simulated and experimental results; logarithmic scale 125
7.23 Concentration distribution after 100 time steps at the distance of 2.64 m from the source – comparison of simulated and experimental results . . 126
7.24 Concentration distribution after 100 time steps at the distance of 2.64 m from the source – comparison of simulated and experimental results; logarithmic scale 126

C.1 Numerical solution with application of different methods of dispersion tensor transformation for the pulse release, $\alpha = 0°$ 138
C.2 Difference between the numerical solution and analytical one for the pulse release, $\alpha = 0°$ 139
C.3 Numerical solution with application of different methods of dispersion tensor transformation for the pulse release, $\alpha = 5°$ 140

C.4 Difference between the numerical solution and analytical one for different methods of dispersion tensor transformation for the pulse release, $\alpha = 5°$ 141
C.5 Numerical solution with application of different methods of dispersion tensor transformation for the pulse release, $\alpha = 15°$ 142
C.6 Difference between the numerical solution and analytical one for different methods of dispersion tensor transformation for the pulse release, $\alpha = 15°$ 143
C.7 Numerical solution with application of different methods of dispersion tensor transformation for the pulse release, $\alpha = 30°$ 144
C.8 Difference between the numerical solution and analytical one for different methods of dispersion tensor transformation for the pulse release, $\alpha = 30°$ 145
C.9 Numerical solution with application of different methods of dispersion tensor transformation for the pulse release, $\alpha = 60°$ 146
C.10 Difference between the numerical solution and analytical one for different methods of dispersion tensor transformation for the pulse release, $\alpha = 60°$ 147
C.11 Numerical solution with application of different methods of dispersion tensor transformation for the continuous release, $\alpha = 0°$ 149
C.12 Numerical solution with application of different methods of dispersion tensor transformation for the continuous release, $\alpha = 5°$ 150
C.13 Difference between the solution by means of *rotation* and the solution with application of one of different methods of dispersion tensor transformation, $\alpha = 5°$ 151
C.14 Numerical solution with application of different methods of dispersion tensor transformation for the continuous release, $\alpha = 15°$ 152
C.15 Difference between the solution by means of *rotation* and the solution with application of one of different methods of dispersion tensor transformation, $\alpha = 15°$ 153
C.16 Numerical solution with application of different methods of dispersion tensor transformation for the continuous release, $\alpha = 30°$ 154
C.17 Difference between the solution by means of *rotation* and the solution with application of one of different methods of dispersion tensor transformation, $\alpha = 30°$ 155
C.18 Numerical solution with application of different methods of dispersion tensor transformation for the continuous release, $\alpha = 60°$ 156
C.19 Difference between the solution by means of *rotation* and the solution with application of one of different methods of dispersion tensor transformation, $\alpha = 60°$ 157

List of Tables

2.1 Orders of magnitude of various mixing coefficients in rivers (Smith, 1992) 10
2.2 Examples for the complete mixing of a passive point source 11
2.3 Parameter a values for transverse dispersion coefficient 19

3.1 Simulation parameters used in the numerical tests 31
3.2 Dispersion coefficients for various α on the basis of the considered methods 31
3.3 Maximum concentration value error expressed in percents 39

4.1 Difference quotients applied for the approximation of the first and the second derivative 48
4.2 Methods implemented in the **RivMix** model 52
4.3 Coefficients in equation (4.9) depending on the signs of velocity components 53
4.4 The number of iterations in a single time step while solving the equation system obtained in CN scheme for example simulation parameters . . . 58

5.1 Values of coefficients of numerical diffusion and dispersion tensors for UP scheme 80
5.2 Values of coefficients of numerical diffusion and dispersion tensors for CN and FI schemes 81
5.3 Comparison of numerical diffusion error calculated using modified equation approach and determined based on the simulation 83
5.4 Values of the coefficients of numerical diffusion and dispersion tensors for the ADI method 88
5.5 Average CPU time and real time in a single time step in case of various schemes, for exemplary simulation parameters 90
5.6 Stability of schemes for example parameters 91

7.1 Simulation parameters used in the tests carried out 106

7.2 Simulation parameters used in the tests carried out 122

B.1 Collection of all difference quotients used in the book 136

D.1 UP scheme; concentration coefficients in equation (4.9) depending on the velocity sign 160
D.2 CN scheme; concentration coefficients in equation (4.11) in the n-th time step for different boundary types 164
D.3 CN scheme; concentration coefficients in equation (4.11) in the $(n+1)$-th time step for different boundary types 165
D.4 ADI scheme, STEP I; concentration coefficients in equation (4.23) for different boundary types 166
D.5 ADI scheme, STEP II; concentration coefficients in equation (4.24) for different boundary types 168
D.6 UP, CN and ADI schemes; concentration coefficients not considered in the previous tables 169

E.1 The table useful when the Modified Equation is created 172

References

Abbott, M.B. & Basco, D.R. (1989). *Computational fluid dynamics*. Longman Scientific and Technical, Great Britain.

Ataie-Ashtiani, B. & Hosseini, S.A. (2005a). Error analysis of finite difference methods for two-dimensional advection-dispersion-reaction equation. *Advances in Water Resources*, **28**:793–806.

Ataie-Ashtiani, B. & Hosseini, S.A. (2005b). Numerical errors of explicit finite difference approximation for two-dimensional solute transport equation with linear sorption. *Environmental Modelling & Software*, **20**:817–826.

Ataie-Ashtiani, B., Lockington, D. & Volker, R. (1996). Numerical correction for finite-difference solution of the advection-dispersion equation with reaction. *Journal of Contaminant Hydrology*, **23**(1-2):149–156.

Ataie-Ashtiani, B., Lockington, D. & Volker, R. (1999). Truncation errors in finite difference models for solute transport equation with first-order reaction. *Journal of Contaminant Hydrology*, **35**:409–428.

Balzano, A. (1999). Mosquito: An efficient finite difference scheme for numerical simulation of 2D advection. *International Journal for Numerical Methods in Fluid*, **31**:481–496.

Beak, K.O. (2004). *Transverse mixing in meandering channels with unsteady pollutant source*. PhD thesis, Seoul National University, Korea.

Beer, T. & Young, P.C. (1983). Longitudinal dispersion in natural streams. *Journal of Environmental Engineering*, **109**(5):1049–1067.

Bielecka-Kieloch, M. (1998). Numerical diffusion and dispersion tensor for 2D linear advection equation. *Archives of Hydro-Engineering and Environmental Mechanics*, **45**(1-4):29–43.

REFERENCES

Björc, A. & Dahlquist, G. (1987). *Metody numeryczne*. PWN, Warszawa.

Boczar, J. (1980). *Wzory służące do modelowania procesów rozprzestrzeniania i przekształcania zanieczyszczeń w rzekach*, vol. 148 , *Prace naukowe Politechniki Szczecińskiej*. Wydawnictwo Uczelniane Politechniki Szczecińskiej, Szczecin.

Boczar, J. (1991). *Modele matematyczne transportu i wymiany pędu i masy w wodach powierzchniowych i gruntowych*, vol. 2 , *Monografie Komitetu Gospodarki Wodnej Polskiej Akademii Nauk*. Wydawnictwa Politechniki Warszawskiej, Warszawa.

Boxall, J.B. (2000). *Dispersion of solutes in sinuous open channel flows*. PhD thesis, University of Sheffield, UK.

Boxall, J.B., Guymer, I. & Marion, A. (2003). Transverse mixing in sinuous natural open channel flows. *Journal of Hydraulic Research*, **41**(2):153–165.

Bronsztejn, I.N. & Siemiendiajew, K.A. (1997). *Matematyka, poradnik encyklopedyczny*. PWN, Warszawa, 14th edn.

Brun, R. & Rademakers, F. (1997). ROOT – an object oriented data analysis framework. *Nuclear Instruments and Methods in Physics Research Section A*, **389**.

Chau, K. & Jiang, Y.W. (2002). Three-dimensional pollutant transport model for the pearl river estuary. *Water Research*, **36**:2029–2039.

Cheong, T.S. & Seo, I.W. (2003). Parameter estimation of the transit storage model by routing method for river mixing processes. *Water Resources Research*, **39**(4), HWC 1-1-11.

Chung, T.J. (2002). *Computational Fluid Dynamics*. Cambridge University Press.

Crank, J. & Nicolson, P. (1947). A practical method for numerical evaluation of solutions of partial differential equations of the heat-conduction type. *Proceedings of the Cambridge Philosophical Society*, **43**:50–67.

Czernuszenko, W. (1987). Dispersion of pollutants in rivers. *Hydrological Sciences Journal*, **32**(1):33–42.

Czernuszenko, W. (1990). Dispersion of pollutants in flowing surface water. In *Encyclopedia of Fluid Mechanics, Surface and Groundwater flow phenomena*, vol. 10, 119–168, Gulf Publishing Company, Houston, London, Paris.

Czernuszenko, W. (2000a). Podstawy modelowania transportu zanieczyszczeń. *Przegląd Geofizyczny*, **XLV**(1):33–42.

Czernuszenko, W. (2000b). Transport zanieczyszczeń w rzekach i kanałach. *Przegląd Geofizyczny*, **XLV**(2):139–150.

Czernuszenko, W. & Rowiński, P. (1994). *Współczesne modele matematyczne procesów transportu i mieszania zanieczyszczeń w rzekach*, vol. 6 , *Monografie Komitetu Gospodarki Wodnej Polskiej Akademii Nauk*. Oficyna Wydawnicza Politechniki Warszawskiej, Warszawa.

Czernuszenko, W. & Rowiński, P.M. (2005). *Water Quality Hazards and Dispersion of Pollutants*. Springer, USA.

Czernuszenko, W. & Rylov, A. (2005). Three-dimensional model of flow and mixing processes in open channels. In W. Czernuszenko & P.M. Rowiński, eds., *Water Quality Hazards and Dispersion of Pollutants*, chap. 1, 35–54, Springer, USA.

Czernuszenko, W., Rowiński, P.M. & Sukhodolov, A. (1998). Experimental and numerical validation of dead-zone model for longitudinal dispersion in rivers. *Journal of Hydraulic Research*, **36**(2):269–280.

Dehghan, M. (2004). Weighted finite difference techniques for the one-dimensional advection–diffusion equation. *Applied Mathematics and Computation*, **147**(2):307–319.

Deng, Z.Q., Bengtsson, L., Singh, V.P. & Adrian, D.D. (2002). Longitudinal dispersion coefficient in single-channel streams. *Journal of Hydraulic Engineering*, **128**(10):901–916.

Directive (2000). Handbook of Implementation of Framework Water Directive EU. Nr 2000/ 60/EC.

Douglas, J. (1955). On the numerical integration of $\frac{\partial^2 u}{\partial x^2} + \frac{\partial^2 u}{\partial y^2} = \frac{\partial u}{\partial t}$ by implicit methods. *Journal of the Society for Industrial and Applied Mathematics*, **3**(1):42–65, USA.

Douglas, J. & Rachford, H. (1956). On the numerical solution of the heat conduction problem in two and three space variables. *Transactions of the American Mathematical Society*, **82**:421–439.

Elder, J.W. (1959). The dispersion of a marked fluid in turbulent shear flow. *Journal of Fluid Mechanics*, **5**(4):544–560.

Elgobashi, S. (1994). On predicting particle-laden turbulent flows. *Applied Scientific Research*, **52**:309–329.

Endrizzi, S., Tubino, M. & Zolezzi, G. (2002). Lateral mixing in meandering channels: a theoretical approach. In D. Bousmar & Y. Zech, eds., *River Flow 2002: Proceedings of the International Conference on Fluvial Hydraulics, Louvain-la-Neuve, Belgium, 4-6 September 2002*, Swets & Zeitlinger, Lisse, The Netherlands.

REFERENCES

Fabritz, J.E. (1995). *A Two Dimensional Numerical Model for Simulating the Movement and Biodegradation of Contaminants in a Saturated Aquifer*. Master's thesis, University of Washington.

Ferziger, J.H. (1988). A note on numerical accuracy. *International Journal for Numerical Methods in Fluid*, **8**:995–996, Special Note.

Fischer, H.B., List, E.J., Koh, R.C.Y., Imberger, J. & Brooks, N.H. (1979). *Mixing in Island and Coastal Waters*. Academic Press, New York.

Fletcher, C.A.J. (1991). *Computational techniques for fluid dynamics*. Springer Series in Computational Physics, Springer-Verlag, Germany.

Grandjouan, N. (1990). The modified equation approach to flux-corrected transport. *Journal of Computational Physics*, **91**:424–440.

Gresho, P.M. & Sani, R.L. (2000). *Incompressible Flow and the Finite Element Method*, vol. 1. Wiley, USA.

Grima, R. & Newman, T. (2004). Accurate discretization of advection-diffusion equations. *Physical Review E*, **70**:036703.

Guan, Y. & Zhang, D. (2005). Finite difference tvd scheme for modeling two-dimensional advection-dispersion. In J.H.W. Lee & K.M. Lam, eds., *Environmental hydraulics and sustainable water management, Proceedings of the 4th International Symposium on Environmental Hydraulics and the 14th Congress of Asia and Pacific Division, International Association of Hydraulic Engineering and Research, Hong Kong, 15-18 December 2004*, 503–509, Taylor & Francis.

Guymer, I. (1998). Longitudinal dispersion in a sinuous channel with changes in shape. *Journal of Hydraulic Engineering*, **124**(1):33–40.

Guymer, I. (2006). Private communication.

Guymer, I., Boxall, J.B., Marion, A., Potter, R., Trevisan, P., Bellinello, M. & Dennis, P. (1999). Longitudinal dispersion in natural formed meandring channel. In M.N. Abbott, ed., *Proceedings of International Association of Hydraulic Engineering and Research 28th Congress, Graz, Austria*.

Holley, E.R. (2001). Field tests for evaluating hydraulic transport processes in rivers. In P.M. Rowiński & J.J. Napiórkowski, eds., *Water quality issues in the Upper Narew valley*, chap. 3, 39–51, Publications of the Institute of Geophysics, Polish Academy of Sciences, Warszawa.

Holley, E.R. & Abraham, G. (1973a). Field tests on transverse mixing in rivers. *Journal of Hydraulic Division, Proceedings of the American Society of Civil Engineers*, **99**(HY 12):2313–2331.

Holley, E.R. & Abraham, G. (1973b). Laboratory studies on transverse mixing in rivers. *Journal of Hydraulic Research*, **11**(3):219–253.

Holley, E.R. & Jirka, G.H. (1986). Mixing in rivers. Tech. rep., US Army Engineer Waterways Experiment Station, Vicksburg, Miss.

Holley, E.R., Siemons, J. & Abraham, G. (1972). Some aspects of analysing transverse diffusion in rivers. *Journal of Hydraulic Research*, **10**:27–57.

Islam, M.R. & Chaudhry, M.H. (1997). Numerical solution of transport equation for applications in environmental hydraulics and hydrology. *Journal of Hydrology*, **191**:106–121.

Jeon, T.M., Baek, K.O. & Seo, I.W. (2007). Development of an empirical equation for transverse dispersion coefficient in natural stream. *Environmental Fluid Mechanics*, **7**:317–329.

Jirka, G.H. & Weitbrecht, V. (2005). Mixing models for water quality management in rivers: continuous and instantaneous pollutant release. In W. Czernuszenko & P.M. Rowiński, eds., *Water Quality Hazards and Dispersion of Pollutants*, chap. 1, 1–34, Springer, USA.

Juntunen, J. & Tsiboukis, T. (2000). Reduction of numerical dispersion in fdtd method through artificialanisotropy. *IEEE Transactions on Microwave Theory and Techniques*, **48**(4):582–588.

Karahan, H. (2006). Implicit finite difference techniques for the advection-diffusion equation using spreadsheets. *Advances in Engineering Software*, **37**(9):601–608.

Kashefipour, S.M., Falconer, R.A. & Lin, B. (2002). Modeling longitudinal dispersion in natural channel flows using ANNs. In D. Bousmar & Y. Zech, eds., *River Flow 2002: Proceedings of the International Conference on Fluvial Hydraulics, Louvain-la-Neuve, Belgium, 4-6 September 2002*, Swets & Zeitlinger, Lisse, The Netherlands.

Lau, L.Y. & Krishnappan, B.G. (1981). Modeling transverse mixing in natural streams. *Journal of the Hydraulics Division, Proceedings of the American Society of Civil Engineers*, **107**(2):209–226.

MacKenzie, T. & Roberts, A. (2003). Holistic discretization of shear dispersion in a two-dimensional channel. *Journal of the Australian Mathematical Society*, **44**(E):C512–C530.

Manson, J.R., Wallis, S.G. & Wang, D. (2002). Application of two-dimensional conservative semi-lagrangian transport algorithm on parallel computers. In S.M. Hassanizadeh, R.J. Schotting, W.G. Gray & G.F. Pinder, eds., *Proceedings of 14th International Conference on Computational Methods in Water Resources, Delft, The Netherlands, June 23-28*, 1011–1018, Elsevier Science.

REFERENCES

McKee, S. & Mitchell, A.R. (1970). Alternating direction methods for parabolic equations in two space dimensions with a mixed derivative. *The Computer Journal*, **13**(1):81–86.

McKee, S. & Mitchell, A.R. (1971). Alternating direction methods for parabolic equations in three space dimensions with mixed derivatives. *The Computer Journal*, **14**(3):295–300.

McKee, S., Wall, D.P. & Wilson, S.K. (1996). An alternating direction implicit scheme for parabolic equations with mixed derivative and convection terms. *Journal of Computational Physics*, **126**:64–76.

Noye, B.J. & Tan, H.H. (1989). Finite difference methods for solving the two-dimensional advection-diffusion equation. *International Journal for Numerical Methods in Fluid*, **9**:75–98.

Noye, J. (1984). Finite difference techniques for partial differential equations. In J. Noye, ed., *Computational Techniques for Differential Equations*, 95–354, North-Holland.

Odman, M.T. (1997). A quantitative analysis of numerical diffusion introduced by advection algorithms in air quality models. *Atmospheric Environment*, **31**(13):1933–1940.

Peaceman, D.W. & Rachford, H.H. (1955). The numerical solution of parabolic and elliptic differential equations. *Journal of the Society for Industrial and Applied Mathematics*, **3**(1):28–42.

Peyret, R. & Taylor, D.T. (1986). *Computational Methods for Fluid Flow*. Springer Series in Computational Physics, Springer-Verlag, New York.

Piotrowski, A. (2005). *Inteligentna analiza danych hydrologicznych*. PhD thesis, Instytut Geofizyki Polskiej Akademii Nauk, Warszawa.

Piotrowski, A., Rowiński, P. & Napiórkowski, J. (2006). Assessment of longitudinal dispersion coefficient by means of different neural models. In *Proceedings of the 7th International Conference in Hydroinformatics, HIC 2006, Nice, France*.

Rieckermann, J., Neumann, M., Ort, J., C.and Huisman & Gujer, W. (2005). Dispersion coefficients of sewers from tracer experiments. *Water Science & Technology*, **52**(5):123–133.

Rowiński, P.M. (2002). Constituent transport. In J.C.I. Dooge, ed., *Encyclopaedia of Life Support Systems (EOLSS)*, chap. Fresh Surface Water, Eolss Publishers Co., Oxford, UK, developed under the auspices of the UNESCO.

Rowiński, P.M. & Kalinowska, M.B. (2006). Admissible and inadmissible simplifications of pollution transport equations. In R.M.L. Ferreira, E.C.T.L. Alves, J.G.A.B. Leal & A.H. Cardoso, eds., *River Flow 2006: Proceedings of the International Conference on Fluvial Hydraulics, Lisbon, Portugal, 6-8 September 2006*, 199–209, Taylor and Francis.

Rowiński, P.M. & Kwiatkowski, K. (2008). Analyses of scenarios of catastrophic releases of hazardous substances into a river. In *River Flow 2008: Proceedings of the International Conference on Fluvial Hydraulics, Cesme – Izmir, Turkey, 3-5 September 2008*.

Rowiński, P.M. & Piotrowski, A. (2008). Estimation of parameters of the transient storage model by means of multi-layer perceptron neural networks. *Hydrological Sciences Journal*, **53**(1):165–178.

Rowiński, P.M., Napiórkowski, J.J. & Owczarczyk, A. (2003a). Transport of passive admixture in a multi-channel river system – the Upper Narew case study. Part II. Application of dye tracer method. *Ecohydrology & Hydrobiology*, **3**(4):381–388.

Rowiński, P.M., Napiórkowski, J.J. & Szkutnicki, J. (2003b). Transport of passive admixture in a multi-channel river system – the Upper Narew case study. Part I. Hydrological survey. *Ecohydrology & Hydrobiology*, **3**(4):371–379.

Rowiński, P.M., Aberle, J. & Mazurczyk, A. (2005a). Shear velocity estimation in hydraulic research. *Acta Geophysica Polonica*, **53**(4):567–583.

Rowiński, P.M., Piotrowski, A. & Napiórkowski, J.J. (2005b). Are artificial network techniques relevant for the estimation of longitudinal dispersion coefficient in rivers? *Hydrological Sciences Journal*, **50**(1):175–187.

Rowiński, P.M., Guymer, I., Bielonko, A., Napiórkowski, J.J., Pearson, J. & Piotrowski, A. (2007). Prediction of dispersion coefficients in a small stream using artificial neural networks. In *Proceedings 32nd Congress of International Association of Hydraulic Engineering and Research, July, 1-6 2007, Harmonizing the Demands of Art and Nature in Hydraulics*, paper 297.

Rowiński, P.M., Guymer, I. & Kwiatkowski, K. (2008). Response to the slug injection of a tracer -– large scale experiment in a natural river. *Hydrological Science Journal*, **53**(6):1300–1309.

Rutherford, J.C. (1994). *River Mixing*. Wiley, Chichester, England.

Rutherford, J.C., Williams, B.L. & Hoare, R.A. (1992). Transverse mixing and surface heat exchange in the Waikato river: a comparison of two models. *New Zealand Journal of Marine and Freshwater Research*, **26**:435–452.

Sawicki, J.M. (2003). *Migracja zanieczyszczeń*. Wydawnictwo PG, Gdańsk.

REFERENCES

Seo, I.W., Baek, K.O. & Jeon, T.M. (2006). Analysis of transverse mixing in natural streams under slug tests. *Journal of Hydraulic Research*, **44**(3):350–362.

Smith, R. (1992). *Physics of Dispersion, Coastal and Estuarine Pollution: Methods and Solutions*. Scottish Hydraulics Study Group, Glasgow, one day seminar 3rd April.

Smith, R. & Yongming, T. (2001). Optimal and near-optimal advection-diffusion finite difference schemes VI. *Proceedings of the Royal Society A*, **457**:2379–2396.

Socolofsky, S.A. & Jirka, G.H. (2005). *Special topics in mixing and transport processes in the environment*. Coastal and Ocean Engineering Division, Texas A & M University, 5th edn., engineering – Lectures, CVEN 489-501.

Stroustrup, B. (2000). *Język C++*. Klasyka informatyki, Wydawnictwa Naukowo-Techniczne, 5th edn.

Sukhodolov, A., Nikora, V.I., Rowiński, P.M. & Czernuszenko, W. (1998). A case study of longitudinal dispersion in small lowland rivers. *Water Environment Research*, **69**(7):1246–1253.

Szymkiewicz, R. (2000). *Modelowanie matematyczne przepływów w rzekach i kanałach*. PWN, Warszawa.

Szymkiewicz, R. (2003). *Metody numeryczne w inżynierii wodnej*. Wydawnictwo PG, Gdańsk.

Szymkiewicz, R. (2006). *Metoda badania dyfuzji i dyspersji numerycznej w rozwiązaniach równań hydromechaniki*. Wydawnictwo PG, Gdańsk.

Tayfur, G. & Singh, V.P. (2005). Predicting longitudinal dispersion coefficient in natural streams by artificial neural network. *Journal of Hydraulic Engineering*, **131**(11):991–1000.

Thom, A. & Apelt, C.J. (1961). *Field computations in engineering and physics*. Van Nostrand, London.

Thomas, J.W. (1995). *Numerical Partial Differential Equations, Finite Difference Methods*. Springer, New York.

Tsai, T.L., Yang, J.C. & Huang, L.H. (2001). An accurate integral-based scheme for advection-diffusion equation. *Communications in Numerical Methods in Engineering*, **17**(10):701–713.

Van Mazijk, A. & Veling, E.J.M. (2005). Mixing models for water quality management in rivers: continuous and instantaneous pollutant release. In W. Czernuszenko & P.M. Rowiński, eds., *Water Quality Hazards and Dispersion of Pollutants*, 143–168, Springer, USA.

Wallis, S., Piotrowski, A., Rowiński, P. & Napiórkowski, J. (2007). Prediction of dispersion coefficients in a small stream using artificial neural networks. In *Proceedings 32nd Congress of International Association of Hydraulic Engineering and Research, July, 1-6 2007, Harmonizing the Demands of Art and Nature in Hydraulics*, paper 175.

Wallis, S.G. & Manson, J.R. (2004). Methods for predicting dispersion coefficients in rivers. *Water Management*, **157**(WM3):131–141.

Wang, Y. & Hutter, K. (2001). Comparisons of numerical methods with respect to convectively dominated problems. *International Journal for Numerical Methods in Fluid*, **37**:721–745.

Warming, R.F. & Hyett, B.J. (1974). The modified equation approach to the stability and accuracy analysis of finite-difference methods. *Journal of Computational Physics*, **14**:159–179.

Wu, Y. & Falconer, R. (1998). Refined two-dimensional ultimate quickest scheme for conservative solute transport modelling. In *3rd International Conference on Hydro-Science and -Engineering Brandenburg University of Technology at Cottbus Cottbus/Berlin, Germany, August 31 - September 3*.

Zoppou, C. & Roberts, S. (1993). Simulation techniques for the advection equation. In D. Singleton, D. Stewart & H. Gardner, eds., *Computational techniques and applications*, 518–526, World Scientific Press.

Index

accuracy, 47, 49, 67–87, 94, 129
advection, 8
- term, 9, 94, 96
advection-diffusion equation, 16, 23–24, 45, 68, 94, 129
- 1D, 8, 11, 15, 17, 23, 46, 68
- 2D, 8, 11, 15–17, 20–24, 46, 68, 77, 96, 122, 133
  - - discretization, 49–65
  - - simplifications, 17, 23–43, 130
- 3D, 8, 10, 11, 15, 23
Alternating Direction Implicit method (ADI), 29, 51, 58–65, 84, 86–87, 89–94, 103, 105–114, 120, 129, 130
analytical solution, 21, 22, 32, 78, 84, 87, 105–107, 111
approximation
- backward, *see* backward difference quotient
- central, *see* central difference quotient
- forward, *see* forward difference quotient
- order, 47, 49, 68
artificial intelligence, 20
averaging process, 9, 11, 16, 23

backward difference quotient, 47–49, 51, 52
band matrix, 56
boundary conditions, 16, 21, 45, 65–66, 99, 159–170

Cartesian coordinate system, 16, 24
central difference quotient, 47–49, 51, 53
channel
- compound, *see* compound channel
- rectangular, *see* rectangular channel
coefficient
- metric, *see* metric coefficient
compound channel, 105, 117–127
computation time, 67, 89–94, 129
- CPU time, *see* CPU time
- real time, *see* real time
concentration, 8
conservative substances, 7
continuous release, 24, 29, 39–43, 105, 106, 113–114, 120, 148
Courant numbers
- advection, 53
- diffusion, 53
CPU time, 89, 90
Crank-Nicolson (CN) scheme, 50, 51, 54–58, 78, 82, 87, 89–94, 103, 105–114, 129, 130
curvelinear coordinate system, 24

difference
- equation, 50
  - - ADI, 59–61, 171
  - - Upwind scheme, 53
  - - explicit scheme, 52
  - - general case, 50, 171
- operators, 46, 50, 135
- quotient, 46, 68, 135
  - - backward, *see* backward difference quotient
  - - central, *see* central difference quotient
  - - forward, *see* forward difference quotient

differential operators, 46, 135
diffusion
- molecular, *see* molecular diffusion
- numerical, *see* numerical diffusion
- term, 9, 94, 96
- turbulent, *see* turbulent diffusion
diffusion coefficient, 8
Dirac delta, 32
discretization grid, 47, 49, 55, 89
dispersion, 10, 11
- coefficient, 16, 18–20
- - longitudinal, *see* longitudinal dispersion
- - transverse, *see* transverse dispersion
- longitudinal, *see* longitudinal dispersion
- numerical, *see* numerical dispersion
- tensor, 17, 23–27, 77, 137
- - diagonal, 24
- - non-diagonal, 24, 130
- transverse, *see* transverse dispersion
dissipation, 68, 76

explicit scheme, 50–53

far field zone, 15
Finite Difference Method (FDM), 45–49, 68
Finite Element Method (FEM), 45, 46
Finite Volume Method (FVM), 45
floodplains, 117
fluorometer, 117
forward difference quotient, 47–49, 51, 52
friction velocity, 18, 120
Fully Implicit (FI) scheme, 50, 51, 54, 78

Gauss distribution, 21, 83, 84, 91, 122
Gauss-Seidel method, 57–58, 89, 90

Identity transformation, 25, 29–43, 137–158
implicit scheme, 50, 54–65, 94
initial conditions, 16, 21, 45, 65, 91, 99, 106, 107, 114
instantaneous release, 24, 29, 32–37, 105–113, 137
iterative methods
- Gauss-Seidel method, *see* Gauss-Seidel method
- Jacobi method, *see* Jacobi method
- Successive Over Relaxation method, *see* Successive Over Relaxation method (SOR)

Jacobi method, 56–58, 89, 90

longitudinal dispersion, 18–20, 24
- coefficient, 121
- coefficient, 17–20, 24, 106, 120

mass conservation law, 8
mass transport, 7, 8, 23, 45, 117
- equation, *see* advection-diffusion equation
matrix
- band, *see* band matrix
- rotation, *see* rotation matrix
- tridiagonal, *see* tridiagonal matrix
metric coefficient, 24
mid field zone, 13
mixed derivatives, 23, 68, 129, 130
mixing coefficients, 10
model
RivMix, *see* River Mixing Model
modified equation, 72, 73, 75, 86, 171
- ADI, 87
- general case, 76, 77
Modified Equation Approach, 69–84
molecular diffusion, 8–10
- coefficient, 10
- tensor, 9

natural coordinate system, *see* curvelinear coordinate system
near field zone, 13
numerical
- diffusion, 67, 68, 77, 78, 82, 84, 94, 111, 129
- - tensor, 77, 78, 82, 87
- dispersion, 67, 68, 76, 78, 94
- - tensor, 77, 78, 82, 87

operators
- difference, *see* difference operators
- differential, *see* differential operators
oscillations, 68, 78, 87, 94, 96, 130

passive substances, 7, 16
Peclet number, 94–96

Quasi rotation, 25, 27, 29–43, 137–158

reaction term, 7

real time, 89, 90
rectangular channel, 18, 19, 29, 30, 105
relaxation parameter, 57, 58, 90, 103
release
- continuous, *see* continuous release
- instantaneous, *see* instantaneous release
Reynolds' hypothesis, 9
Rhodamine, 117
River Mixing Model, 29, 51, 58, 97, 105, 120, 129
RivMix, *see* River Mixing Model
Rotation, 24–26, 29–43, 137–158
rotation matrix, 26
round-off error, 90

scheme
- Alternating Direction Implicit method (ADI), *see* Alternating Direction Implicit method (ADI)
- Crank-Nicolson, *see* Crank-Nicolson (CN) scheme
- Fully Implicit, *see* Fully Implicit (FI) scheme
- Upwind, *see* Upwind (UP) scheme
- explicit, *see* explicit scheme
- implicit, *see* implicit scheme
series expansion, *see* Taylor series
shear dispersion, *see* dispersion
shear velocity, *see* friction velocity
square method, 46
stability, 67, 89–94
- criteria, 91
Successive Over Relaxation method (SOR), 57–58, 89, 90

Taylor series, 46, 47, 49, 68–71, 86, 171
Thomas method, 61–65, 89, 90, 94
tracer test, 19, 20, 105, 106, 117, 120, 130
transport equation, *see* advection-diffusion equation
transverse dispersion, 18–20, 24
- coefficient, 17–20, 24, 117, 120
transverse mixing coefficient, *see* transverse dispersion, 117
tridiagonal matrix, 61–64
truncation error, 10, 49, 67–87, 130
turbulence, 18
turbulent diffusion, 9, 23
- coefficient, 10, 17
- tensor, 10, 23
turbulent diffusion tensor, 9

Upwind (UP) scheme, 51–53, 78, 80–84, 89–94, 103, 105–114, 129, 130

Vector-like rotation, 25, 27, 29–43, 137–158

water quality, 7, 8